



UNIVERSIDAD AUTÓNOMA DE MADRID  
FACULTAD DE CIENCIAS  
DEPARTAMENTO DE FÍSICA TEÓRICA



---

# HIGGS COSMOLOGY

*From the Early to the Late Universe*

---

Memoria de Tesis Doctoral realizada por

**Javier Rubio Peña**

presentada ante el Departamento de Física Teórica  
de la Universidad Autónoma de Madrid  
para la obtención del Título de Doctor en Ciencias.

Tesis Doctoral dirigida por

**Juan García-Bellido Capdevila**

del Departamento de Física Teórica y el I.F.T.  
de la Universidad Autónoma de Madrid

Madrid, Junio 2011.



## Abstract

Inflation is nowadays a well established paradigm consistent with all the observations, related both to the background and to the matter perturbations in the Universe. The nature of the inflaton, as well as the overall picture of the transition between the inflationary and radiation eras, depend crucially on the different microphysics models in which inflation is embedded. The absence of a suitable candidate in the usual formulation of the Standard Model has motivated the search for alternatives in different extensions of the standard theory, as Supersymmetry or String Theory. Unfortunately, the strength of the couplings among the inflaton and the different matter species present in those models is generically unknown. This fact makes difficult the determination of the dominant reheating mechanism at the end of inflation and the associated efficiency of the reheating stage. In this PhD thesis we adopt a very different and reductionist point of view. We study the possibility of inflation to be a natural consequence of the Standard Model, rather than an indication of its weakness. The role of the inflaton is played by the Higgs boson, non-minimally coupled to gravity. No new degrees of freedom apart from those already present in the electroweak theory are initially added. The non-minimal coupling rescues the Higgs field from the known difficulties for generating inflation, being its value determined by cosmological observations. The novelty and great advantage of the model is precisely its connection with a well-known microphysical mechanism, hopefully accessible in the present accelerator experiments. All the couplings among the Higgs and the Standard Model particles are known at the electroweak scale and can be extrapolated to the reheating era through the renormalization group equations. For the first time, the initial conditions of the hot Big Bang can be potentially determined, without invoking new speculative physics beyond the electroweak scale. Some modest extensions of the simplest Higgs Inflation model, based on scale invariance and Unimodular Gravity, are able to accommodate not only the early but also the late time acceleration of the Universe. Contrary to other *beyond the Standard Model theories*, they introduce just an extra degree of freedom, the dilaton, which plays however a central role, tracking the present expansion rate of the Universe. The close connection between the inflationary and dark energy dominated eras leads to highly non-trivial consistency relations between the spectral tilt of CMB anisotropies and the present equation of state of dark energy.





## Resumen

Inflación es a día de hoy un paradigma bien establecido consistente con todas las observaciones. Su naturaleza, así como los aspectos globales de la transición entre el estado inflacionario y la época dominada por materia, dependen en gran medida de los diferentes modelos microscópicos en los que se implementa. La ausencia de un candidato a inflatón en el Modelo Estándar ha motivado la búsqueda de alternativas en extensiones de esta teoría, como Supersimetría o teoría de cuerdas. Desafortunadamente, desconocemos la intensidad de los acoplos entre el inflatón y el contenido de materia de dicho modelos. Este hecho dificulta la determinación del mecanismo de recalentamiento dominante y su eficiencia. En esta tesis abordaremos el problema desde un punto de vista muy diferente y reduccionista. Estudiaremos el inflatón no como una indicación de la debilidad del modelo estándar, sino como una consecuencia natural del mismo. Será el propio campo de Higgs, ya presente en el Modelo Estándar, el que juegue el papel de inflatón mediante un acoplo no mínimo a gravedad. No se incorporarán inicialmente nuevos grados de libertad, más allá de los ya presentes en la teoría electrodébil. La novedad, y al mismo tiempo gran ventaja, de este modelo es precisamente su conexión con un mecanismo microfísico bien conocido, y que podría ser accesible en los aceleradores de partículas actuales. Todos los acoplos entre el Higgs y las partículas del Modelo Estándar se conocen a la escala electrodébil, pudiéndose extrapolar a la era del recalentamiento mediante las ecuaciones del grupo de renormalización. La determinación de las condiciones iniciales del Big Bang es por primera vez posible sin la necesidad de invocar nueva y especulativa física más allá de la escala electrodébil. Algunas extensiones relativamente modestas de *Higgs Inflation*, basadas en invarianza de escala y gravedad unimodular, son capaces de acomodar no sólo el estadio inflacionario, sino también la aceleración del universo actual. Contrariamente a otros modelos, estas extensiones introducen solamente un grado de libertad adicional, el dilatón, que juega sin embargo un papel central en el modelo, determinando la tasa de expansión actual del mismo. La gran conexión entre el proceso inflacionario y la energía oscura da lugar a relaciones de consistencia altamente no triviales entre el tilte espectral de las anisotropías del CMB y la ecuación de estado de energía oscura.



*A mi familia, que me lo ha dado todo.*



## Acknowledgements

A todos los que la presente  
vieren y entendieren.

---

Inicio de las Leyes Orgánicas.

I am indebted to many people for their help and support during the last few years. I am particularly thankful to my supervisor Juan García-Bellido for sharing with me his insight in the interplay between particle physics and cosmology. My view of understanding the physics, my critical view of it as well as maybe my prejudices are clearly influenced by him. I would like also to thank all the members of SISSA-Trieste, MPI-Munich and EPFL-Lausanne for the hospitality and very pleasant working environment during the development of part of the research presented in this thesis. I am particularly thankful to Stefano Liberati, Ignacio Cirac and Mikhail Shaposhnikov for allowing me to visit those institutions and for guiding me in the exploration of their very diverse disciplines. Great thanks to Daniel Zenhausern and Daniel G. Figueroa for the fruitful and enjoyable collaborations we had in Madrid and Lausanne respectively. Thanks also to Anupam Mazumdar, Jose Pedro Mimoso and Stefano Liberati for their comments and suggestions about this manuscript and for bringing to my attention references which would have otherwise missed in the large literature. Finally I would like to mention the efficient secretarial staff of the Department and Institute of Theoretical Physics for all the bureaucratic help along the past few years.

In the most personal part of these acknowledgments, I would like to thank my co-PhD students and friends in Madrid: Roberto, Bea, Domenico, Luis, Norberto, Jaime, Joao, Brian, Ana, Josu, Javis, Migueles and many others who will surely forgive me not to include their name in this long list. Among them I would like to convey my special affection to Fran and Pilar, for all we have shared during these years and for helping me so much with the *technicalities* of this thesis. In the past few years, I met a lot of people in different workshops and meetings and some of them have also become good friends. Thanks Hector, Aurelio, Guillem, Noela, Marco, Julien, Iker for all the good moments we lived. Among my *carissimi amici* out of the Institute deserve a special mention Cristina and Jose, for being there in all my bad moments before, during and hopefully after the preparation of this thesis. They are

a central part of my life. Great friends are also María y Pedro, with whom I spent one of the best vacations of my life and hopefully many others. Thanks María for that wonderful piece of advise that you gave me in Zamora.

Last, but not least, I wish to thank my fathers Tino and Emilia, my sister Beatriz and my lovely grandparents for their invaluable and unconditional support along all my life. Everything I am I owe to you.

Qué te parece desto, Sancho? -  
dijo Don Quijote - Bien podrán  
los encantadores quitarme la  
ventura, pero el esfuerzo y el  
ánimo, será imposible.

---

*Segunda parte del Ingenioso  
Caballero Don Quijote de la  
Mancha*  
MIGUEL DE CERVANTES

- Buena está - dijo Sancho -;  
fírmela vuestra merced. No es  
menester firmarla -dijo Don  
Quijote-, sino solamente poner  
mi rúbrica.

---

*Primera parte del Ingenioso  
Caballero Don Quijote de la  
Mancha*  
MIGUEL DE CERVANTES





## Declaration

The material presented in this PhD thesis is based on original contributions done during the course of my PhD studies. In particular the results scattered through Chapters 2, 3 and 5 are based on Ref. 2 on the list below, while the main results of Chapter 4 are contained in Ref. 1. This last chapter is also influenced by Ref. 3. although the details have not been included for being yet work in progress. Chapter 1 describe the motivation of the Higgs-driven inflationary models considered in this PhD thesis, while a summary of the main results of this thesis is presented in Chapter 6. The appendices A and B contains mainly non-original contributions included to clarify some technical aspects of this PhD thesis. On the other hand the results presented in Appendix C constitute also original material.

1. *Preheating in the Standard Model with the Higgs-Inflaton Coupled to Gravity.*  
Juan Garcia-Bellido, Daniel G. Figueroa and Javier Rubio  
[Phys. Rev. D \*\*79\*\* 063531 \(2009\)](#)
2. *Higgs Cosmology: From the Early to the Late Universe.*  
Juan Garcia-Bellido, Javier Rubio, Mikhail Shaposhnikov and Daniel Zenhausern.  
To be published soon.
3. *Dilaton production at Higgs-Dilaton Inflation.*  
Juan Garcia-Bellido, Javier Rubio, Mikhail Shaposhnikov and Daniel Zenhausern.  
In preparation.



<b>Glossary and Notation</b>	<b>i</b>
<b>1 Beyond the Standard Model</b>	<b>1</b>
1.1 The Standard Models . . . . .	1
1.2 Troubles in paradise . . . . .	2
1.3 Beyond or not Beyond? . . . . .	5
1.4 The $\nu$ MSM: an alternative approach . . . . .	6
1.5 Higgs Cosmology . . . . .	8
<b>2 The Higgs field and Gravity</b>	<b>11</b>
2.1 Inertia here arises from mass there . . . . .	11
2.2 The Minimal Non-Minimally Coupled Standard Model . . . . .	13
2.3 The No-Scale scenario . . . . .	16
2.4 A very useful Noether's Current . . . . .	18
<b>3 The Higgs boson in the Sky</b>	<b>21</b>
3.1 The Higgs field as the inflaton . . . . .	21
3.2 Higgs Inflation . . . . .	22
3.2.1 Slow-roll inflation and attractor solutions . . . . .	25
3.3 Higgs-Dilaton Inflation . . . . .	27
3.3.1 Slow-roll inflation and attractor solutions . . . . .	29
3.4 Cosmological Perturbations . . . . .	33
3.5 CMB constraints on parameters . . . . .	36
3.6 Quantum Corrections . . . . .	42
<b>4 The Higgs field and (P)reheating</b>	<b>49</b>
4.1 From Inflation to the hot Big Bang . . . . .	49
4.2 Higgs-Dilaton Inflation meets Higgs Inflation . . . . .	51

4.3	The Standard Model in the Einstein frame . . . . .	57
4.4	Perturbative Decay of the Higgs field . . . . .	59
4.5	Tachyonic preheating . . . . .	62
4.6	Bose-Einstein Condensation and Parametric Resonance . . . . .	62
4.7	Spontaneous boson production and decay into fermions . . . . .	67
4.7.1	Instant Preheating . . . . .	70
4.7.2	Successive Instant Preheating . . . . .	72
4.8	A new preheating mechanism: <i>Combined Preheating</i> . . . . .	73
4.9	Backreaction and the end of (p)reheating . . . . .	80
4.10	Similar but not equal: Dilaton production . . . . .	82
<b>5</b>	<b>The Higgs field and Dark Energy</b>	<b>85</b>
5.1	Scale invariance and the Cosmological Constant . . . . .	85
5.2	Dilaton Quintessence . . . . .	86
5.3	From the Early to the Late Universe . . . . .	89
5.3.1	Consistency relations . . . . .	89
5.3.2	Dark energy constraints on the initial inflationary conditions . . . . .	93
<b>6</b>	<b>Conclusions and Outlook</b>	<b>97</b>
<b>7</b>	<b>Resumen y Perspectivas</b>	<b>103</b>
	<b>Appendices</b>	<b>107</b>
	<b>Appendix A Parametric resonance as a quantum mechanical problem</b>	<b>109</b>
	<b>Appendix B Conformal transformations</b>	<b>113</b>
	B.1 Geometrical quantities . . . . .	113
	B.2 Matter quantities . . . . .	114
	B.3 Cosmological perturbations . . . . .	115
	<b>Appendix C Higgs-Dilaton trajectories in the Jordan frame</b>	<b>119</b>
	<b>List of Tables</b>	<b>123</b>
	<b>List of Figures</b>	<b>125</b>
	<b>Bibliography</b>	<b>131</b>

## Conventions and Units

The signature of the metric is taken to be  $(-, +, +, +)$ . Greek indices refer to coordinates in the full spacetime, ranging from 0 to 4, while latin indices refer to coordinates in field space or to spatial coordinates, depending on the context. Repeated indices are generally summed, unless otherwise indicated. Colon and semicolon denote respectively ordinary and covariant differentiation. Spatial three-vectors are indicated by letters in boldface. A tilde is used for those quantities defined in the Einstein frame and the subscript 0 is usually preserved for quantities evaluated at the present time. Dot denotes differentiation with respect to the coordinate time.

Keeping the conventional system of units in cosmology and particle physics, the speed of light  $c$ , the reduced Planck constant  $\hbar$  and the Boltzmann constant  $k_B$  are set to 1 throughout this thesis. Masses and temperatures are therefore measured in energy units. Regarding the gravitational interaction, we define the *reduced Planck mass* as

$$M_P \equiv \sqrt{\frac{\hbar c}{8\pi G}} = 2.436 \times 10^{18} \text{ GeV} , \quad (1)$$

and use it interchangeably with the gravitational Newton's constant  $G$ , depending on the context. The word *reduced* is frequently omitted in the text.

## Cosmological Parameters

In Table 1 we summarize the value of the different cosmological parameters used in this work [1]. Their value depends on the different data sets used and the number of parameters allowed to vary. We choose a  $\Lambda$ CDM cosmology with a power-law initial spectrum, spatial flatness, a cosmological constant. Tensor perturbations are assumed to be zero, except in quoting a limit on them. The pivot scale is  $k^* = 0.002 \text{ Mpc}$ . Unless otherwise stated, the uncertainties presented in the parameters are at the 68% confidence level and should not be extrapolated to higher levels, without the knowledge of the assumed priors and non-gaussian likelihoods.

Parameter	Symbol	Value
Hubble parameter	$h$	$0.704 \pm 0.013$
Present Hubble constant	$H_0$	$H_0 = 100 h \text{ km} \cdot \text{s}^{-1} \text{Mpc}^{-1}$
Present critical density	$\Omega_{cr}$	$\Omega_{cr} h^2 = 0.1123 \pm 0.0035$
Present total matter density	$\Omega_M$	$\Omega_M h^2 = 0.1349 \pm 0.0036$
Present baryon density	$\Omega_B$	$\Omega_B h^2 = 0.02260 \pm 0.00053$
Present Radiation Density	$\Omega_R$	$\Omega_R h^2 = 2.42 \times 10^{-5}$
Present Cosmological constant	$\Omega_\Lambda$	$\Omega_\Lambda = 0.728 \pm 0.015$
Density perturbation amplitude	$\Delta_\zeta^2(k^*)$	$(2.44 \pm 0.09) \times 10^{-9}$
Density perturbation spectral index	$n_s$	$n = 0.963 \pm 0.012$
Tensor to scalar ratio	$r$	$r < 0.24$ (95% C.L.)

Table 1: Cosmological Parameters for a  $\Lambda$ CDM cosmology with a power-law initial spectrum, spatial flatness and cosmological constant [1].

## Glossary

An attempt has been made to keep acronyms and abbreviations as standard as possible. The following list will hopefully be a useful tool for clarifying the use of the non-standard ones. In general, irrespectively of whether they have been included in this guide, they are also defined at their first occurrence in the text and in all places where ambiguities may arise.

BAU	Baryonic Asymmetry of the Universe
BBN	Big Bang Nucleosynthesis
BOSS	Baryon Oscillation Spectroscopic Survey
BSM	Beyond the Standard Model
CMB	Cosmic Microwave Background
<i>dof</i>	degrees of freedom
<i>ecom</i>	equation of motion
DE	Dark Energy
DES	Dark Energy Survey
DM	Dark Matter
EW	Electroweak
FRW	Friedmann-Robertson-Walker
GR	General Relativity
GUT	Grand Unified Theory
hBB	hot Big Bang
$\Lambda$ CDM	Lambda Cold Dark Matter
LEP	Large Electron-Positron collider
LHC	Large Hadron Collider
LSS	Large Scale Structure
$\nu$ MSM	Neutrino Minimal Standard Model

PAU	Physics of the Accelerating Universe
QCD	Quantum Chromodynamics
QED	Quantum Electrodynamics
QFT	Quantum Field Theory
SEP	Strong Equivalence Principle
SM	Standard Model
SSB	Spontaneous Symmetry Breaking
SUSY	Supersymmetry
UG	Unimodular Gravity
<i>vev</i>	vacuum expectation value
WEP	Weak Equivalence Principle
<i>wrt</i>	with respect to
1PI	One Particle Irreducible





# CHAPTER 1

## Beyond the Standard Model

Ubi materia, ibi geometria.

JOHANNES KEPLER

### 1.1 The Standard Models

It is an ancestral belief that the universe is composed of simple materials governed by a set of universal and unified laws. Our current understanding of the structure of the universe, in the absence of a unified theory for all the fundamental interactions, is based on two basic pillars of Modern Physics: the Standard Model (SM) of particle physics and General Relativity (GR).

The Standard Model [2, 3, 4], based on the  $SU(3)_C \times SU(2)_L \times U(1)_Y$  gauge symmetry group, unifies the strong, weak and electromagnetic interactions. The gauge symmetry is spontaneously broken to  $SU(3)_C \times U(1)_{EM}$  by a weak isodoublet complex scalar field, giving mass to the SM particles<sup>1</sup>. Intermediate gauge bosons acquire masses by absorbing three of the four components of the scalar field, the so-called Goldstone bosons (see for instance Ref. [5]). The remaining degree of freedom becomes a physical particle: the Higgs field, still undiscovered. The many particle's experiments in the 80's and 90's gave rise to a vast array of data, which, with unprecedented precision, allowed to test the different interaction vertices and masses of the model. The central theoretical principles of the SM have remained in place for decades and it is nowadays understood as an extremely successful description of particle physics at energies below TeV scales.

On the other hand, General Relativity [6], a classical geometrical theory, constitutes a very elegant, comprehensive and coherent framework for the description of gravity and matter at the macroscopic level. Its predictions and deviations from Newtonian gravity (in

---

<sup>1</sup>In the original formulation of the SM the neutrinos remain massless.

its weak-field, small velocities limit) have been tested in and out the solar system, although its consequences go far beyond these scales. Indeed it can be considered as the origin or seed of Modern Cosmology. In General Relativity, space and time are promoted to dynamical quantities, whose evolution is dictated by the matter and energy content. For the first time in history the universe as a whole became a dynamical entity that can be modelled and measured.

The symbiosis between GR and the SM is also surprising. Their combination gives rise to the successful hot Big Bang (hBB) scenario, describing the evolution of the universe and its content from the first fraction of a second till the present era. The expansion of the universe [7, 8], the relative abundance of light nuclei [9, 10] or the discovery of the Cosmic Microwave Background [11] give confidence in the basic picture, the expansion of a initial primordial soup. Many of the key cosmological parameters describing the universe have been accurately determined [1] (cf. also Table. 1 in the Glossary), which have led to the establishment of a precision cosmological model known as  $\Lambda$ CDM. At the same time, these parameters provide useful information for particle physics. The stringent limits on the sum of neutrino masses [1, 12] and on the variations of the fundamental constants [13] clearly illustrate the entanglement between cosmology and high-energy physics.

## 1.2 Troubles in paradise

In spite of the success of both theories for describing our observed universe, they are not without shortcomings [14]; there are a handful of fundamental questions unanswered. Strong experimental, observational and theoretical arguments lead us to believe that none of them should be understood as complete theories of nature. Before considering extensions, it is important to notice that we are facing different kinds of troubles.

On the one hand, there are well established facts, whose explanation is not satisfactory within the SM. The first, and maybe the most evident one, is the existence of neutrino masses. When the SM was formulated, the neutrinos were considered to be massless, and therefore, the particle content of the model was chosen to forbid the mass terms. Nevertheless, the situation changed dramatically with the discovery of neutrino oscillations, from which there is nowadays overwhelming evidence [15]. These are transitions between neutrinos of different flavours and can occur only if neutrinos have non-degenerate masses [16, 17]. The initial version of the SM must be then extended in order to accommodate this fact. We will come back to this point in Section 1.3.

Regarding also the particle content, one of the basic tenets of the SM is the symmetry between matter and antimatter. According to the CPT theorem for any given particle exists an antiparticle with opposite charges but identical masses and decay widths [18]. This basic principle seems to be in contradiction with a variety of observations, ranging from the solar system to the whole observable universe [19, 20, 21]. For some unknown reason, there are many more protons than antiprotons and antimatter is indeed only detected in accelerators or

cosmic rays. Moreover, the number of photons substantially exceed the number of protons<sup>2</sup>. This fact is usually called the baryon asymmetry problem. As established on general grounds by Sakharov [23] in 1967, to successfully create the primeval baryon asymmetry of the universe (BAU), the particle processes violating baryon number conservation must take place out of thermal equilibrium. Besides, C and CP symmetries must be violated. Although the SM alone has *a priori* all the ingredients to generate the baryonic asymmetry, the absence of a first order electroweak phase transition [24] and the smallness of the Jarlskog determinant in the quark sector [25] excludes the possibility of generating the measured value within the standard theory. For a review, see for instance [26].

Even if a satisfactory baryogenesis mechanism was known, the baryonic matter would not be able to account for all the matter content in the universe. Several astrophysical and cosmological observations, coming from many different scales, seem to suggest that our universe should contain a new type of invisible or Dark Matter (DM) component. The new species would help to explain processes so unrelated as primordial nucleosynthesis, large-scale structure formation, or the galactic rotation curves (see Ref. [27] for a review). The concept of Dark Matter does not find however a satisfactory explanation within the framework of the Standard Model, since all the SM particles either emit photons or would have left an imprint on nucleosynthesis. The now massive neutrinos would constitute a natural choice, but they are essentially ruled out by observations. As relativistic species, neutrino erase density fluctuations as scales below their free-streaming length, of order  $40 \text{ Mpc} \times m_\nu / 30 \text{ eV}$  (see [12] for a review of this topic.). This erasing would imply a top-down process for the structure formation in the universe. As a consequence, galaxies would only appear at redshifts  $z \leq 1$ , which is in clear contradiction with the observation of galaxies at redshifts  $z > 4$ , cf. Ref [28]. A new dark candidate beyond the Standard Model matter content seems therefore unavoidable.

This invisible matter is indeed not the only dark or unknown component in our universe. In the concordance  $\Lambda$ CDM model, the redshift dependence of type Ia Supernovae [29, 30] is interpreted as a consequence of a present accelerated expansion of the universe. The present energy content is dominated by a cosmological constant term  $\Lambda$ , which, as happens with Dark Matter, has been only inferred by its gravitational interaction on cosmological scales. Although this term is a completely natural part of Einstein equations, it encounters consistency or interpretation problems when particle physics, in its standard formulation, is taken into account [31, 32, 33]. In the usual Quantum Field Theory (QFT) approach, the  $\Lambda$  term cannot be distinguished from vacuum energy fluctuations. When the standard renormalization procedure in flat space-time is applied, it fails to reproduce the observed value by 120 orders of magnitude<sup>3</sup>. No explanation is neither known for the so called *coincidence problem*, which wonders about why the cosmological constant started to dominate *right now*,

<sup>2</sup>This is usually defined in terms of the quantity  $\eta = n_B/n_\gamma$  where  $n_B$  is the difference between the number of baryons and antibaryons per unit volume and  $n_\gamma$  is the photon number density at temperature T. The value of  $\eta$  is severely constrained by nucleosynthesis,  $5.1 \times 10^{-11} \leq \eta \leq 6.5 \times 10^{-11}$  at 95% C.L. [22].

<sup>3</sup>The flat spacetime hypothesis does not apply if the bare (or renormalized) value of  $\Lambda$  is different from zero. If this happens, Minkowsky spacetime is not a solution of Einstein's equations [34]. This observation diminishes the predictive power of the estimate, since perturbation theory is being performed around a spacetime that does not satisfy the equations of motion. Although it can be argued that spacetime is locally flat, the observable effects of the cosmological constant appear at very large scales, where clearly the spacetime is not flat.

in our present epoch [35, 36, 37] (see also Ref. [34] for a critical point of view). These difficulties have motivated the study of alternatives such as Modified Gravity [38], Extra Dimensions, Dark Energy [39] or inhomogeneous Lemaître-Tolman-Bondi cosmologies [40]

Finally, we believe that the early universe also underwent a period of accelerated expansion, as that it is experiencing in the present epoch. In the old hot Big Bang theory questions such as the origin of the surprising flatness, homogeneity and isotropy of the present universe remained unexplained. Our universe should have been originated from very unnatural and non-generic initial conditions. As we will discuss below, naturalness is just a question of taste. One could simply argue that the most symmetric or simple initial conditions are more physical, but this is not very convincing from the point of view of the self-consistency of the theory, specially if some of those conditions are unstable, as happens for instance in the flatness problem. What singles out cosmology from the rest of sciences is the uniqueness of our universe. The usual particle physics experimental control of the initial conditions cannot be applied. A cosmological theory can claim to be a successful physical theory only if it can explain the state of the observed universe using simple physical ideas and starting with the most general initial conditions. The first attempts to solve these problems appeared in the early 80s [41, 42, 43, 44]. These works were the *shot heard around the world* and initiated what has become to be the most successful paradigm in modern cosmology: Inflation. The new ideas revolutionized cosmology by introducing an early period of accelerated expansion of the universe, ending in the radiation dominated epoch within which the usual hot Big Bang model starts. Note that inflation is not a model, but rather a paradigm including hundreds of particular models parametrizing the very simple idea (for a review of inflationary models see for instance Ref. [45, 46, 47]). The beauty of inflation is that all these (beyond the standard) models give rise to very similar predictions, which differs only in the details<sup>4</sup>. As we will see in Section 3.2.1, the easiest way to violate the strong energy condition is by an (effective or fundamental) homogeneous scalar field, evolving in a sufficiently flat potential. Unfortunately, the only existing scalar field in the Standard Model, the Higgs field, is not able to produce an early exponential expansion of universe. The lower bound on the Higgs mass makes it incompatible with CMB constraints on inflation. The question about the origin of the otherwise successful inflationary scenario remains therefore unexplained in the standard theory.

Any fundamental or effective theory beyond the SM and GR should try to solve, or at least alleviate, the previously described troubles. They clearly constitute a *smoking gun* for physics Beyond the Standard Model. On the other hand, there are man-made or aesthetic problems. The SM contains many parameters, which are unrelated, at least in the context of the theory itself. In addition to the Yukawa couplings for quark and lepton masses, one should specify three mixing angles and a complex phase in the CKM matrix, as well as other CP violation parameters. Something similar happens in the neutrino sector. If mass terms are allowed, three further mixing angles together with three phases must be considered. This counting gives rise to 26 free parameters. The amount and strange hierarchy

---

<sup>4</sup>If the existence of so many candidates to be the inflaton based on unknown speculative physics is an advantage or not for inflation is very researcher-dependent. From the point of view of the author the best models are those with an unification character (as should happen always in physics) and with the least number of assumptions based on unknown physics (simply Ockham's razor). This is precisely the approach followed in this thesis.

of the parameters, or the non-unification of the gauge couplings [48], are usually invoked to justify new physics beyond the SM, such as Grand Unified Theories [49]. The large set of couplings is thought to be the dynamical outcome of a simpler and more fundamental structure, as happens for instance with the transport coefficients of fluids. Although this is a very interesting possibility, one should always keep in mind that, contrary to the troubles described before, these parameters can be safely accommodated by the SM and do not express an inconsistency of the underlying theory.

### 1.3 Beyond or not Beyond?

There is a large number of proposals for extending the Standard Model, commonly refers to as *Beyond the Standard Model* (BSM) theories [14]. Inspired by the success of weak interactions, they share the belief that new energy scales, and their associated physics, should appear beyond the Electroweak (EW) scale. The new symmetries and particles introduced would allow to partially alleviate some of the SM problems, providing candidates for Dark Matter, new Baryogenesis mechanisms or flat inflationary potentials. Given the huge difference between the weak and gravitational scales, the relevance of gravity in those theories is usually neglected and new physics is expected to appear at energies well below the Planck scale.

As an example, let us consider the generation of neutrino masses. The absence of a singlet,  $\nu_R(1,1)_0$ , under the SM gauge group excludes the generation of neutrino masses via the usual Higgs mechanism. No Dirac mass term  $\langle\phi\rangle\bar{\nu}_L\nu_R$  can be written. One could consider the possibility of introducing neutrino masses *a la* Majorana<sup>5</sup>. Notice however that the combination  $\bar{\nu}_L^c\nu_L$  transforms as a  $SU(2)$  triplet. Since the SM does not contain scalar triplets,  $\Delta(1,3)_1$ , no invariant Majorana mass term  $\langle\Delta\rangle\bar{\nu}_L^c\nu_L$  can then be constructed. The situation changes dramatically if three right-handed neutrinos singlets are introduced. This constitutes a very economical approach which restores the symmetry between quarks and leptons in the SM. After all, there is no strong reason to banish this state, since there is an appropriate right-handed partner to all the other fermions<sup>6</sup>. The new neutrinos behave as pure singlets under the SM gauge symmetries, and therefore, Majorana mass terms can also be added to the theory. In this case, the most general renormalizable lagrangian for neutrino masses has the form

$$\mathcal{L}_\nu = y_{ij}\bar{L}_i\nu_{jR}\tilde{H} + \frac{\mathcal{M}_{ij}}{2}\nu_{iR}^c\nu_{jR} + \text{c.c.} \quad (1.1)$$

where  $y_{ij}$  are neutrino Yukawa couplings to the SM Higgs  $\tilde{H}$  and  $\mathcal{M}_{ij}$  are Majorana masses. The resulting mass matrix  $M$  has the structure

$$\hat{M} = \begin{pmatrix} 0 & m \\ m^T & \mathcal{M} \end{pmatrix}, \quad (1.2)$$

<sup>5</sup>Notice that Majorana terms  $\bar{\nu}_L^c\nu_L$  break the accidental L symmetry in the SM by two units. Global symmetries are not imposed at the level of the action and are just a consequence of the particular matter field content of the theory. Indeed, lepton number symmetry is anomalous at the quantum level. Note however, that B-L is conserved, even at the quantum level.

<sup>6</sup>Contrary to other right-handed particles interacting strongly or electromagnetically, right handed neutrinos were not originally included in the Standard Model particle content since they were not needed to explain the electroweak phenomena.

with Dirac mass matrices  $m_{ij} = \frac{y_{ij}}{\sqrt{2}}v$  coming from the Yukawa interactions. Let us now assume a big hierarchy between the Dirac and Majorana masses, namely  $\mathcal{M}_{ij} \gg m_{ij}$ . In this case,  $\hat{M}$  has approximately three heavy eigenvalues of order  $\mathcal{O}(\mathcal{M})$ , as well as three light ones of order

$$m_\nu \sim y^2 \frac{v^2}{\mathcal{M}}. \quad (1.3)$$

According to the previous expression, the effective neutrino masses depends now not only the Yukawa couplings, but also on the Majorana mass  $\mathcal{M}$ . Although the absolute scale of active neutrino masses has not yet been measured<sup>7</sup>, the simple assumption of a mass hierarchy provide an upper cosmological bound on the sum of all neutrino species, namely  $\sum_\nu m_\nu < 0.58$  eV at 95% C.L. [1] (see also [50]). If we take into account that the measured differences between neutrino masses squared range from  $10^{-3}$  to  $10^{-5}$  eV [22], it is not unreasonable to assume the largest neutrino mass  $m_\nu$  to be of the same order of magnitude, lets say about 0.1 eV. In order to reproduce this value via Eq. (1.3), we must first specify the Yukawa couplings and Majorana masses. The standard Seesaw mechanism [51, 52, 53] implicitly assumes neutrino Yukawa couplings of the same order as any other Yukawa in the Standard model. This assumption gives rise to a big hierarchy between the EW scale and the Majorana mass  $\mathcal{M}$ . Indeed, for  $y \sim 1$ , Eq. (1.3) implies  $\mathcal{M} \sim 10^{14}$  GeV, close therefore to the unification scale. In the standard approach, this scale is frequently interpreted as a physical cutoff for the SM effective theory<sup>8</sup>. However, one should keep in mind that this result is based on the assumption of large Yukawa couplings. It constitutes therefore an *upper bound* for the scale at which new physics should appear, rather than an estimate of its value. For sufficiently small Yukawa couplings, even Majorana masses at the EW scale would be enough to generate the small masses of the active neutrinos.

## 1.4 The $\nu$ MSM: an alternative approach

The Neutrino Minimal Standard Model ( $\nu$ MSM) proposed in Ref. [55] adopt precisely the alternative approach described at the end of the previous section. As the usual Seesaw mechanism described before, it introduces only three right-handed neutrinos, enlarging the SM with a mass term (1.1) (for the total particle content of the  $\nu$ MSM cf. Table 1.1). Nevertheless, the standard requirement of *Yukawa naturalness* is translated into *scale naturalness*. What is now considered to be *natural* is to have Majorana masses of the same order of any other mass term in the lagrangian, even if this implies very small Yukawa couplings for the neutrinos. No intermediate scales between the EW and Planck scales are introduced<sup>9</sup>. The number of additional degrees of freedom is therefore extremely restricted, contrary to what happens in

<sup>7</sup>Oscillation experiments provide only information about mass-squared differences between neutrino flavours, but not about their absolute value.

<sup>8</sup>Indeed, when integrating out the Majorana masses one obtains the effective non-renormalizable Weinberg operator [54]

$$\mathcal{O}_\nu = \frac{y_{ij}}{\mathcal{M}} \left( L_i^\dagger \phi^c \right)^\dagger \left( L_j^\dagger \phi^c \right). \quad (1.4)$$

This operator is indeed the lowest dimensional operator compatible with gauge and Lorentz invariance that can be constructed with the usual SM fields.

<sup>9</sup>Similar arguments can be also found in [56, 57].

Fermions					
Quarks			Leptons		
$\begin{pmatrix} u \\ d \end{pmatrix}_L$	$\begin{pmatrix} c \\ s \end{pmatrix}_L$	$\begin{pmatrix} t \\ b \end{pmatrix}_L$	$\begin{pmatrix} \nu_e \\ e \end{pmatrix}_L$	$\begin{pmatrix} \nu_\mu \\ \mu \end{pmatrix}_L$	$\begin{pmatrix} \nu_\tau \\ \tau \end{pmatrix}_L$
$u_R$	$c_R$	$t_R$	$e_R$	$\mu_R$	$\tau_R$
$d_R$	$s_R$	$b_R$	$\nu_{e,R}$	$\nu_{\mu,R}$	$\nu_{\tau,R}$
Vector Bosons			Scalars		
$\gamma, W^+, W^-, Z^0, g_{1\dots 8}$			$H, \chi$ (Dilaton)		

Table 1.1: Particle content of the Standard Model with a minimal Higgs sector (in black) and the  $\nu$ MSM extensions (in blue). The number of degrees of freedom in the Standard Model is 98, while there exist 28 bosonic degrees of freedom. The  $\nu$ MSM simply restores the symmetry between quarks and leptons in the SM by adding three right handed neutrinos, or equivalently 6 ( $3 \times 2$ ) fermionic degrees of freedom. In the scale-invariant extension of the  $\nu$ MSM an extra scalar singlet  $\chi$  (in brick red) is added.

other SM extensions such as Grand Unified Theories [48] or Supersymmetry [58, 59]. It is precisely this restriction which makes the model extremely appealing and predictive, but at the same time rather fragile. The success of the model depends on the outcome of a batch of experiments. If any the predictions [60] of the  $\nu$ MSM is not verified the whole idea would be ruled out. Given the absence of any intermediate scale, the  $\nu$ MSM should be able to accommodate the SM problems. As shown in [61, 62, 63], it is possible to simultaneously explain the dark matter abundance, the neutrino masses and the baryon asymmetry of the universe within the considered model, albeit with non-trivial conditions on the sterile neutrino masses and relatively fine-tuned parameters. In the  $\nu$ MSM dark matter is accounted by a keV-scale sterile neutrino, while baryogenesis occurs via leptogenesis due to sterile neutrino oscillations. As a bonus, the anomaly cancellation procedure in the new model gives rise to charge quantization [64], not present in the usual Standard Model. Other SM problems such as the Landau pole of the Higgs self-coupling [65, 66] are still present in the  $\nu$ MSM. Notice that some of those problems could be due to a misunderstanding of the gravitational theory and its relations with the SM. Moreover, the merging between gravitation and the SM could not even occur in the framework of Quantum Field Theory (QFT). Perhaps QFT is just an emergent approximation of a deeper framework, like String Theory [67]. The  $\nu$ MSM adopts a conservative point of view, postponing the solution of the Landau pole of the Higgs till the Planck scale. For a restricted value of Higgs masses<sup>10</sup>, the position of the pole is beyond the Planck mass [72, 73, 74], leaving therefore the ultraviolet completion of the SM to a quantum theory of gravity.

<sup>10</sup>For very small masses the Standard Model vacuum is believed to be unstable [68, 69, 70]. For arguments again this perturbative claim based on lattice simulations see for instance [71].



## 1.5 Higgs Cosmology

The  $\nu$ MSM must also provide an inflationary mechanism, able to give rise to the surprising flatness, homogeneity and isotropy of the universe. This mechanism should incorporate a graceful exit, able to recover the hot Big Bang scenario. This constitutes *a priori* a difficult task, since, as we pointed out in Section 1.2, the usual SM does not contain any suitable candidate to be the inflaton. However, this situation changes dramatically when gravity comes into play. In Chapter 2 we introduce a non-minimal coupling between the Higgs field and gravity. Again, in the philosophy of the  $\nu$ MSM, no new scales between the EW and Planck scales are introduced. In this new scalar-tensor framework, the metric is not the only gravitational degree of freedom coupled to local matter. Contrary to what happens in GR any measurements of the inertial mass of a given object would depend, through the Higgs field, on the surrounding matter distribution. The Higgs field seems therefore to unify the concept of mass in particle physics with the Mach's principle, which inspired Einstein to construct GR.

This unified description of the origin of the masses in gravity and particle physics, becomes somehow obscured by the presence of scales completely unrelated to the Higgs mechanism. Scales such as  $\Lambda_{QCD}$  appear through dynamical transmutation, a process that has nothing to do with the spontaneous symmetry breaking mechanism, responsible for the masses of the quarks, leptons, or gauge bosons. Other scales, such as the vacuum expectation value ( $vev$ ) of the Higgs or the Planck mass, are just dimensional parameters in the action. A unified description of all the masses in the universe, within the present understanding of the SM and gravity, seems therefore unlikely. Among the three ways of generating mass, a spontaneous symmetry breaking mechanism seems unavoidable, given the gauge character of the SM. From this point of view, an interesting possibility is to consider a scale-invariant extension of the  $\nu$ MSM [75, 76]. This is also done in Chapter 2. In this case, the Higgs'  $vev$  is promoted to a dynamical field, the dilaton, which also couples to gravity. All the scales, including the Planck mass, are now generated by spontaneous symmetry breaking of the underlying scale invariance. As a consequence, the dilaton field becomes exactly massless, as corresponds to a Goldstone boson. As we will show in Chapter 3, the existence of the non-minimal interaction between the Higgs field and the metric can give rise, in both models, to a successful inflationary stage with a graceful exit. All the parameters of the theory, except the Higgs mass, turn out to be determined by CMB observations, making the models extremely predictive. The similarities between the two models are indeed noticeable. As we will see in Chapter 4, the production of gauge bosons and fermions take place, up to some small corrections, in the same way in the two models. The explosive production of particles by parametric resonance is however diminished by the perturbative decay of the created quanta into lighter particles. This gives rise to a very complicated process, that we called *Combined Preheating* [77] in which perturbative and non-perturbative effects are mixed. Eventually, the energy stored in the light particles will dominate, recovering the standard hot Big Bang picture. The scale-invariant extension of the SM is nevertheless not free of caveats. The otherwise so useful scale-invariance of the theory forbids the existence of a cosmological constant at the level of the action, which is in contradiction with the observed accelerated expansion of the late universe. This term can be recovered at the level



of the equations of motion, if we allow for a slight modification of GR. The combination of Unimodular gravity and non-minimal couplings described in Chapter 5 gives rise to a runaway dark energy potential for the dilaton [75, 76]. This makes the Higgs-Dilaton scenario unique. For the first time, a single well motivated particle physics model is able to explain simultaneously the Early and Late universe in a consistent way, recovering the standard hot Big Bang picture and the late time acceleration of the universe, after a successful inflationary period<sup>11</sup>. The common origin of these three stages allows to derive extra bounds on the initial inflationary conditions, as well as potentially testable relations between the Early and Late universe observables [76].

---

<sup>11</sup>Related unifying ideas have been proposed in the literature in the context of *Quintessential Inflation* (see for instance [78, 79, 80, 81]), but never within the well-known Standard Model and therefore without the knowledge of the couplings among the inflaton and matter fields.



## CHAPTER 2

# The Higgs field and Gravity

The Higgs mechanism is just a  
reincarnation of the Communist  
party: it controls masses.

V.I. ULYANOV

### 2.1 Inertia here arises from mass there

This chapter explores the close relation between the Higgs, General Relativity and the concept of mass. Where does the mass of the particles come from? Mass is such a fundamental property of matter that an explanation of its origin seems not to be needed. However, when examining the problem in detail, one realizes that it is difficult to find descriptions of mass compatible with other ideas of modern physics. From the particle physics point of view, the naive inclusion of masses within the Standard Model turns out to be incompatible with the gauge symmetry. A new scalar field, the Higgs, and a spontaneous symmetry breaking mechanism, are needed to account for the masses of the Standard Model particles. The dimensional Fermi coupling constant  $G_F$  becomes, in the light of the new electroweak (EW) theory, not fundamental. It rather corresponds to a low energy effective coupling, that depends on the dimensionless couplings of the  $SU(2)_L \times U(1)_Y$  group and on the vacuum expectation value ( $vev$ ) of the Higgs field. The weakness of the EW interactions is translated now to the largeness of the Higgs'  $vev$ ,  $v \propto G_F^{-1/2}$ .

On the other hand, from the gravitational point of view, the inertial mass of an object, understood as a measure of its resistance to changes in its motion, is thought to be a consequence of its gravitational interaction with the rest of matter in the Universe. This idea is known as Mach's principle [82]. Einstein, strongly influenced by Mach, proposed General Relativity, the first theory with a dynamical background depending on the matter distribution. A detailed analysis of GR reveals however almost no observable effects of how

distant matter affects local measurements<sup>1</sup>, except gravitomagnetism or frame dragging [85]. In fact, if we take into account that the metric field can always be locally transformed to the Minkowsky metric

$$g_{\mu\nu}(x) = \eta_{\mu\nu} + \mathcal{O}(R_{\mu\sigma\nu\eta}(x - x_0)^\sigma(x - x_0)^\eta) , \quad (2.1)$$

then, neglecting gravitational tidal fields, the laws of physics are locally identical throughout the spacetime. As Brans and Dicke realized [86], the previous reasoning changes dramatically if the metric is not the only field coupled to local matter. If extra fields are present, they will generally vary in space and time and, even if the metric field is made locally Minkowskian. Any measurements of an object's mass will be influenced by the local value of these new fields, permeating all of space. In this new picture, not only the active gravitational masses, but also the Newton's gravitational "constant"  $G$  or passive mass, will be a function determined by the matter distribution in the Universe. Similarly to the EW case, the weakness of the gravitational constant would be related to the *vev* of these fields. In order to preserve Lorentz invariance and isotropy of local physical laws [87, 88], no vector or second order fields should be introduced, unless they were extremely weak as to avoid appreciable preferred-frame effects. Therefore, we are just left with a scalar "arena". The new scalar field could of course belong to a new theory beyond the Standard Model, but, if we do not want to introduce new highly speculative degrees of freedom apart from those already in the standard theory, we are just left with one possibility: The Higgs field. The idea of unifying the Higgs and Brans-Dicke fields in an unique field, responsible both for the gravitational and EW interaction is known as Induced Gravity (IG) [89, 90].

But, is it natural to consider the Higgs field as a *gravitational* degree of freedom? The Higgs mechanism lies precisely in the same direction of the original Mach's idea of producing mass by a gravitational-like interaction. The Higgs boson couples to all the particles in the Standard model in a very specific way, with a strength proportional to their masses, and mediates a scalar Yukawa type gravitational interaction [91, 92]. The masses act as the source of the scalar Higgs field and the Higgs field backreacts by its gradient on the masses in the momentum law. According to the Equivalence Principle, it seems natural to identify the gravitational and particle physics approaches to the origin of the masses. From this point of view, the Induced Gravity theory could be considered as an indication of a connection between the Higgs, gravity and inertia.

On the other hand, choosing the Higgs field implies that, not only all the masses in the Standard Model would be due to their interactions with the Higgs field, but also the Planck mass, which seems to contradict the standard lore that gravity does not play any role in elementary particle physics. Somehow, the hierarchy between the EW and gravitational scales should be maintained in order to avoid undesirable effects. The standard way, within models of symmetry breaking with several fields, is to assume that the different fields have very different expectation values, but similar values of the coupling constants, in order to keep the theory perturbative at all scales. However, if the *vev* of the Higgs field is chosen to be responsible both for the Planck and EW scales, we are compelled to consider another possibility to preserve the hierarchy: the coupling constants must be widely different. The important physical question is not if the value of the couplings constant is *natural* or not, but if the model is indistinguishable from the Standard Model at low energy.

---

<sup>1</sup>Some of their solutions as the Gödel universe [83] of the exact *pp*-waves [84] are indeed clearly anti-Machian

## 2.2 The Minimal Non-Minimally Coupled Standard Model

Let us apply now the previous arguments to the Standard Model. The Glashow-Weinberg-Salam lagrangian density [2, 3, 4] is divided into four parts: a fermion sector ( $F$ ) which includes the kinetic terms for the fermions and their interaction with the gauge bosons, a gauge sector ( $G$ ), including the kinetic terms for the intermediate bosons as well as the gauge fixing and Faddeev-Popov terms, a Spontaneous Symmetry Breaking sector ( $SSB$ ), with a Higgs potential and the kinetic term for the Higgs field including its interaction with the gauge fields, and finally, a Yukawa sector ( $Y$ ), with the interaction among the Higgs and the fermions of the Standard Model,

$$\mathcal{L}_{SM} = \mathcal{L}_F + \mathcal{L}_G + \mathcal{L}_{SSB} + \mathcal{L}_Y. \quad (2.2)$$

In the presence of gravity, the previous lagrangian density is supplemented with extra terms, containing the usual Einstein-Hilbert term, possible extensions of GR and/or non-minimal couplings of the Higgs field to gravity. The simplest versions of this lagrangian in curved spacetime follows the principles of general covariance and locality, for both matter and gravitational sectors. To preserve the fundamental features of the original theory in flat space-time, one must also require the gauge invariance and other symmetries in flat space-time to hold for the curved space-time theory. The number of possible terms in the action is unbounded even in this case and some additional restrictions are needed. A natural requirement could be renormalizability and simplicity. Following this three principles (locality, covariance and restricted dimension), and the previously motivated requirement of not introducing new dynamical degrees of freedom, the lagrangian density  $\mathcal{L}$  involving the Higgs field and gravity is fixed to be of the form

$$\frac{\mathcal{L}}{\sqrt{-g}} = f(h)R - \frac{1}{2}(\partial h)^2 - U(h) - \Lambda, \quad (2.3)$$

where we have neglected all matter fields for the time being and allowed for a possible cosmological constant  $\Lambda$ . Here

$$U(h) = \frac{\lambda}{4}(h^2 - v^2)^2, \quad (2.4)$$

is the usual Higgs potential of the Standard Model in the unitary gauge,  $2H^\dagger H = h^2$ . The direct measurement of the intermediate gauge bosons masses,  $m_W^2 = 80.398 \pm 0.025$  GeV and  $m_Z^2 = 91.1876 \pm 0.0021$  GeV, sets the value of vacuum expectation value of the Higgs field at a value  $v \simeq 246$  GeV, that we will use throughout this thesis. The function  $f(h)$  includes only terms up to second order in the the Higgs field  $h$ . Including a direct coupling of the Higgs field to matter we are opening the door not just to a possible violation of the Strong Equivalence Principle (SEP), but also to a violation of the Weak Equivalence Principle (WEP). Notice however that the terrestrial and solar system experimental bound of the WEP [93] do not necessarily apply at high energies, so this kind of arguments do not apply here. Indeed, the WEP is guaranteed once the Higgs reaches its vacuum expectation value  $v$ , since, from there on, it will take the same value all over the space.

In the pure Induced Gravity scenario this function depends only on the Higgs field and therefore, no bare Planck mass is included in the action. In this case, the Higgs-Gravity

sector takes the form

$$\frac{\mathcal{L}}{\sqrt{-g}} = \frac{1}{2}\xi_h h^2 R - \frac{1}{2}(\partial h)^2 - U(h) - \Lambda, \quad (2.5)$$

where the non-minimal coupling  $\xi_h$  must have a very large value in order to reproduce the huge hierarchy between the electroweak and Planck scales,  $\xi_h \sim M_P^2/v^2 \sim 10^{32}$ . The lagrangian density (2.5) is, at least at the classical level and for  $\Lambda = 0$ , just a different representation of the first inflationary *proposal*<sup>2</sup>, the Starobinsky's model [97, 98, 99, 100],

$$\frac{\mathcal{L}_g}{\sqrt{-g}} = \frac{1}{2\kappa^2} \left( R - \frac{R^2}{6M^2} \right), \quad (2.6)$$

where inflation is entirely a property of the gravitational sector. Here  $\kappa = M_P^{-1}$ , with  $M_P \equiv \sqrt{8\pi G} = 2.436 \times 10^{18}$  GeV the reduced Planck mass. Both representations of the same theory are simply related by a Legendre transformation [101, 102]. The Higgs field  $\phi$  plays therefore the role of the scalaron in the Starobinsky model of inflation. This means that *all* the results obtained in Starobinsky inflation can be also applied to Induced Gravity. In particular, the IG scenario will present inflationary solutions. This is very interesting, because, apart from the motivated connection between the Higgs sector and gravity, we obtain an inflationary solution as a bonus, without imposing any *ad hoc* requirements to the potential or explicitly introducing a new field parametrizing the inflaton. This is not very common and makes the model extremely appealing. Notice, that the naturalness of inflation is directly related to the origin of the inflaton. Most of the Quantum Field Theory based inflationary models proposed so far require the introduction of new degrees of freedom

<sup>2</sup>The original motivation of the model was however not related to the modern concept of inflation. It was conceived to solve the singularity problem taking into account one loop corrections

$$\langle T_{\mu\nu} \rangle = k_1 H_{\mu\nu}^{(1)} + k_3 H_{\mu\nu}^{(3)} + H_{\mu\nu}^{(4)},$$

of conformally invariant fields (which are indeed a good approximation of realistic matter fields in the high-curvature limit) to the semiclassical Einstein equations of motion

$$G_{\mu\nu} \equiv R_{\mu\nu} - \frac{1}{2}g_{\mu\nu}R = \kappa^2 \langle T_{\mu\nu} \rangle.$$

Here

$$\begin{aligned} H_{\mu\nu}^{(1)} &= 2(\nabla_\mu \nabla_\nu - g_{\mu\nu} \nabla^2) R + 2R R_{\mu\nu} - \frac{1}{2}g_{\mu\nu} R^2, \\ H_{\mu\nu}^{(3)} &= R_\mu{}^\lambda R_{\lambda\nu} - \frac{2}{3}R R_{\mu\nu} - \frac{1}{2}g_{\mu\nu} R^{\rho\sigma} R_{\rho\sigma} + \frac{1}{4}g_{\mu\nu} R^2, \end{aligned}$$

are purely geometric terms expressed through invariants of the curvature tensor and  $H_{\mu\nu}^{(4)}$  is a traceless boundary term that cannot be written in terms of curvature tensors.  $H_{\mu\nu}^{(1)}$  is identically conserved and can be obtained by varying a local action

$$H_{\mu\nu}^{(1)} = -\frac{2}{\sqrt{-g}} \frac{\delta}{\delta g^{\mu\nu}} \int d^4x \sqrt{-g} R^2,$$

while the term  $H_{\mu\nu}^{(3)}$ , although conserved, cannot in general be obtained from a local lagrangian density. The constants  $k_1, k_3$  are fixed by the number of matter fields considered, and then just by microphysical conditions (see for instance Ref.[94, 95]). The local action for  $H_{\mu\nu}^{(1)}$  admits a certain class of non-singular, homogeneous and isotropic solutions of de Sitter type. As shown in Ref. [96], the existence of such solutions is a rather common phenomenon in effective theories of gravity involving arbitrary functions of the Riemann and Ricci tensors in 4 dimensions.

to drive inflation. The nature of the inflaton is completely unknown, and its role could be played by any candidate able to imitate a scalar condensate (typically in the slow-roll regime), such as a fundamental scalar field, a fermionic or vector condensate [103, 104], or even higher order terms of the curvature invariants, as in the Starobinsky's model (2.6). The number of particle physics motivated candidates is as big as the number of extensions of the Standard Model (Grand Unified Theories, Supersymmetry, Extra Dimensions, etc.), where it is not very difficult to find a field able to play the role of the inflaton [46]. Even minimal models as that recently proposed in Ref. [105] for solving the dark matter and baryon asymmetry problems with a matter content identical to that in the  $\nu$ MSM introduce new inflationary fields. The non-minimal coupling of the Higgs field to gravity in the IG scenario rescues the Higgs field from the known difficulties<sup>3</sup>, without introducing new highly speculative degrees of freedom.

Regarding preheating after inflation the previous scenario is also appealing. Given an inflationary model we must find a graceful exit to inflation as well as a mechanism to bring the Universe from a cold and empty post-inflationary state to the highly entropic and thermal Friedmann Universe, cf. Chapter 4. Unfortunately, the theory of reheating is far from being complete, since not only the details, but even the overall picture, depend crucially on the different microphysical models. From this point of view, it is very difficult to single out a given model of inflation, and even more difficult to understand the details of the reheating process via the experimental access to the couplings. Notice that the situation is completely different in the Induced Gravity scenario. All the couplings between the Higgs field and the SM particles are known and no new highly speculative degrees of freedom, apart from those already present in the usual Standard Model, are introduced.

Unfortunately, in spite of its many advantages, the Induced Gravity model cannot be accepted as a satisfactory inflationary scenario [107, 108, 109]. To see this, consider for instance the masses of the Z and W bosons (at tree level)

$$m_W = \frac{g_2 h}{2}, \quad m_Z = \frac{m_W}{\cos \theta_w}, \quad (2.7)$$

with  $\theta_w$  the weak mixing angle, defined as  $\theta_w = \tan^{-1}(g_1/g_2)$ , and  $g_1$  and  $g_2$  are the coupling constants corresponding to the  $U(1)_Y$  and  $SU(2)_L$  gauge groups respectively. The length scales are conventionally defined in such a way that elementary particle masses are the same for all times and in all places. This implies that, if under a conformal transformation<sup>4</sup>  $\tilde{g}_{\mu\nu} = \Omega^2 g_{\mu\nu}$ , the lagrangian of a free particle transforms as

$$\mathcal{L}_{1P} = \int m ds \longrightarrow \tilde{\mathcal{L}}_{1P} = \int \frac{m}{\Omega} \tilde{ds}, \quad (2.8)$$

the mass should be accordingly redefined as  $\tilde{m} \equiv \frac{m}{\Omega}$  to express it in the new system of units. Therefore, under a conformal transformation to the Einstein frame, the gauge boson masses

<sup>3</sup>Models of inflation in terms of a Higgs-like quartic self-interaction potential  $\lambda h^4$  need an extremely small coupling constant  $\lambda \sim 10^{-13}$  [44], incompatible with the lower bounds on the Higgs mass [22]. Besides, they are also nowadays excluded at around  $3\sigma$  by the present observational data (non observation of tensor modes) [106].

<sup>4</sup>For a review of conformal transformation and their properties cf. Appendix B.

(2.7) are redefined as

$$\tilde{m}_W = \frac{m_W}{\Omega} = \frac{g_2}{2\xi^{1/2}} M_P, \quad \tilde{m}_Z = \frac{\tilde{m}_W}{\cos \theta_W}, \quad (2.9)$$

where we have used  $\Omega^2 = \xi_h h^2 / M_P^2$ . As can be seen in the previous equations the gauge bosons acquire a constant mass in the Einstein frame and are therefore totally decoupled from the Higgs (inflaton) field, excluding the possibility of successful reheating.

Notice however that the lagrangian density (2.5) is not the most general one that can be written in a nontrivial background. As shown in [110, 111], the simultaneous existence of a reduced *bare* Planck mass  $M_P$  and a non-minimal coupling of a symmetry breaking field to the scalar curvature

$$\frac{\mathcal{L}}{\sqrt{-g}} = \frac{M_P^2 + \xi_h h^2}{2} R - \frac{1}{2} (\partial h)^2 - U(h) - \Lambda, \quad (2.10)$$

avoid the decoupling of the gauge bosons and can give rise to an inflationary expansion of the Universe together with a potentially successful reheating. In this case, the non-minimal coupling  $\xi_h$  must have a value large enough as to reproduce the interesting inflationary features of the Induced Gravity scenario, but sufficiently small as to allow for the decay of the Higgs field after that period,  $1 \ll \xi_h \ll 10^{32}$ . We will come back to this model in Section 3.2.

### 2.3 The No-Scale scenario

The non-minimally coupled Standard Model (2.10) accounts, as the usual Standard Model, for the masses of all the elementary particles induced by the *vev* of the Higgs field. It also provides a nice connection with the Mach's principle and therefore, with the concept of inertia. However, the model contains, at the classical and quantum level, dimensional parameters or scales, such as the Newton's constant  $G$ , the *vev* of the Higgs field or  $\Lambda_{\text{QCD}}$ . These scales are *a priori* completely unrelated to the Higgs mechanism, and questions such as the origin of the Planck, the Higgs or the proton mass remain unexplained. Would it be feasible that all the scales were generated dynamically from one and the same source? To explore this possibility, let these scales be dynamical and consider a theory invariant under global scale transformations,

$$g_{\mu\nu}(x) \mapsto g_{\mu\nu}(\omega x), \quad \Psi(x) \mapsto \omega^d \Psi(\omega x), \quad (2.11)$$

where  $\Psi(x)$  stands for the different particle physics fields,  $d$  is their associated scaling dimension and  $\omega$  is an arbitrary real parameter. In order to induce all the scales and masses in the theory, this symmetry is required to be spontaneously broken by a symmetry breaking classical ground state<sup>5</sup>. The choice of scale invariance among all other possible symmetries is very tempting from the quantum point of view. If the classical theory including gravity remains scale invariant at the quantum level to all orders in perturbation theory, several fine-tuning problems of the Standard Model, such as the quadratic corrections to the Higgs

<sup>5</sup>Scale symmetry might be also broken by the pure presence of a time-dependent cosmological background [112, 113].



mass [114, 115] or the cosmological constant problem would be automatically solved. In what follows we will assume that quantization procedure does not spoil the essential features of the classical theory. We will come back to this point in Section 3.6.

As before, the most natural choice, without introducing new degrees of freedom, would be to let the Higgs field be responsible for all the physical scales. The corresponding lagrangian density is quite similar to the Induced Gravity lagrangian (2.5), but does not include the dimensional constants  $v$  and  $\Lambda$ , now forbidden by scale-invariance,

$$\frac{\mathcal{L}_{SI}}{\sqrt{-g}} = \frac{1}{2}\xi_h h^2 R - \frac{1}{2}(\partial h)^2 - \frac{\lambda}{4}h^4. \quad (2.12)$$

Notice that those terms would be neither generated dynamically if the quantization procedure respects the exact scale invariance of the theory [116, 117]. As required, the lagrangian density (2.12) possesses a continuous family of classical ground states satisfying  $h^2 = h_0^2$  and  $R = 4\lambda h_0^2/\xi_h$ , where  $h_0$  is an arbitrary constant. A non-zero background value of  $h_0$  is enough to generate the Planck scale together with the masses all the Standard Model particles. However, as occurred in the Induced Gravity model, these particles are completely decoupled from the Higgs field, which makes the model phenomenologically non viable from an inflationary point of view. Besides, it is excluded by EW constraints [22], since the Higgs field itself becomes massless, as corresponds to the Goldstone boson associated to the spontaneous breakdown of scale invariance. This can be easily proved by noting the shift symmetry displayed by the lagrangian density (2.12) when it is transformed to the Einstein-frame

$$\frac{\tilde{\mathcal{L}}_{SI}}{\sqrt{-\tilde{g}}} = \frac{M_P^2}{2}\tilde{R} - \frac{1}{2}\tilde{g}^{\mu\nu}\partial_\mu\phi\partial_\nu\phi - \frac{\lambda M_P^4}{4\xi_h^2}, \quad (2.13)$$

where  $\phi = \phi(h)$  is a new field defined to make the kinetic term canonical.

The next simplest possibility is to add a new singlet scalar field to the theory [75]. We will refer to it as the dilaton  $\chi$ . Similar extensions to the Minimal Non-Minimally Coupled Standard Model (2.10) have been suggested in Ref.[118, 119], although with a very different physical motivation and without the requirement of an exact scale-invariance at the level of the action. In our case, the scale-invariant extension of the minimal non-minimally coupled Standard Model reads

$$\frac{\mathcal{L}_{SI}}{\sqrt{-g}} = \frac{1}{2}(\xi_\chi\chi^2 + \xi_h h^2)R - \frac{1}{2}(\partial h)^2 - \frac{1}{2}(\partial\chi)^2 - U(h, \chi), \quad (2.14)$$

where the scalar potential is given by

$$U(h, \chi) = \frac{\lambda}{4}\left(h^2 - \frac{\vartheta}{\lambda}\chi^2\right)^2 + \beta\chi^4. \quad (2.15)$$

We will only consider positive values for  $\xi_\chi$  and  $\xi_h$ , for which the coefficient in front of the scalar curvature is positive, whatever values the scalar fields take, e.g. conformally invariant scalar fields in 4 dimensions have  $\xi = 1/6$ . The chosen parametrization of the scalar potential assumes that  $\lambda \neq 0$ . This only excludes the phenomenologically unacceptable case where a quartic term  $\lambda h^4$  is absent. As before, we will require the theory to possess a symmetry breaking classical ground state. To have a theory with electroweak symmetry breaking we

imposed  $h = h_0 \neq 0$ . The condition  $\chi_0 \neq 0$  is also needed in order to avoid the case of a massless Higgs described above. The classical ground states for  $\beta \neq 0$  are given by

$$h_0^2 = \frac{\vartheta}{\lambda} \chi_0^2 + \frac{\xi_h}{\lambda} R, \quad (2.16)$$

with  $R = \frac{4\beta\lambda\chi_0^2}{\lambda\xi_\chi + \vartheta\xi_h}$ . Notice that if gravitational interactions are neglected the previous set of ground states corresponds to the minimum of the potential. The solutions with  $\chi_0 \neq 0$  spontaneously break scale invariance. All mass scales are therefore induced and proportional to  $\chi_0$ . It is important to notice however, that physical observables will be independent of the particular value of  $\chi_0$ , since they correspond to ratios between scales or masses. The model does not however address the origin of the differences among these scales. For instance, the hierarchy between the electroweak and gravitational interaction  $v^2/M_P^2 \sim 10^{-32}$  is translated into the value of the  $\vartheta$  parameter, while the ratio between the cosmological constant and the electroweak scale  $\Lambda/v^4 \sim 10^{-56}$  determines the value of  $\beta$ . In terms of the couplings these ratios are given by  $v^2/M_P^2 \sim \frac{\vartheta}{\xi_\chi}$  and  $\Lambda/v^4 \sim \frac{\beta}{\xi_\chi^2}$ . To reproduce the hierarchy the parameters must satisfy  $\vartheta \ll \beta \ll \xi_\chi$ .

Depending on the value of  $\beta$ , the background corresponds to flat spacetime ( $\beta = 0$ ), de Sitter ( $\beta > 0$ ) or Anti-de Sitter ( $\beta < 0$ ) spacetime of constant curvature  $R$ . From the cosmological point of view, the Anti-de Sitter case is clearly disfavoured, since it can not explain the present accelerated expansion of the Universe. One should be tempted to think that, as happens in GR, the only plausible choice would be the de Sitter  $\beta > 0$  case. Nevertheless, if slight modifications of the fundamental theory of gravity are allowed, even the case  $\beta = 0$  can be phenomenologically satisfactory. Indeed, as we will see in Chapter 5, scalar-tensor theories formulated in the framework of Unimodular Gravity are able to produce a dynamical dark energy component, even if  $\beta = 0$ . In this new setup, the choice  $\beta = 0$  seems favoured from a pragmatismal point of view, since only in that case the dark energy component becomes purely dynamical. This choice would increase the predictive power of the model, providing important relations between the observables in the Early and Late Universe that we will describe in detail in Chapter 5. Besides, the  $\beta = 0$  case allows to successfully break scale invariance, even in the absence of gravity, allowing for a flat spacetime with  $(h_0, \chi_0) \neq (0, 0)$ . On the other hand, the  $\beta = 0$  choice does not present any of the instability problems for massless degrees of freedom usually associated to the de Sitter and Anti-de Sitter backgrounds [98, 120, 121, 122, 123, 124].

## 2.4 A very useful Noether's Current

To finish this chapter let us notice an important point that will be extremely useful in the following developments. By construction, all terms in the action associated to the lagrangian (2.14) are invariant under continuous scale transformations and therefore, according to Noether's Theorem [125], there must exist an almost conserved Noether's current associated to this symmetry. Note that under infinitesimal scale transformations the metric and scalar fields transform respectively as

$$g_{\mu\nu} \rightarrow g_{\mu\nu} + \omega \Delta g_{\mu\nu}, \quad \varphi^a \rightarrow \varphi^a + \omega \Delta \varphi^a, \quad (2.17)$$

where again, we have introduced an infinitesimal real parameter  $\omega$ . Here, latin indices  $a, b, \dots = 1, 2$  are used to label, in a compact notation, the two real scalar fields present in the model: the dilaton field,  $\varphi^1 = \chi$ , and the Higgs field in the unitary gauge,  $\varphi^2 = h$ . The Noether's current associated to (2.17) is given by

$$\sqrt{-g}J^\mu = \frac{\partial \mathcal{L}}{\partial [\partial_\mu g_{\alpha\beta}]} \Delta g_{\alpha\beta} + \frac{\partial \mathcal{L}}{\partial [\partial_\mu \varphi^a]} \Delta \varphi^a. \quad (2.18)$$

The explicit expressions for  $\Delta g_{\mu\nu}$  and  $\Delta \varphi^a$  depend on the field variables chosen. In terms of the Higgs and dilaton fields,  $h$  and  $\chi$ , we have  $\Delta g_{\mu\nu} = -2g_{\mu\nu}$ ,  $\Delta \chi = \chi$  and  $\Delta h = h$ . Note that in order to apply the Noether's theorem (2.18) to the gravitational part of the Lagrangian (2.14), it must contain only terms up to first order derivatives. Let us therefore write the Ricci scalar as the sum of two contributions  $R = R_1 + R_2$ , given respectively by

$$R_1 = g^{\mu\nu} \left( \partial_\lambda \Gamma_{\mu\nu}^\lambda - \partial_\nu \Gamma_{\mu}^\lambda \right), \quad R_2 = \Gamma_\lambda C^\lambda + \frac{1}{2} \Gamma_{\rho\sigma}^\lambda \partial_\lambda g^{\rho\sigma}, \quad (2.19)$$

with

$$\Gamma_\mu \equiv \Gamma_{\rho\mu}^\rho = \frac{\partial_\mu \sqrt{-g}}{\sqrt{-g}} = \frac{1}{2} g^{\rho\sigma} \partial_\mu g_{\rho\sigma}, \quad C^\lambda \equiv g^{\mu\nu} \Gamma_{\mu\nu}^\lambda = -\partial_\sigma g^{\lambda\sigma} - g^{\lambda\nu} \Gamma_\nu, \quad (2.20)$$

The quantities  $R_1$  and  $R_2$  are indeed related by

$$\sqrt{-g}R_1 = \partial_\lambda \left( \sqrt{-g}G^\lambda \right) - 2\sqrt{-g}R_2. \quad (2.21)$$

where we have defined  $G^\lambda \equiv C^\lambda - g^{\lambda\mu} \Gamma_\mu$ . Inserting this quantity into the action (2.14) and integrating by parts we obtain an expression for the Ricci scalar containing only first derivatives of the metric tensor

$$f(\varphi)R = -G^\lambda \partial_\lambda f - fR_2, \quad (2.22)$$

with  $2f(\varphi) \equiv (\xi_h h^2 + \xi_\chi \chi^2)$ . Taking into account (2.22) and performing the variation of the lagrangian with respect to the metric and scalar fields, the conservation law for the current (2.18) can be rewritten as

$$D_\mu J^\mu = 0, \quad (2.23)$$

where

$$J^\mu = g^{\mu\nu} \sum_a (1 + 6\xi_a) \partial_\nu \varphi_a^2. \quad (2.24)$$

Notice that the previous expression is not independent of the equations of motion. Indeed, it can be also obtained directly from the Friedmann equations

$$3H^2 f(\varphi) = \frac{1}{2} \dot{\varphi}^a \dot{\varphi}_a + \frac{1}{2a^2} \partial_i \varphi^a \partial_i \varphi_a + U(\varphi) + (\partial^i \partial_i - 3H\partial_0) f(\varphi), \quad (2.25)$$

$$f(\varphi)R = 3\Box f(\varphi) + (\partial\varphi^a)^2 + 4U(\varphi). \quad (2.26)$$

and the equations of motion for the scalar fields

$$\ddot{\varphi}_a + 3H\dot{\varphi}_a + U_{,a} - \frac{1}{2} f_{,a} R = 0. \quad (2.27)$$

Combining Eqs. (2.27) and (2.26) we obtain

$$\sum_a (1 + 6\xi_a) \square \varphi_a^2 = 2 \left( \sum_a \varphi_a U_{,a} - 4U(\varphi) \right), \quad (2.28)$$

which, for the scale invariant potential (2.15), reduces to (2.23). As we will see in Chapter 3, this conservation law will have important consequences for the study of the inflationary trajectories, since it effectively reduces by one the number of independent dynamical variables.

## CHAPTER 3

# The Higgs boson in the Sky

*Entia non sunt multiplicanda  
praeter necessitatem.*

WILLIAM OF OCKHAM

### 3.1 The Higgs field as the inflaton

Inflation is nowadays a well established paradigm, consistent with all the observations. It solves most of the puzzles of the hot Big Bang Model in a very simple and elegant way. The inflationary paradigm is able to explain not only the homogeneity and isotropy of the present universe on large scales, but also the causal generation of an almost scale invariant spectrum of primordial perturbations [126] that give rise to the observed large scale structure. This perturbations arise from the amplification of vacuum fluctuations, which become a highly two-mode squeezed state during inflation [127]. Therefore, inflation can be considered as a link between the large scale structure of the universe and its microphysics. As pointed out in the previous chapter, the Higgs field strongly non-minimally coupled to gravity is able to give rise to an inflationary stage. This chapter is devoted to the detailed study of that epoch in the minimal non-minimally coupled extension of the Standard Model and its scale-invariant version, and to the determination of the free parameters of the theory from Cosmic Microwave Background physics.

Although the model was originally formulated in the so-called Jordan frame, in which the non-minimal coupling to gravity is explicit, we will perform the analysis in another conformally-related representation of the theory. Choosing a representation is equivalent to choosing the physical variables used to describe the problem. The frame dependence of the spacetime curvature is accompanied by a change in the matter lagrangian, and therefore in the definition of ideal clocks used to measure the curvature. The change from one frame to another does not correspond to a change in the physics and different representations are

completely equivalent at the classical level. Useful discussion of this equivalence can be found in [128]. The inevitable arbitrariness in choosing the physical variables will of course affect the clarity of the predictions in the representation. Purely gravity phenomena in a given frame could be interpreted as matter effects in another, and *vice versa*. We choose to perform the study in the so-called Einstein frame. This frame is defined as that in which the gravity sector takes the usual Einstein-Hilbert form. This will simplify considerably the computation of the measurable quantities and their comparison with those in the literature.

This chapter is organized as follows. In Section 3.2 we transform the Higgs Inflation model to the Einstein frame and derive an approximate inflationary potential, from which we determine the corresponding slow-roll parameters and attractor solutions. Similarly, the scale-invariant Higgs-Dilaton extension, is studied in detail in Section 3.3. The inflationary trajectories are classified making use of the conserved current associated to the scale-invariance of the model. A general treatment of the cosmological perturbations produced during inflation and the inflationary observables is presented in Section 3.4. The derivation of their specific form in Higgs-driven inflationary models is left for Section 3.5, where we derive observational constraints on the value of the non-minimal couplings for both Higgs and Higgs-Dilaton models. Finally, in Section 3.6, we comment on the different quantum aspects that might modify the previous classical treatment.

## 3.2 Higgs Inflation

We start by considering the lagrangian density (2.10) for the non-minimally coupled Higgs introduced at the end of Section 2.2

$$\frac{\mathcal{L}}{\sqrt{-g}} = f(h)R - \frac{1}{2}(\partial h)^2 - U(h), \quad (3.1)$$

where the function  $f(h)$  is defined as

$$f(h) = \frac{M_P^2 + \xi_h h^2}{2}, \quad (3.2)$$

and  $U(h)$  is the standard Higgs potential (2.4) in the unitary gauge  $2H^\dagger H = h^2$ ,

$$U(h) = \frac{\lambda}{4}(h^2 - v^2)^2. \quad (3.3)$$

A possible cosmological constant term has been omitted, since its effects during the inflationary period under consideration are completely negligible. Motivated by the Induced Gravity scenario (cf. the end of Section 2.2), we will assume the non-minimal coupling of the Higgs field to gravity to be in the region  $1 \ll \xi_h \ll 10^{32}$ . This range avoids the decoupling of the Standard Model particles from the Higgs field and allows for an inflationary stage.

As mentioned in the previous section, we will work in the Einstein frame. In order to get rid of this non-minimal coupling to gravity, we perform a conformal transformation [129]

$$\tilde{g}_{\mu\nu} = \Omega^2(h)g_{\mu\nu}, \quad (3.4)$$

which, contrary to standard coordinate transformations, alters the curvature of spacetime by mixing the gravitational and matter degrees of freedom. This conformal transformation allows us to obtain the lagrangian density in the Einstein frame<sup>1</sup>,

$$\frac{\tilde{\mathcal{L}}}{\sqrt{-\tilde{g}}} = \frac{f(h)}{\Omega^2} \left( \tilde{R} + 3\tilde{g}^{\mu\nu} \tilde{\nabla}_\mu \tilde{\nabla}_\nu \ln \Omega^2 - \frac{3}{2} \tilde{g}^{\mu\nu} \tilde{\nabla}_\mu \ln \Omega^2 \tilde{\nabla}_\nu \ln \Omega^2 \right) - \frac{\tilde{g}^{\mu\nu} \partial_\mu h \partial_\nu h}{2\Omega^2} - \frac{U(h)}{\Omega^4}, \quad (3.5)$$

where we can recover the standard Einstein-Hilbert term by simply identifying the prefactor of the Ricci scalar with the Planck mass, i.e.

$$\frac{f(h)}{\Omega^2} \equiv \frac{M_P^2}{2}. \quad (3.6)$$

This step implies the following relation between the conformal transformation and the Higgs field

$$\Omega^2(h) = 1 + \frac{\xi_h h^2}{M_P^2}, \quad (3.7)$$

which allows us to write the Einstein-frame lagrangian density (3.5) completely in terms of  $h$

$$\frac{\tilde{\mathcal{L}}}{\sqrt{-\tilde{g}}} = \frac{M_P^2}{2} \tilde{R} - \frac{1}{2} \left( \frac{\Omega^2 + 6\xi_h^2 h^2/M_P^2}{\Omega^4} \right) \tilde{g}^{\mu\nu} \partial_\mu h \partial_\nu h - \frac{U(h)}{\Omega^4}. \quad (3.8)$$

Here we have neglected a boundary term that does not contribute to the equations of motion. As we will be working in the Einstein frame, from now on, we will skip over the tilde in all the variables to simplify the notation.

Notice that the conformal transformation (3.4) leads to a non-minimal kinetic term for the Higgs field. However, it is possible to get a canonically normalized kinetic term by introducing a new field  $\phi$  via the field redefinition

$$\frac{d\phi}{dh} \equiv \sqrt{\frac{\Omega^2 + 6\xi_h^2 h^2/M_P^2}{\Omega^4}} = \sqrt{\frac{1 + \xi_h(1 + 6\xi_h)h^2/M_P^2}{(1 + \xi_h h^2/M_P^2)^2}}. \quad (3.9)$$

In terms of it the lagrangian density (3.8) becomes

$$\frac{\tilde{\mathcal{L}}}{\sqrt{-\tilde{g}}} = \frac{M_P^2}{2} R - \frac{1}{2} g^{\mu\nu} \partial_\mu \phi \partial_\nu \phi - V(\phi), \quad (3.10)$$

with

$$V(\phi) \equiv \frac{U(\phi)}{\Omega^4(\phi)}, \quad (3.11)$$

the Higgs potential in the Einstein frame. To find the explicit form of this potential in term of  $\phi$ , we must find the expression of  $h$  in terms of  $\phi$ . This can be done by integrating (3.9), whose general solution is given by

$$\frac{\sqrt{\xi_h}}{M_P} \phi(h) = \sqrt{1 + 6\xi_h} \sinh^{-1} \left( \sqrt{1 + 6\xi_h} u \right) - \sqrt{6\xi_h} \sinh^{-1} \left( \sqrt{6\xi_h} \frac{u}{\sqrt{1 + u^2}} \right), \quad (3.12)$$

<sup>1</sup>The detailed relations between the Ricci scalar in two different frames can be found in Appendix B.

with  $u \equiv \sqrt{\xi_h} h / M_P$ . Since  $\xi_h \gg 1$ , we can take  $1 + 6\xi_h \approx 6\xi_h$  and, using the identity  $\sinh^{-1} x = \ln(x + \sqrt{x^2 + 1})$  for  $-\infty < x < \infty$ , we can approximate (3.12) by

$$\frac{\sqrt{\xi_h}}{M_P} \phi(h) \approx \sqrt{6\xi_h} \ln(1 + u^2)^{1/2}, \quad (3.13)$$

or, equivalently,

$$\Omega^2 = e^{\alpha\kappa\phi}, \quad (3.14)$$

where  $\alpha = \sqrt{2/3}$  and  $\kappa = M_P^{-1}$ . The  $\phi$  field is therefore directly related in this approximation (just in the limit  $\xi_h \gg 1$  and far from  $u = 0$ ) to the conformal transformation  $\Omega^2$  in a very simple way. The inflationary potential (3.11) is just given by

$$V(\phi) = \Omega^{-4} U(h) = V_0 \left[ e^{\alpha\kappa\phi} - \left( 1 + \xi_h \frac{v^2}{M_P^2} \right) \right]^2 e^{-2\alpha\kappa\phi}. \quad (3.15)$$

where we have defined an amplitude  $V_0 \equiv \frac{\lambda M_P^4}{4\xi_h^2}$ . Given the large hierarchy between the electroweak and Planck scales,  $v \ll M_P$ , the term in parenthesis in the previous expression becomes<sup>2</sup>  $1 + \xi_h \frac{v^2}{M_P^2} \approx 1$ , which implies that we can safely ignore the *vev* of the Higgs field for the evolution during inflation and (p)reheating, and simply consider the potential

$$V(\phi) = V_0 \left( 1 - e^{-\alpha\kappa\phi} \right)^2. \quad (3.16)$$

Notice however that (3.16) only parametrizes partially the original potential (3.3), as can be seen in Fig. 3.1, where we compare the exact solution (red continuous line) obtained parametrically from (3.12), with the analytic formula (3.16) (blue dashed line). Although both solutions agree very well in the region of positive  $\phi$ , they substantially differ for negative values of the Higgs field,  $\phi < 0$ . The conformal transformation is even ill-defined in the negative field region. From (3.7) and (3.14) we have

$$\frac{\xi_h h^2}{M_P^2} = \Omega^2 - 1 = e^{\alpha\kappa\phi} - 1 = (1 - e^{-\alpha\kappa\phi}) e^{\alpha\kappa\phi}, \quad (3.17)$$

which is inconsistent, since the left-hand side of this equation is positive definite, while the right hand is negative definite for  $\phi < 0$ . Taking this into account will turn out to be important for the study of the different (p)reheating mechanisms of the post-inflationary regime, where the field oscillate around the minimum of the potential. In what follows, we will then use the parametrization

$$V(\phi) = V_0 \left( 1 - e^{-\alpha\kappa|\phi|} \right)^2, \quad (3.18)$$

which correctly describes the potential obtained from (3.12), for the whole field range of interest. In Fig. 3.1, this parametrization (green dotted line) is again compared to the exact solution (red continuous line) obtained from (3.12).

<sup>2</sup>Note that the non-minimal coupling is chosen to be in the region  $1 \ll \xi_h \ll M_P^2/v^2$ .



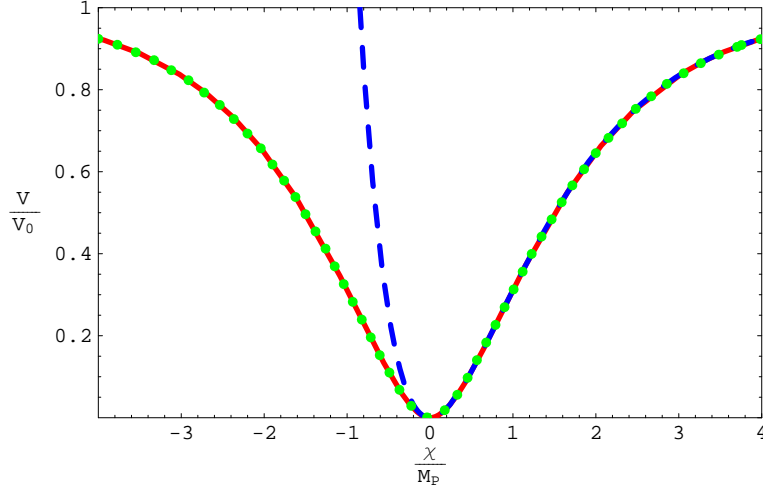


Figure 3.1: Comparative plot of the exact solution (red continuous line) obtained parametrically from (3.12), the analytic formula (3.16) for the potential (blue dashed line), and their parametrization (3.18) (green dotted line). Although the three different expression nicely agrees for positive values of the Higgs field, it can be clearly seen that the analytic formula (3.16) substantially differs from the parametric exact solution.

### 3.2.1 Slow-roll inflation and attractor solutions

In the new representation (3.10) the Klein-Gordon equation for the Higgs takes the form

$$\ddot{\phi} + 3H\dot{\phi} - \frac{\nabla^2 \phi}{a^2} + V'(\phi) = 0, \text{ size} \quad (3.19)$$

where prime denotes derivative with respect to the field. We have implicitly assumed a flat Friedmann-Robertson-Walker (FRW) metric

$$ds^2 = -dt^2 + a^2(t)d\mathbf{x}^2, \quad (3.20)$$

and defined the Hubble rate  $H \equiv \frac{\dot{a}}{a}$ . Dots denotes derivatives *wrt* the previous coordinate time. Equation (3.19) should be understood as a semiclassical evolution equation for the Higgs field, where the quantum fluctuations (of typical size  $H/2\pi$ ) are considered as small perturbations above the classical background. Regarding the evolution of the scale factor, in the context of a perfect fluid description on General Relativity, we have

$$H^2 = \frac{\rho_\phi}{3M_P^2}, \quad \frac{\ddot{a}}{a} = -\frac{\rho_\phi + 3p_\phi}{6M_P^2}. \quad (3.21)$$

where the energy and pressure densities associated to the Higgs condensate are simply given by

$$\rho_\phi = \frac{1}{2}\dot{\phi}^2 + V(\phi) + \frac{(\nabla\phi)^2}{2a^2}, \quad p_\phi = \frac{1}{2}\dot{\phi}^2 - V(\phi) - \frac{(\nabla\phi)^2}{6a^2}. \quad (3.22)$$

Note that, although we have included the spatial gradient terms for completion, they rapidly decrease with the expansion of the universe for wavelengths  $\gtrsim H^{-1}$ , and quickly become negligible.

In order to explain the present homogeneity and flatness of the observable universe on large scales the only ingredient needed is an early period of accelerated expansion, previous to the radiation and matter dominated eras. Such a stage is known as inflation [46]. Obtaining the benefits of such an accelerated expansion,  $\ddot{a} > 0$ , requires an unusual negative pressure density

$$p_\phi < -\frac{1}{3}\rho_\phi, \quad (3.23)$$

as can be seen from the second Friedmann equation in (3.21). Taking into account (3.22), we realize that this condition can be easily satisfied in the Higgs Inflation model. Notice that the potential (3.18) is exponentially flat for large field values<sup>3</sup>. If the initial value of the Higgs condensate is sufficiently large<sup>4</sup>, then, according to the first Friedmann equation in (3.21), the Hubble parameter would be also large. This translates into an important friction term ( $3H\dot{\phi} \gg \ddot{\phi}$ ) in the Klein-Gordon equation for the Higgs field, cf. (3.19), that slows down its motion in the potential ( $\dot{\phi}^2 \ll V(\phi)$ ), so that (3.21) and (3.19) become respectively

$$H \simeq \frac{1}{\sqrt{3}M_P} V(\phi)^{1/2}, \quad \dot{\phi} \simeq -\frac{M_P}{\sqrt{3}} \frac{V'(\phi)}{V^{1/2}(\phi)}. \quad (3.24)$$

As can be seen from (3.22) the slow rolling ( $\dot{\phi}^2 \ll V(\phi)$ ) gives rise to an effective equation of state of vacuum-energy type for the inflaton,  $p_\phi \simeq -\rho_\phi$ , which automatically satisfies the inflationary condition (3.23).

The previous considerations are usually encoded in the smallness of the so-called *potential slow roll parameters* (PSR) [130]

$$\epsilon = \frac{M_P^2}{2} \left( \frac{V'(\phi)}{V(\phi)} \right)^2 \ll 1, \quad \eta = M_P^2 \frac{V''(\phi)}{V(\phi)} \ll 1, \quad (3.25)$$

characterizing the flatness and curvature of the potential. Taking into account the explicit form of the Einstein frame potential (3.18), they become

$$\epsilon = \frac{2\alpha^2}{(e^{\alpha\kappa\phi} - 1)^2}, \quad \eta = \frac{2\alpha^2(2 - e^{\alpha\kappa\phi})}{(e^{\alpha\kappa\phi} - 1)^2}, \quad (3.26)$$

which, as expected, agree with those for the scalaron potential in the Starobinsky model of inflation [97, 98, 99, 100]. Inflation comes to an end when the  $\epsilon$  parameter reaches unity,  $\epsilon \simeq 1$ , due to the rolling of the Higgs down to the minimum of the potential. Using the exact expression (3.26) this corresponds to a field value

$$\phi_{\text{end}} = \frac{1}{\alpha\kappa} \ln \left( 1 + \frac{2}{\sqrt{3}} \right). \quad (3.27)$$

Note that the slow roll parameter  $\eta$  is then negative,  $\eta_{\text{end}} = 1 - \frac{2}{\sqrt{3}} < 0$ , so there is a small region of negative curvature in the potential just after the end of inflation. The effective

<sup>3</sup>We implicitly assume that quantum corrections do not spoil the classical flatness of the potential. We will come back to this point at the end of this chapter, cf. Section 3.6.

<sup>4</sup>It must be larger than the Planck scale, but its value is otherwise arbitrary.

curvature of the potential will be negative until  $\phi_* = \frac{1}{\alpha\kappa} \ln 2$ , which corresponds to the inflection point, given by  $\eta_* = 0$ . As we will point out in Section 4.5, this region might have dramatic effects on particle production after inflation.

We end this section by noticing that the slow-roll conditions (3.26) only restrict the shape of the potential. They are necessary but not sufficient conditions for inflation. Recall that the evolution equations for the Higgs must be supplemented with a specification of the initial conditions [130]. In particular the value of  $\dot{\phi}$  in (3.24) could be chosen in such a way that (3.26) becomes violated. Contrary to what happens in other fields of physics, we don't have the opportunity of repeating *the experiment of creation*. The inflationary paradigm will be predictive only if our observed universe can be explained from simple ideas and the most generic initial conditions. Fortunately, in the case of Higgs Inflation (as in any other scalar single field inflationary scenario) there exist a slow-roll attractor solution [131, 130]. This can be easily seen in the Hamilton-Jacobi formulation [131], in which the Higgs field  $\phi$  itself is taken as the evolution *clock*. In this formalism the Friedmann equation (3.21) takes the form

$$[H'(\phi)]^2 - \frac{3}{2M_P^2} H^2(\phi) = -\frac{1}{2M_P^4} V(\phi). \quad (3.28)$$

A linear homogeneous perturbation<sup>5</sup>  $\delta H(\phi)$  above a general solution of (3.28),

$$H(\phi) = H_0(\phi) + \delta H(\phi) \quad (3.29)$$

satisfies

$$\frac{d \log \delta H}{d\phi} \simeq \frac{3}{2M_P^2} \frac{H_0}{H'_0} = -\frac{1}{2M_P^4}. \quad (3.30)$$

The general solution of the previous differential equation can be expressed in terms of the number of e-folds

$$\Delta N \equiv \int_{t_i}^t H dt = -\frac{1}{2M_P^2} \int_{\phi_i}^{\phi} d\phi \quad (3.31)$$

to obtain

$$\delta H(\phi) = \delta H(\phi_i) e^{-3\Delta N}. \quad (3.32)$$

with  $\phi_i$  the initial value of the Higgs field. The attractor behaviour (3.32) clearly shows that any inflationary solution, independently of the initial conditions, will end up in a single trajectory in field space, becoming therefore all trajectories equivalent up to unmeasurable global time shifts.

### 3.3 Higgs-Dilaton Inflation

In this section we extend the results of the Higgs Inflation model described above to its scale invariant version (2.14). For doing it, let us rewrite that lagrangian density in the compact notation

$$\frac{\mathcal{L}}{\sqrt{-g}} = f(\varphi)R - \frac{1}{2}g^{\mu\nu}\delta_{ab}\partial_\mu\varphi^a\partial_\nu\varphi^b - U(\varphi), \quad (3.33)$$

<sup>5</sup>Linear perturbations are chosen for simplicity. The final conclusion remains unchanged if non-linear perturbations are taken into account.

with the non-minimal coupling  $f(\varphi)$  now given by

$$f(\varphi) \equiv \frac{1}{2} \sum_a \xi_a \varphi^{a^2}. \quad (3.34)$$

Greek indices  $\mu, \nu, \dots = 0, 1, 2, 3$  denote spacetime coordinates, while latin indices  $a, b, \dots = 1, 2$  are used to label the two real scalar fields present in the model: the dilaton field,  $\varphi^1 = \chi$ , and the Higgs field in the unitary gauge,  $\varphi^2 = h$ . The abstract notation in terms of  $\varphi^i$  will allow us to interpret the scalar fields as the coordinates of a two-dimensional  $\sigma$ -model manifold. We will be able to write expressions and equations that are covariant under changes of variables  $\varphi \mapsto \varphi'(\varphi)$ .

As before, whenever the non-minimal coupling is non-zero,  $f(\varphi) \neq 0$ , one can define a new conformal metric

$$\tilde{g}_{\mu\nu} = \Omega^2(\varphi) g_{\mu\nu}, \quad (3.35)$$

and identify, as in the Higgs Inflation case, the prefactor of the Ricci scalar in the Einstein frame with the Planck mass  $M_P$  to obtain

$$\frac{\tilde{\mathcal{L}}}{\sqrt{-\tilde{g}}} = \frac{M_P^2}{2} \tilde{R} - \frac{1}{2} \gamma_{ab} \tilde{g}^{\mu\nu} \partial_\mu \varphi^a \partial_\nu \varphi^b - V(\varphi), \quad (3.36)$$

where  $\gamma_{ab}$  is the non-diagonal and non-canonical field space metric given by

$$\gamma_{ab} = \frac{1}{\Omega^2} \left( \delta_{ab} + \frac{3}{2} M_P^2 \frac{\Omega_{,a}^2 \Omega_{,b}^2}{\Omega^2} \right). \quad (3.37)$$

The Einstein frame potential is defined as  $V(\varphi) \equiv \frac{U(\varphi)}{\Omega^4}$  and given explicitly by

$$V(h, \chi) = \frac{\lambda}{4} \frac{(h^2 - \frac{\vartheta}{\lambda} \chi^2)^2 + \beta \chi^4}{(\xi_\chi \chi^2 + \xi_h h^2)^2} M_P^4. \quad (3.38)$$

We will assume all the parameters in the previous expression to be positive, i.e.  $\vartheta, \lambda, \xi_\chi, \xi_h > 0$ . Note that the Einstein frame potential becomes singular for  $\chi = h = 0$ , where the conformal transformation (3.35) is ill-defined and the change to the Einstein frame is forbidden. Let us qualitatively discuss the shape of the potential for the different values of the parameters and its consequences, cf. Fig. 3.2. For sufficiently large values of the fields, the potential (3.38) is sufficiently flat as to allow for a slow-roll inflationary phase. On the other hand, as happened in the Jordan frame, the previous potential displays two degenerate classical ground states, reminiscent of those at  $\pm v$  in the no-scale invariant Higgs potential (3.3). Those valleys,  $h^2 \simeq \frac{\vartheta}{\lambda} \chi^2$  are located at very small angles  $\theta \approx \pm \arctan(\vartheta)$  with respect to the  $\chi$ -axis. The value of the potential along them depends on the value of the  $\beta$  parameter. In the absence of a quartic dilaton term in the Jordan frame,  $\beta = 0$ , the potential vanishes at its minimum, while a non-zero  $\beta$  gives rise to a classical ground state with dS or AdS background. As we pointed in Section 2.3, given its implications for further developments, only the  $\beta = 0$  case will be considered here. After the inflationary and reheating period the scalar fields will eventually come to rest in the valley due to effective dissipation produced

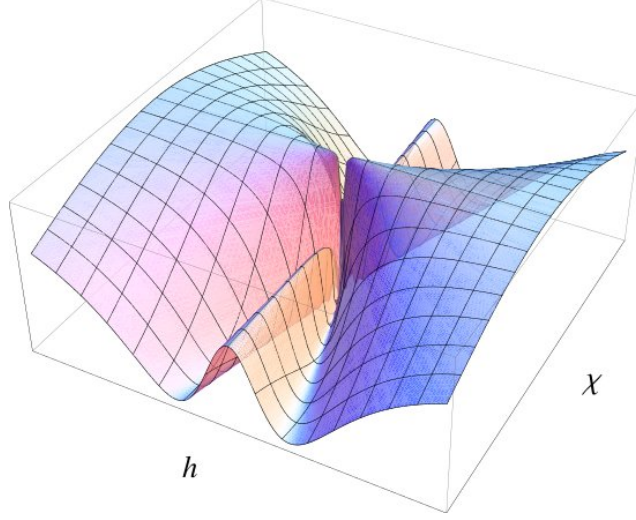


Figure 3.2: Shape of the Higgs-Dilaton potential in the Einstein frame (3.38) for the  $\beta = 0$  case (not to scale). The potential displays asymptotic flat regions that can give to inflation. It also possesses two completely degenerate classical ground states that spontaneously break the scale invariance of the corresponding action.

by the expansion of the Universe and possible decays. Perturbations around this constant background can be interpreted as Standard Model particles, as is done with the perturbations above the Higgs  $vev$  in the Standard Higgs procedure. Apart from them, there will exist an extra massless degree of freedom, the dilaton, completely decoupled from the Standard Model particles.

### 3.3.1 Slow-roll inflation and attractor solutions

This section is devoted to the study of the different inflationary trajectories in Higgs-Dilaton inflation. Since inflation will take place very far away from the minima of the potential, we can safely ignore the small angle formed by them with respect to the  $\chi$  axis, and set  $\vartheta = 0$  for the rest of this chapter. As pointed out in the previous section, an ideal inflationary scenario will be completely successful only if the physical outcome is independent of the initial conditions. Unfortunately, no slow-roll attractor solution generically exist in the two-field case. However, in the present Higgs-Dilaton scenario, the corresponding inflationary trajectories are not completely undetermined, thanks to the Noether's current associated to the scale-invariance. To show this, let us consider the Einstein's field equations corresponding to the lagrangian density (3.36)

$$\tilde{G}_{\mu\nu} = -\gamma_{ab} \left( \partial_\mu \varphi^a \partial_\nu \varphi^b - \frac{1}{2} \tilde{g}_{\mu\nu} \tilde{g}^{\rho\sigma} \partial_\rho \varphi^a \partial_\sigma \varphi^b \right) + \tilde{V} \tilde{g}_{\mu\nu} , \quad (3.39)$$

where  $\tilde{G}_{\mu\nu}$  is the Einstein tensor computed from the Einstein frame metric  $\tilde{g}_{\mu\nu}$ , which we will assume to be of FRW type. On the other hand, the Klein-Gordon type equations of motion

for the Higgs and dilaton scalar fields are given by

$$\square\varphi^c + \tilde{g}^{\mu\nu}\Gamma_{ab}^c\partial_\mu\varphi^a\partial_\nu\varphi^b = \gamma^{cd}\tilde{V}_{,d} , \quad (3.40)$$

where the action of the d'Alembertian  $\square$  on the scalar field is given by

$$\square\varphi^c = \frac{1}{\sqrt{-\tilde{g}}}\partial_\mu(\sqrt{-\tilde{g}}\tilde{g}^{\mu\nu}\partial_\nu\varphi^c) \quad (3.41)$$

and  $\Gamma_{ab}^c$  is the affine connection computed from the field space metric  $\gamma_{ab}$

$$\Gamma_{ab}^c = \frac{1}{2}\gamma^{cd}(\gamma_{da,b} + \gamma_{db,a} - \gamma_{ab,d}) . \quad (3.42)$$

Note that (3.39) and (3.40) are covariant under scalar field redefinitions  $\varphi \mapsto \varphi'(\varphi)$ . Assuming the scalar fields to be homogeneous during inflation,  $\varphi^i = \varphi^i(t)$ , they reduce to the Friedmann and coupled Klein-Gordon equations

$$H^2 = \frac{1}{3M_P^2} \left( \frac{1}{2}\gamma_{ab}\dot{\varphi}^a\dot{\varphi}^b + \tilde{V} \right) , \quad (3.43)$$

$$\ddot{\varphi}^c + \Gamma_{ab}^c\dot{\varphi}^a\dot{\varphi}^b + 3H\dot{\varphi}^c = -\tilde{V}^c , \quad (3.44)$$

where as before dots stand for derivative *wrt* the coordinate time  $t$ . As we pointed out in Section 2.4, there must exist an almost conserved current associated to the scale-invariance symmetry of the theory, which can be obtained from the Noether's theorem or directly derived from the equations of motion. For homogeneous fields, we have

$$\frac{1}{a^3} \frac{d}{dt} \left( a^3 \gamma_{ab} \dot{\varphi}^a \Delta\varphi^b \right) = 0 . \quad (3.45)$$

As a consequence, the quantity  $a^3 \gamma_{ab} \dot{\varphi}^a \Delta\varphi^b$  is exactly conserved. Rewriting it as

$$\gamma_{ab} \dot{\varphi}^a \Delta\varphi^b = \frac{\text{cst.}}{a^3} , \quad (3.46)$$

we realize that, in those cases in which the scale factor grows large, as happens during the considered inflationary stage, the right-hand side of the previous equation vanishes and the quantity

$$\gamma_{ab} \dot{\varphi}^a \Delta\varphi^b \simeq 0 . \quad (3.47)$$

becomes approximately conserved. The previous equation can be understood as an effective dynamical constraint that reduces by one the number of independent dynamical variables. To identify the normal modes let us consider the first two slow-roll parameters in the generalized two field case [132]

$$\epsilon = \frac{M_P^2 \gamma^{ab} \tilde{V}_{,a} \tilde{V}_{,b}}{2\tilde{V}^2} , \quad N_{ab} = \frac{M_P^2 \tilde{V}_{;ab}}{\tilde{V}} . \quad (3.48)$$

with  $\tilde{V}_{;cb} = \tilde{V}_{,cb} - \Gamma_{bc}^a(\varphi)\tilde{V}_{,a}$ . Note that in the two-field case the curvature of the potential along the different field directions is encoded in the eigenvalues  $\eta_i$  of the matrix  $N_b^a$ .

The system describes an inflating universe as long as the slow-roll parameters satisfy the conditions  $\epsilon \ll 1$  and  $\eta_i \ll 1$ . In that case, the Friedmann (3.43) and Klein-Gordon (3.44) equations reduce to

$$\tilde{H}^2 \simeq \frac{\tilde{V}}{3M_P^2}, \quad 3\tilde{H}\dot{\varphi}^c \simeq -\tilde{V}^c. \quad (3.49)$$

Combined them we obtain a parametric equation for the slow-roll trajectories

$$\frac{d\chi}{dh} = -\frac{(1+6\xi_h)h}{(1+6\xi_\chi)\chi}, \quad (3.50)$$

that can be solved exactly to get

$$r^2 \equiv (1+6\xi_\chi)\chi^2 + (1+6\xi_h)h^2 = \text{cst}. \quad (3.51)$$

The above solution describes an ellipse in field space. In spite of having being derived in the slow roll approximation, these trajectories are a good approximation, even beyond the slow-roll approximation as can be seen in Fig. 3.3. The existence of  $r^2$  leads us to the definition of new polar variables<sup>6</sup>

$$\rho = \frac{M_P}{\gamma} \ln \left( \frac{r}{M_P} \right), \quad \theta = \arctan \left( \sqrt{\frac{1+6\xi_h}{1+6\xi_\chi}} \frac{h}{\chi} \right), \quad (3.52)$$

with  $\gamma = \sqrt{\frac{\xi_\chi}{1+6\xi_\chi}}$ . As the initial  $r$  the new radial coordinate  $\rho$  is conserved by the evolution. On the other hand, the angular variable  $\theta$  satisfies the equation

$$\theta' = -\frac{4\xi_\chi}{1+6\xi_\chi} \cot \theta \left( 1 + \frac{6\xi_\chi \xi_h}{\xi_\chi \cos^2 \theta + \xi_h \sin^2 \theta} \right). \quad (3.53)$$

As a consequence of the scale-invariance, the previous equation is independent of the precise value of  $\rho$ . The radial coordinate does not move during the whole inflationary period and can be in practice excluded from the discussion. The evolution of the number of e-folds  $N$  as a function of  $\theta$  can be obtained by simply integrating (3.53) to get

$$N = \frac{1}{4\xi_\chi} \left[ \ln \left( \frac{\cos \theta_{\text{end}}}{\cos \theta} \right) + 3\xi_\chi \ln \left( \frac{\xi_\chi \cos^2 \theta_{\text{end}} + \xi_h \sin^2 \theta_{\text{end}} + 6\xi_\chi \xi_h}{\xi_\chi \cos^2 \theta + \xi_h \sin^2 \theta + 6\xi_\chi \xi_h} \right) \right]. \quad (3.54)$$

Here  $\theta_{\text{end}}$  stands for the value of angular variable  $\theta$  at the end of inflation. Inflation will end when the  $\epsilon$  parameter equals one,  $\epsilon = 1$ , which implies

$$\frac{8\xi_\chi^2(1+6\xi_h)}{1+6\xi_\chi} \frac{\cot^2 \theta_{\text{end}}}{\xi_\chi \cos^2 \theta_{\text{end}} + \xi_h \sin^2 \theta_{\text{end}}} = 1. \quad (3.55)$$

The previous equation will be important to derive a lower bound on the initial conditions for inflation  $\theta_{\text{initial}} > \theta_{\text{min}}$  for a minimal number of e-folds  $N = N_{\text{min}}$ . For doing this we need before to derive bounds on the non-minimal couplings  $\xi_\chi$  and  $\xi_h$  from cosmological observables. This is the purpose of the following sections.

<sup>6</sup>We would like to notice, that, although it is not the first time that a similar change of variables is proposed [133, 134], an explicit relation with the conservation law associated to the scale invariance (2.23) has been never pointed out.

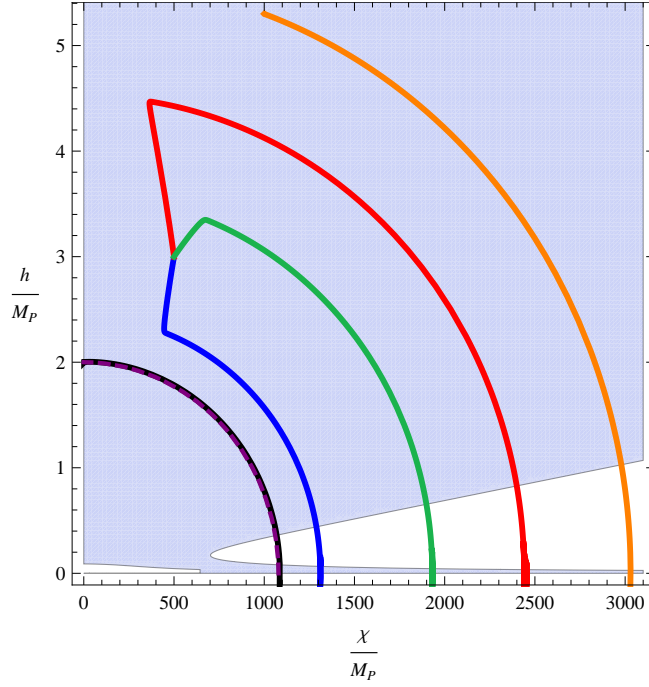


Figure 3.3: Numerically computed trajectories of Higgs and Dilaton fields in the Einstein-frame. The lower and upper curves correspond to slow-roll initial conditions. From the very beginning the fields satisfy the constraint  $r^2 = (1 + 6\xi_h)\chi^2 + (1 + 6\xi_\chi)h^2 = \text{const.}$ , represented by the dotted line above the lower curve. On the other hand, the initial values for the velocities of the intermediate solid curves have been chosen to be highly non-slow roll. Although the trajectory is initially influenced by the initial conditions, the fields end up describing an ellipse of constant radius in field space.



### 3.4 Cosmological Perturbations

In this section we review the inflationary observables for a general multiple field case [135], particularizing when needed to the single field case. Notice that the Higgs and Higgs-Dilaton lagrangian densities, given by (3.10) and (3.36) respectively, are invariant under general coordinate transformations. This gauge freedom on the unperturbed spacetime background will influence the perturbed physical spacetime. Cosmological perturbations are not unique and the theory is generically plagued by gauge or non-physical modes. The problem can be solved by defining how the points in the perturbed manifold relate to those in the unperturbed manifold, i.e. by fixing a gauge, or by working with gauge invariant quantities, with a clear geometrical meaning. The latter are invariant under infinitesimal coordinate transformations and can be obtained by simply requiring them to have vanishing Lie derivative along every infinitesimal vector field.

The independent components of the metric perturbations can be reduced to 6 gauge independent degrees of freedom, classified according to their behaviour under the rotation group  $SO(3)$ . The reasons for this classification are twofold. From a mathematical point of view, it turns out that the scalar, vector and tensor perturbations decouple and evolve independently, at least at the level of first order perturbed Einstein equations. From the physical point of view, these components give rise to different phenomena. Scalar perturbations are the only ones that can give rise to gravitational collapse, while vectors and tensor perturbations give rise to vorticity and gravitational waves respectively. In what follows we will only consider scalar and tensor perturbations, since vector perturbations rapidly decay with the expansion of the Universe (for a general review see for instance [136]).

In particular, two gauge-invariant scalar quantities – the Bardeen potentials  $\Phi$  and  $\Psi$  [137] – can be constructed. Any combination of gauge invariant quantities will be also scale invariant. Among all the possible combinations, we will consider the comoving curvature perturbation [137, 138]

$$\zeta \equiv \Psi - \frac{\mathcal{H}}{\mathcal{H}' - \mathcal{H}^2} (\Psi' + \mathcal{H}\Phi) . \quad (3.56)$$

Here  $\mathcal{H}$  is the comoving Hubble parameter  $\mathcal{H} \equiv aH$  and primes stand for derivative with respect to comoving time  $\eta$ .

The comoving curvature perturbation is especially interesting given its properties outside the horizon. In the single Higgs inflation case its temporal evolution is given by

$$\zeta' = \frac{1}{\epsilon\mathcal{H}} \nabla^2 , \quad (3.57)$$

which implies that the comoving curvature perturbation is constant for adiabatic superhorizon modes  $k \ll aH$ . As a consequence, the amplitude of the perturbations (3.56) expelled out of the horizon by the inflationary mechanism remains frozen during the radiation or matter eras, until they eventually reentry in the horizon. This constancy of super-horizon modes is crucial for testing inflation, since it directly relates the scalar and tensor perturbations seeding the CMB anisotropies and LSS matter distribution to the the primordial power spectrum of fluctuations at the end of inflation. The reconstruction of the inflationary potential becomes then independent of the (p)reheating details. The influence of subsequent reheating stage on

metric perturbations produced during inflation was considered in Refs. [139, 140, 141, 142, 143, 144, 145]. In the single field case under consideration, no instability of adiabatic metric perturbations is produced during the (p)reheating stage [141]. Related numerical studies beyond the linear regime can be found in Refs. [146, 147, 148, 149, 150, 151].

Contrary to the single field case, in generic multiple-field models, as Higgs-Dilaton inflation, the curvature or adiabatic perturbation might evolve on super-horizon scales. At linear order in perturbations we have

$$\zeta' = \frac{2\mathcal{H}}{\sigma'^2} \Delta\Psi - \frac{2\mathcal{H}}{\sigma'^2} P_d^c a^2 \tilde{V}_{,c} \delta\varphi^d, \quad (3.58)$$

where  $\delta\varphi^d$  are the perturbations to the background field trajectory and  $P_{ab}$  is the projector orthogonal to the trajectory  $P_{ab} = \gamma_{ab} - u_a u_b$ , with  $u^a \equiv \frac{\varphi'^a}{\sigma'} = \frac{\dot{\varphi}^a}{\dot{\sigma}}$ . In the long wavelength limit, the previous equation reduces to<sup>7</sup>

$$\zeta' = -\frac{2\mathcal{H}}{\sigma'^2} P_d^c a^2 \tilde{V}_{,c} \delta\varphi^d. \quad (3.59)$$

Therefore, the amplitude of the curvature perturbation  $\zeta$  at re-entry cannot be longer equated with that at horizon crossing. It must be rather integrated along the whole subsequent trajectory. Even if we assume an initial slow-roll regime, there will exist many inequivalent inflationary trajectories, given the absence of general attractor solutions in the multifield case.

Should we consider the evolution of the curvature perturbation in the two-field Higgs-Dilaton inflationary model? To answer this question let us write the conservation equation (3.46) in term of the polar variables  $(\rho, \theta)$ , cf. (3.52). We obtain

$$\frac{d\rho}{dN} = \frac{\text{cst}}{H\gamma_{\rho\rho}} \cdot e^{-3N}. \quad (3.60)$$

with  $N$  the number of e-folds in the Einstein frame. The constant in the previous expression depends on the initial conditions. The explicit form of the bounded metric component  $\gamma_{\rho\rho}$  is irrelevant for the discussion, although the reader can easily deduce it from the lagrangian density (4.11). During inflation the factor  $H^{-1}$  in (3.60) is generically nearly constant, but grows at most like  $e^N$  at the end of inflation. For instance, for matter domination we have  $H^{-1} \sim e^{\frac{1}{2}N}$ , while for radiation domination  $H^{-1} \sim e^{\frac{2}{3}N}$ . Therefore,  $\dot{\rho} = 0$  acts like an attractor of the equations of motion, which reduces the dynamical degrees of freedom to one, corresponding to the fluctuations back and forth the angular variable  $\theta$ . We then recover the single field case, where the comoving curvature perturbation is conserved for superhorizon modes. As shown in Ref. [145] (see also [154] for a general perspective) the large scale suppression of entropy perturbations during inflation avoid the resonant growth of these fluctuations also during the (p)reheating stage.

To describe the nature of perturbations in the Universe we make use of statistical descriptors such as the dimensionless scalar power spectrum  $\mathcal{P}_\zeta(k)$  or two-point correlation

<sup>7</sup>An explicit computation of this quantity for the Higgs-Dilaton model written in terms of the variables used in (4.11) can be found in Ref. [152, 153].

function in Fourier space

$$\langle 0 | \hat{\zeta}_{\mathbf{k}} \hat{\zeta}_{\mathbf{k}'}^* | 0 \rangle \equiv \frac{\mathcal{P}_\zeta(k)}{4\pi k^3} (2\pi)^3 \delta^2(\mathbf{k} - \mathbf{k}') , \quad (3.61)$$

which provides a complete description of the properties of Gaussian perturbations<sup>8</sup>. To the first non-trivial order in the slow-roll parameters it can be expressed as [126, 155, 135]

$$\mathcal{P}_\zeta(k) \simeq \Delta_\zeta^2(k^*) \left( 1 - 2(C + 3)\epsilon^* + 2C\eta_{\text{eff}}^* - (6\epsilon^* - 2\eta_{\text{eff}}^*) \ln \frac{k}{k^*} \right) , \quad (3.62)$$

where  $C = 2 - \ln 2 - \gamma$  and we have defined

$$\eta_{\text{eff}} \equiv p_{ab} N^{ab} , \quad p_{ab} = \frac{\tilde{V}_{,a} \tilde{V}_{,b}}{\gamma^{cd} \tilde{V}_{,c} \tilde{V}_{,d}} , \quad (3.63)$$

corresponding to the projection of the matrix  $N_{ab}$  in (3.48) on the background trajectory. Quantities marked with a star  $*$  are evaluated at the moment when the pivot scale  $k^*$  leaves the Hubble horizon,  $k^* = a(N^*)H(N^*)$ . This scale  $k^*$  is given by the *statistical center* of the range of scales explored by the data. The amplitude  $\Delta_\zeta^2(k^*)$  of the power spectrum is given by

$$\Delta_\zeta^2(k^*) \equiv \frac{\kappa^2}{2\epsilon^*} \left( \frac{H^*}{2\pi} \right)^2 . \quad (3.64)$$

Notice that, due to the approximate constancy of the Hubble rate  $H$  during inflation, the power spectrum (3.62) is expected to be nearly scale-invariant, i.e  $\mathcal{P}_\zeta(k) \propto k^{n_s-1}$ , with  $n_s$  very close to one. Therefore, it is customary to perform a Taylor expansion of  $\log \mathcal{P}_\zeta^2$  to obtain

$$\log \mathcal{P}_\zeta^2(k) = \log \Delta_\zeta^2(k^*) + (n_s(k^*) - 1) \log \frac{k}{k^*} + \frac{1}{2} \frac{dn_s}{d \log k} \Big|_* \log^2 \frac{k}{k^*} + \dots , \quad (3.65)$$

where  $n_s$  and  $\frac{dn_s}{d \log k} \Big|_*$  are often called the *spectral index* and *therunning* respectively. In terms of the slow-roll parameters, they are given by

$$n_s(k^*) - 1 \equiv \frac{d \ln \mathcal{P}_\zeta}{d \ln k} \Big|_{k=k^*} \simeq -6\epsilon^* + 2\eta_{\text{eff}}^* . \quad (3.66)$$

and

$$\frac{dn_s}{d \log k} \Big|_* = -16\epsilon^* \eta_{\text{eff}}^* + 24\epsilon^{*2} + 2\xi_{\text{eff}}^* . \quad (3.67)$$

Let us consider now the metric perturbations over the Friedmann-Robertson-Walker perturbed metric

$$ds^2 = -a^2 d\eta^2 + (\delta_{ij} + h_{ij}) dx^i dx^j \quad (3.68)$$

where  $h_{ij}$  is a divergenceless and traceless tensor perturbation

$$\nabla^i h_{ij} = \delta^{ij} h_{ij} = 0 . \quad (3.69)$$

---

<sup>8</sup>For Gaussian perturbations we mean the property of the initial seeds produced during inflation. Non-Gaussianities can of course appear in the posterior structure formation stage through gravitational instabilities.

The associated equation of motion is given by

$$h''_{ij} + 2\mathcal{H}h'_{ij} - \nabla^2 h_{ij} = 0 . \quad (3.70)$$

As we did for scalar perturbations, we define the primordial dimensionless spectrum tensor perturbations with all polarizations  $\mathcal{P}_g(k)$  as

$$\sum_i \langle 0 | h_{k,i} h_{k,i} | 0 \rangle \equiv \frac{\mathcal{P}_h(k)}{4\pi k^3} (2\pi)^3 \delta^2(\mathbf{k} - \mathbf{k}') \quad (3.71)$$

To first order in the slow-roll approximation, it becomes [126, 155]

$$\mathcal{P}_g(k) \simeq \Delta_g^2(k^*) \left( 1 - 2(C+1)\epsilon^* - 2\epsilon^* \ln \frac{k}{k^*} \right) , \quad (3.72)$$

where we have defined an amplitude

$$\Delta_g^2(k^*) \equiv 8\kappa^2 \left( \frac{H^*}{2\pi} \right)^2 \quad (3.73)$$

As the scalar power-spectrum, the gravitational power spectrum  $\mathcal{P}_g(k)$  is expected to be nearly scale invariant. The associated tensorial spectral index

$$n_g(k^*) \equiv \left. \frac{d \ln \mathcal{P}_g}{d \ln k} \right|_{k=k^*} \simeq -2\epsilon^* , \quad (3.74)$$

is always smaller than zero. Since both scalar and gravitational perturbations are generated from the same inflationary mechanism, there exist a *consistency condition* between them, defined by the ratio of the tensor and the scalar dimensionless spectra, namely,

$$r^* \equiv \frac{\mathcal{P}_g}{\mathcal{P}_\zeta} \simeq 16\epsilon^* = -2n_g^* , \quad (3.75)$$

to first order in slow-roll. If contrary to what happens in Higgs-Dilaton inflation, the comoving curvature perturbation evolved outside the horizon, then the previous equality would become an inequality  $r^* \leq -2n_g^*$ . The consistency condition (3.75) show that the tensor-to scalar ratio  $r$  and the tensor tilt  $n_g$  are not independent parameters. For this reason, from now on, we will take  $\Delta_\zeta^2$ ,  $n_s$ ,  $dn_s/d \log k|_{k^*}$  and  $r$  at the pivot scale  $k^*$  as the parameters to be compared with the inflationary predictions

### 3.5 CMB constraints on parameters

In this section we will study the primordial perturbations in the Higgs-driven inflationary models and derive approximate analytical results for different inflationary observables as functions of the couplings  $\xi_\chi$ ,  $\xi_h$ ,  $\lambda$ .

Let us solve (3.55) to obtain  $\theta_{end} = \theta_{end}(\xi_\chi, \xi_h)$ . Although this cannot be done analytically, numerical evaluation shows that for the spectral parameters to lie in the region allowed

for CMB constraints, the non-minimal couplings to gravity must satisfy  $\xi_\chi \ll 1$  and  $\xi_h \gg 1$  (cf. Fig. 3.6), which allow us to derive an approximate solution

$$\theta_{end} \simeq 2 \times 3^{\frac{1}{4}} \sqrt{\xi_\chi} , \quad (3.76)$$

at the leading order in  $\xi_\chi$  and  $1/\xi_h$ . Inserting this small quantity into (3.54) we can obtain the value of the angular variable  $\theta^* = \theta^*(\xi_\chi, \xi_h, N^*)$  for a number of e-folds  $N^*$  between the moment at which a given scale  $k^*$  exits the horizon and the end of inflation. Neglecting the small contribution on the second term in the right hand side of (3.54) we get<sup>9</sup>

$$\cos \theta^* \simeq e^{-4\xi_\chi N^*} . \quad (3.77)$$

Combining (3.77) with (3.66), (3.75) and (3.64) we obtain the following analytical expressions for the inflationary observables

$$n_s(k^*) \simeq 1 - 8\xi_\chi \coth(4\xi_\chi N^*) , \quad (3.78)$$

$$\Delta_\zeta^2(k^*) \simeq \frac{\lambda \sinh^2(4\xi_\chi N^*)}{1152\pi^2 \xi_\chi^2 \xi_h^2} , \quad (3.79)$$

$$r(k^*) \simeq 192\xi_\chi^2 \sinh^{-2}(4\xi_\chi N^*) , \quad (3.80)$$

at leading order in the couplings  $\xi_\chi, 1/\xi_h$ . In the relevant parameter range (see below) the accuracy of the approximate formula for  $n_s(k^*)$  is of the per mill level, while that  $r(k^*)$  are good at the percent level. The comparison between the previous expressions and observational WMAP7 bounds can be found in Fig. 3.4. To make explicit the connection with the Higgs Inflation model, let us notice that, although the quantity  $4\xi_\chi N^*$  might be of the order one,  $4\xi_\chi N^* \sim \mathcal{O}(1)$ , the series expansions of the hyperbolic functions converge rapidly and we can further approximate

$$n_s(k^*) \simeq 1 - \frac{2}{N^*} \left( 1 + \frac{1}{3}(4\xi_\chi N^*)^2 + \dots \right) , \quad (3.81)$$

$$\Delta_\zeta^2(k^*) \simeq \frac{\lambda N^{*2}}{72\pi^2 \xi_h^2} \left( 1 + \frac{1}{3}(4\xi_\chi N^*)^2 + \dots \right) , \quad (3.82)$$

$$r(k^*) \simeq \frac{12}{N^{*2}} \left( 1 - \frac{1}{3}(4\xi_\chi N^*)^2 + \dots \right) . \quad (3.83)$$

The scalar spectral index predicted by the present model has therefore an absolute maximum,

$$n_s(k^*) < 0.967 \simeq 1 - \frac{2}{N^*} . \quad (3.84)$$

This extreme value is obtained  $\xi_\chi \rightarrow 0$ , and corresponds to the value predicted by the Higgs-Inflation model [111]. The differences between the two models are completely encoded in the value of the non-minimal coupling  $\xi_\chi$ . The predicted tensor-to-scalar ratio has also a strong upper bound, i.e.

$$r(k^*) < 0.0035 \simeq \frac{12}{N^{*2}} , \quad (3.85)$$

---

<sup>9</sup>Although a more accurate result could be obtained iteratively, it becomes rather complicated, so we stick to the first order approximation.

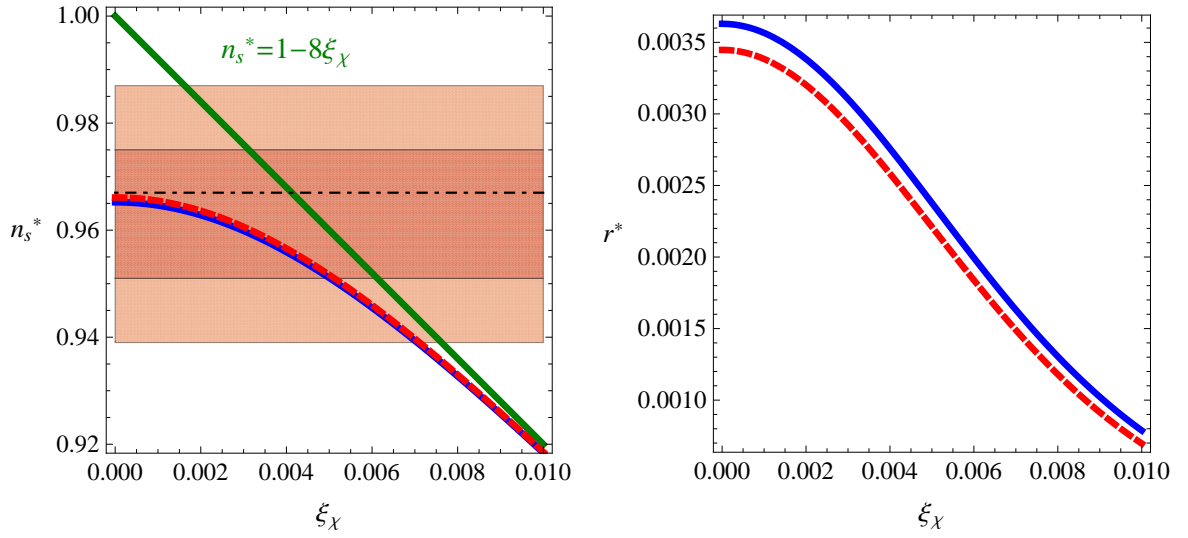


Figure 3.4: The approximate expressions (3.78) and (3.80) for the spectral tilt (left) and the tensor-to-scalar ratio (right) respectively as a function of the non-minimal coupling  $\xi_\chi$ . The red dashed curve is evaluated at  $N^* = N_{max}^*$ , corresponding to the fast reheating case,  $\rho_{rh} = \rho_{rh}^{max}$ . On the other hand, the blue solid curve represents the slow reheating case  $\rho_{rh} = \rho_{rh}^{min}$  with  $N^* = N_{min}^*$ . The green diagonal line correspond to the limiting case  $n_s = 1 - 8\xi_\chi$ . The dot-dashed horizontal line and the shaded regions correspond to the absolute maximum (3.84) and the observational  $1\sigma$  and  $2\sigma$  WMAP7 bounds for the scalar tilt respectively, cf. (3.90).

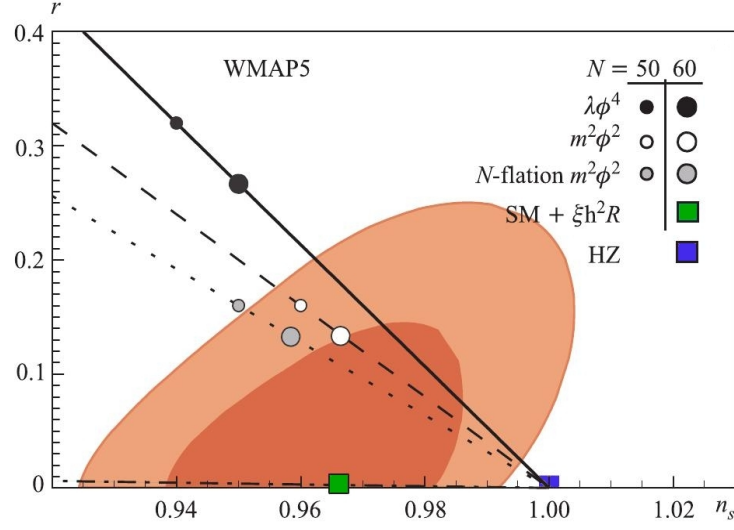


Figure 3.5: The allowed WMAP5  $1\sigma$  and  $2\sigma$  regions in the  $(r, n_s)$ . The prediction of Higgs Inflation (green box) are compared with those of the standard  $m^2\phi^2$  and  $\lambda\phi^4$  chaotic models and the Harrison-Zeldovich spectrum.

much smaller than the current observational constraint,  $r < 0.24$  (95% C.L.), cf. Ref. [1]. Also here, the extreme value agrees with that of Higgs Inflation [111]. The obtained values lie well inside the  $2\sigma$  WMAP7 allowed region in the  $(r, n_s)$  plane, as can be seen in Fig. 3.5. For completion we compare them with the predictions of the standard chaotic models and the Harrison-Zeldovich spectrum. At this point, it is interesting to notice that the predictions of Higgs inflation with  $\phi \gg v$  and large coupling  $\xi_h \gg 1$  coincide with those obtained in a scalar tensor theory with  $\phi < v$  and negative coupling  $\xi_h < 0$ . This duality was pointed out in Ref. [156].

The value of  $N^*$  in the previous expressions depends on the post-inflationary evolution of the universe, including not only the radiation and matter dominated eras, but also the details of (p)reheating. As we will see in the next chapter, this stage turns out to be extremely complicated. However, an estimation of the number of e-folds  $N^*$  can be obtained as follows. We will assume, as is indeed the case (cf. Chapter 4), that the evolution of scale factor during (p)reheating is that of a matter dominated universe,  $a \sim t^{2/3}$ , and that the transitions between the different eras are instantaneous. In this case, one can derive the following relation [155]

$$N^* \simeq 59 - \ln \frac{k^*}{a_0 H_0} - \ln \left( \frac{\rho^{cr}/\Omega_R}{\tilde{V}(\theta^*)} \right)^{1/4} + \ln \left( \frac{\tilde{V}(\theta^*)}{\tilde{V}(\theta_{end})} \right)^{1/4} - \frac{1}{3} \ln \left( \frac{\tilde{V}(\theta_{end})}{\rho_{rh}} \right)^{1/4}, \quad (3.86)$$

where  $a_0$ ,  $H_0$ ,  $\rho^{cr}$  and  $\Omega_R$  stand for present values of the scale factor, the Hubble parameter, the critical density and the present radiation density respectively. Numerically this

corresponds to

$$N^* \simeq 59 - \ln \frac{k^* \text{Mpc}}{0.002 a_0} - \ln \frac{10^{16} \text{GeV}}{\tilde{V}(\theta^*)^{1/4}} + \ln \left( \frac{\tilde{V}(\theta^*)}{\tilde{V}(\theta_{end})} \right)^{1/4} - \frac{1}{3} \ln \left( \frac{\tilde{V}(\theta_{end})}{\rho_{rh}} \right)^{1/4}. \quad (3.87)$$

with  $\rho_{rh}$  the radiation energy density at the end of reheating. It is clear that the maximum energy density transferred into radiation  $\rho_{max}$  has to be smaller than the energy scale at the end of inflation. This case corresponds to what we have called *fast reheating* approximation, where almost all the energy density of the inflaton is converted into relativistic matter. The lower value of the energy transfer  $\rho_{min}$  is dictated by the transition value  $\phi_t \sim M_P/\xi_h$  (cf. Section 4.2), below which the non-minimal coupling of the Higgs field to gravity can be neglected and we recover the standard Higgs quartic behaviour. This second case is referred as *long reheating*. We then have  $\rho_{max} \leq \rho_{rh} \leq \rho_{min}$ , with

$$\rho_{rh}^{max} = V(\theta_{end}) \simeq (7 - 4\sqrt{3}) \frac{\lambda M_P^4}{\xi_h^2}, \quad \rho_{rh}^{min} \simeq \frac{\lambda M_P^4}{4\xi_h^4}. \quad (3.88)$$

In these two limits,

$$N_{max}^* \simeq 64.55 - \frac{1}{2} \ln \frac{\xi_h}{\sqrt{\lambda}}, \quad N_{min}^* \simeq 64.55 - \frac{1}{12} \ln \lambda - \frac{2}{3} \ln \frac{\xi_h}{\sqrt{\lambda}}, \quad (3.89)$$

where we have taken into account the approximate expressions (3.76) and (3.77).

The approximate formulas (3.78)-(3.80), as well as (3.89), are useful to understand the parametric dependence of the observables. In the slow reheating case  $\rho_{rh} = \rho_{rh}^{max}$ , all of them depend on the different couplings only through the ratio  $\xi_h/\sqrt{\lambda}$ , while in the fast reheating case  $\rho_{rh} = \rho_{rh}^{min}$ , there appears an explicitly on the Higgs self-coupling  $\lambda$  through  $N_{min}$ , cf. (3.89). Changes in the value of  $\lambda$ , for fixed ratio  $\xi_h/\sqrt{\lambda}$ , give therefore rise to a shift in the minimal number of e-folds  $N_{min}^*$ . However, the influence of this small shift ( $\Delta N \sim 0.2$ ) on the observables can be completely neglected for values of  $\lambda$  in the range  $0.1 < \lambda < 1$ . It is therefore sufficient to discuss their dependence on  $\xi_\chi$  and  $\xi_h/\sqrt{\lambda}$ . In Fig. 3.4 we plot the approximate expressions (3.78) and (3.80) for the scalar spectral tilt and the tensor-to-scalar ratio respectively as functions of the coupling  $\xi_\chi$  for both the fast and slow reheating cases. The horizontal line in the left plot corresponds to the upper bound on the spectral tilt (3.84).

Accurate predictions for the parameter regions yielding the observables  $n_s(k^*)$ ,  $\Delta_\zeta^2(k^*)$  and  $r(k^*)$  in the allowed CMB range can be found numerically by combining (3.55), (3.54) and (3.87). Since the amplitude of tensor perturbations are expected to be very small, cf. (3.85), we will consider as observational bounds for the scalar tilt, and the amplitude of the scalar power spectrum those of the concordance  $\Lambda$ CDM model without tensor perturbations<sup>10</sup>

$$n_s(k^*) = 0.963 \pm 0.012, \quad \Delta_\zeta^2(k^*) = (2.44 \pm 0.09) \times 10^{-9}, \quad (3.90)$$

where  $k^*/a_0 = 0.002 \text{ Mpc}^{-1}$  is the pivot scale. The previous bounds take into account data from WMAP 7-year results, Baryonic Acoustic Oscillations (BAO) [157] and the value of the Hubble constant  $H_0$  [158]. Errors indicate the 68% confidence level. The results are plotted in Fig. 3.6. The band-shape of the two regions (associated to the fast and slow reheating



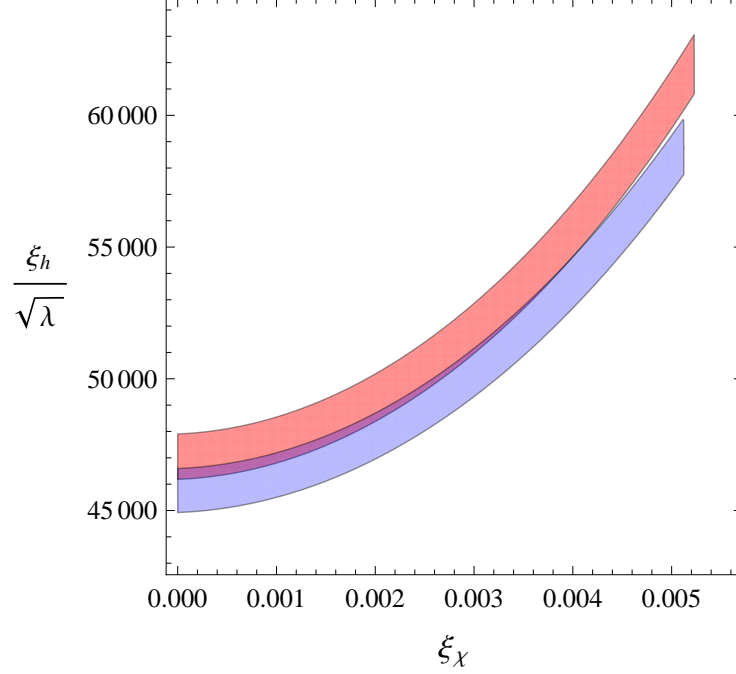


Figure 3.6: Parameter regions for which the values of the scalar tilt  $n_s(k^*)$  and the amplitude of the scalar spectrum  $\Delta_\zeta^2(k^*)$ , lie in the observationally allowed range 3.90, for  $0.1 < \lambda < 1$ . The red area is obtained for  $\rho_{rh} = \rho_{rh}^{max}$  (fast reheating), while the blue one corresponds to  $\rho_{rh} = \rho_{rh}^{min}$  (slow reheating). The fact that the bands are cut on the right hand side is due to the constraint on the scalar tilt  $n_s(k^*)$ , cf. (3.78). On the other hand, the band-shape comes from the constraint on the scalar perturbation amplitude  $\Delta_\zeta^2(k^*)$ , cf. (3.79).

<i>Fast reheating</i>	$0 < \xi_\chi < 0.0052$	$46200 < \frac{\xi_h}{\sqrt{\lambda}} < 63100$
<i>Slow reheating</i>	$0 < \xi_\chi < 0.0051$	$44900 < \frac{\xi_h}{\sqrt{\lambda}} < 59900$

Table 3.1: Bounds from the CMB observables on the non-minimal couplings of the Higgs ( $h$ ) and dilaton fields to gravity ( $\chi$ ) for fast ( $\rho_{rh} = \rho_{max}$ ) and slow ( $\rho_{rh} = \rho_{max}$ ) reheating stages.

cases) is due to the constraint on the spectrum amplitude (3.79), depending both on  $\xi_h$  and  $\xi_\chi$ . On the other hand, the cut on the right of the bands comes from the constraint on scalar tilt (3.78), which only depends on  $\xi_\chi$ . The associated bounds on parameters are shown in Table 3.1.

We derive this section by computing the constraints on the region of initial conditions for the scalar fields which lead to successful inflation. The initial conditions for inflation have to be such that  $\theta_{in} \geq \theta^*$ , where  $\theta^*$ , given by (3.77), is the field value close to which the observable scales exit the Hubble horizon during inflation. In terms of the original variables this condition reads

$$\frac{h_{in}}{\chi_{in}} \geq \sqrt{\frac{1+6\xi_\chi}{1+6\xi_h}} \tan \theta^* . \quad (3.91)$$

For typical values of the parameters,  $\xi_\chi = 0.003$ ,  $\xi_h = 50000$  and  $N^* = 60$ , we have  $\theta^* \sim 1.2$ , or equivalently  $\frac{h_{in}}{\chi_{in}} \gtrsim 0.004$ . We will come back to the initial conditions for inflation in Chapter 5, where considerations related to the late evolution of the universe will yield additional constraints on the initial conditions.

### 3.6 Quantum Corrections

The study of the cosmological aspects of Higgs-driven scenarios throughout this chapter have mostly remained at the level of classical field theory. However, both inflation and the subsequent reheating stage, cf. Chapter 4, take place at energies well above the electroweak scale. Some important assumptions, such as the validity of the effective theory at the scales involved or the flatness of the potential during inflation, strongly depend on the quantum theory. Although a complete study of the quantum aspects of Higgs inflationary models goes clearly beyond the scope of this thesis, we would like to summarize the state of the art and clarify the controversies between the different approaches to the problem [159, 160, 161, 162, 163, 164, 165, 166, 167]. The discussion closely follows that in Ref. [167], although other discussions have been also taken into account.

Let us start by noting that Higgs-driven inflationary models are clearly non-renormalizable, due to the non-minimal coupling to gravity in the Jordan frame or to the non-linear interactions of the Einstein frame potential. Therefore, they should be understood as effective field theories valid up to a given cutoff scale  $\Lambda_c$ . At this scale the theory becomes either inconsistent or strongly interacting, making it impossible to apply the standard QFT techniques. The usual criterion for determining the cutoff of the theory is based on the violation of tree level unitarity, whose lower value is frequently estimated by simple power counting. This is precisely the approach adopted in [164, 165], where it was claimed that the tree level amplitudes of scattering of scalars above the EW vacuum in Higgs inflation hit the unitarity bounds at energies  $\Lambda_c \sim \frac{M_P}{\xi_h}$ . This point is however rather subtle. In order to clarify it, let us decompose the Higgs field and the Jordan frame metric around their corresponding vacuum

<sup>10</sup>These numbers are taken from [http://lambda.gsfc.nasa.gov/product/map/current/params/lcdm\\_sz\\_lens\\_wmap7\\_bao\\_h0.cfm](http://lambda.gsfc.nasa.gov/product/map/current/params/lcdm_sz_lens_wmap7_bao_h0.cfm).

solutions

$$h = v + \delta\hat{h}, \quad g_{\mu\nu} = h_{\mu\nu} + \frac{\delta\hat{g}_{\mu\nu}}{M_P}, \quad (3.92)$$

where  $\delta\hat{h}$  are the quantum excitations of the Higgs field and  $h_{\mu\nu}$  is a canonically normalized metric perturbation. At the leading order one obtains a dimension 5 operator

$$\frac{\xi_h}{M_P} (\delta\hat{h})^2 \square \delta\hat{g}, \quad (3.93)$$

arising from the non-minimal coupling to gravity in the Jordan frame  $\xi_h h^2 R$ . As correctly pointed out in [164], the contribution of the previous term to tree level amplitudes is of order

$$\mathcal{M} \sim \frac{\xi_h^2 E_{cm}^2}{M_P^2}, \quad (3.94)$$

with  $E_{cm}$  the typical center of mass energy of the process. Then, taking into account just the naive power counting mentioned before, one should be tempted to say that the effective field theory (EFT) description breaks down at a scale  $\Lambda_c \sim M_P/\xi_h$ . Notice however that this kind of reasoning can be misleading, since there can exist non-trivial cancellations between the different channels involved that could give rise to a higher cutoff. As an example of this we can consider the  $hh \rightarrow hh$  scattering via graviton exchange with on-shell external legs. Summing over all the possible intermediate channels (s,t,u) one obtains [168, 169]

$$\mathcal{M}_{total} \sim \frac{E_{cm}^2}{M_P^2}, \quad (3.95)$$

which, rather than to the GUT scale  $\Lambda_c \sim M_P/\xi_h$ , points directly to the Planck scale as the true cutoff of the theory. Although one could argue that this kind of cancellations might not take place for other scattering processes, recovering therefore the original cutoff, there exist additional arguments in favour of a higher scale. As always the devil is in the details. It is very important to notice that the cutoff  $\Lambda_c$  is not a static quantity, but rather depends on the background  $\bar{h}$  above the instantaneous expectation value of the Higgs field. During the inflationary and reheating stages the system is not described by perturbations above the vacuum solutions. Let us illustrate how this is applied to Higgs Inflation. Let us assume the background to be approximately static, which is indeed a good approximation compared with the temporal scale of the relevant high-frequency excitations  $\delta\hat{h}$  appearing in non-renormalizable operators as (3.93). Expanding the metric and the Higgs field around their corresponding background values

$$h = \bar{h} + \delta\hat{h}, \quad g_{\mu\nu} = \bar{g}_{\mu\nu} + \delta\hat{g}_{\mu\nu}, \quad (3.96)$$

we obtain (after diagonalizing and redefining the Higgs field) the leading order term

$$\frac{\xi_h \sqrt{M_P^2 + \xi_h \bar{h}^2}}{M_P^2 + \xi_h (1 + 6\xi_h) \bar{h}^2} (\delta\hat{h})^2 \square \delta\hat{g}, \quad (3.97)$$

which corrects the dimension 5 operator (3.93). Note that the associated cutoff

$$\Lambda_c(\bar{h}) = \frac{M_P^2 + \xi_h(1 + 6\xi_h)\bar{h}^2}{\xi_h\sqrt{M_P^2 + \xi_h\bar{h}^2}}, \quad (3.98)$$

reduces indeed to the previous one in the low energy limit  $\bar{h} \ll M_P/\xi_h$ . However, they clearly differ for large values of the Higgs field,  $\bar{h} \gg M_P/\xi_h$ , as those that occur during inflation. In that case, the power counting cutoff scale (3.98) reduces to  $\Lambda_c \sim \sqrt{\xi_h\bar{h}}$ , or in other words, to the approximate effective Planck mass in the Jordan frame  $M_{P,\text{eff}}^2 = M_P^2 + \xi_h\bar{h}^2 \simeq \xi_h\bar{h}^2$ .

A similar analysis can be performed in the Einstein frame [167]. After doing the field redefinition (3.9), the non-linearities in the Einstein frame kinetic term are translated into the potential

$$V(\phi) = \frac{\lambda M_P^4}{4} \frac{h^4(\phi)}{(M_P^2 + \xi_h h^2(\phi))^2}, \quad (3.99)$$

which expanded around the background,  $\bar{\phi} + \delta\hat{\phi}$ , becomes

$$V(\bar{\phi} + \delta\hat{\phi}) = V(\bar{\phi}) + \sum_{n=1}^{\infty} \frac{1}{n!} \frac{d^n V}{d\phi^n} (\delta\hat{\phi})^n, \quad (3.100)$$

The specific form of the operators with  $n > 4$  and the associated cutoff in the previous expression depend, as before, on the value of the background field, and therefore on the position of the Higgs field in the inflationary potential. As we saw in Section 3.2 the relation  $\phi(h)$  simplifies considerably during the inflationary stage,  $\bar{\phi} \gg M_P/\sqrt{\xi_h}$  and (3.99) becomes<sup>11</sup>

$$V(\phi) = V_0 \left(1 - e^{-\alpha\kappa\phi}\right)^2, \quad (3.101)$$

where we have assumed the field  $\phi$  to be positive and omitted the absolute value in (3.18). Expanding around the background, the non-renormalizable terms in (3.100) have the form

$$V_0 \frac{e^{-\alpha\kappa\bar{\phi}}}{M_P^n} (\delta\hat{\phi})^n. \quad (3.102)$$

The exponential factors in the previous expression effectively extend the cutoff of the theory up to the Planck scale,  $\Lambda_c \sim M_P$ , in clear agreement with the results obtained in the Einstein frame. All the relevant scales during inflation are parametrically well below this cutoff, which justifies the semiclassical approximation used in this thesis. The conclusion can be extended to the subsequent (p)reheating and hot Big Bang stages [167].

Note that the Einstein frame potential (3.101) displays, for large field values, an approximate shift symmetry  $\phi \rightarrow \phi + c$ , respected also by the minimally coupled gravitational interaction. As is known from the works on Natural inflation [170], an approximate shift symmetry is enough to preserve the flatness of the Einstein frame potential from radiative

<sup>11</sup>A similar analysis, albeit much more tedious, can be of course performed for the remaining parts of the potential [167].

corrections. Quantum corrections can indeed be computed with the standard renormalization prescriptions and taken into account in a consistent way [171, 167]. For the perturbation theory to make sense, the counterterms must be chosen such that the effective potential has a flat direction to allow for the spontaneous breaking of scale invariance. This conclusion also holds upon the inclusion of fermion and gauge fields, provided that their couplings also obey shift symmetry [167], as indeed happens in Higgs Inflation.

The previous ideas about field dependent cutoffs can be also applied to the computation of quantum effective inflationary potential. Note that the large field region of Higgs Inflation in the Einstein frame displays an approximate scale-invariance symmetry, which becomes exact for all field values in the Higgs-Dilaton model. All the standard regularization procedures [125] (cutoff, Pauli-Villars, dimensional regularization, lattice regularization) introduce a new scale in the theory, breaking this scale-invariance at the quantum level. We have seen above that a fixed renormalization point or cutoff in that frame corresponds to a field-dependent one in the Jordan frame. This suggest to modify the standard regularization prescriptions in the Jordan frame to make them depend on the fields. For the case of cutoff or Pauli-Villars regularizations this can be done by simply choosing the cutoff scale or the Pauli-Villars masses to be field dependent [172]. Similarly, the t'Hooft-Veltman parameter<sup>12</sup>  $\mu^{2\epsilon}$  [173] appearing for instance in the standard dimensional regularization of the Higgs' self-coupling<sup>13</sup>  $\lambda$  [125]

$$\lambda = \mu^{2\epsilon} \left( \lambda_R + \sum_{i=1}^{\infty} \frac{a_i}{\epsilon^i} \right), \quad (3.103)$$

should be promoted to [116]

$$\mu^{2\epsilon} \rightarrow (\xi_h h^2 + \xi_\chi \chi^2)^{\frac{\epsilon}{1-\epsilon}}, \quad (3.104)$$

in order to solve the dimensional mismatch between the bare ( $\lambda$ ) and renormalized ( $\lambda_R$ ) couplings constants. Notice that the previous schemes are completely perturbative and indeed make sense only if there exist a spontaneously broken ground state over which perform the perturbative expansion. The use of a dynamical lattice could extend the previous perturbative treatments to the non-perturbative regime [117]. Using the above renormalization prescriptions it is possible to compute the effective potential in the inflationary region with the normalization point chosen in order to minimize higher order terms. The values of the coupling constants must be evaluated at the energy scale of inflation, making use of the renormalization group equations. The effective potential obtained in this way can be used to put constraints on the Higgs mass through the known value of the cosmological parameters. A detailed computation of the two loop<sup>14</sup> quantum corrections to the Higgs Inflation potential can be found in Ref. [162]. Higgs Inflation turns out to be possible only in an specific interval of Higgs masses, namely  $m_{\min} < m_H < m_{\max}$ , with

$$m_{\min} = \left[ 126.1 + \frac{m_t - 171.2}{2.1} \times 4.1 - \frac{\alpha_s - 0.1176}{0.002} \times 1.5 \right] \text{ GeV}, \quad (3.105)$$

<sup>12</sup>We use the convention  $d = 4 - 2\epsilon$ .

<sup>13</sup>The parameters  $a_n$  are the coefficients of the Laurent series in  $\epsilon$  (counterterms) and must be fixed by requiring finite renormalized Green's functions at every order in perturbation theory.

<sup>14</sup>The main effect of the 2-loop computation is widening the window for the Higgs field *wrt* the one-loop computation.

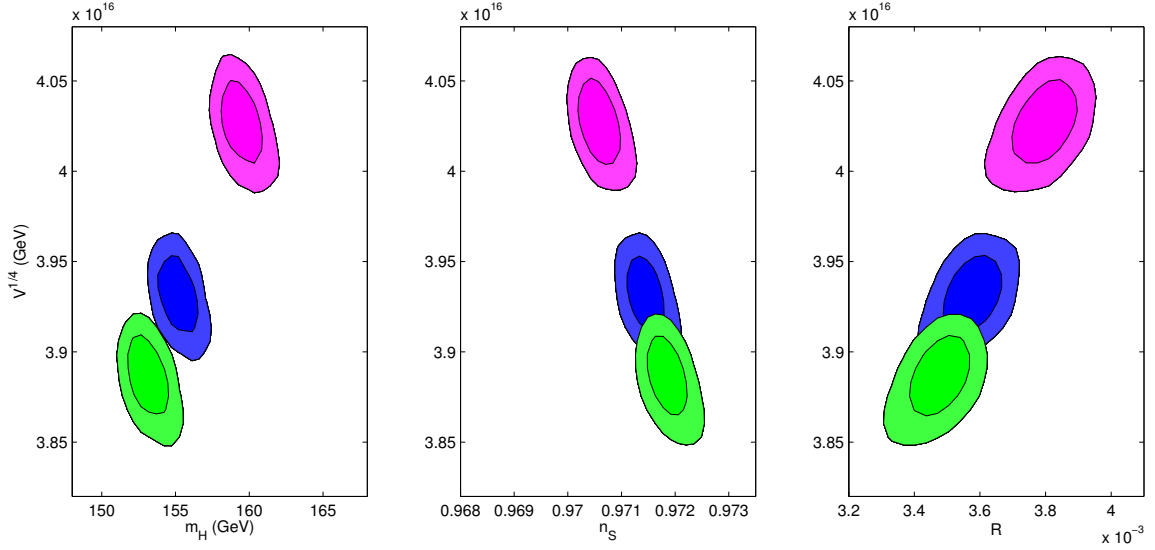


Figure 3.7: Reconstructed Higgs inflationary potential from the WMAP+SN+BA0 dataset as a function of the Higgs mass  $m_H$ , the spectral tilt  $n_s$  and the tensor to scalar ratio  $r$ . The different contours correspond to quark pole masses  $m_t = 168$  GeV (green),  $m_t = 171.3$  GeV (blue),  $m_t = 173$  GeV (magenta) at 68% and 95% C.L. Taken from [174].

$$m_{\max} = \left[ 193.9 + \frac{m_t - 171.2}{2.1} \times 0.6 - \frac{\alpha_s - 0.1176}{0.002} \times 0.1 \right] \text{ GeV} . \quad (3.106)$$

The theoretical uncertainty is about  $\pm 2.2$  GeV [162]. Here  $m_t$  and  $\alpha_s$  stand for the top mass and strong coupling constant respectively. It is important to understand the differences among the computation procedure of the previous bounds and others in the literature. The results obtained in Ref. [159] are particularly controversial, since they imply a significantly different Higgs mass,  $m_H \simeq 230$  GeV. However, it should be mentioned that in that work the running of the coupling constants up to the inflationary scale  $M_P/\xi_h$  was not taken into account and the mass of the Goldstone boson was overestimated, due to the approximation  $m_G^2 = \lambda v^2$ , which clearly differs from the real one

$$m_G^2 = \frac{\lambda v^2}{\left(1 + \frac{\xi_h v^2}{M_P^2}\right)^3} \ll \lambda v^2 . \quad (3.107)$$

On the other hand, the results obtained in [163, 160] are in good numerical agreement (at the one and two-loop level respectively) with the cited bounds (3.105) and (3.106), in spite of the fact that the formalism used in [160] is not gauge invariant. This translates into a different running of the coupling constants and gauge dependent matching conditions at the EW scale.

The values (3.105) and (3.106) are just based on the mapping between the renormalization group equations and the spectral index. These results can be further refined by using Markov Chain Montecarlo (MCMC) techniques to reconstruct the inflationary potential [174]. The WMAP7 data are complemented with geometric probes from Type Ia Supernovae (SN)

and baryon acoustic oscillations (BAO). The dependence of the reconstructed Higgs potential at 68% and 95% C.L. for several top quark pole masses is shown in Fig. 3.7. Note that an accurate reconstruction of the Higgs potential requires a precise determination of the top quark mass<sup>15</sup>. A value of the top quark pole  $m_t = 171.3$  GeV and effective QCD coupling constant  $\alpha_s(m_Z) = 0.1176$  provide a bound for the Higgs mass [174]

$$143.7\text{GeV} \leq m_H \leq 167.0\text{GeV} \quad (3.108)$$

at 95 % C.L. It is interesting to compare this window with the direct experimental constraints on the Higgs mass, coming from  $e^+e^-$  and  $p\bar{p}$  experiments at LEP and Tevatron (CDF and D0) respectively [22]. The final mass limit<sup>16</sup> arrived by LEP2 through the channel  $e^+e^- \rightarrow hZ$

$$m_H > 114.4 \text{ GeV}, \quad (3.109)$$

at 95% C.L., while that obtained by the combined effort of CDF and D0 through channels such as  $gg \rightarrow h^* \rightarrow WW$  or  $q\bar{q} \rightarrow Wh \rightarrow l\nu b\bar{b}$  *excludes* the intermediate region

$$160 \text{ GeV} < m_H < 170 \text{ GeV}. \quad (3.110)$$

also at 95% C.L. We conclude therefore that there still exist an experimentally allowed (although narrow) window of Higgs masses able to provide us with a successful inflationary stage. These experimental bounds together with the upper limits on the Higgs mass obtained from CMB observables place Higgs Inflation to the reach of the LHC, which will allow to verify or falsify the prediction.

---

<sup>15</sup>A summary of the present experimental status can be found in [http://www-cdf.fnal.gov/physics/new/top/public\\_mass.html](http://www-cdf.fnal.gov/physics/new/top/public_mass.html).

<sup>16</sup>We only consider the direct lower bounds. For a review of the theoretical upper bounds on the Higgs mass the reader is referred for instance to Ref. [175].





## CHAPTER 4

# The Higgs field and (P)reheating

I believe there are  $136 \times 2^{256}$   
protons in the universe and an  
equal number of electrons.

---

*Philosophy of Physical Science*  
SIR ARTHUR EDDINGTON

### 4.1 From Inflation to the hot Big Bang

The key ability of inflation to homogenize the universe also means that it effectively leaves the cosmos empty of particles and at zero temperature. Any particle content previous to the inflationary era is diluted away by the inflationary expansion. For the minimal number of e-folds needed to obtain the observed homogeneity and flatness of the universe [46],  $N \sim 60$ , the dilution factor of any primordial number density becomes at least as large as  $e^{-3N} \sim e^{-210}$ . Thus, the universe at the end of inflation is in a cold, low-entropy state with few degrees of freedom, very much unlike the present hot and highly-entropic universe. The energy density of the universe is locked up in a combination of kinetic and potential energy, stored in the zero-momentum mode of the inflaton field. To recover the standard hot Big Bang picture, this energy has to be somehow converted into the Standard Model particles. The diverse perturbative or non-perturbative mechanisms to defrost the universe are known as reheating [176, 177, 178] and preheating [179, 180, 181, 182, 183] respectively, and constitute one of the most important applications of the quantum theory of particle creation. A review of the different preheating mechanism can be found in Ref. [184, 185]. Whatever the mechanism of particle production, the created particles interact among themselves and

eventually reach an approximate state of thermal equilibrium<sup>1</sup>. This is understood as a decoherent distribution of particles with small occupation numbers for all momentum modes. It is the state of maximum uniformity and highest entropy and is completely characterised by the temperature and the chemical potentials associated to the existing conserved charges. The maximal temperature at this stage is called the reheating temperature. A viable (p)reheating scenario must lead to a radiation-dominated universe at least at a temperature above a few MeV, when nucleosynthesis begins. From there on, the universe expands and cools down, in the way described by the standard hot Big Bang.

(P)reheating is not at all a generic process. The overall picture of the transition between the *quasi*-inflationary and radiation dominated eras depends crucially on the inflaton amplitude and the strength of the interactions involved, and therefore on the different microphysics models in which inflation is embedded. The study of the details of (p)reheating in each concrete model without the experimental access to the couplings among the inflaton and the matter fields is a very difficult task. Most of the works on (p)reheating are therefore focused on the generic features of the different mechanisms that could play a role in the process, without considering any specific model. The novelty and great advantage of Higgs inflationary models is their connection with a well-known microphysical mechanism, hopefully accessible in the near future accelerator experiments. The measurement of the Higgs mass will complete the list of the couplings of the Standard Model and. Known the couplings, one should be able to study all the (p)reheating details and determine from them the initial conditions for the hot Big Bang. This makes the models under consideration extremely interesting and, potentially, predictive.

As we did in Chapter 3, we choose to work in the Einstein frame, where the action takes the usual Einstein-Hilbert form and the familiar (p)reheating techniques can be directly applied. Different perturbative and non-perturbative aspects of reheating in the context on induced gravity [186, 187, 188] and general scalar-tensor theories [189, 190, 191, 192, 193, 194, 195] have been previously considered in the literature, but not with the Higgs field playing the role of the inflaton. The main features of the following analysis will be common to both Higgs and Higgs-Dilaton Inflation. Indeed, as we will show in Section 4.2, the Higgs-Dilaton model can be reduced, with a proper choice of variables, to the single field case studied in Ref. [77]. All the relevant physical scales, including the effective gauge and fermion masses presented in Section 4.3, agree, up to small corrections, with those of Higgs Inflation. Given the strength of the interactions between the Higgs and the Standard Model particles, we will start by considering the perturbative decay of the Higgs field right after the end of inflation. As we will show in Section 4.4, the process turns out to be not efficient enough, and non-perturbative effects must be taken into account. Among the different possibilities, the shape of the potential in the Einstein frame suggests the study of tachyonic preheating [196, 197, 198] and parametric resonance [179, 181, 182, 183], which are presented in Sections 4.5 and 4.6 respectively. Once created, the Standard Model particles would decay into lighter states, as happens for instance in instant preheating [199]. This analysis is presented in Section 4.7, leaving for Section 4.8 the study of the combined effect of parametric resonance

---

<sup>1</sup>Properly speaking, a precise thermal equilibrium does not exist in an expanding universe. However, this state constitutes a good approximation if the rate of change of the quantities describing the system is much smaller than the expansion rate.

and perturbative decays, that we called *Combined Preheating* [77]. The backreaction of the produced particles on the Higgs oscillations and the end of inflation are finally considered in Section 4.9.

## 4.2 Higgs-Dilaton Inflation meets Higgs Inflation

In this section we make explicit the similarities between Higgs and Higgs-Dilaton Inflation during (p)reheating. Let us start by considering the single field Higgs Inflation case presented in Section 3.2 and study its evolution around the minimum of the potential. For small field values, the potential (3.18) can be approximated as

$$V(\phi) = \frac{1}{2}M^2\phi^2 + \Delta V(\phi), \quad (4.1)$$

where  $M = \sqrt{\frac{\lambda}{3}} \frac{M_P}{\xi_h} \sim \mathcal{O}(10^{13} \text{ GeV})$  is the typical frequency of oscillation and  $\Delta V$  are some corrections to the quadratic approximation

$$\Delta V(\phi) = -\frac{\beta_1}{3}|\phi|^3 + \frac{\beta_2}{4}\phi^4 + \mathcal{O}(|\phi|^5), \quad (4.2)$$

with  $\beta_1 = \lambda M_P / \sqrt{6} \xi_h^2$  and  $\beta_2 = 7\lambda / 27 \xi_h^2$ . As we will see at the end of this section, they soon become negligible after the end of inflation. The potential around the minimum behaves therefore, to very good approximation, as an standard quadratic chaotic potential. Note, nevertheless, that the approximation (3.13), and as a consequence the parametrized potential (3.18), does not properly describe the shape of the potential in the region  $v \ll \phi \ll M_P / \xi_h$ . For these small values,  $|\phi| \ll \phi_t \equiv M_P / \xi_h$ , the effect of the non-minimal coupling becomes irrelevant and we recover the minimally coupled case, in which the Jordan and Einstein frames agree,  $\Omega^2 \approx 1$ . This translates into a transition in the inflationary potential from (4.1) to  $V(\phi) \approx \frac{\lambda}{4}\phi^4$ . As will be argued in Section 4.6, this region will turn out to be irrelevant for the analysis of the preheating stage. Therefore, from now on, we will neglect the change in the behaviour of the potential (from  $\frac{1}{2}M^2\phi^2$  to  $\frac{\lambda}{4}\phi^4$ ) in this “small” field region.

To make explicit the connection of (4.1) with the scale invariant Higgs-Dilaton extension presented in Section 3.3, let us rewrite the lagrangian density (3.36) in the appropriate variables. The tilde over all Einstein frame variables will be skipped to simplify the notation. Unlike in the single-field case, the non-canonical kinetic term in (3.36) cannot be recasted in canonical form by simply redefining the scalar field. In fact, in the present two-dimensional manifold case, the Ricci scalar<sup>2</sup> associated to the field space metric  $\gamma_{ab}$ ,

$$R_\gamma = (\xi_\chi - \xi_h) \frac{2}{M_P} \frac{\xi_\chi^2(1 + 6\xi_\chi)\chi^4 - \xi_h^2(1 + 6\xi_h)h^4}{(\xi_h(1 + 6\xi_h)h^2 + \xi_\chi(1 + 6\xi_\chi)\chi^2)^2}, \quad (4.3)$$

does not identically vanishes, unless  $\xi_\chi = \xi_h$ . This case is however not allowed by observations, cf. Section 3.5. Nevertheless, it is possible to write the kinetic term in a quite simple diagonal

<sup>2</sup>In two dimensions, the Riemann tensor has only one independent component and therefore, it is enough to consider the Ricci scalar.

form. As pointed out at the end of Section 3.3, the conserved quantity (3.51) suggests to introduce the polar decomposition (3.52), in terms of which the lagrangian density (3.36) for the  $\beta = 0$  case can be written as

$$\frac{\mathcal{L}}{\sqrt{-g}} = \frac{M_P^2}{2} R - \frac{1}{2} K_D - V(\theta). \quad (4.4)$$

Here  $K_D$  is a diagonal, although non-canonical, kinetic term

$$K_D = \frac{\sigma}{\sin^2 \theta + \sigma \cos^2 \theta} (\partial \rho)^2 + \frac{M_P^2 \sigma}{\xi_\chi} \frac{\tan^2 \theta + \mu}{\cos^2 \theta (\tan^2 \theta + \sigma)^2} (\partial \theta)^2. \quad (4.5)$$

and we have defined

$$\mu \equiv \frac{\xi_\chi}{\xi_h}, \quad \sigma \equiv \frac{(1 + 6\xi_h) \xi_\chi}{(1 + 6\xi_\chi) \xi_h}. \quad (4.6)$$

Recall that the CMB bounds in Table 3.1 imply  $\mu \ll 1$ , which allows to simplify the second term in (4.5) to obtain

$$K_D = \frac{\sigma}{\sin^2 \theta + \sigma \cos^2 \theta} (\partial \rho)^2 + \frac{M_P^2 \sigma}{\xi_\chi} \frac{\sin^2 \theta}{(\sin^2 \theta + \sigma \cos^2 \theta)^2} (\partial \theta)^2. \quad (4.7)$$

The potential term in (4.4) is given by

$$V(\theta) = V_0 \left( \frac{\sin^2 \theta}{\sin^2 \theta + \sigma \cos^2 \theta} \right)^2, \quad (4.8)$$

where we have neglected the contribution of the dilaton  $\chi$ , given the small value of  $\vartheta$ . Notice that this is analogous to neglect the vacuum expectation value  $v$  in the single field case, cf. (3.15). The amplitude  $V_0$  is defined as  $V_0 \equiv \frac{\lambda M_P^4}{4\xi_h^2}$ , which agrees with that of the Higgs Inflation potential (3.18). Let us finally perform an extra field redefinition to write the angular dependence of the kinetic term (4.7) in a simpler form. We set

$$\tanh[\bar{\alpha} \kappa (\phi_0 - |\phi|)] = \sqrt{1 - \sigma} \cos \theta, \quad (4.9)$$

with  $\kappa = M_P^{-1}$  and  $\bar{\alpha} = \sqrt{\xi_\chi (1 - \sigma) / \sigma}$ . The constant quantity  $\phi_0$  is defined by

$$\cosh^2(\bar{\alpha} \kappa \phi_0) = \frac{1}{\sigma}. \quad (4.10)$$

As we will see below, this choice simply sets the minimum of the potential at  $\phi = 0$ . Notice that, as happened in Higgs Inflation, the absolute value in the left hand-side of (4.9) is required for  $\phi$  to maintain the symmetry of the initial angular variable  $\theta$  around the minimum. In terms of the new variables the lagrangian density in the Einstein frame can be written in a very simple form

$$\frac{\tilde{\mathcal{L}}}{\sqrt{-g}} = \frac{M_P^2}{2} R - \frac{e^{2b(\phi)}}{2} (\partial \rho)^2 - \frac{1}{2} (\partial \phi)^2 - V(\phi), \quad (4.11)$$

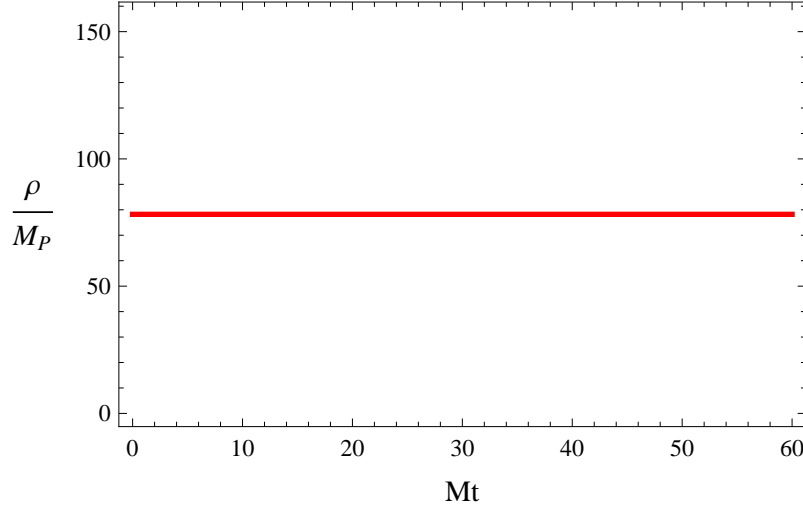


Figure 4.1: Numerical evolution of the radial coordinate  $\rho$  during the (p)reheating stage. The field displays the shift symmetry  $\rho \rightarrow \rho + c$ , associated to the conservation of the dilatational current. This fact reduces the background evolution during preheating to the single field Higgs inflationary case.

previously studied in the literature [152, 200, 153]. As shown in Fig. 4.1 the radial variable  $\rho$  displays an exact shift symmetry  $\rho \rightarrow \rho + c$ . The function  $b(\phi)$  is defined as

$$b(\phi) = \frac{1}{2} \ln [\sigma \cosh^2 (\bar{\alpha} \kappa (\phi_0 - |\phi|))] , \quad (4.12)$$

while the potential  $V$  is given by

$$V(\phi) = \tilde{V}_0 [1 - \sigma \cosh^2 (\bar{\alpha} \kappa (\phi_0 - |\phi|))]^2 , \quad (4.13)$$

where we have defined a new amplitude  $\tilde{V}_0 \equiv \frac{V_0}{(1-\sigma)^2}$ . As shown in Fig. 4.2, the shape of the Higgs-Dilaton potential in these new variables clearly resembles that of the simplest Higgs Inflation scenario (3.18). In spite of the slight differences, both of them present an exponentially flat region for large field values and nicely agree for small ones. Indeed, the relation between them becomes explicit if we approximate (4.13) around its minimum, to obtain

$$V(\phi) \simeq \frac{1}{2} M_{HD}^2 \phi^2 + \Delta V_{HD}(\phi) . \quad (4.14)$$

where

$$M_{HD}^2 = (1 + 6\xi_\chi) M^2 , \quad \Delta V_{HD}(\phi) \simeq (1 + 6\xi_\chi) \Delta V(\phi) . \quad (4.15)$$

The comparison between the previous expression and the exact potential (4.13) is shown in Fig. 4.3. The small value of  $\xi_\chi$  allows us to identify  $M^2 \simeq M_{HD}^2$  and  $\Delta V \simeq \Delta V_{HD}$  and study, simultaneously for the two models, the evolution of the inflaton around the minimum of the potential. Let us start by considering the Klein-Gordon equation for the inflaton,

$$\ddot{\phi} + 3H\dot{\phi} + V'(\phi) = 0 , \quad (4.16)$$

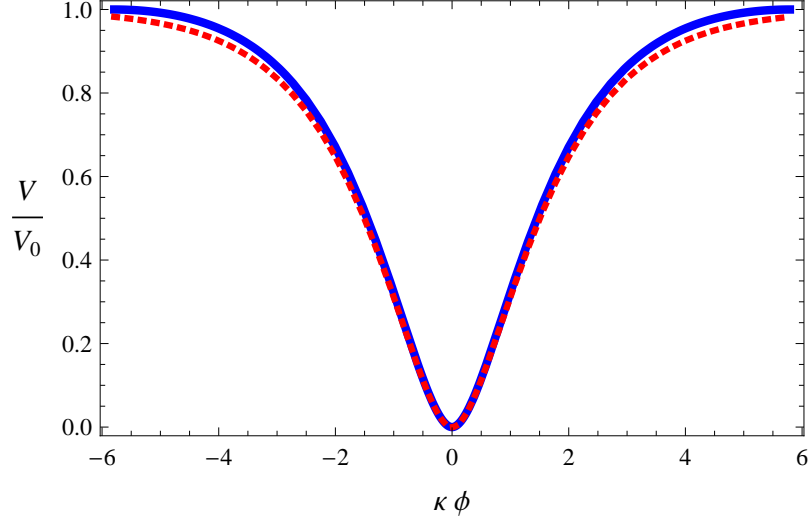


Figure 4.2: Comparison between the Higgs-Dilaton inflationary potential (blue continuous line) obtained from (4.13) and the corresponding one for the Higgs Inflation model (3.18) (red dotted line). In spite of the slight differences in the upper inflationary region, they nicely agree in the lower part, where the (p)reheating stage takes place.

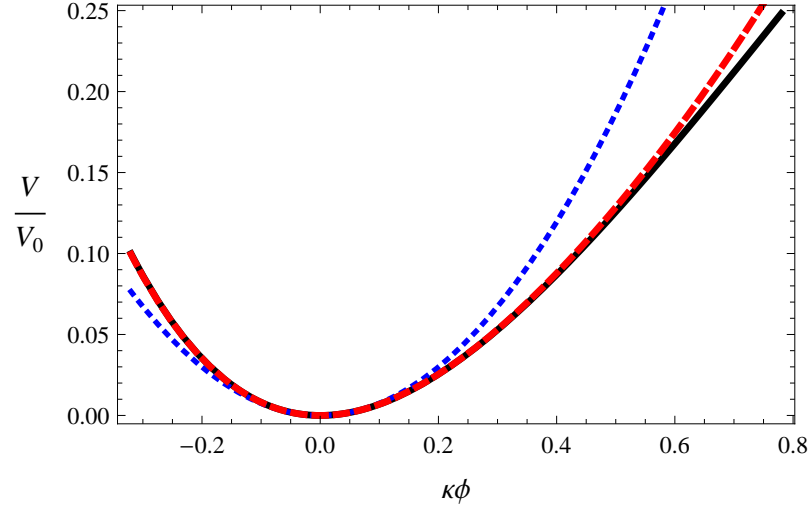


Figure 4.3: Comparison among the exact inflationary potential (4.13) in Higgs-Dilaton inflation (solid black line) and the quadratic approximation in (4.14) with (red dashed line) and without (blue dotted line) taking into account the corrections  $\Delta V_{HD}$ . Similar results can be found for Higgs Inflation.

which, for a power-law evolution  $a \propto t^p$ , can be written as

$$\ddot{\phi} + 3\frac{p}{t}\dot{\phi} + M^2[1 + \delta M^2(\phi)]\phi = 0, \quad (4.17)$$

with  $\delta M^2 \approx -\beta_1|\phi| + \beta_2\phi^2 + \mathcal{O}(\phi^3)$ . As we will justify *a posteriori*, these non-linear terms will be negligible from the very beginning of (p)reheating,  $|\delta M^2(\phi)| \ll 1$ . Notice that the interactions with the Standard Model fields are also neglected. As we will see in Section 4.9, the backreaction of these fields into the Higgs' dynamics will only be relevant once their occupations numbers have grown sufficiently.

The general solution of the evolution equation (4.17) in the  $|\delta M^2(\phi)| \ll 1$  case can be expressed as

$$\phi(t) = \frac{1}{(Mt)^\nu} [C_1 J_\nu(Mt) + C_2 J_{-\nu}(Mt)], \quad (4.18)$$

with  $C_1$  and  $C_2$  constants depending on the field values at the end of inflation, and  $J_{\pm\nu}(x)$  Bessel functions of order  $\pm\nu$ , with  $\nu = (3p - 1)/2$ . For a reasonable power index<sup>3</sup>,  $p > 1/3$ , the second term in the right-hand side of (4.18) diverges in the limit  $Mt \rightarrow 0$  and therefore should be discarded on physical grounds. The physical solution is then simply given by

$$\phi(t) = C_1 (Mt)^{-\nu} J_\nu(Mt), \quad (4.19)$$

which making use of the large argument expansion ( $Mt \gg 1$ ) of fractional Bessel functions [201], can be approximated by a cosine function

$$\phi(t) \approx A (Mt)^{-\frac{3p}{2}} \cos(Mt - (3p/2)(\pi/2)). \quad (4.20)$$

where  $A \propto C_1$  is a normalization constant that will be fixed later. The energy and pressure densities associated to the general solution (4.19) are given, after averaging over several oscillations, by

$$\begin{aligned} \rho_\phi &\approx \left\langle \frac{1}{2}\dot{\phi}^2 + \frac{1}{2}M^2\phi^2 \right\rangle \approx \frac{1}{2}M^2X^2[\langle \cos^2(Mt - 3\pi p/4) \rangle + \langle \sin^2(Mt - 3\pi p/4) \rangle] = \frac{1}{2}M^2X^2, \\ p_\phi &\approx \left\langle \frac{1}{2}\dot{\phi}^2 - \frac{1}{2}M^2\phi^2 \right\rangle \approx \frac{1}{2}M^2X^2[\langle \cos^2(Mt - 3\pi p/4) \rangle - \langle \sin^2(Mt - 3\pi p/4) \rangle] = 0. \end{aligned}$$

where we have neglected the change in  $X(t) \equiv A(Mt)^{-3p/2}$ , since  $M \gg H$ . The equation of state for the inflaton is then that of pressureless non-relativistic matter,  $p_\phi \approx 0$ . Taking into account the conservation equation  $\dot{\rho}_\phi + 3H(\rho_\phi + p_\phi) = 0$ , we obtain  $\rho_\phi \sim a^{-3}$ . The inflation behaves therefore as a wave of particles at rest, oscillating coherently with conserved number of particles per comoving volume

$$\frac{d}{dt}(a^3 n_\phi) = 0, \quad (4.21)$$

or in other words, as a Bose condensate. In this case, the scale factor evolves as  $a(t) \propto t^{2/3}$ , which allows to express the final physical solution as

$$\phi(t) = \frac{\phi_{\text{end}}}{Mt} \sin(Mt). \quad (4.22)$$

---

<sup>3</sup>This condition includes both the matter  $p = 2/3$  and radiation  $p = 1/2$  dominated cases.

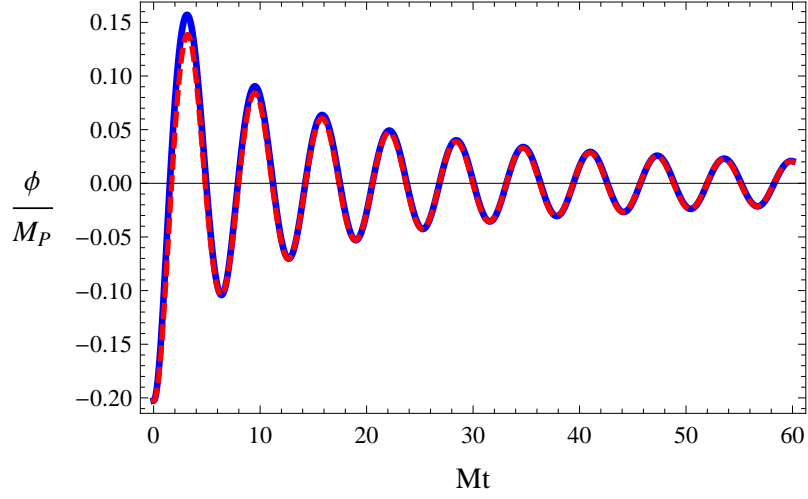


Figure 4.4: Numerical evolution during the preheating of the field  $\phi$  in (4.11). The amplitude of the oscillations decreases with time due to the expansion of the Universe. The blue solid line corresponds to the evolution on the exact Higgs-Dilaton potential (4.13), while the red dashed line comes from simple quadratic potential (4.14). The curves nicely agree from the very beginning of the preheating stage.

where we have assumed that the oscillatory behaviour starts just at the end of inflation,  $A = \phi_{\text{end}}$ . Rewriting the previous equation in terms of the number of times the inflaton crosses zero,  $j = (Mt)/\pi$ , we get

$$\phi(t) \approx \frac{\phi_{\text{end}}}{j\pi} \sin(\pi j) = X(j) \sin(\pi j) . \quad (4.23)$$

The Higgs condensate oscillates with a decreasing amplitude  $X(j) \equiv \frac{\phi_{\text{end}}}{j\pi}$ . We can obtain an upper bound,  $\alpha\kappa|\phi| < 0.122/N$ , on the amplitude of the Higgs field after  $N = j/2$  oscillations, which in terms of the correction of  $\delta M^2$  to 1, see (4.17), implies  $|\delta M^2| < 0.122, 0.0615$  or  $0.0244$ , after the first  $N = 1, 2$  and  $5$  oscillations, respectively. Thus, from the very beginning, the effective potential of the Higgs field tends very rapidly to that of a harmonic oscillator, which justifies *a posteriori* the approximation  $|\delta M^2| \ll 1$  used in the derivation of (4.18) and (4.23). This fact can be observed in the numerical result displayed in Fig. 4.4

If we neglect the presence of other fields and consider the Higgs-condensate as a free field, only damped by the expansion of the universe, then we can easily estimate the number of semi-oscillations before the amplitude of the field becomes smaller than the transition value  $\phi_t \sim M_p/\xi_h$ . For  $|\phi| < \phi_t$ , the conformal transformation (3.7) equals one and ceases to distinguish between Jordan and Einstein frames. In this case, the Higgs potential will not be anymore approximated by the quadratic potential (4.1), but rather by a quartic interaction  $(\lambda/4)\phi^4$ . This will happen when

$$X(j_t)/\phi_t \sim \frac{\xi_h \kappa \phi_{\text{end}}}{\pi j_t} < 1 , \quad (4.24)$$



or equivalently after

$$j \geq j_t \equiv \frac{\xi_h \kappa \phi_{\text{end}}}{\pi} \approx (10^4) \quad (4.25)$$

semi-oscillations. If before such a time, the energy stored in the Higgs condensate has not yet been transferred into the Standard Model fields, the transition in the behaviour of the potential will change the expansion rate from matter-like to radiation-like, characteristic of quartic potentials.

### 4.3 The Standard Model in the Einstein frame

The efficiency of the energy transfer from the Higgs field to the Standard Model particles will depend on their mutual couplings, and therefore, on the specific form of the Standard Model lagrangian in the Einstein frame. Let us start by considering the spontaneous symmetry breaking sector, responsible of the masses of the intermediate gauge  $W$  and  $Z$  bosons, i.e.

$$\frac{\mathcal{L}_{SBB}}{\sqrt{-g}} \supset m_W^2 W_\mu^+ W^{\mu-} + \frac{1}{2} m_Z^2 Z_\mu Z^\mu. \quad (4.26)$$

Contrary to what happens in the usual Standard Model, where the constant  $v_{\text{ev}}$  of the Higgs field makes the masses of the  $SU(2)$  bosons independent of time, the dynamical evolution during inflation gives rise to variable effective masses that depend on the instantaneous value of the Higgs condensate

$$m_W(t) = \frac{g_2 h(t)}{2}, \quad m_Z = \frac{m_W}{\cos \theta_w}. \quad (4.27)$$

The weak mixing angle  $\theta_w = \tan^{-1}(g_1/g_2)$  depends on the coupling constants  $g_1$  and  $g_2$  of the  $U(1)_Y$  and  $SU(2)_L$  groups respectively. Notice that these couplings must be evaluated at the scale  $M$ , where all the relevant physical processes during preheating will take place. Making use of the renormalization group equations it can be shown [202, 77] that numerically this corresponds to  $g_1^2 \approx g_2^2 \approx 0.30$ , or equivalently,  $\sin^2 \theta_w = \cos^2 \theta_w \approx 1/\sqrt{2}$ . From now on we will use these values for numerical estimates.

In agreement with the prescription for transforming masses and fields firstly introduced in Section 2.2, the lagrangian density (4.26) preserves its form under a generic conformal transformation,  $\tilde{g}_{\mu\nu} = \Omega^2 g_{\mu\nu}$ ,

$$\frac{\tilde{\mathcal{L}}_{SBB}}{\sqrt{-\tilde{g}}} \supset \tilde{m}_W^2 \tilde{W}_\mu^+ \tilde{W}^{\mu-} + \frac{1}{2} \tilde{m}_Z^2 \tilde{Z}_\mu \tilde{Z}^\mu, \quad (4.28)$$

if the fields and masses are redefined with the corresponding conformal weights as

$$\tilde{W}_\mu^\pm \equiv \frac{W_\mu^\pm}{\Omega}, \quad \tilde{Z}_\mu \equiv \frac{Z_\mu}{\Omega}, \quad \tilde{m}_W^2 = \frac{m_W^2}{\Omega^2}, \quad \tilde{m}_Z^2 = \frac{m_Z^2}{\cos^2 \theta_w}. \quad (4.29)$$

The same procedure can be applied to the Yukawa sector. As before, the specific form of the action is maintained in the new frame if the conformal factors coming from the transformation

of the metric determinant are incorporated in the definition of fields and masses. In particular, for fermionic fields  $\psi$ , we must require  $\tilde{\psi} \equiv \frac{\psi}{\Omega^{3/2}}$  and  $\tilde{m}_f \equiv m_f/\Omega$ .

It is interesting to notice that, not only the masses, but also the form of the interactions between the Standard Model particles, remain invariant under conformal transformations. Let us consider for instance the interactions between gauge bosons and fermions

$$\frac{\mathcal{L}_F}{\sqrt{-g}} \supset \frac{g_2}{\sqrt{2}} W_\mu^+ J_\mu^- + \frac{g_2}{\sqrt{2}} W_\mu^- J_\mu^+ + \frac{g_2}{\cos \theta_w} Z_\mu J_Z^\mu, \quad (4.30)$$

where

$$J_\mu^- \equiv \bar{d}_L \gamma^\mu u_L, \quad J_\mu^+ \equiv \bar{u}_L \gamma^\mu d_L, \quad (4.31)$$

are the charged currents carrying the information about the couplings of the  $W^\pm$ , and

$$J_Z^\mu \equiv \frac{1}{2} \bar{u}_L \gamma^\mu u_L - \frac{1}{2} \bar{d}_L \gamma^\mu d_L - \frac{2 \sin^2 \theta_w}{3} \bar{u}_L \gamma^\mu u_L + \frac{\sin^2 \theta_w}{3} \bar{d}_L \gamma^\mu d_L, \quad (4.32)$$

is the neutral current with the information of the couplings of the  $Z$  boson. Under a generic conformal transformation, we obtain

$$\frac{\tilde{\mathcal{L}}_F}{\sqrt{-\tilde{g}}} \supset \frac{g_2}{\sqrt{2}} \tilde{W}_\mu^+ \tilde{J}_\mu^- + \frac{g_2}{\sqrt{2}} \tilde{W}_\mu^- \tilde{J}_\mu^+ + \frac{g_2}{\cos \theta_w} \tilde{Z}_\mu \tilde{J}_Z^\mu, \quad (4.33)$$

where we have redefined the currents as

$$\tilde{J}_Z^\mu \equiv \frac{J_Z^\mu}{\Omega^3}, \quad \tilde{J}_\mu^\pm \equiv \frac{J_\mu^\pm}{\Omega^3}, \quad (4.34)$$

in agreement with the redefinitions of fermionic fields previously discussed.

The invariance of the total lagrangian density under generic conformal transformations allows us to compute any scattering or decay in the new frame, without introducing different Feynman rules from those already present in the original frame. In particular, we will be interested in the total decay widths of the intermediate gauge bosons into lighter states. Summing over all the allowed decay channels and boson polarizations, we obtain [203]

$$\tilde{\Gamma}_{W^\pm} = \frac{3g_2^2 \tilde{m}_W}{16\pi} = \frac{3 \cos^3 \theta_w}{2 \text{Lips}} \tilde{\Gamma}_Z, \quad (4.35)$$

where  $\tilde{m}_{W^\pm}, \tilde{m}_Z$ , are the dynamical masses in the Einstein frame and Lips denotes *Lorentz invariant phase-space* factors  $\text{Lips} \equiv \frac{7}{4} - \frac{11}{3} \sin^2 \theta_w + \frac{49}{9} \sin^4 \theta_w$ . Notice that the previous expressions assume that the gauge bosons are non-relativistic, while the fermions produced in the decay are relativistic. The relativistic or non-relativistic nature of a given particle is something intrinsic to the particle and should not depend on the conformal frame. Indeed, since both momenta and masses transform in the same way under conformal transformations, if a gauge boson is allowed to decay into a pair of fermions in a given frame, it will also be able to decay in another frame, and the other way round. For instance forbidden transitions in the Jordan frame such as  $Z \rightarrow \bar{t}t$ ,  $W \rightarrow tb$  are neither allowed in the Einstein frame. We will come back to this point in Section 4.8, cf. (4.100).

The explicit form of gauge boson and fermion masses in the expressions above depends *a priori* on the particular conformal transformation used, and therefore on the non-minimally coupled model considered. For the Higgs Inflation case, making use of the conformal transformation (3.7), we have

$$\tilde{m}_{\mathcal{A},f}^2 = \frac{g^2 M_P^2}{4\xi_h} \left(1 - e^{-\alpha\kappa|\phi|}\right), \quad (4.36)$$

with  $g = g_2, g_2/\cos\theta_w$  and  $\sqrt{2}y_f$ , for  $\mathcal{A} = W, Z$  bosons and fermions  $f$ , respectively. On the other hand, for the Higgs-Dilaton scenario, associated with a much more complicated conformal transformation, we obtain

$$(\tilde{m}_{\mathcal{A},f}^2)_{HD} = \frac{g^2 M_P^2}{4\xi_h} \left( \frac{1 - \sigma \cosh^2(\alpha\kappa(\phi_0 - |\phi|))}{1 - \sigma} \right). \quad (4.37)$$

Around the minimum of the potential we find an interesting connection between the masses in the two models, namely,  $(\tilde{m}_{\mathcal{A},f}^2)_{HD} = \tilde{m}_{\mathcal{A},f}^2 (1 + 6\xi_\chi)$  with

$$\tilde{m}_{\mathcal{A},f}^2 \simeq \frac{\alpha g^2 M_P}{4\xi_h} |\phi|. \quad (4.38)$$

All the physical scales in Higgs and Higgs-Dilaton Inflation coincide, up to small corrections proportional to the small parameter  $\xi_\chi$  (cf. Table 3.1). This will allow us to apply the results of the following sections to both models. From now on, we will focus on the Higgs Inflaton scenario, extrapolating the main results to the Higgs-Dilaton case. As we did with the gravitational sector, we will simplify the notation by omitting the tilde over all the Einstein frame quantities in the matter sector.

## 4.4 Perturbative Decay of the Higgs field

A natural reheating mechanism, given the strength of the interactions of the Higgs boson with the Standard Model particles, would be a single body perturbative decay of the inflaton quanta into the Standard Model particles right after the end of slow-roll. In this picture, the inflaton is understood as a collection of independent scalar particles with a finite probability of decaying into the particles to which it is coupled [176, 177, 178]. During the inflationary stage those couplings are usually neglected<sup>4</sup>, since, even if the excitations of those fields are produced, the *quasi*-exponential expansion dilutes them almost instantaneously. In those cases in which the mass of the decaying particle is larger than the Hubble rate, the curvature of the spacetime can be neglected and the decay probabilities computed using the perturbative Feynman rules in Minkowsky spacetime. In particular, we can modify the Higgs' equation of motion (4.16) to account for the proper quantum propagator. We have

$$\ddot{\phi} + 3H\dot{\phi} + (M^2 + \Pi(M))\phi = 0, \quad (4.39)$$

---

<sup>4</sup>These couplings are however fundamental for determining the radiative corrections during inflation. In most of the inflationary models, they are assumed to be small in order to prevent radiative corrections from *lifting* the flatness of the inflationary potential [46].

First family	Second family	Third family
$y_e \sim 2.9 \times 10^{-6}$	$y_\mu \sim 5.7 \times 10^{-4}$	$y_\tau \sim 10^{-2}$
$y_u \sim 1 \times 10^{-5}$	$y_c \sim 7.5 \times 10^{-3}$	$y_t \sim 1$
$y_d \sim 2.5 \times 10^{-5}$	$y_s \sim 5 \times 10^{-4}$	$y_b \sim 2.4 \times 10^{-2}$

Table 4.1: Approximate values of the Yukawa couplings in the Standard Model assuming a vacuum expectation value for the Higgs field  $v = 249$  GeV.

where  $\Pi(M)$  is the polarization operator for the zero mode,  $k^\mu = (M, \mathbf{0})$ . This operator can be understood as the sum of all the one-particle irreducible (1PI) Green functions. Diagrammatically, these functions are constructed as the sum of all Feynman diagrams that cannot be split into disconnected parts by cutting a single propagator line. Applying the optical theorem in Minkowsky spacetime [125],  $\text{Im } \Pi(M) = M \Gamma_{\text{tot}}$ , the imaginary part of the polarization operator<sup>5</sup> can be related to the total decay width  $\Gamma_{\text{tot}}$ , obtained by adding all the partial decays corresponding to each open channel. The effect of the polarization operator and the associated particle decays can be phenomenologically described by an effective (and somehow controversial from the point of view of the fluctuation-dissipation theorem [204]) damping term [176, 177, 178]

$$\ddot{\phi} + (3H + \Gamma_{\text{tot}}) \dot{\phi} + M^2 \phi = 0. \quad (4.40)$$

If the frequency of oscillations is sufficiently large compared with the Hubble rate and the decay width, i.e  $M^2 \gg \{H^2, \text{Im } \Pi(M)\}$ , we can safely neglect the temporal dependence of these quantities to obtain

$$\phi(t) \propto \exp \left[ -\frac{1}{2} (3H + \Gamma_{\text{tot}}) t \right] \sin(Mt). \quad (4.41)$$

The perturbative decay of the Higgs field into the Standard Model species translates in this approach into an additional decrease of the oscillation amplitude and the non-conservation of associated number of particles (4.21),

$$\frac{d}{dt} (a^3 n_\phi) = -\Gamma_\phi n_\phi a^3. \quad (4.42)$$

Notice that for the previously described perturbative decay to happen, two conditions must be fulfilled :

- i) There should be enough phase-space in the final states for the Higgs field to decay, i.e.  $M > 2m_{\mathcal{A},f}$ , which will only happen when the amplitude of the Higgs field becomes

---

<sup>5</sup>The real part simply *renormalizes* the bare particle mass  $M^2$ .

smaller than a certain value  $\phi_c$ . In particular, for a decay into gauge bosons and/or fermions, in the light of (4.38), one needs

$$\phi \gtrsim \phi_c \equiv \frac{1}{g^2} \sqrt{\frac{\lambda}{2}} M, \quad (4.43)$$

which can be compared to the initial amplitude of the Higgs at the end of inflation to obtain

$$\frac{\phi_c}{\phi_{\text{end}}} \simeq \frac{1}{3g^2 \xi_h}. \quad (4.44)$$

- ii) The decay rate of the Higgs field  $\Gamma \sim \frac{g^2}{8\pi} M$  has to be greater than the rate of expansion  $H \approx \frac{1}{\sqrt{6}} \frac{M}{M_P} \frac{\phi_{\text{end}}}{\pi j}$ , or in other words, its half-lifetime must be smaller than the age of the universe at that time. Such a condition,  $\Gamma > H$ , can be translated into the following inequality

$$j \geq j_c \equiv \frac{4(\alpha \kappa \phi_{\text{end}})}{g^2}, \quad (4.45)$$

which defines the critical number of semi-oscillations required for this second condition to be true.

The critical amplitude (4.43) below which the Higgs is allowed to decay into gauge bosons is of order  $\phi_c \sim 0.1M$ . When compared to the initial amplitude (3.27) of the Higgs at the end of inflation  $\phi_{\text{end}} \approx M_p \approx 10^6 M$ , we see that this critical amplitude is very small for the gauge bosons. The Higgs condensate would need to oscillate  $\sim 10^6$  times before being able to decay through this channel. The same applies to the top quark. In the case of other fermions, due to the wide range of the Yukawa couplings, cf. Table 4.1, several situations can take place. For instance, the decay channel into bottom and charm quarks is opened only after a few oscillations of the Higgs, while for the rest of quarks and leptons, the decay-channel has sufficient phase space from the very end of inflation. In general, the smaller the Yukawa coupling of a given fermion to the Higgs, the less oscillations the Higgs will go through before there is enough phase-space for it to decay into such a fermion. Notice however that the smallness of the Yukawa coupling implies also a smaller decay rate. Consider for instance the decay of the Higgs into electrons, whose Yukawa coupling is of order  $y_e \approx 10^{-6}$ . From the very end of inflation, see (4.43), there is phase-space in this channel for the Higgs to decay into. However, it is precisely the smallness of the electron's Yukawa coupling that allows the decay to be possible, which prevents the condition ii) to be fulfilled. The decay width is much smaller than the Hubble rate for a huge number of oscillations. Looking at (4.45), we realize that the Higgs condensate should oscillate  $j \sim 10^{12}$  times before the decay rate into electrons overtakes the Hubble rate.

One can check that the previous conclusions also hold for the rest of fermions of the Standard Model. When there is phase-space for the Higgs to decay into a given species, the decay rate does not catch up with the expansion rate and, *vice versa*, if the decay rate of a

given species overtakes the expansion rate, there is no phase-space for the decay to happen<sup>6</sup>. The universe has then to wait to be old enough for the Higgs field to decay into the Standard Model particles. Before any of those decay channels is opened, many other interesting non-perturbative effects will take place. Their study is the purpose of the following sections.

## 4.5 Tachyonic preheating

As we pointed out in Section 3.2, the effective square mass  $m_{\phi,\text{eff}}^2$  of the Higgs field is negative just after the end of inflation and will be so till the inflection point. When this happens spinoidal instability takes place and long wavelengths quantum fluctuations  $\phi_k$ , with momenta  $k = |\mathbf{k}| < m_{\phi,\text{eff}}$ , grow exponentially,  $\phi_k(t) \propto \exp\left(t\sqrt{m_{\phi,\text{eff}}^2 - k^2}\right)$ , giving rise to an infrared band. This effect is usually called *Tachyonic Preheating* [196, 197, 198]. Notice that this is a strongly nonlinear and non-perturbative effect. The perturbative description presented in the previous section has therefore a limited applicability. The width of the tachyonic band will be limited in our case by the point of maximum particle production, i.e. the end of inflation. At this point the effective mass  $m_{\phi,\text{eff}}$  takes a value

$$m_{\phi,\text{eff}}^2(\phi_{\text{end}}) = \left. \frac{\partial^2 V(\phi)}{\partial \phi^2} \right|_{\phi_{\text{end}}} \approx -\frac{M^2}{30}, \quad (4.46)$$

which corresponds to a maximum momentum for the tachyonic band  $k_{\text{max}} = 0.2M$ . This comes from vacuum quantum fluctuations,  $\phi_k(t) \propto \exp(Mt\sqrt{1/30 - (k/M)^2})$ , which grow exponentially. In the usual hybrid inflation scenarios [205] this give rise to large occupation numbers [196, 197, 198]. However, in our case, since the inflaton is fast rolling down the potential towards the positive curvature region, the duration of the tachyonic preheating stage is so short that the occupation numbers of those modes in the band do not grow significantly and the effect can be neglected. In particular, the time interval from the end of inflation till the inflection point is just  $M\Delta t \approx 0.5$  and therefore, even for the fastest growing mode,  $k = 0$ , its growth is only  $\sim e^{0.5/\sqrt{30}} \approx 1.09$ . This is a negligible effect and thus, one can still consider an initial spectrum of quantum vacuum fluctuations even at the inflection point. All the analytical estimates of the following sections will ignore this period of tachyonic instability, taking as initial conditions the amplitude (3.27) of the Higgs condensate at the end of inflation and quantum vacuum fluctuations.

## 4.6 Bose-Einstein Condensation and Parametric Resonance

As we pointed in Section 4.2, the occupation number of the inflaton  $\mathbf{k} = 0$  mode at the end of inflation is very large and the Higgs field effectively behaves, at least at zeroth order, as a Bose-Einstein condensate. This implies that, contrary to the assumptions of Section

---

<sup>6</sup>Note that the condition (4.43) (which prevents Higgs decay into gauge bosons and top quarks) assumes an averaged amplitude over a single Higgs oscillation, while smaller values are attained around the minimum of the potential when  $X(t) < \phi_c$ . However, when this happens, the Higgs field is well inside the non-adiabatic range (4.57), in which the very concept of particle is not properly defined (see Section 4.6 for details).

4.4, it should not be considered an ensemble of statistically independent static particles, but rather a coherent zero-mode oscillating field, whose spatial and temporal coherence can cause radical departures from the previous picture [179, 180]. To qualitatively understand this let us consider any of the trilinear Einstein-frame couplings among the Higgs field and the gauge bosons, forgetting for simplicity about polarizations. The direct decay probability,  $\mathcal{P}_D \equiv \mathcal{P}_{\phi \rightarrow \mathcal{A}\mathcal{A}}$ , of a Higgs particle  $\phi$  with zero momentum into two gauge bosons  $\mathcal{A}$  with same momenta  $\mathbf{k}$ , but opposite directions (as dictated by momentum conservation), is proportional to

$$\mathcal{P}_D \propto |\langle n_\phi - 1, n_{\mathbf{k}} + 1, n_{-\mathbf{k}} + 1 | a_{\mathbf{k}}^\dagger a_{-\mathbf{k}}^\dagger a_\phi | n_\phi, n_{\mathbf{k}} + 1, n_{-\mathbf{k}} + 1 \rangle|^2 = (n_{-\mathbf{k}} + 1)(n_{\mathbf{k}} + 1)n_\phi, \quad (4.47)$$

where  $a_{\pm\mathbf{k}}^\dagger$  and  $a_{\pm\mathbf{k}}$  are the gauge boson creation and annihilation operators and  $n_{\mathbf{k}}$  are the corresponding occupation numbers. Accordingly, the probability for the inverse decay,  $\mathcal{P}_I \equiv \mathcal{P}_{\mathcal{A}\mathcal{A} \rightarrow \phi}$ , to occur will be proportional to

$$\mathcal{P}_I \propto |\langle n_\phi + 1, n_{\mathbf{k}} - 1, n_{-\mathbf{k}} - 1 | a_{\mathbf{k}} a_{-\mathbf{k}} a_\phi^\dagger | n_\phi, n_{\mathbf{k}} + 1, n_{-\mathbf{k}} + 1 \rangle|^2 = n_{\mathbf{k}} n_{-\mathbf{k}} (n_\phi + 1). \quad (4.48)$$

If we assume spatial isotropy we can identify  $n_{\mathbf{k}} = n_{-\mathbf{k}} \equiv n_k$ . Taking into account that the effective decay width of the Higgs field in this channel will be given by the total decay width times the difference between the direct (4.47) and inverse (4.48) probabilities, then

$$\Gamma_{\text{eff}} \approx (1 + 2n_k) \Gamma_{\mathcal{A}}. \quad (4.49)$$

Therefore, for  $n_k < 1$  the effective decay width is determined just by the perturbative one,  $\Gamma_{\text{eff}} \approx \Gamma_{\text{tot}}$ . However, for a high occupation number  $n_k \gg 1$  the transition rates depend on the number of identical bosons in that state. This effect, known as Bose stimulation, is the familiar gain mechanism of an optical laser or a Bose-Einstein condensate<sup>7</sup> and constitutes the basis of *Parametric resonance* [179, 181, 182, 183], one of the most efficient preheating mechanisms.

Let us see how this parametric resonance takes place in the Standard Model. Strictly speaking the previous arguments apply only to gauge bosons. Fermions obey the Pauli exclusion principle, which implies that the occupation numbers for a given mode are restricted to be  $n_k \leq 1$ , so the system is severely constrained. While the number of gauge bosons can grow exponentially, that of fermions cannot and Fermi quantum statistic effectively transfers their energy to the higher momentum modes (for a study of fermionic preheating see for instance [206, 207]). Although it is hard to determine the relative importance of this effect in the self-consistent non-linear dynamics of Bose and Fermi fields, if the production of fermions is, as expected, proportional to the Yukawa coupling squared [208], then only the top quark production would be non-negligible. Let us focus therefore on the interaction of the Higgs field with the intermediate gauge bosons. The equation of motion for the fluctuations of each gauge field with a given polarization is given by

$$\mathcal{A}_k'' + \left( \frac{k^2}{a^2} + \tilde{m}_{\mathcal{A}}^2(t) + \Delta \right) \mathcal{A}_k = 0, \quad (4.50)$$

---

<sup>7</sup>Indeed the Bose-Einstein distribution function can be obtained simply from bosonic stimulation and detailed balance.

where the rate of expansion has been absorbed in the field definition<sup>8</sup>, i.e  $\mathcal{A} \rightarrow a^{-3/2}\mathcal{A}$ , and the corrections  $\Delta = -\frac{3}{4}\frac{\dot{a}}{a} - \frac{3}{2}\frac{\ddot{a}}{a}$  are always small for the matter dominated stage under consideration,  $a \propto t^{2/3}$ . The physical momentum  $k_{ph} \equiv k/a$  redshifts with time due to the expansion of the universe. Motivated by the inflationary dilution of any primordial abundances, the initial conditions are chosen to be the vacuum for scales well inside the horizon at the end of inflation. This corresponds to the initial-positive frequency solution

$$\mathcal{A}_k(kt \rightarrow -\infty) = \frac{1}{\sqrt{2\omega_k}} e^{-i\omega_k t}, \quad (4.51)$$

with  $\omega_k^2 = k_{ph}^2 + \tilde{m}_{\mathcal{A}}^2$ . Notice that the familiar notion in which positive energy solutions to the wave equation corresponds to particles, while negative energy solutions correspond to antiparticles is meaningless in time-dependent background fields. In Quantum Field Theory the definition of particle depends on the choice of modes. The vacuum state is usually defined as the eigenstate of minimal energy of the Hamiltonian, which must have a diagonalized form. Particles and antiparticles are associated with those creation and annihilation operators that diagonalize the Hamiltonian. Nevertheless, in the present case, the Hamiltonian is an explicit function of time, due to the presence of a time-dependent mass term. Consequently, the energy of individual particles is not conserved and the vacuum cannot be chosen as a time-independent eigenstate of the Hamiltonian. Notice however that, when the temporal dependences are not very rapidly varying in time, and the so-called adiabaticity condition

$$\left| \frac{\dot{\omega}_k}{\omega_k^2} \right| \ll 1 \quad (4.52)$$

is satisfied, we should expect to recover a meaningful definition of particle number. Around the minimum of the potential the masses of the intermediate gauge bosons (4.36) can be approximated by the trilinear interaction (4.38). These masses are much greater than the inflaton mass  $M$  for the main part of the Higgs oscillation. As a result, the typical frequency of oscillation of the gauge bosons is much higher than the one of the Higgs. This implies that, during most of the time, the effective masses of the intermediate bosons are changing adiabatically, which allows us to adopt a physically reasonable definition of particle by introducing instantaneous positive and negative energy solutions<sup>9</sup>

$$i \frac{d}{dt} \tilde{f}_k(t) = \pm \omega_k(t) \tilde{f}_k(t). \quad (4.53)$$

In terms of these functions, the solution of (4.50) can be expressed as a superposition of *integrated plane waves*

$$\mathcal{A}_k(t) = \frac{\alpha_k(t)}{\sqrt{2\omega}} e^{-i \int^t \omega_k(t') dt'} + \frac{\beta_k(t)}{\sqrt{2\omega}} e^{+i \int^t \omega_k(t') dt'}. \quad (4.54)$$

Here, the  $\alpha_k$  and  $\beta_k$  coefficients satisfy the Wronskian condition  $|\alpha_k|^2 - |\beta_k|^2 = 1$ . Note that the previous expression does indeed reduce to the standard *Born approximation* in the

<sup>8</sup>Notice that we maintain the notation  $\mathcal{A}$  for the new conformal field.

<sup>9</sup>Notice that the use of the particle picture defined by the instantaneous positive and negative frequency solutions is merely an ansatz which must be justified by physically reasonable results, such as an asymptotic finite number of particles.



constant  $\omega_k$  case. The associated instantaneous number of particles is defined as the ratio of the total energy in a given mode  $k$  divided by the energy quantum  $\omega_k$  at a given time

$$n_{\mathcal{A}} \equiv |\beta_k|^2 = \frac{\omega_k}{2} \left( \frac{|\dot{\mathcal{A}}_k|^2}{\omega_k^2} + |\mathcal{A}_k|^2 \right) - \frac{1}{2}. \quad (4.55)$$

The subtraction  $-1/2$  effectively eliminate quantum vacuum fluctuations from the counting. One can easily check that the initial-positive frequency solution (4.51), corresponds to the initial absence of particles within the horizon  $n_{\mathcal{A}}(kt \rightarrow \infty) = 0$ .

On the other hand, if the effective gauge boson masses change rapidly with time, as happens for values of the Higgs field very close to zero, the previous analysis breaks down. In that region the number of particles (4.55) is no longer an adiabatic invariant. The inequivalence between the vacua before and after the passage of  $\phi$  through the minimum of the potential can be interpreted as particle production [179, 181, 182, 183]. The violation of the adiabaticity condition  $|\dot{\tilde{m}}_{\mathcal{A}}|/\tilde{m}_{\mathcal{A}}^2 \ll 1$  corresponds to the region

$$|\phi| \lesssim \phi_a = \left( \frac{\xi_h |\dot{\phi}(t)|^2}{\alpha g^2 M_P} \right)^{1/3}, \quad (4.56)$$

where, again,  $g = g_2$ ,  $g_2/\cos\theta_w$  for the  $W$  or  $Z$  bosons respectively. Only outside this region, the notion of particle makes sense and an adiabatic invariant can be defined. Taking into account that and approximating the velocity of the field around zero as  $\dot{\phi}(j) \approx MX(j)$ , see Eq. (4.23), the general expressions (4.56) can be approximated as

$$\phi_a(j) = \left( \frac{\xi_h M^2 |\phi_{\text{end}}|^2}{\alpha j^2 g^2 \pi^2 M_P} \right)^{\frac{1}{3}} = \left( \frac{\lambda \pi}{3 \xi_h g^2 \alpha \kappa \phi_{\text{end}}} \right)^{\frac{1}{3}} j^{\frac{1}{3}} X(j). \quad (4.57)$$

Note that the previous region is indeed very narrow compared to the amplitude of the oscillating Higgs,  $\phi_a \sim 10^{-2} j^{1/3} X(j)$ . Therefore, the particle production in that region happens within a very short period of time as compared to the inflatons' oscillation period  $T = 2\pi/M$ ,

$$\Delta t_a(j) \sim \frac{2\phi_a}{|\dot{\phi}|} \sim 10^{-2} j^{1/3} M^{-1} \ll T, . \quad (4.58)$$

Different values of  $\lambda$  do not change appreciably the above conclusions about the smallness of the non-adiabatic regions. Given the weak dependence of  $\Delta t \propto j^{1/3}$ , many semi-oscillations ( $\sim 10^3$ ) will take place before the fraction of time spent in the non-adiabatic zone increases from a 1 % to a 10 %, as compared with the period of oscillations.

Moreover, despite the smallness of  $\phi_a$  as compared to the amplitude  $X(j)$ , it is important to note that the field range corresponding to the region of non-adiabaticity is still several orders of magnitude greater than those critical regions defined in Section 3.2. In particular, let us recall that there is a field value,  $\phi_t \sim M_P/\xi_h$ , below which there is a transition of the effective potential from a quadratic to quartic behaviour. However, this is well inside the region of non-adiabaticity,  $\phi_t \ll \phi_a$ , inside which the concept of particle during preheating is not properly defined. Besides, there is an interval of Higgs field values,  $|\phi| < \phi_c$ , for which

the Higgs perturbative decay into  $W$ ,  $Z$  and top quarks can occur (see (4.43) in Section 4.4), but it is also much smaller than the non-adiabaticity interval,  $\phi_c \ll \phi_a$ .

Let us discuss the non-perturbative creation of particles in the non-adiabatic region. This production is formally equivalent to the quantum mechanical problem of a particle scattering in a periodic potential, see Appendix A. Expanding (4.23) around the  $j$ -th zero at time  $t_j = \pi j$ , the evolution equation of the fluctuations (4.50) can be approximated as

$$\mathcal{A}_k'' + \left( \frac{k^2}{a^2} + \frac{\alpha g^2 M_p \phi_{\text{end}} |\sin(M(t - t_j))|}{4\pi j \xi_h} \right) \mathcal{A}_k = 0. \quad (4.59)$$

The violations of the adiabaticity condition are localized in the vicinity of  $t_j$ . Around these points the sinusoidal behaviour  $|\sin(M(t - t_j))|$  can be very well approximated by its argument,  $|\sin(M(t - t_j))| \approx M|t - t_j| \equiv |\tau|$ , which allows us to rewrite (4.59) as

$$\mathcal{A}_k'' + \omega_k^2(j) \mathcal{A}_k = 0, \quad (4.60)$$

where primes denote derivatives with respect to the rescaled time  $\tau = Mt$  and

$$\omega_k^2(j) \equiv \frac{q}{j} |\tau| + \frac{1}{j^{2/3}} \frac{k^2}{M^2}. \quad (4.61)$$

Note that the previous expression is reminiscent of models with cubic interactions as those considered in Refs. [209, 210, 211]. The possibility of *Tachyonic Resonance preheating* [210] is however excluded in our case due to the presence of the absolute value. The resonance parameter  $q$  in (4.61) is given by

$$q \equiv \frac{3g^2 \xi_h \alpha \kappa \phi_{\text{end}}}{4\pi \lambda}, \quad (4.62)$$

and depends, through the coupling  $g$ , on the gauge boson considered. Each zero crossing can be interpreted therefore as the quantum mechanical scattering problem of a particle crossing an inverted triangular potential. The coefficients  $\alpha_k$  and  $\beta_k$  in the expansion (4.54) before  $(-)$  and after  $(+)$  the  $j$  crossing are related by a Bogoliubov transformation

$$\begin{pmatrix} \alpha_k^{j+} e^{-i\Theta_k^j} \\ \beta_k^{j+} e^{+i\Theta_k^j} \end{pmatrix} = \begin{pmatrix} 1/T_k & R_k^*/T_k^* \\ R_k/T_k & 1/T_k^* \end{pmatrix} \begin{pmatrix} \alpha_k^{j-} e^{-i\Theta_k^j} \\ \beta_k^{j-} e^{+i\Theta_k^j} \end{pmatrix}, \quad (4.63)$$

where

$$\Theta_k^j(t) = \int_0^{t_j} \omega_k(t') dt', \quad (4.64)$$

and  $T_k$  and  $R_k$  are the transmission and reflection probabilities for a single scattering, satisfying  $|T_k|^2 + |R_k|^2 = 1$ . The details of the derivation of (4.63) can be found in the Appendix A. The general solution of the mode equation (4.60) can be written in terms of Airy functions  $\text{Ai}(z)$ ,  $\text{Bi}(z)$  for times before and after the zero crossing. Matching this solution with the adiabatic *integral plane wave* basis (4.60) before and after the crossing we obtain [212]

$$\mathcal{C}(x_j) \equiv T_k^{-1}(j) - 1 = \pi^2 [\text{Ai}(-x_j^2) \text{Ai}'(-x_j^2) + \text{Bi}(-x_j^2) \text{Bi}'(-x_j^2)]^2, \quad (4.65)$$

where we have used the Wronskian condition,  $\text{Ai}(z)\text{Bi}'(z) - \text{Bi}(z)\text{Ai}'(z) = \pi^{-1}$ . The argument of the Airy functions is defined as  $x_j \equiv k/k_*(j)$ , being  $k_*(j) \equiv q^{1/3}j^{1/3}M$  the typical momentum scale of the problem. Its order of magnitude coincide indeed with the one obtained via the Heisenberg uncertainty principle (see (4.58)),  $k(j) \sim a_j(\Delta t_a)^{-1} \approx k_*(j)/2^{1/3}$ . Notice that any momenta range will be red-shifted due to the expansion of the universe and, even the comoving typical moment  $k_*$ , is not a static quantity but rather depends on  $j$ .

The number of particles just after the  $j$ -th scattering,  $n_k(j^+)$ , in terms of the number of particles  $n_k(j^-)$  just before that scattering, can be computed from (4.63) to obtain<sup>10</sup> [181, 183]

$$n_k(j^+) = \mathcal{C}(x_j) + (2\mathcal{C}(x_j) + 1)n_k(j^-) + 2 \cos \theta_j \sqrt{\mathcal{C}(x_j)(\mathcal{C}(x_j) + 1)} \sqrt{n_k(j^-)(n_k(j^-) + 1)} \quad (4.66)$$

where  $\theta_j = 2\Theta_k^j - \phi_k + \text{Arg}\alpha_k + \text{Arg}\beta_k$  are some accumulated phases at each scattering. The first term in the right hand side of the previous expression corresponds to the spontaneous particle production, while the rest of terms depend on the number of previously existing bosons, and account therefore for the stimulated emission effects described at the beginning of this section. The previous expression is very enlightening. Let us emphasize its main properties. Expanding the combination of Airy functions in (4.65), we obtain

$$\mathcal{C}(x_j) = \frac{1}{3} e^{-D \frac{k^2}{k_*^2}}, \quad D = 4 \frac{3^{1/3} \Gamma(2/3)}{\Gamma(1/3)}, \quad (4.67)$$

The occupation number decay exponentially for large momenta, which reflects the fact that particle production is intrinsically an infrared effect. Notice also that the typical momentum scale  $k_*(j)$  is proportional to the coupling,  $k_*(j) \propto g^{1/3}$ , making the previous expression non-analytical for  $g = 0$ . The occupation number (4.66) is the result of a strong non-perturbative effect that cannot be obtained from any perturbative computation.

## 4.7 Spontaneous boson production and decay into fermions

Let us start by considering the spontaneous particle creation of  $W$  and  $Z$  bosons in each zero-crossing, corresponding to the low occupation limit  $n_k(j^-) \ll 1$ . It tells us about the number of particles produced in the first zero-crossing  $j = 1$  and in those successive scatterings  $j > 1$  in which the gauge bosons produced in the previous semioscillations have fully decayed into other SM particles. Retaining only the first term in the spectral number densities (4.66)

$$n_k(j^+) \approx \mathcal{C}(x_j), \quad (4.68)$$

we obtain the total number of particles of a given species with a given polarization associated to the spontaneous production

$$\Delta n(j^+) = \frac{1}{2\pi^2 a_j^3} \int_0^\infty dk k^2 \mathcal{C}(x_j) = \frac{q}{2j} \mathcal{I} M^3, \quad (4.69)$$

<sup>10</sup>See also the Appendix A for details.

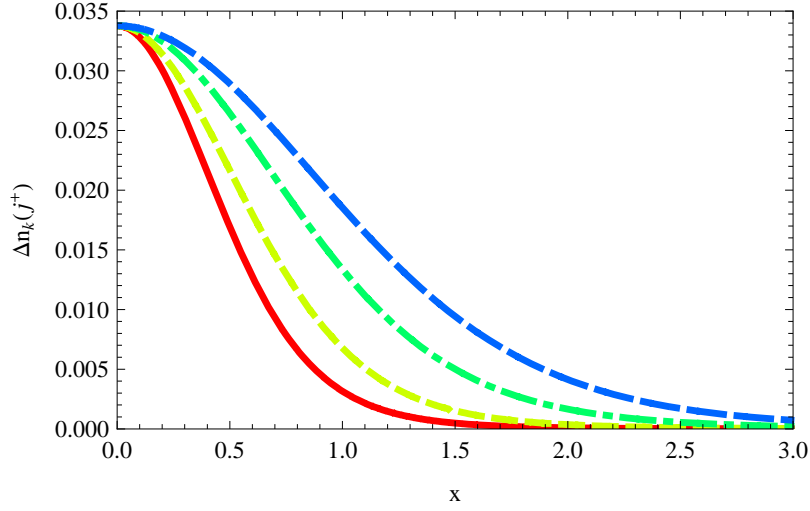


Figure 4.5: Spectral distributions (4.68) for the gauge bosons created in a single zero crossing through the first term of (4.66), calculated after  $j = 1, 2, 5$  and  $10$  oscillations (from left to right). The horizontal axis represents  $x_j = k/k_*(j)$ , so  $x = 1$  is the typical width of the band of momenta of particles created at the first scattering. For later times, the distributions broaden out to greater momenta, since the argument of (4.68),  $x_j$  behaves as  $\propto j^{-1/3}$ . The typical momenta of the distribution agree with the one calculated in Section 4.6.

where  $\mathcal{I} = \int_0^\infty \mathcal{C}(x_j)x^2 dx \approx 0.0046$  and  $q$  are the resonant parameters given by (4.62). The non-perturbative production of these particles is proportional to the coupling square. If the couplings of the Higgs field to the intermediate gauge bosons were not so large ( $g_2^2 \sim 0.3$ ), then their production would be very suppressed. Notice that non-perturbative parametric resonance is not the only place in which changing effective masses might play a role. After the passage through the minimum of the potential, the created number of  $W$  and  $Z$  particles remains almost constant, while their effective masses (4.38) are *boosted* due to the coupling with the Higgs field,  $m_A^2(t) \propto |\phi(t)|$ , which increases their probability of decaying into fermions. The process is schematically represented in Fig. 4.6.

The total number density of gauge bosons just previous to the  $(j+1)$ -th zero crossing,  $n((j+1)^-)$ , is then given by

$$n((j+1)^-) = n(j^+)e^{-\int_{t_j}^{t_{j+1}} \Gamma dt} = n(j^+)e^{-\langle \Gamma \rangle_j \frac{T}{2}}, \quad (4.70)$$

where the exponential factor  $e^{-\langle \Gamma \rangle_j \frac{T}{2}}$  accounts for the decay into fermions between those two crossings. The number of fermions produced in that time is simply

$$\Delta n_F(j) = 2 \times 3 \times \left[ n_Z(j^+)(1 - e^{-\langle \Gamma_Z \rangle_j \frac{T}{2}}) + 2 n_W(j^+)(1 - e^{-\langle \Gamma_W \rangle_j \frac{T}{2}}) \right], \quad (4.71)$$

where the factor  $2 \times 3$  reflects that each gauge boson can have one out of three polarizations and decay into two fermions, while the extra factor 2 in front  $n_W$ , accounts both for the  $W^+$

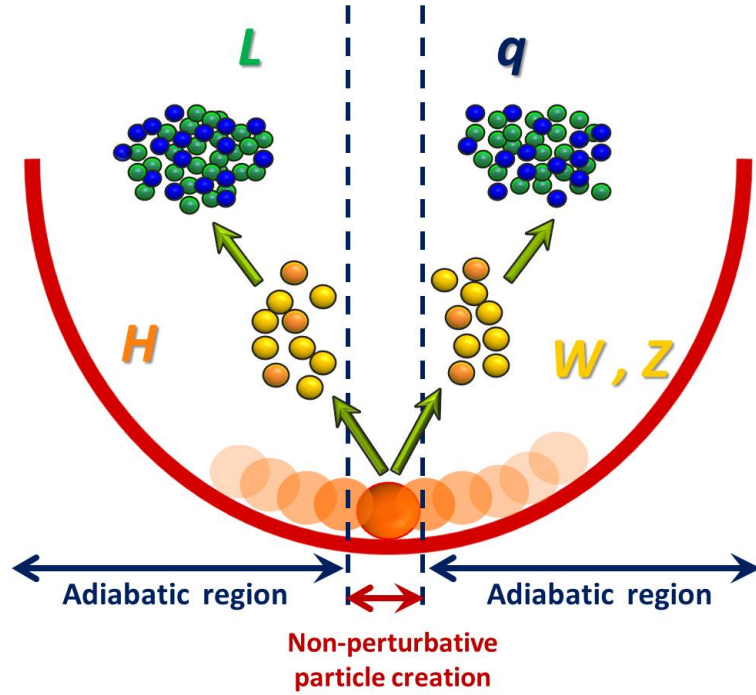


Figure 4.6: Schematic view of gauge boson and fermion production in Higgs Inflation: the slow evolution of the Standard Model effective masses allows to adopt a physically reasonable adiabatic definition of particle during most of the oscillation period. Nevertheless, for values of the Higgs field very close to the minimum of the potential, the adiabaticity condition becomes violated, which can be interpreted as particle production. Most of the created particles are intermediate gauge bosons, since the production of fermions is limited by Pauli blocking. The latter are produced as secondary products of the created gauge bosons, which tend to decay into them via the Standard Model decay widths, amplified by the growing Higgs amplitude.

and  $W^-$  decays. The averaged value of the decay widths (4.23) in the previous expressions can be estimated as

$$\begin{aligned}\langle \Gamma_{Z \rightarrow all} \rangle_j &= \left( \frac{g_2}{\cos \theta_w} \right)^3 \frac{M_P \text{Lips}}{16\pi \sqrt{\xi_h}} \left\langle (1 - e^{-\alpha \kappa |\phi|})^{1/2} \right\rangle_j \equiv \frac{2\gamma_Z}{T} F(j), \\ \langle \Gamma_{W \rightarrow all} \rangle_j &= \frac{3 \cos^3 \theta_w}{2\text{Lips}} \langle \Gamma_{Z \rightarrow all} \rangle_j \equiv \frac{2\gamma_W}{T} F(j),\end{aligned}\quad (4.72)$$

where  $T = 2\pi/M$  is the typical oscillation period and we have averaged the field dependence between two crossings as

$$F(j) \equiv \left\langle \left( 1 - e^{-\alpha \kappa |\phi|} \right)^{1/2} \right\rangle_j \approx \frac{0.3423}{\sqrt{j}}. \quad (4.73)$$

The constants  $\gamma_Z, \gamma_W$  are just numerical factors depending on the model's parameters and decaying species,

$$\gamma_Z = \left( \frac{g_2}{\cos \theta_w} \right)^3 \frac{\sqrt{3}\xi_h^{1/2}}{16\lambda^{1/2}} \text{Lips} \approx 14.23 \lambda^{-\frac{1}{4}}, \quad \gamma_W \equiv \frac{3 \cos^3 \theta_w}{2\text{Lips}} \gamma_Z \approx 5.91 \lambda^{-\frac{1}{4}}, \quad (4.74)$$

The gauge bosons will tend to decay into fermions in a time inversely proportional to their mean lifetime (4.72). The typical time of decay turns out to be of order  $\Delta t \simeq j^{1/2} M^{-1}$ , where the  $j$ -dependence comes from (4.73). Numerically, after  $j = 1, 2, 10, 15$  and  $20$  zero-crossings, the 99.5 %, 98.5 %, 94.2 %, 87.4 %, 81.9 %, 77.4 % of the produced  $Z$  particles have decayed into fermions (and a similar, though smaller, fraction of the  $W$  bosons). Although significant during the first few oscillations, the number of created fermions becomes smaller and smaller as time goes by. Notice however that the relevant quantity for recovering the radiation dominated era is not the number of particles, but rather the energy density transferred from the inflaton to the fermions (through the gauge bosons). In what follows we study this energy transfer in two different scenarios. Both of them neglect the contribution of the residual gauge bosons that have not decayed into fermions and the corresponding stimulated emission. They are therefore just based on the combination of spontaneous particle creation and perturbative decays. The first one considers what is usually called *Instant Preheating* [199], in which the transferred energy from the inflaton to the fermions is so large that the universe reheats in a single oscillation. The second one, that we called *Successive Instant Preheating*, extends the *Instant Preheating* scenario to multiple oscillations.

#### 4.7.1 Instant Preheating

Let us focus on the first oscillation. As we pointed out at the end of the previous section, roughly a 99.5 % of the gauge bosons produced in the first oscillation decay into fermions. The large decay rate allows us to neglect the exponential factors  $e^{-\gamma \langle \Gamma \rangle_j} \ll 1$  in (4.71) and compute the averaged energy density of the fermions as

$$\Delta \rho_F(1) \sim 6 [\Delta n_Z(1) E_{F_Z}(1) + 2 \Delta n_W(1) E_{F_W}(1)], \quad (4.75)$$

where

$$E_{F\mathcal{A}}(j) \equiv \left\langle \sqrt{k_f^2 + m_f^2} \right\rangle_j \approx \langle k_f \rangle_j \approx \frac{1}{2} \langle m_{\mathcal{A}} \rangle_j \approx \frac{g}{4\xi_h^{1/2}} F(j) M_p, \quad (4.76)$$

denotes the mean energy of the decay products. Notice that we have taken into account that every gauge boson decay into two fermions and assumed that the produced fermions are relativistic, while the gauge bosons are non-relativistic. This assumption will be justified in Section 4.8.

Using (4.69) the averaged energy density (4.75) becomes

$$\Delta\rho_F(1) = \varepsilon \left( \frac{1}{2} M^2 \phi_{\text{end}}^2 \frac{1}{\pi^2} \right) F(1) \quad (4.77)$$

with

$$\varepsilon \equiv \frac{3^{1/2} \pi (2 + \cos^{-3} \theta_w) \mathcal{I} g_2^3}{4 \lambda^{1/2} \xi_h^{1/2} (\alpha \kappa \phi_{\text{end}})} \approx 3 \times 10^{-5} \lambda^{-3/4}. \quad (4.78)$$

Comparing this quantity with the energy density of the inflaton

$$\rho_\phi(j) = \frac{1}{2} M^2 \phi_{\text{end}}^2 \left( \frac{j + 1/2}{\pi} \right)^2, \quad (4.79)$$

evaluated at the maximum amplitude of the first semi-oscillation,  $Mt \approx 1.5\pi$ , we obtain the ratio

$$\epsilon(1) \equiv \frac{\rho_F(1)}{\rho_\phi(1)} = \frac{\varepsilon F(1)}{(2/3)^2} \approx 2 \times 10^{-5} \lambda^{-3/4}. \quad (4.80)$$

The energy transferred to the fermions during the first oscillation is therefore just a tiny percentage ( $\sim 0.004\%$  for  $\lambda = 0.4$ ) of the inflaton's energy. Thus, the so called *Instant Preheating* [199] mechanism results frustrated here. In order to make it work efficiently, the couplings of the theory must be fine-tuned, in such a way that a significant fraction of the energy of the inflaton was transferred (in the first semi-oscillation) to the decay products of the bosons to which the inflaton is coupled. Moreover, in the *Instant Preheating* scenario, the produced fermions must be non-relativistic while the effective behaviour of the background inflaton should be effectively mimicking that of relativistic matter (like *e.g.* in  $\lambda\phi^4$  models). Only in this case it would be guaranteed that the remnant energy of the inflaton would decay faster than that of the fermions. If the inflaton would effectively behave as non-relativistic matter and the produced fermions were relativistic, the energy of the inflaton could again overtake very soon that of the fermions, because the fermion's energy would decrease faster than that of the background. That is, precisely, the situation we have in the scenario under discussion. Even if we had found that  $\epsilon(1) \sim \mathcal{O}(1)$ , the relativistic nature of the fermions and the non-relativistic effective behaviour of the Higgs would prevent the universe to instantaneously reheat at that point.

### 4.7.2 Successive Instant Preheating

One could hope that, after a certain number of oscillations  $j_p$ , the successively produced fermions might accumulate enough energy as to finally equal that of the Higgs condensate,  $\epsilon(j_p) \sim \mathcal{O}(1)$ . Since the total energy stored in the Higgs field decreases as the universe expands (cf. Eq. (4.79)), also does the amount of energy that must be transferred to the fermions. Moreover, the number of created fermions increases monotonically with time, adding energy in each semi-oscillation. These two effects contribute therefore to increase the ratio  $\epsilon(j_p)$ . On the other hand, the relativistic nature of the fermions and the decrease of their production rate with the expansion of the universe (cf. Eq. (4.72)) tend to decrease this ratio. In order to obtain the temporal evolution of the energy transferred to the fermions, all these competing effects must be incorporated in an unified formalism. To do this, let us start assuming, both for simplicity as for making the mechanism more efficient, that the gauge bosons do not accumulate significantly, neglecting then the surplus between successive decays. The intermediate gauge bosons are then produced just through spontaneous creation at each zero-crossing and only the first term in (4.66) is considered. In this case the averaged energy density of the fermions produced between  $t_j$  and  $t_{j+1}$  will be

$$\begin{aligned} \Delta\rho_F(j) &\sim 6 \left[ (1 - e^{-\gamma_Z F(j)}) \Delta n_Z(j) E_{F_Z}(j) + 2(1 - e^{-\gamma_W F(j)}) \Delta n_W(j) E_{F_W}(j) \right] \\ &= \varepsilon \left( \frac{1}{2} M^2 \phi_{\text{end}}^2 \frac{1}{\pi^2} \right) \frac{F(j)}{j} \Upsilon(j), \end{aligned} \quad (4.81)$$

where  $\varepsilon$  is given by (4.78) and we have defined

$$\Upsilon(j) \equiv 1 - \frac{e^{-\gamma_Z F(j)} + 2 \cos^3 \theta_w e^{-\gamma_W F(j)}}{1 + 2 \cos^3 \theta_w}. \quad (4.82)$$

The ratio between the total fermionic energy density after the  $j$ -th zero crossing and that of the Higgs condensate is generically given by

$$\varepsilon(j)_F \equiv \frac{\rho_F(j)}{\rho_\phi(j)} = \frac{2\pi^2 \left(j + \frac{1}{2}\right)^2}{M^2 \phi_{\text{end}}^2} \sum_{i=1}^j \Delta\rho_F(i) \left(\frac{i}{j}\right)^{8/3}, \quad (4.83)$$

where we have used (4.79) and taken into account the relativistic behaviour of the fermionic fluid

$$\rho_F(j) = \sum_{i=1}^j \Delta\rho_F(i) \left(\frac{a_i}{a_j}\right)^4 = \sum_{i=1}^j \Delta\rho_F(i) \left(\frac{i}{j}\right)^{8/3}. \quad (4.84)$$

For the particular averaged energy density (4.81), the ratio (4.83) becomes

$$\varepsilon(j)_F \equiv \frac{\rho_F(j)}{\rho_\phi(j)} \approx \varepsilon \frac{\left(j + \frac{1}{2}\right)^2}{j} \sum_{i=1}^j F(i) \Upsilon(i) \left(\frac{i}{j}\right)^{5/3}. \quad (4.85)$$

Notice that, even for large values of the couplings ( $g_2^2 \sim 0.3$ ), the initial transfer of energy is very small. For  $\lambda = 0.4$ , the numerical values (4.85) after  $j = 1, 2, 5, 10, 15, 20$  semi-oscillations are respectively  $\varepsilon(j)[\times 10^5] \sim 3.90, 5.97, 11.82, 37.26, 65.04, 97.59$ . If we could



extrapolate the previous formalism to the creation of fermions around the minimum of the potential, we would obtain even more ridiculous numbers, due to the smallness of the Yukawa couplings<sup>11</sup>. As clearly seen, the energy ratio (4.85) is also a very slowly growing function of time. After 20 zero-crossings, only  $\sim 0.03\%$  of the Higgs energy has been transferred into fermions. Indeed, if the former formalism could be applied up to arbitrary times, we will need at least  $j_p \sim \mathcal{O}(10^4)$  semi-oscillations to achieve the critical value  $\varepsilon(j) \sim \mathcal{O}(1)$ . The *successive Instant Preheating* mechanism seems therefore not efficient enough as to rapidly reheat the universe. Nevertheless, as we will see in the next section, the up-to-now neglected parametric resonance effects will completely modify the previous picture.

## 4.8 A new preheating mechanism: *Combined Preheating*

In this section, the *successive Instant Preheating* mechanism developed in the previous section is extended to accommodate the stimulated creation of gauge bosons. As pointed out in Section 4.6, this effect becomes the dominant one in the large occupation limit  $n_k \gg 1$ . In this case, the first term in (4.66) can be neglected to obtain

$$n_k(j^+) \approx n_k(j^-) \left( (2\mathcal{C}(x_j) + 1) - 2 \cos \theta_j \sqrt{\mathcal{C}(x_j)(\mathcal{C}(x_j) + 1)} \right) \equiv n_k(j^-) e^{2\pi\mu_k(j)}, \quad (4.86)$$

where  $n_k(j^\pm)$  denote the spectral number densities of the produced gauge bosons before  $(-)$  and after  $(+)$  the  $j$ -th scattering and the Floquet or growth index  $\mu_k(j)$  is given by [181, 183]

$$\mu_k(j) \approx \frac{1}{2\pi} \log \left( (2\mathcal{C}(x_j) + 1) - 2 \cos \theta_j \sqrt{\mathcal{C}(x_j)(\mathcal{C}(x_j) + 1)} \right). \quad (4.87)$$

The accumulated phases at the  $j$ -th scattering,  $\theta_j$  play a very important role, since they can enhance ( $\cos \theta_j < 0$ ) or decrease ( $\cos \theta_j > 0$ ) the production of particles at each scattering. Depending on their value, we can consider three different cases:

- i) The typical behaviour of the Floquet index, for  $\cos \theta = 0$ ,

$$\mu_k^{(\text{typ})} = \frac{1}{2\pi} \log (2\mathcal{C}(x_j) + 1), \quad (4.88)$$

- ii) The maximum index, achieved for  $\cos \theta = -1$

$$\mu_k^{(\text{max})} = \frac{1}{\pi} \log \left( \sqrt{\mathcal{C}(x_j)} + \sqrt{\mathcal{C}(x_j) + 1} \right), \quad (4.89)$$

- iii) The average index over an oscillation

$$\mu_k^{(\text{av})} = \frac{1}{2\pi} \int_0^{2\pi} \mu_k(\theta) d\theta = \frac{1}{2\pi} \log (\mathcal{C}(x_j) + 1). \quad (4.90)$$

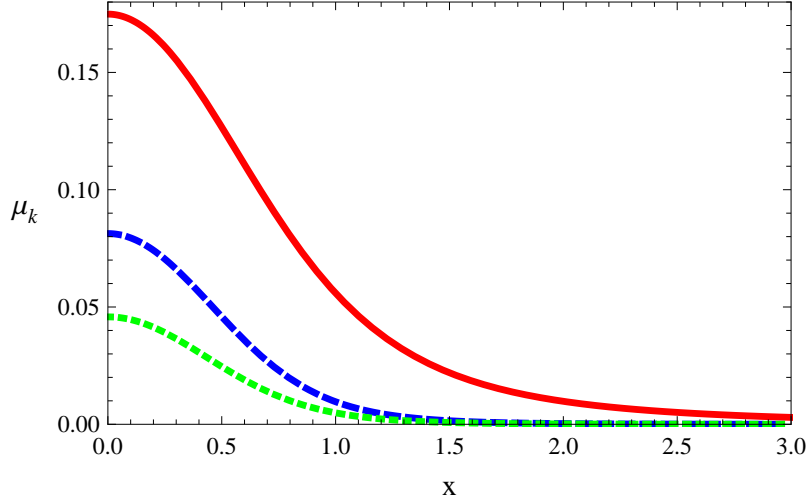


Figure 4.7: The Floquet index for a given polarization of the  $W$  and  $Z$  bosons as a function of the variable  $x_j = k/k_*(j)$ . Here we show the maximum (continuous red), the average (short dashed green) and the typical (long dashed blue) indices.

All these possibilities are shown in Fig. 4.7, as a function of  $x_j \equiv k/k_*(j)$ , the natural argument of the transmission probability scattering functions (4.65).

As explained in Ref. [183], when  $\Delta\theta_j \equiv \theta_{j+1} - \theta_j \gg \pi$ , the effect of resonance will be chaotic, being then the phases essentially random at each scattering. For instance, using the effective frequencies of the fluctuations (4.61) of the gauge fields  $\mathcal{A} = W, Z$ , these phases can be estimated, for the relevant range of momenta, as

$$\Delta\theta_j = \frac{1}{M} \int_{t_j} t_{j+1} dt \sqrt{\frac{k^2}{a^2} + \tilde{m}_{\mathcal{A}}^2} \approx \frac{g\pi\sqrt{3\xi_h}}{2\sqrt{\lambda}} F(j) \simeq 65\pi \frac{g}{\lambda^{1/4}} j^{-1/2}. \quad (4.91)$$

Note that, in obtaining the second equality, we have neglected the momenta of the gauge bosons, since, as we will justify later, they are completely non-relativistic.

Comparing the above formula with  $\pi$ , we see that the end of the stochastic behaviour will occur after  $j \sim 5 \times 10^3 g_2^2 / \sqrt{\lambda} \sim 10^3$  zero crossings. Therefore, since, for the first thousand of oscillations of the Higgs, the accumulated phases of the fluctuations of the gauge bosons will be chaotic, we will average out the phases and work with  $\mu_k^{(\text{av})}$ .

On the other hand, the perturbative decay of the produced vector bosons occurs, as before, between two successive Higgs zero-crossings,  $n((j+1)^-) = n(j^+) \exp(-\gamma F(j))$ , where  $F(j)$  is given by (4.73) and  $\gamma = \gamma_Z, \gamma_W$  by (4.74). Taking into account (4.86), we can express the number of gauge bosons just after the  $(j+1)$ -th scattering in terms of the number just after the previous one

$$n_k((j+1)^+) = n_k((j+1)^-) e^{2\pi\mu_k(j+1)} = n_k(j^+) e^{-\gamma F(j)} e^{2\pi\mu_k(j+1)}. \quad (4.92)$$

<sup>11</sup>A possible exception would be the top quark.

Applied recursively, this formula allows us to obtain the occupation number for each species and polarization, just after the  $(j+1)$ -th scattering, in terms of the initial abundances  $n_k(1^+)$ ,

$$n_k((j+1)^+) = n_k(1^+) \exp \left[ -\gamma F_\Sigma(j) \right] \exp \left[ 2\pi \sum_{i=1}^j \mu_k(i+1) \right], \quad (4.93)$$

where we have defined  $F_\Sigma(j) \equiv \sum_{i=1}^j F(i)$ . The total number density of created particles just after the  $j$ -th scattering is given by

$$\begin{aligned} n(j^+ \geq 2) &= \frac{1}{2\pi^2 a_j^3} e^{-\gamma F_\Sigma(j-1)} \int dk k^2 n_k(1^+) e^{\{2\pi \sum_{i=1}^j \mu_k(i)\}} \\ &= \frac{qM^3}{2\pi^2 a_j^3} e^{-\gamma F_\Sigma(j-1)} \int du u^2 \mathcal{C}(u) \prod_{l=2}^j (1 + \mathcal{C}(u l^{-1/3})), \end{aligned} \quad (4.94)$$

where we have defined a new variable  $u \equiv j^{1/3} x_j < 1$ . This expression plays a central role in what we have called *Combined Preheating* [77]. It encodes the effect of non-perturbative parametric resonance at the bottom of the potential and perturbative decay during the rest of the semi-oscillation. As we will see in what follows, this combination gives rise to a very rich phenomenology, clearly different from that appearing in other preheating mechanisms, such as *Parametric Resonance* or *Instant Preheating*. In order to clarify and make explicit the consequences of *Combined Preheating*, let us expand the combination of Airy functions  $\mathcal{C}$  in (4.94) for small arguments. We obtain

$$\begin{aligned} n(j^+ \geq 2) &\approx \frac{qM^3}{2\pi^2 j^2} e^{-\gamma F_\Sigma(j-1)} A^{j-1} C \int du u^2 e^{-Du^2} e^{-B(\sum_{i=2}^j i^{-2/3})u^2} \\ &= \frac{qM^3}{2\pi^2 j^2} e^{-\gamma F_\Sigma(j-1)} A^{j-1} C \frac{\sqrt{\pi}}{4} \left( D + B \sum_{i=2}^j i^{-2/3} \right)^{-3/2}, \end{aligned} \quad (4.95)$$

where we have defined

$$A = \frac{4}{3}, \quad B = 3^{1/3} \frac{\Gamma(2/3)}{\Gamma(1/3)}, \quad C = \frac{1}{3}, \quad D = 4B. \quad (4.96)$$

The comparison, for different  $j$ 's, between the exact expression (4.94) and the Gaussian approximation (4.95) is shown in Fig. 4.8. In this approximation, the resonant behaviour is encoded in the factor  $A^{j-1}$ . Notice that, since  $A$  is bigger than one, for sufficiently large  $j$ , the resonant effects will eventually overtake the decaying factor  $e^{-\gamma F_\Sigma(j-1)}$ . Taking into account the factor  $1/j^2$ , due to the expansion of the universe, we conclude that this will happen for those values of  $j$  for which

$$(j-1) \log A - 2 \log j > \gamma F_\Sigma(j-1). \quad (4.97)$$

On the other hand, the maximum value

$$u_p \equiv (D + B \sum_{i=2}^j i^{-2/3})^{-1/2} \quad (4.98)$$

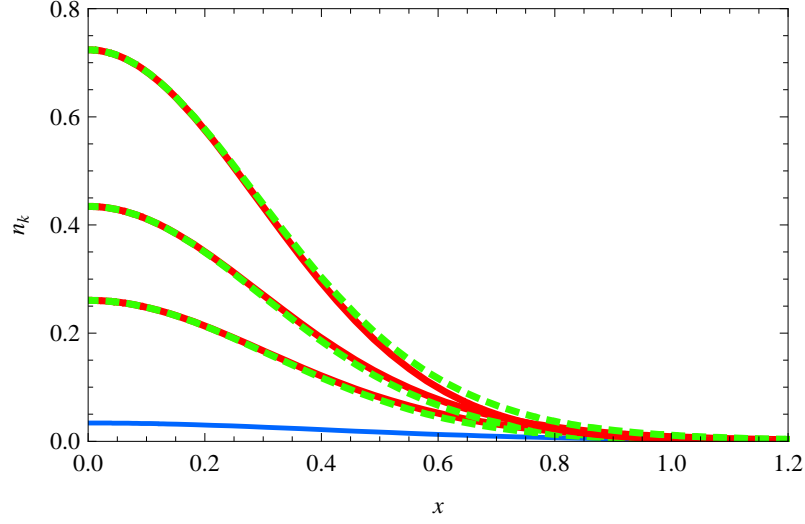


Figure 4.8: The initial spectral distribution  $n_k(1^+)$  (lower blue curve) and the Gaussian approximation (4.95) for different  $j$ 's greater than 2 (rest of the curves), describing the resonant behaviour. The approximation is so good that it is hard to distinguish it from the real curve, presenting small deviations just on the tail. The horizontal axis is  $x = k/k_*(1)$  and the curves correspond to different  $j$ 's. It is clearly distinguishable the fact that only the range  $x < 1$  ( $k < k_*(1)$ ) is filtered and therefore excited through parametric resonance, no matter if  $j \gg 2$ .

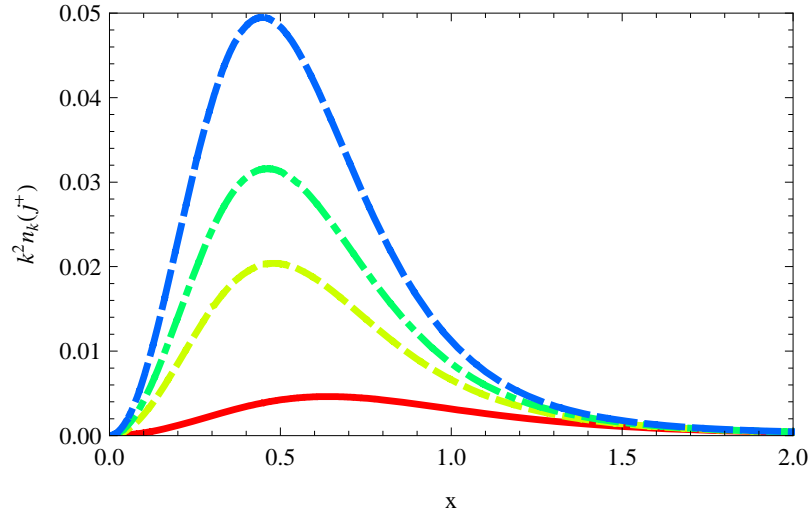


Figure 4.9: Successive spectral distributions  $k^2 n_k(1^+) e^{2\pi \sum_{k=2}^j \mu_k(j)}$ , at different  $j$ 's, including the volume factor  $k^2$ . One can see the predicted (4.99) slow displacement of the maxima of the distribution. The x-axis is given in terms of  $x = k/(k_*(1))$ .

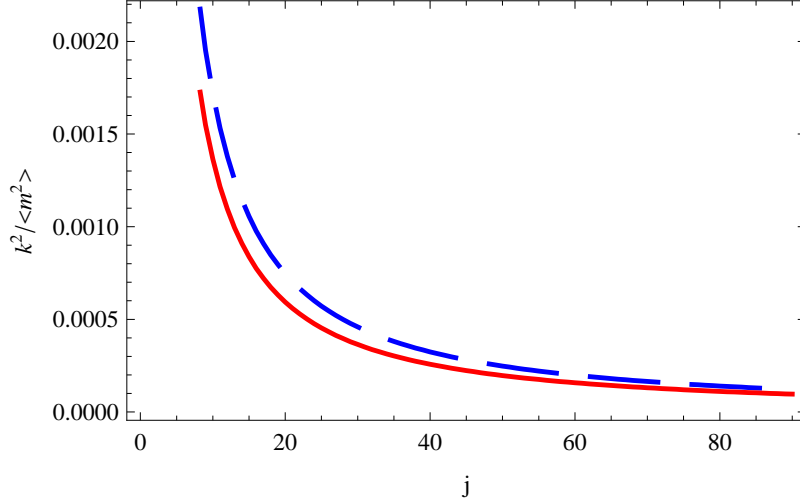


Figure 4.10: The ratio  $k^2/\langle m^2 \rangle$  between the typical momenta produced around zero and the averaged mass in every oscillation for the  $W$  (dashed blue line) and  $Z$  bosons (continuous red line) as a function of the number of oscillations. This ratio is significantly smaller than 1 for all crossings, which allows us to consider the produced gauge bosons as non-relativistic.

of the integrand  $u^2 e^{-(D+B \sum_{i=2}^j i^{-2/3})u^2}$  inside (4.95) determines the typical (comoving) excited momentum

$$k_p \approx \frac{k_*(1)}{(D + B \sum_{i=2}^j i^{-2/3})^{1/2}}. \quad (4.99)$$

Its behaviour can be observed in Fig. 4.9. According to the previous expression, the peaks of the successive spectral distributions  $k^2 n_k(1^+) e^{2\pi \sum_{k=2}^j \mu_k(j)}$ , slowly evolve to smaller momenta for larger  $j$ . Notice that the typical momentum  $k$  of the resonant fluctuations is always of order  $k_*(1)$ , independently of how many oscillations are performed by the Higgs field. This can be understood as a consequence of the filtering  $k \lesssim k_*(1)$  performed by the initial spectral distribution  $n_k(1^+)$ , cf. Eq. (4.93). On the other hand, comparing the evolution of the typical momenta (4.99) with the averaged masses of the gauge bosons in every oscillation we realize that the ratio

$$\frac{(k_p/a_j)^2}{\langle m_A \rangle_j^2} = \frac{4\lambda q^{2/3}}{3g^2 \xi_h (D + B \sum_{i=2}^j i^{-2/3}) (a_j F(j))^2} \propto \frac{1}{g^{2/3}} \frac{1}{j^{1/3} (D + B \sum_{i=2}^j i^{-2/3})}, \quad (4.100)$$

is not only initially smaller than one, but also a monotonically decreasing function of time. This behaviour is shown in Fig. 4.10. We can conclude therefore that the vector bosons produced at the bottom of the potential are always non-relativistic, which justifies *a posteriori* the calculation of the energy of the fermions (4.76) performed in Section 4.7.1. If we could extrapolate (4.100) to the case of fermions, we would realize that they would be mainly relativistic, due to the smallness of the Yukawa couplings. The only exception would be the top quark.

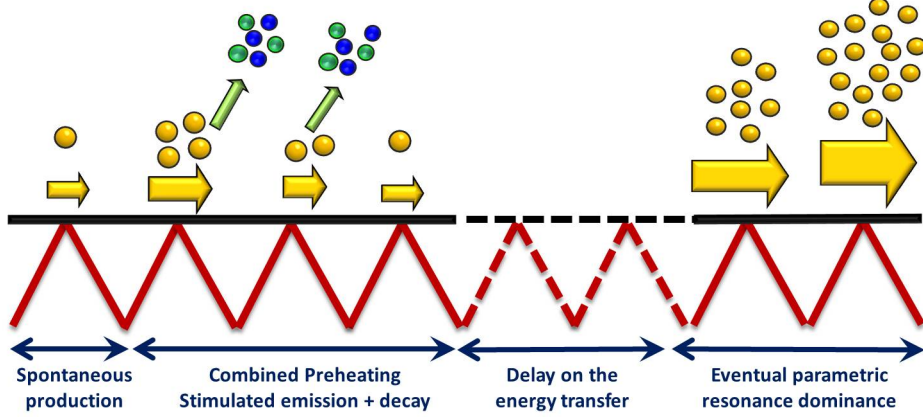


Figure 4.11: Schematic representation of the *Combined Preheating* process: The non-perturbatively created gauge bosons in the successive scatterings in the inverted periodic triangular potential (first spontaneously and then via stimulated emission) tend to decay into fermions while their effective masses (4.38) are *boosted* due to the coupling with the Higgs field. These decays initially delay the development of parametric resonance and the consequent exponential particle production. Eventually, the resonant effects overtake the perturbative decays and parametric resonance develops as usual, i.e. as if the produced bosons would not decay perturbatively during each semi-oscillation.

The energy density transferred to the fermions between the  $j$ -th and the  $(j + 1)$ -th scatterings, will be

$$\begin{aligned}
 \Delta\rho_F(j) &= 6 \left[ (1 - e^{-\gamma_Z F(j)}) n_Z(j^+) E_{F_Z}(j) + 2(1 - e^{-\gamma_W F(j)}) n_W(j^+) E_{F_W}(j) \right] \\
 &= \tilde{\epsilon} \left( \frac{1}{2} M^2 \phi_{\text{end}}^2 \frac{1}{\pi^2} \right) A^{j-1} C \frac{\sqrt{\pi}}{4} \left( D + B \sum_{l=2}^j l^{-2/3} \right)^{-\frac{3}{2}} \frac{q_*}{j^2} F(j) \times \\
 &\quad \times \left( (1 - e^{-\gamma_Z F(j)}) e^{-\gamma_Z \Gamma_\Sigma(j-1)} + 2 \cos \theta_w^3 (1 - e^{-\gamma_W F(j)}) e^{-\gamma_W \Gamma_\Sigma(j-1)} \right), \tag{4.101}
 \end{aligned}$$

where we have used (4.76) and defined a factor  $q_* \equiv q/g^{2/3}$  common to both bosonic species. The gauge coupling dependence is nonetheless incorporated into the definition of the  $\tilde{\epsilon}$  parameter

$$\tilde{\epsilon} \equiv \frac{3g_2^3 \lambda^{1/2}}{(\cos \theta_w)^3 \xi_h^{5/2} (\alpha \kappa \phi_{\text{end}})^2}, \tag{4.102}$$

which modulates the strength of the effect. The ratio of the total energy density transferred into the fermions to that of the inflaton is again (4.81), but now with  $\Delta\rho_F$  given by (4.101). Here we can clearly see the two competing effects; schematically represented in Fig. 4.11. On the one hand we have the perturbative decay of the bosons, given by the factors  $(1 - e^{-\gamma F(j)}) e^{-\gamma F_\Sigma(j-1)}$ , which tend to decrease the rate of production of bosons and fermions. On the other the factors  $e^{2\pi \sum_{i=2}^j \mu_k(i)}$ , encoded in the form of the gaussian approximation,

describe the resonant effect due to the accumulation of the previously produced bosons. Initially, the perturbative decay prevents the resonance to be effective. However, after a certain number of oscillations, the resonant effect overtakes the perturbative decays and parametric resonance develops as usual, i.e. as if the produced bosons would not decay perturbatively during each semi-oscillation. In order to estimate the time at which this happens, let us evaluate numerically the ratio

$$\sigma \equiv \frac{2\pi \sum_{i=2}^j \mu_k(i)}{\gamma \Gamma_\Sigma(j-1)}, \quad (4.103)$$

for the fastest growing mode (4.99), and find the number of semi-oscillations  $j_R$  for which it becomes greater than one,  $\sigma \geq 1$ . We find  $j_R \approx 70$  for the  $W$  bosons and  $j_R \approx 300$  for the  $Z$  bosons. The fact that parametric resonance becomes important much earlier for  $W$  than for  $Z$  bosons is not a surprise, since their decay rate (4.35) differs in a factor  $\gamma_Z/\gamma_W \approx 2.4$ , which simply means that many more  $W$  survive every semioscillation. Therefore, the *Combined Preheating* of the  $W$  bosons is much faster driven into the parametric-like behaviour, while the evolution of the  $Z$  bosons is much more affected by the perturbative decays, delaying (or even completely preventing) the development of parametric resonance. Obviously, after a dozen of oscillations, the transfer of energy from the inflaton to the gauge bosons will be completely dominated by the  $W$  channel, since by that time they will be fully resonant, while the  $Z$  bosons will still be severely affected by their perturbative decay.

To conclude this section and achieve an overall complete picture of all the details, let us also estimate the transferred energy from the inflaton to the gauge bosons. In particular, the total energy transferred to them just after the  $j$ -th scattering,  $\rho_B(j)$ , is given by

$$\rho_B(j) = 3 \left( n_Z(j^+) \langle m_Z \rangle_j + 2n_W(j^+) \langle m_W \rangle_j \right), \quad (4.104)$$

where we have used taken into account that the gauge bosons are non-relativistic and have 3 polarizations. Therefore, the ratio of the energy of the gauge bosons to the energy of the inflaton,  $\varepsilon_B(j) \equiv \rho_B(j)/\rho_\phi$ , can be expressed as

$$\varepsilon_B(j) = \tilde{\epsilon} \left( j + \frac{1}{2} \right)^2 \left( \frac{1}{\cos \theta_w} \right)^2 \frac{\sqrt{\pi} k_*^3 F(j) A^{j-1} C}{4j^2 \left( D + B \sum_{i=2}^j i^{-2/3} \right)^{3/2}} \left( e^{-\gamma_Z F_\Sigma(j)} + 2 \cos \theta_w^3 e^{-\gamma_W F_\Sigma(j)} \right), \quad (4.105)$$

where we have used (4.95). As in the fermionic case, the amplitude of this growing function is modulated by the parameter  $\tilde{\epsilon}$ , defined in (4.102).

Using Eqs. (4.83) and (4.105), we can estimate the time at which the energy of the inflaton would be finally transferred to the fermions and bosons. Defining that moment as  $\varepsilon_F(j_{\text{eff}}) \equiv 1$  and  $\varepsilon_B(j_{\text{eff}}) \equiv 1$  respectively, we obtain the numbers presented in Table 4.2. Note that although the number of oscillations  $j_{\text{eff}}$  required for an efficient energy transfer depends on the parameter  $\lambda$ , the overall order of magnitude does not change appreciably. Unfortunately, as we will see in the next subsection, before reaching the stage  $\epsilon_{F,B} \sim 1$ , the backreaction of the produced gauge fields into the homogeneous Higgs condensate will become significant, and it will must be taken into account.

$\lambda$	0.2	0.4	0.6	0.8	1.0
$j_{\text{eff}}^{(F)}$	107	111	113	114	115
$j_{\text{eff}}^{(B)}$	111	113	115	116	117
$j_{\text{BR}}$	107	110	112	113	114

Table 4.2: Number of semi-oscillations of the Higgs required, as a function of  $\lambda$ , for an efficient transfer of energy from the inflaton to the fermions (F) and/or to the gauge fields (B). The numbers are compared with the number of semi-oscillations for the backreaction (BR) of the gauge fields into the Higgs background to become significant.

## 4.9 Backreaction and the end of (p)reheating

The perturbations in cosmology usually depend on the background but no *vice versa*. However, during the preheating stage, the production of particles is so explosive that it rapidly affects the dynamics of the inflaton itself. In this section we study the backreaction of the  $W$  and  $Z$  bosons into the Higgs condensate and the end of preheating. In the so-called Hartree-Fock approximation [213, 214], the amplification effects of the created particles on the inflaton are encoded in the variance of the created fields,  $\langle \mathcal{A}^2 \rangle$ , which modifies the equation of motion for the inflaton

$$\ddot{\phi} + 3H\dot{\phi} - \frac{1}{a^3}\nabla^2\phi + \left[ M^2 + \frac{\alpha g^2 M_p}{4\xi_h|\phi|} e^{-\alpha\kappa|\phi|} \langle \mathcal{A}^2 \rangle \right] \phi = 0, \quad (4.106)$$

where we implicitly assume a sum over polarizations and gauge boson species and neglect the vectorial nature of the fields. Although the variance is initially small,  $\langle \mathcal{A}^2 \rangle \ll 1$ , it will eventually grow enough as to modify the curvature of the potential around the minimum  $M$ . When this happens the amplitude of the oscillations decreases, as in the standard harmonic oscillator, diminishing the  $q$  parameter (4.62), and therefore, stopping the non-perturbative production of gauge bosons.

Whenever the Higgs frequency evolves adiabatically, we can compute the expectation value of the bosonic field components  $\mathcal{A}$  as

$$\langle \mathcal{A}^2 \rangle \equiv \frac{1}{2\pi^2 a^3} \int dk k^2 |\mathcal{A}_k|^2 = \frac{1}{2\pi^2 a^3} \int \frac{dk k^2}{\omega_k} \left( \frac{1}{2} + n_k + \text{Re}\{\alpha_k \beta_k^* e^{-i2 \int^t \omega dt' + \text{Arg } \alpha_k + \text{Arg } \beta_k} \} \right)$$

where  $n_k \equiv |\beta_k|^2$  denotes the spectral number densities of the produced gauge bosons and  $\alpha_k$  and  $\beta_k$  are related by the Wronskian condition  $|\alpha_k|^2 - |\beta_k|^2 = 1$ . Taking into account the non-relativistic nature of the produced gauge bosons  $\omega_k \simeq m_{\mathcal{A}}$  (cf. Eq. (4.36)), the previous expression becomes

$$\langle \mathcal{A}^2 \rangle \approx \frac{1}{2\pi^2 a^3} \frac{2\sqrt{\xi_h}}{gM_p} \frac{1}{\sqrt{1 - e^{-\alpha\kappa|\phi|}}} \int dk k^2 n_k \left[ 1 + \cos\left(\frac{2\pi}{M} \sum_j \langle \omega \rangle_j + \text{Arg } \alpha_k + \text{Arg } \beta_k\right) \right] \quad (4.107)$$



with averaged frequency  $\langle\omega\rangle_j = \frac{M}{\pi} \int_{t_j}^{t_{j+1}} dt' \omega(t')$ . The coupling  $g$  appearing in the denominator of the previous expression clearly reflects that we are dealing with non-perturbative processes. Following [183], we will rewrite the previous equation as

$$\langle\mathcal{A}^2\rangle \approx \frac{2\sqrt{\xi_h}}{gM_p} \frac{n_{\mathcal{A}}}{\sqrt{1 - e^{-\alpha\kappa|\phi|}}} \left[ 1 + a \cos\left(\frac{2\pi}{M} \sum_j \langle\omega\rangle_j\right) \right], \quad (4.108)$$

where the coefficient  $a < 1$  hides the uncertainty about the accumulated phases  $\text{Arg } \alpha_k$  and  $\text{Arg } \beta_k$ , and  $n_{\mathcal{A}} \equiv (2\pi^2 a^3)^{-1} \int dk k^2 n_k$ . From here, we can define the effective frequency of the Higgs condensate as

$$M_{\text{eff}}^2 \equiv M^2 + \frac{\alpha g n_{\mathcal{A}}}{2\sqrt{\xi_h}|\phi|} \frac{\left[ 1 + a \cos\left(\frac{2\pi}{M} \sum_j \langle\omega\rangle_j\right) \right]}{\sqrt{e^{2\alpha\kappa|\phi|} - e^{\alpha\kappa|\phi|}}}. \quad (4.109)$$

The backreaction of the gauge bosons on the Higgs field dynamics, will become relevant when the last term in the right hand side of the previous expressions becomes of order  $M^2$ . The initial blocking of parametric resonance due to the perturbative decays into fermions prevents this to happen during the first oscillations. However, when parametric resonance becomes efficient, the number of gauge bosons  $n_{\mathcal{A}}$  grows exponentially fast within few Higgs oscillations, and the second term in (4.109) becomes eventually dominant. In terms of the number densities of the  $Z$  and  $W$  bosons, i.e. summing the contribution over all polarizations and species, this will happen at a time  $t_j = j\pi/M$ , in which

$$\left( n_Z(j)/\cos\theta_w + 2n_W(j) \right) \gtrsim \frac{2\sqrt{\xi_h}|\phi(t_j)|(\alpha\kappa\langle\phi(t)\rangle_j)^{1/2}M^2}{3\alpha g_2}, \quad (4.110)$$

where we have expanded  $\sqrt{e^{2\alpha\kappa|\phi|} - e^{\alpha\kappa|\phi|}} \approx (\alpha\kappa|\phi|)^{1/2}$  around the minimum of the potential and replaced  $\phi(t)$  by its averaged value per semi-oscillation

$$\langle\phi(t)\rangle_j = \frac{\phi_{\text{end}}}{\pi j} \left( \frac{1}{\pi} \int_0^\pi \sin(x) \right) = \frac{2}{\pi} \frac{\phi_{\text{end}}}{\pi j}. \quad (4.111)$$

Using the analytical expressions (4.95) for the gauge boson occupation numbers we can translate the above condition into the following one

$$\left( e^{-\gamma_Z \Gamma_\Sigma(j-1)} / \cos^3 \theta_w + 2e^{-\gamma_W \Gamma_\Sigma(j-1)} \right) \frac{A^{(j-1)}C}{j^{1/2} \left( D + B \sum_{i=2}^j i^{-3/2} \right)} \geq \frac{16\sqrt{6}\xi_h^{3/2}(\alpha\kappa\phi_{\text{end}})^{3/2}}{\lambda^{1/2}g_2^3\pi^{7/2}k_*^3}. \quad (4.112)$$

The moment at which backreaction of the bosonic fields becomes significant can be determined numerically from the previous expression. Table 4.2 shows the results obtained for different values of the undetermined Higgs self-coupling  $\lambda$ . We clearly see that backreaction seems to become important at a time slightly earlier than that at which we were expecting the Higgs to have transferred efficiently its energy to the bosons and fermions. This means that our analytical estimates of these transfers were biased, and a careful numerical study of the process via a modification of the numerical packages available [215, 216, 217] is required. Beyond backreaction, the strength of the resonance very quickly decreases due to

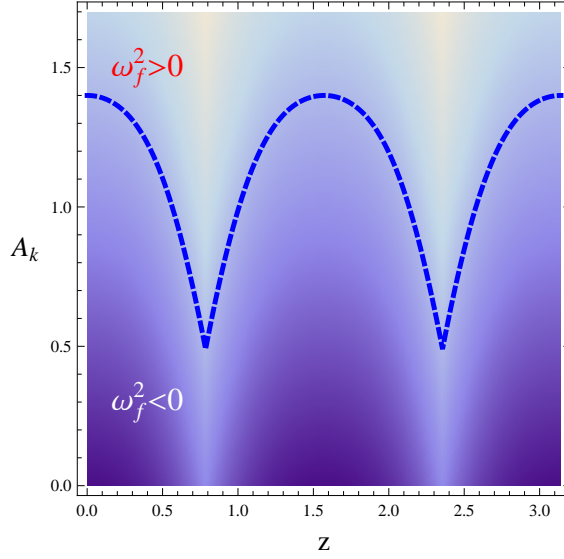


Figure 4.12: The dependence of the frequency of oscillation in (4.121) as a function of  $A_k$  and  $z$ . The region under the blue dashed line corresponds to  $A_k - 2p|\cos 2z| - p^2 \sin^2 2z < 0$ . Note the periodicity  $T = \pi/2$ .

the increased frequency of oscillations of the Higgs. Eventually, the broad resonance driving the production of gauge bosons and thus their decay into Standard Model particles becomes narrow and finally shuts off. From then on, the inflaton will oscillate like a matter field, while the produced particles will redshift as radiation, becoming their effect on the expansion completely negligible after a few hundred oscillations.

## 4.10 Similar but not equal: Dilaton production

Throughout this chapter we have assumed that Higgs and Higgs-Dilaton inflation give rise to one and the same (p)reheating. Notice however that Higgs-Dilaton Inflation incorporates an extra degree of freedom, the dilaton field. The constancy of the classical background component is of course guaranteed by the scale invariance current conservation, but this reasoning does not apply to the corresponding quantum excitations. As suggested in [218], these modes can be excited through the non-canonical kinetic term in the Einstein-frame lagrangian (4.11), which mixed quantum excitations and background solutions. Although the perturbative estimate of dilaton production via the effective field mixing is very small (due to the small value of  $\xi_\chi$ ), non-perturbative effects can play a very important role [219]. To illustrate the point let us consider the equations of motion for the scalar perturbations [152, 153]

$$\delta\ddot{\phi}_k + 3H\delta\dot{\phi}_k + \left(\frac{k^2}{a^2} + V_{,\phi\phi}\right)\delta\phi_k = 0, \quad (4.113)$$

$$\delta\ddot{\rho}_k + (3H + 2\dot{b})\delta\dot{\rho}_k + \frac{k^2}{a^2}\delta\rho_k = 0. \quad (4.114)$$

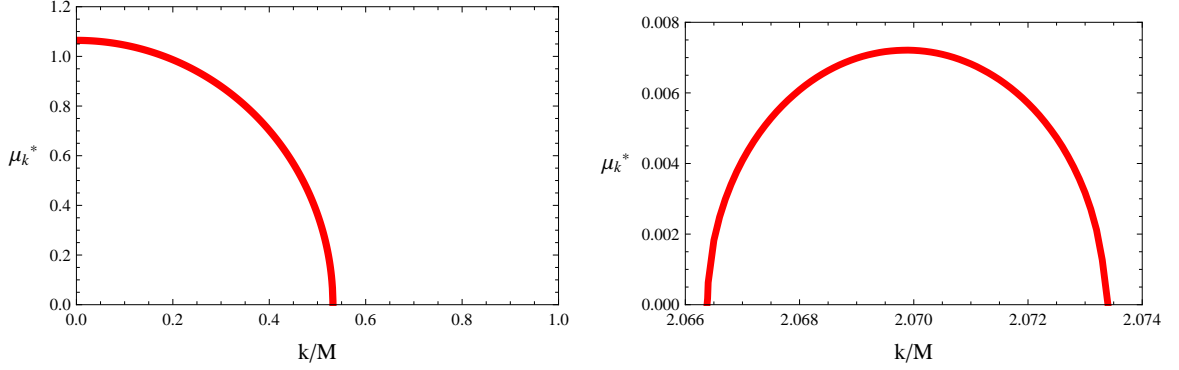


Figure 4.13: The Floquet index  $\mu_k$  for dilaton production. It presents a large infrared band at low momenta is reminiscent of a tachyonic mechanism, and a smaller band at higher momenta. The results neglect the expansion of the universe.

Note that we have ignored metric perturbations and taking into account the constancy of the background field  $\rho$ . The function  $b = b(\phi)$  (cf. (4.12)) plays the role of an addition oscillatory damping term for the dilaton perturbations. Let us focus of the effect of this term, neglecting therefore the expansion of the universe as a first approximation. In this case, the amplitude  $\phi_{\text{end}}$  of the angular background oscillations in (4.23) becomes constant, which allows us to further approximate  $\dot{b}$  as

$$\dot{b} = -\bar{\alpha}\kappa \frac{d|\phi|}{dt} \tanh(\alpha\kappa(\phi_0 - |\phi|)) \approx -\alpha\kappa M \phi_{\text{end}} \frac{d|\cos Mt|}{dt} \quad (4.115)$$

Performing a change of variables  $Mt \rightarrow 2z$  we can now rewrite (4.114) as

$$\delta\rho_k'' + 2p \sin(2z) \delta\rho_k' + A_k \delta\rho_k = 0 \quad \cos Mt > 0, \quad (4.116)$$

$$\delta\rho_k'' - 2p \sin(2z) \delta\rho_k' + A_k \delta\rho_k = 0 \quad \cos Mt \leq 0, \quad (4.117)$$

where primes denote derivatives wrt to  $z$  and we have defined

$$p \equiv 2\bar{\alpha}\kappa\phi_{\text{end}}, \quad A_k \equiv \frac{4k^2}{M^2} \quad (4.118)$$

Notice that the previous equations closely resemble an Ince's equation. This suggests to introduce a version of the standard field redefinition

$$f_k(z) = \delta\rho_k(z) e^{\frac{p}{2}|\cos 2z|} \quad (4.119)$$

to recast (4.116) as a modified version of the Hill-Whittaker equation [220]

$$f_k''(z) + \omega_f^2 f_k(z) = 0, \quad (4.120)$$

with frequency

$$\omega_f^2 \equiv A_k - 2p|\cos 2z| - p^2 \sin^2 2z. \quad (4.121)$$

As for the original equation Hill-Whittaker, the Floquet or Bloch theorem can be applied, which open the possibility of exponential particle production of those quantum modes for which the Floquet index acquires an imaginary part [218]. Following [94, 221] we define the number of created particles at time  $z$  as

$$n_k(z) = 2 \sinh^2(\mu_k z) , \quad (4.122)$$

where the Floquet index  $\mu_k$  is determined by

$$\cosh(\mu_k T) = \text{Re} \left[ f_k^{(1)}(T) \right] \quad (4.123)$$

where  $T = \pi/2$  is the periodicity associated to the frequency (4.121) (cf. Fig. 4.12) and  $f_k^{(1)}$  also satisfies (4.120), but now with initial conditions  $f_k^{(1)}(0) = 1$  and  $f_k^{(1)'}(0) = 0$ . The shape of the resulting Floquet index is shown in Fig. 4.13. It presents a large infrared band, reminiscent of tachyonic preheating, as well a smaller band at larger momenta. One should expect therefore a large production of dilatons, which might spoil completely the analysis presented in this chapter. The problem requires however a careful numerical study that takes into account the expansion of the universe, which could change the band structure previously described. We are at present studying such particle production.

## CHAPTER 5

# The Higgs field and Dark Energy

Like a great poet, Nature knows  
how to produce the greatest  
effects with the most limited  
means.

HEINRICH HEINE

### 5.1 Scale invariance and the Cosmological Constant

As we argued in Chapter 2 a spontaneously broken scale invariance symmetry constitutes a very natural extension of the Standard Model, able to generate all the dimensional parameter of the theory, at the classical and quantum level. Note however that it forbids the appearance of a cosmological term, required (in the most conventional approaches) to explain the late time acceleration of the universe. Although one could argue that the cosmological constant term might reappear due to quantum effects or to the pure presence of a time-dependent cosmological background, it is worth exploring the possibilities of solving the problem already at the classical level. One interesting possibility is to consider a quite modest modification of General Relativity, firstly considered by Einstein in 1919, known as Unimodular Gravity (UG) [31, 222, 223, 224, 225]. Unimodular Gravity is a very particular case of the much more general set of theories invariant under the group of transverse diffeomorphisms TDiff [222, 226, 227, 228, 229, 230]. These are coordinate transformations

$$x^\mu \mapsto \tilde{x}^\mu(x), \quad \left| \frac{\partial \tilde{x}^\mu}{\partial x^\mu} \right| = 1 \quad (5.1)$$

generated by the subalgebra of transverse vectors

$$x^\mu \mapsto x^\mu + \xi^\mu(x), \quad \partial_\mu \xi^\mu = 0. \quad (5.2)$$

TDiff theories generically contain an extra scalar degree of freedom on top of the massless graviton. Unimodular Gravity reduces the dynamical components of the metric by requiring the metric determinant  $g \equiv \det(g_{\mu\nu})$  to take some fixed constant value, conventionally  $|g| = 1$ . Unimodular gravity is then only invariant under volume-preserving diffeomorphisms. As shown in [222, 75], the field equations for UG in combination with arbitrary matter fields with arbitrary couplings to gravity are classically equivalent to the solutions obtained from the Diff invariant action<sup>1</sup>

$$\Sigma_e = \int d^4x \mathcal{L}_e = \int d^4x \sqrt{-g} \left( \mathcal{L}(g_{\mu\nu}, \partial g_{\mu\nu}, \Phi, \partial \Phi) + \Lambda_0 \right), \quad (5.3)$$

except that, while in the standard theory the  $\Lambda_0$  term appears directly in the action, in UG it is an integration constant related to some initial conditions. Indeed, if we reformulate UG in terms of an unconstrained metric by taking into account the unimodular constraint on the metric determinant ( $|g| = 1$ ) through an undetermined lagrange multiplier  $\lambda(x)$ , then, it can be shown [75] that, for all possible infinitesimal transformations,  $\lambda(x) = \Lambda_0$  is a constant of motion

$$\partial_\mu \lambda(x) = 0. \quad (5.4)$$

Note that this conserved quantity should not be understood as a cosmological constant, since although it plays that role in minimally coupled theories, things are different if Newton's constant is induced dynamically (non-minimal coupling). Let us see this explicitly in the Higgs-Dilaton inflationary model.

## 5.2 Dilaton Quintessence

In Unimodular Gravity the Einstein frame potential (4.13) in the lagrangian density (4.11) becomes

$$V_{UG} = V + V_{\Lambda_0}. \quad (5.5)$$

where

$$V(\phi) = V_0 \left[ 1 - \sigma \cosh^2(\bar{\alpha}\kappa(\phi_0 - |\phi|)) \right]^2, \quad (5.6)$$

was already defined in Section 4.2 and  $V_{\Lambda_0}$  is a new term proportional to the arbitrary integration constant  $\Lambda_0$

$$V_{\Lambda_0}(\phi, \rho) = \Lambda_0 \left( \frac{1 + 6\xi_\chi}{\xi_\chi} \right)^2 \sigma^2 \cosh^4[\bar{\alpha}\kappa(\phi_0 - |\phi|)] e^{-4\gamma\kappa\rho}. \quad (5.7)$$

We see that once transformed to the Einstein frame the up-to-now  $\Lambda_0$  constant term in the equations of motions becomes the strength of a potential.

As can be seen in Fig. 5.1 the new  $\Lambda_0$  term does not significantly modify the asymptotic flat regions of the former potential, cf. Fig. 3.2. The effects of the cosmological constant become however dominant around the  $(h, \chi) = (0, 0)$  point, giving rise to chimney and well shapes. Note that the conformal transformation is indeed not properly defined at that point,

---

<sup>1</sup>For a choice of coordinates such that the metric determinant is equal to one, which is always possible [231].

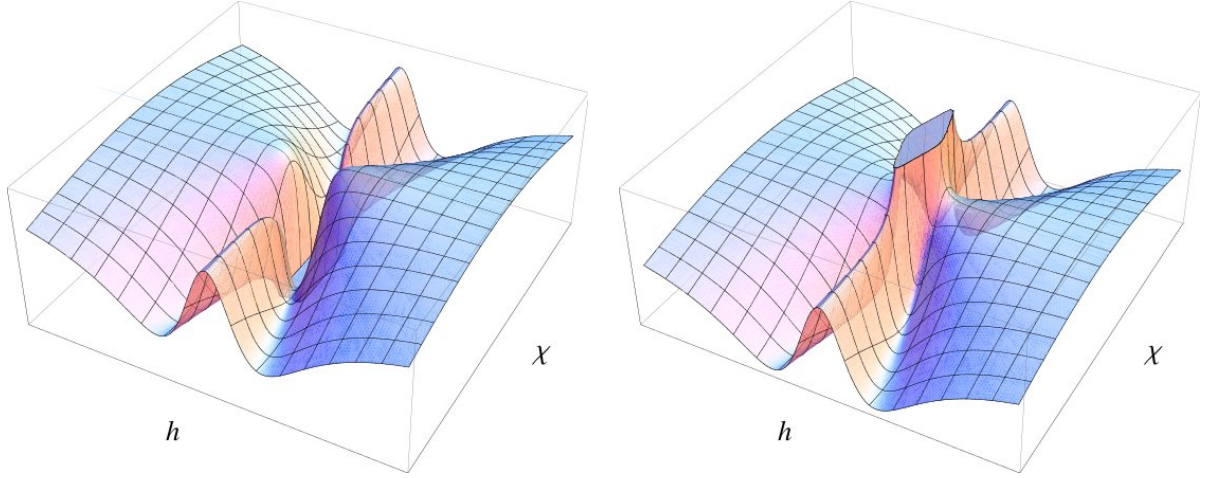


Figure 5.1: Shape of the Einstein-frame Higgs-Dilaton potential in the original field variables  $h$  and  $\chi$  for  $\Lambda_0 < 0$  (left) and  $\Lambda_0 > 0$  (right). The non-equal zero value of  $\Lambda_0$  gives rise to the well and chimney shapes in the center of the figures. Its main effect is lifting the valleys, breaking therefore the degeneracy of the classical ground state. For  $\Lambda_0 < 0$  the valleys are tilted towards the origin, which induces a trivial classical ground state  $(h, \chi) = (0, 0)$ . On the other hand, for  $\Lambda_0 > 0$  the potential becomes of runaway type, with an asymptotic ground state at large field values.

and therefore it should be skipped from the discussion. Their main effect of the tubular shapes is lifting the valleys, breaking therefore the degeneracy of the classical ground state. For  $\Lambda_0 < 0$  the valleys are tilted towards the origin, and the fields will tend to approach to the trivial  $h = \chi = 0$  ground state. Much more interesting is the  $\Lambda_0 > 0$  case, where the potential becomes of runaway type with an asymptotic ground state at large field values ( $\chi \rightarrow \infty$ ). Let us analyze the consequences of this behaviour.

Assume that the backreaction of the created particles on the inflaton dynamics during inflation does not modify the analytical estimates about the efficiency of the energy transfer from the inflaton to the fermions (cf. Section 4.8). In this case, the system will eventually thermalize, acquiring a reheating temperature  $T_{rh}$  and entering in the radiation dominated era. At the beginning of this stage, the energy density of the Universe will be completely dominated by the relativistic energy density  $\rho_{\text{total}} \simeq \rho_{\text{rad}}(T_{rh}) = \frac{\pi^2}{30} g_{\text{eff}}(T_{rh}) T_{rh}^4$ . At that time, the scalar fields have almost settled down<sup>2</sup> in one of the two almost degenerate classical ground states of the potential, i.e.  $h \simeq \pm \vartheta \chi$ . In this case, the lagrangian density (4.11) becomes independent of the angular variable,

$$\frac{\mathcal{L}}{\sqrt{-g}} = \left[ \frac{M_P^2}{2} R - \frac{1}{2} (\partial\rho)^2 - V_{\Lambda_0}(\rho) \right], \quad (5.8)$$

We are left therefore with just one dynamical degree of freedom, the field  $\rho$ , which, as pointed out in Ref. [75], keeps on rolling down the potential with the dynamics of a “thawing”

<sup>2</sup>The trajectory along the valley is indeed asymptotic, not an exact solution of the equations of motion.

quintessence model [232, 233]

$$\tilde{V}_{\Lambda_0}(\rho) = \Lambda_0 \left( \frac{1 + 6\xi_\chi}{\xi_\chi} \right)^2 e^{-4\gamma\kappa\rho} \simeq \frac{\Lambda_0}{\xi_\chi^2} e^{-4\gamma\kappa\rho}. \quad (5.9)$$

The Klein-Gordon equation of motion for the dilaton field  $\rho$  in a flat FRW background is given by

$$\ddot{\rho} + 3H\dot{\rho} + \frac{dV_{\Lambda_0}}{d\rho} = 0, \quad (5.10)$$

where we have assumed the field to be homogeneous,  $\rho = \rho(t)$ . In what follows it will be useful to adopt a perfect fluid description of the problem. Defining the energy and pressure densities of the dilaton field as<sup>3</sup>

$$\varrho_\rho \equiv \frac{1}{2}\dot{\rho}^2 + V_{\Lambda_0}, \quad p_\rho \equiv \frac{1}{2}\dot{\rho}^2 - V_{\Lambda_0}. \quad (5.11)$$

we can rewrite (5.10) as

$$\dot{\varrho}_\rho = -3H\varrho_\rho(1 + w_\rho). \quad (5.12)$$

with  $w_\rho \equiv \frac{p_\rho}{\varrho_\rho}$  the associated equation of state for the barotropic fluid. On the other hand, the first Friedmann equation is given by

$$H^2 = \frac{1}{3M^2}(\varrho_m + \varrho_\rho), \quad (5.13)$$

where  $\varrho_m$  represents generically the dominant fluid component of the remaining particle or energy content. That fluid is assumed to have a constant equation of state but it is otherwise completely generic. It can be simply relativistic or non-relativistic matter, or even an extra dark energy component with constant equation of state,  $w_m < -1/3$  (at that appearing in Higgs-Dilaton Inflation if we allow for a non-zero value of  $\beta$  in the initial scale-invariant potential (2.15)). Note that no explicit interactions between the two fluids have been included. The dilaton field interacts with matter and radiation components only through the gravitational interactions, since it does not couple directly to the Standard Model fields.

Let us rewrite the Klein-Gordon equations (5.12) and Friedmann (5.13) equations as

$$\eta'_\rho = -3\eta_\rho(2 - \eta_\rho) + 4\gamma(2 - \eta_\rho)\sqrt{3\eta_\rho\Omega_\rho}, \quad (5.14)$$

$$\Omega'_\rho = 3(\eta_m - \eta_\rho)\Omega_\rho(1 - \Omega_\rho), \quad (5.15)$$

and study the critical points of the system. Here primes denote derivatives *wrt* the number of e-folds and we have defined the observable quantities ( $i = \rho, m$ )

$$\eta_i \equiv 1 + w_i, \quad \Omega_i \equiv \frac{\varrho_i}{3M_P^2 H^2}, \quad (5.16)$$

where the latter satisfy the cosmic sum rule  $\Omega_m + \Omega_\rho = 1$ . As shown in Refs. [172, 233], the behaviour of 5.14 and 5.15 depends on the value of the  $\gamma$  parameter. For  $4\gamma > \sqrt{3\eta_m}$ , the

---

<sup>3</sup>Note that we have slightly modified the notation for the energy density used in the thesis ( $\rho \rightarrow \varrho$ ) to avoid confusion with the radial field coordinate  $\rho$ .



dilaton inherits the equation of state of the barotropic fluid,  $\eta_\rho = \eta_m$ , evolving towards the stable fixed point

$$\Omega_\rho = \frac{3\eta_m}{16\gamma^2}. \quad (5.17)$$

These so-called *scaling solutions*<sup>4</sup> can not be responsible for the late-time acceleration of the universe. For the dilaton field to be responsible of the late time evolution of the universe it should be the dominant contribution from the very beginning, excluding therefore the existence of a radiation dominated era. A *scaling dilaton* can at best provide a small contribution to dark energy.

The previous conclusion changes completely if  $4\gamma < \sqrt{3\eta_m}$ . In this case the stable fixed point is given by

$$\Omega_\rho = 1, \quad \eta_\rho = \frac{16\gamma^2}{3}, \quad (5.18)$$

which means that if  $4\gamma < \sqrt{2}$ , or equivalently  $\xi_\chi \lesssim \frac{1}{2}$  the asymptotic solution is that of an accelerating universe, opening the possibility for the dilaton field  $\rho$  to be responsible of the present dark energy dominated era if the stable fixed point (5.18) has not yet been attained<sup>5</sup>. Note that this is precisely the case of Higgs-Dilaton Inflation in the absence of another dark energy component with  $\eta < 4\gamma/\sqrt{3}$ . Indeed, taking into CMB bound  $\xi_\chi \lesssim 5 \times 10^{-3}$  derived in Section 3.5 we obtain  $4\gamma \simeq 4\sqrt{\xi_\chi} < \sqrt{2}$ .

The dilaton energy density must be negligible ( $\Omega_\rho \ll 1$ ) during the radiation and matter dominated stages and become important ( $\Omega_\rho \simeq 0.74$ ) in the recent era [234]. If  $\Omega_\rho \ll 1$  the second term on the right-hand side of (5.15) is small compared to the first one, the system evolves towards  $\eta_\rho \ll 1$  or equivalently towards the cosmological constant case  $w_\rho \simeq -1$ . Then, the value of  $\rho$  is almost constant during the radiation and matter dominated epochs, remaining essentially equal to its value at the end of (p)reheating. Nevertheless, the larger dilution of radiation and matter densities with the expansion of the universe would eventually lead the inflaton to be the dominant contribution. At this point,  $\rho$  starts rolling down the potential and  $\eta_\rho$  starts to evolve towards its attractor value. The described scenario in which the dilaton field remains constant for a long time to eventually start rolling down the exponential potential (5.9) belongs to the so-called *thawing quintessence* models [232] and has been previously studied in the literature [235, 236].

## 5.3 From the Early to the Late Universe

### 5.3.1 Consistency relations

As we showed in Chapter 3, the value of the non-minimal couplings of the Higgs and dilaton fields to gravity in Higgs and Higgs-Dilaton Inflation can be directly constrained by CMB observations, in particular by the scalar tilt and the amplitude of curvature perturbations,

<sup>4</sup>The name comes from the tendency of the dilaton's energy density to scale as that of the additional fluid.

<sup>5</sup>The limits of the present dark energy abundance [1] set an upper bound on the contribution of the dilaton  $\rho$  to the present energy density,  $\Omega_\rho^0 \lesssim \Omega_{\text{DE}}^0 \simeq 0.74$ , with the inequality becoming an equality if the dilaton the only dark energy component of dark-energy. The bound shows that the present universe must not have reached its fixed-point yet.

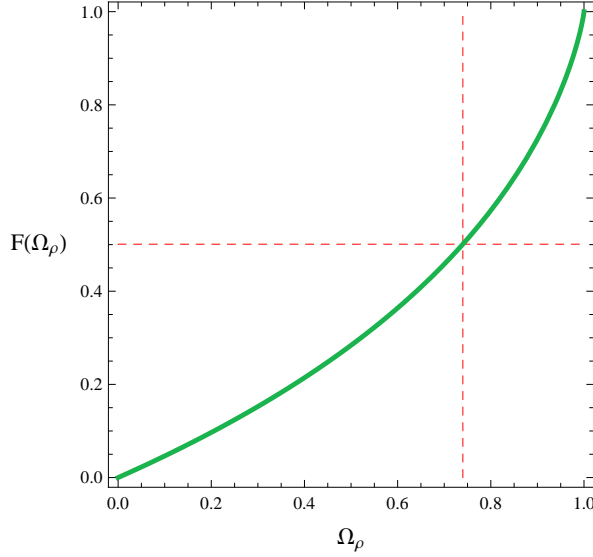


Figure 5.2: The monotonically increasing function  $F(\Omega_\rho)$  (green solid line). Note that it becomes exactly  $1/2$  for  $\Omega_\rho = 0.74$  (red dashed lines).

cf. Fig. 3.6. The theory is therefore completely specified at the inflationary stage and any subsequent period, as the mentioned dark energy dominated stage, should be consistent with that choice of parameters. In this section we will derive several consistency conditions among the inflationary observables and those of the equation of state of dark energy.

Let us start by combining (5.14) and (5.15) in the approximation where  $1 + w_\rho \ll 1$  to obtain the following interesting relation [235]

$$1 + w_\rho \simeq \frac{16\gamma^2}{3} F(\Omega_\rho) , \quad (5.19)$$

where

$$F(\Omega_\rho) = \left[ \frac{1}{\sqrt{\Omega_\rho}} - \frac{1}{2} \left( \frac{1}{\Omega_\rho} - 1 \right) \ln \frac{1 + \sqrt{\Omega_\rho}}{1 - \sqrt{\Omega_\rho}} \right]^2 . \quad (5.20)$$

As can be seen in Fig. 5.2  $F(\Omega_\rho)$  is a monotonic increasing function. Note that if no extra dark energy components apart from the dilaton field  $\rho$  are present, then we can equate  $\Omega_\rho^0 = \Omega_{\text{DE}}^0 \simeq 0.74$ , from which one gets  $F(\Omega_{\text{DE}}^0 = 0.74) = 0.5$ . Inserting this inequality into (5.19) we obtain the bound

$$1 + w_\rho^0 \lesssim \frac{8}{3} \frac{\xi_\chi}{1 + 6\xi_\chi} \simeq \frac{8\xi_\chi}{3} + \mathcal{O}(\xi_\chi^2) , \quad (5.21)$$

on the present equation of state of the dilaton field. From equations (5.14) and (5.15) it can be easily understood that if dark energy is mainly due to a barotropic component, its corresponding  $\eta$  must be smaller than  $\eta_\rho$ . Therefore, the previous bound can be translated into a bound on the equation of state parameter of the total dark energy

$$1 + w_{\text{DE}}^0 \lesssim \frac{8}{3} \frac{\xi_\chi}{1 + 6\xi_\chi} \simeq \frac{8\xi_\chi}{3} + \mathcal{O}(\xi_\chi^2) . \quad (5.22)$$

Note that this is a rather non-trivial result: Observations related to the very early universe provide information about observables of the very late universe. The Higgs-driven inflationary models give again rise to very precise predictions or consistency relations, able to confirm or rule out the model. Indeed, taking into account the upper bound  $\xi_\chi < 0.0052$  derived in the previous chapter (cf. Table 3.1), we obtain a very strong bound on the equation of state of dark energy, namely

$$0 \leq 1 + w_{\text{DE}}^0 \lesssim 0.014 . \quad (5.23)$$

Unfortunately the current observational constraint  $-0.04 < 1 + w_{\text{DE}}^0 < 0.2$  [1] is much weaker than (5.23). From this point of view, the energy density  $\varrho_{\text{DE}}^0$  is practically indistinguishable from a cosmological constant. Nevertheless, the observational bound is expected to improve considerably in the near future. A measurement precision at the percent level would make it possible to check the prediction of our model.

The relation between the scalar spectral index  $n_s^*$  and the dark energy equation of state  $w_{\text{DE}}^0$  can be further refined if the dilaton  $\rho$  alone is responsible from the late time accelerated expansion of the universe, i.e.  $\Omega_\rho^0 = \Omega_{\text{DE}}^0$ . Recall that in the Higgs-Dilaton model under consideration this corresponds to the absence of a dilaton quartic interaction in the original Jordan frame (cf. Section 2.3), i.e. to  $\beta = 0$ . In that case, the associated dark energy component becomes purely dynamical. Combining (5.22) (where inequality is replaced by equality) with the approximate relation (3.78) allows us to express the scalar tilt  $n_s^*$  as a function of  $\eta_{\text{DE}}^0$  and the number of e-folds  $N^*$  as

$$n_s^* \simeq 1 - \frac{12\eta_{\text{DE}}^0}{4 - 9\eta_{\text{DE}}^0} \coth \left( \frac{6N^*\eta_{\text{DE}}^0}{4 - 9\eta_{\text{DE}}^0} \right) . \quad (5.24)$$

This relation is plotted in Fig. 5.3 for the fast and slow reheating assumption. The plot is equivalent to that in Fig. 3.4, except that the independent variable is changed from  $\xi_\chi$  to  $w_{\text{DE}}^0$  with the help of (5.19). As before, the result is rather insensitive to variations of the number of e-folds  $N^*$  within the estimated range (3.89). For intermediate values of  $\xi_\chi$ , the previous equation can be approximated as

$$-3(w_{\text{DE}}^0 + 1) \approx (n_s^* - 1) , \quad (5.25)$$

which can be written as a relation between the zero and first orders in the early and late universe

$$\frac{d \ln \varrho_{\text{DE}}^0}{d \ln a} \approx \frac{d \ln P_\zeta(k)}{d \ln k} . \quad (5.26)$$

The comparison between (5.24) and (5.25) is also shown in Fig. (5.3). Note that although (5.25) completely fails to describe the behaviour of (5.24) for values of  $w_{\text{DE}}^0$  very close to the cosmological constant case  $w_{\text{DE}}^0 = -1$ , it can constitute a good approximation, within the expected accuracy of the Planck mission, for slightly larger values of  $w_{\text{DE}}^0$ . Moreover, it is also possible to derive a relation among the first and second order respectively,

$$3w_a \approx \frac{dn_s^*}{d \log k} , \quad (5.27)$$

relating the rate of change of the equation of state parameter  $w(a) = w_0 + w_a(1 - a)$  with the logarithmic running of the scalar tilt.

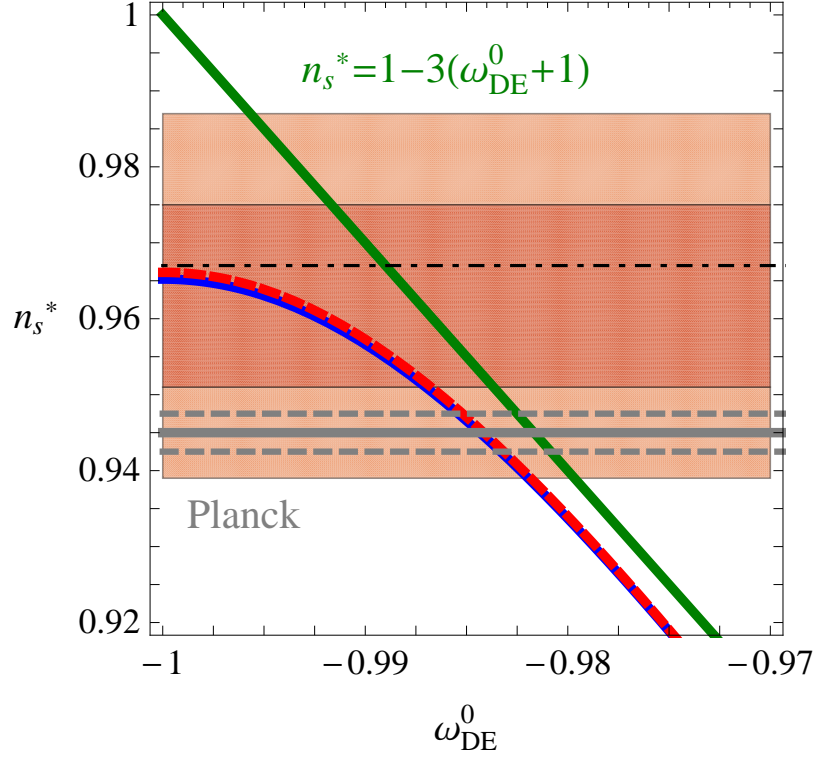


Figure 5.3: Approximate functional relationship (5.24) between the spectral tilt and the dark energy equation of state. The red dashed curve is obtained for fast reheating  $\rho_{rh} = \rho_{rh}^{max}$  with  $N^* = N_{max}^*$ , while the blue solid curve represents the case of slow reheating  $\rho_{rh} = \rho_{rh}^{min}$  with  $N^* = N_{min}^*$ . The shaded region shows the WMAP7  $1\sigma$  and  $2\sigma$  bounds. The green diagonal line corresponds to the further approximation (5.25). Note that this extra approximation completely fails to describe the behaviour of (5.24) close to the cosmological constant case  $w_{DE}^0 = -1$ . However, it might constitute a good approximation, within the expected precision of the forthcoming surveys, for slightly larger values of  $w_{DE}^0$ . Gray horizontal dot-dashed line represent the expected accuracy to be achieved by the Planck satellite [237] around an hypothetical central value of the spectral tilt.

Equations (5.26) and (5.27) should be seen as consistency relations for the unimodular Higgs-Dilaton model under consideration, that could allow us either to confirm or exclude it in the near future. Let us stress again that the links between the observable  $n_s^*$  and  $\frac{dn_s^*}{d \ln k}$ , related to inflation, and  $w_{\text{DE}}^0$  and  $w_a$ , related to dark energy, are non-trivial predictions of the present model. They constitute an intriguing relation between inflation and dark energy, relating two periods a priori totally independent, that allows us to use the measurable observables from CMB anisotropies to make firm testable predictions in the widely unknown DE sector. On the other hand one should also mention that this result relies on several important assumptions. In particular, the functional relation (5.24) is based on the requirement that the J-frame potential has a flat direction ( $\beta = 0$ ).

### 5.3.2 Dark energy constraints on the initial inflationary conditions

As we saw in Section 5.1, if General Relativity is replaced by Unimodular Gravity the exact scale invariance of the original Higgs-Dilaton model is explicitly broken by the appearance of an arbitrary integration constant  $\Lambda_0$ . Note that the shape of the potential is dramatically modified around the vicinity of the  $(h, \chi) = (0, 0)$  point (cf. Fig 5.1), which could potentially spoil the analysis of the inflationary trajectories performed in Chapter (3). The non-conservation of the radial component during inflation could give rise to the generation of isocurvature perturbations, which would hinder the determination of the non-minimal couplings  $\xi_h$  and  $\xi_\chi$  from the CMB observables. In what follows we will explicitly show that all the conclusions of the previous chapters hold also if scale-invariance is explicitly broken. To do this, let us characterize the departure of scale invariance by the dimensionless ratios

$$v_1 \equiv \frac{V_{\Lambda_0}}{V}, \quad v_2 \equiv \sqrt{\frac{V_{\Lambda_0}^a V_{\Lambda_0}^a}{V^b V^b}}, \quad (5.28)$$

Here latin indices denote as usual the Higgs and dilaton field coordinates. The interpretation of (5.28) is rather obvious. The parameter  $v_1$  compares the strength of the scale invariance breaking part of the potential  $V_{\Lambda_0}$  with that of the scale invariant one  $V$ . Similarly, the parameter  $v_2$  encodes, in a coordinate invariant way, the relation between the derivatives of both parts. In those regions of (5.5) where both  $v_1, v_2 \ll 1$ , the effect of the  $\Lambda_0$ -term can be completely neglected at the level of the classical equations of motion, recovering therefore the scale-invariant case studied in the preceding chapters.

Among all the possible inflationary trajectories, only those able to give rise to a late dark energy stage can be considered as phenomenologically acceptable. As can be inferred from the theoretical bound (5.23), the energy density of the dilaton field at the minimum of the potential (5.5) is completely dominated by the potential energy contribution,  $\rho_\rho \simeq V_{\Lambda_0}(\rho)$ . Taking this into account we can translate the observational upper bound on  $\Omega_\rho^0 \leq \Omega_{DE}^0 \simeq 0.74$  [1] into a lower bound on the current value of the dilaton field

$$\rho_0 \gtrsim -\frac{1}{4\gamma} M_P \ln \left( \xi_\chi^2 \frac{\Lambda_{\text{eff}}}{\Lambda_0} \right), \quad (5.29)$$

where

$$\Lambda_{\text{eff}} \equiv 3M_P^2 H_0^2 \Omega_{DE}^0 \simeq 10^{-120} M_P^4, \quad (5.30)$$

denotes the present value of the effective cosmological constant in Planck units. The slow evolution of the dilaton field along the minimum of the potential from the end of inflation till today makes it possible to approximate the present value of  $\rho_0$  by that at the end of inflation<sup>6</sup>. Making then use of (5.29) and (5.28) we obtain

$$v_1 \lesssim \frac{144\xi_\chi^2\xi_h^2}{\lambda} \frac{\Lambda_{\text{eff}}}{M_P^4} \frac{1}{\sin^4\theta}, \quad v_2 \lesssim \frac{24\xi_\chi\xi_h^2}{\lambda} \frac{\Lambda_{\text{eff}}}{M_P^4} \frac{1}{\sin^2\theta \cos^2\theta}. \quad (5.31)$$

The small value of the effective cosmological constant  $\Lambda_{\text{eff}}$  extremely suppresses the value of the previous parameters ( $v_1, v_2 \ll 1$ ) for the whole evolution of the angular variable,  $\theta_{\text{end}} < \theta < \theta^*$  (cf. Eqs. (3.76) and (3.77)). We conclude therefore that any phenomenologically viable field trajectory originated from an inflationary region in which the effect of the  $\Lambda_0$ -term was completely negligible.

The minimal value (5.29) of the radial field and its slow evolution from horizon crossing during inflation until today allows indeed to further restrict the initial inflationary conditions discussed at the end of Chapter 3. For a scale-invariant trajectory ( $v_1, v_2 \ll 1$ ), the bound (5.29) translates into

$$\rho_{\text{in}} \simeq \rho^* \simeq \rho_{\text{end}} \gtrsim -\frac{1}{4\gamma} M_P \ln \left( \xi_\chi^2 \frac{\Lambda_{\text{eff}}}{\Lambda_0} \right), \quad (5.32)$$

which in terms of the original variables can be written as

$$\frac{\chi_{\text{in}}^2}{\Lambda_0^{1/2}} + 6\xi_h \frac{h_{\text{in}}^2}{\Lambda_0^{1/2}} \gtrsim \frac{1}{\xi_\chi} \frac{M_P^2}{\Lambda_{\text{eff}}^{1/2}} \sim 10^{60}. \quad (5.33)$$

If we combine this bound with (3.91) we conclude that appropriate initial conditions must be much larger than the arbitrary scale  $\Lambda_0^{1/4}$ , namely  $h_{\text{in}}/\Lambda_0^{1/4} \gtrsim 10^{30}$ . Notice that the associated region is a bidimensional surface in the  $(h, \chi)$  plane. If  $\rho$  is completely responsible from the observed dark energy abundance and no additional component are allowed ( $\beta = 0$ ), then, the inequalities become equalities and the initial values lie on a very precise line in the  $(\rho, \theta)$  plane. Let us note that, although this kind of fine-tuning on the initial conditions is an undesirable feature, it does not constitute a consistency problem. Indeed, it is just a manifestation of the Cosmic Coincidence problem permeating all Dark Energy models. A summary of the different kind of evolutions in Higgs-Dilaton inflation according to the different initial conditions in presented in Fig. 5.4.

---

<sup>6</sup>The numerical solution shows that the changes of  $\rho$  during the (p)reheating and thawing quintessence stages are around the percent level.

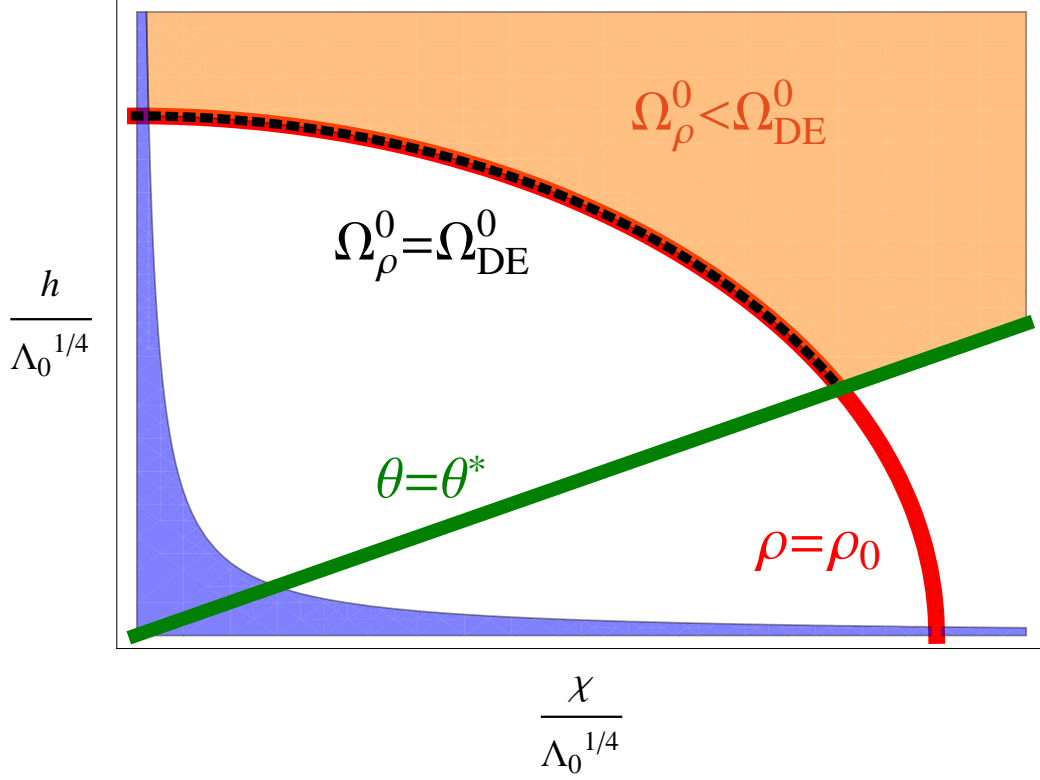


Figure 5.4: In this schematic plot we summarize the different kind of evolutions that can take place in Higgs-Dilaton inflation according to the different initial conditions. In order to guarantee a sufficient number of e-folds, the initial values of the Higgs and dilaton fields have to lie above the green line, which corresponds to  $\theta = \theta^*$ , given by (3.77). For  $\Lambda_0 > 0$  the dilaton contributes to the dark energy density in the late universe. For this contribution not to exceed the observational value  $\Omega_{\text{DE}}^0$ , the initial conditions have to lie above the arc of an ellipse  $\rho \simeq \rho_0$ , with  $\rho_0$  given by (5.29). The orange region in the figure corresponds therefore to initial field values giving rise to a successful inflationary stage as well as to a dark energy dominated era compatible with the observations. If the dilaton field is completely responsible from the present dark energy, the initial conditions must be fine-tuned to lie on the dotted black segment of the ellipse. The blue region below the hyperbola corresponds to the non-scale-invariant region where the  $\Lambda_0$  term becomes dominant. Trajectories starting in that area tend to move away from the origin before entering the scale-invariant region. Such initial conditions can also be acceptable as long as the corresponding trajectories enter the scale-invariant region above the line given by  $\rho \simeq \rho_0$ .





## CHAPTER 6

# Conclusions and Outlook

You alwaies end ere you begin.

---

*The two Gentlemen of Verona*  
W. SHAKESPEARE

## From the Early to the Late Universe

General Relativity and the Standard Model of Particle Physics constitute two well-founded pillars of modern physics, albeit not free of caveats. Questions such as the origin of neutrino masses, the dynamics of cosmic inflation or the nature of the dark components of the Universe remain unexplained. In the usual *Beyond the Standard Model* approach new physical scales are usually invoked in order to solve or alleviate the Standard Model problems. In this thesis we adopted an alternative and *minimalistic* approach, relying only on those elements that are known to be there or that can be discovered in the near future: The Standard Model is assumed to be valid up to the Planck scale and the number of additional degrees of freedom is severely restricted. The resulting models are therefore rather fragile, but at the same time extremely predictive. If any of their predictions is not verified the whole idea would be ruled out. Among all the phenomenological consequences, we focused on the cosmological aspects, especially on their relevance in the context of inflation, preheating and dark energy. Let us summarize the main results.

## The Higgs field and Inflation

We started by complementing the Einstein-Hilbert action with a non-minimal coupling of the Higgs field to gravity. A conformal transformation shows that the model is, at the level of the equations of motion, indistinguishable from the Starobinsky scenario [97, 98, 99, 100]. Indeed, the model admits inflationary solutions for relatively large values of the non-minimal coupling,

$\xi_h \sim 10^4$ , which rescues the Higgs field from the known difficulties for generating inflation. In spite of the large value of the coupling, it does not leave any observable signature at low energy scales and solar system physics. After the end of inflation, the symmetry breaking potential forces the Higgs field to acquire a vacuum expectation value, which is many orders of magnitude smaller than the Planck mass. The evolution of the, otherwise dynamical, gravitational Newton's constant freezes and the Weak Equivalence Principle bounds [93] can be satisfied.

In order to unify the different mechanisms for mass generation, the previous extension of the Standard Model was supplemented with a classical scale invariance symmetry, which can be extended to the quantum level if a specific renormalization scheme [116, 117] is used. The vacuum expectation value of the Higgs is made dynamical and promoted into a singlet scalar field, the dilaton. The coupling between the new singlet and the Standard Model particles is forbidden by quantum numbers, not violating therefore any experimental bound. Nevertheless, non-minimal couplings to gravity can be included, in the spirit of the Induced Gravity scenario. The resulting lagrangian density does not display any scale or mass parameter. All the scales, including the Newton's constant, originate from one and the same source: the spontaneous breaking of scale invariance. Due to quantum scale invariance the Higgs mass is stable against quantum corrections [116]. As a bonus, the model also provides a successful inflationary scenario. In spite of dealing with a multi-field inflationary model, no isocurvature perturbations are produced during the whole inflationary stage. The conserved current associated to the symmetry of scale invariance effectively reduces the number of degrees of freedom to a single field. Indeed, by choosing the appropriate set of variables, it was shown that the inflationary trajectories are well described, when rescaled, by circumferences of constant radius in field space, whose evolution depends only on an angular variable. In this case, the primordial power spectra can be directly related to the observations of the CMB [1] to obtain bounds on the non-minimal couplings of the Higgs and dilaton fields to gravity, which turn out to be of order  $\xi_h \sim 10^4$  and  $\xi_\chi \sim 10^{-3}$  respectively.

## On the initial conditions of the hot Big Bang

The number of Standard Model particles per comoving volume at the end of inflation is completely negligible. Any particle abundance previous to the inflationary stage has been completely diluted by the inflationary expansion. In order to recover the standard hot Big Bang picture, the potential and kinetic energy stored in the Higgs condensate must be transferred to the Standard Model particles during the (p)reheating stage. Given the hierarchical structure of the non-minimal couplings to gravity, with one of them much larger than the other, the study of the (p)reheating stage in Higgs-Dilaton inflation effectively reduces to that in Higgs inflation, up to small corrections and dilaton production [219]. All the couplings of the Higgs (inflaton) to matter fields are experimentally known at the electroweak scale, and can be extrapolated to the (p)reheating scale using the renormalization group equations. Contrary to other (p)reheating models, no *ad hoc* assumptions about their values are done. The process becomes more complicated than expected, and a series of subsequent stages take place, where essentially all different types of particle production mechanisms at preheating occur [77, 202].

After a negligible tachyonic particle production after the end of inflation, the Higgs field starts to oscillate around the minimum of its potential with a curvature scale of order  $10^{13}$  GeV. Given the initial large occupation of the Higgs zero-mode, the standard Quantum Field Theory techniques for particle production in non-trivial backgrounds [94, 238] can be applied. Indeed, the oscillating Higgs condensate gives rise to a homogeneous time-dependent mass term for all the fields to which it is coupled. Notice that the concept of particle can only be properly defined in those cases in which the frequency of oscillations changes adiabatically. Although this condition is satisfied during most of the oscillation period, it is certainly violated around the minimum of the potential, where the temporal variation of the Higgs field is maximal. This gives rise to an inequivalence between the vacua before and after the zero crossing, which can be interpreted as non-perturbative particle production [181, 183]. While there is no restriction on the number of created weak bosons, the direct production of SM fermions is severely restricted by Fermi-Dirac statistics [206]. Based on the experience on other preheating scenarios, the number density of gauge bosons would be expected to grow exponentially due to bosonic stimulation. However, the couplings among the gauge and fermionic fields in the Standard Model are non-negligible, which gives rise to a very complicated process in which perturbative and non-perturbative effects are mixed. We called this process *Combined Preheating* [77], to distinguish it from all the other existing (p)reheating mechanisms. The created weak bosons, triggered by the increasing Higgs amplitude after the zero crossing, acquire a large mass and decay (perturbatively) into quarks and leptons within half a Higgs oscillation, rapidly depleting the occupation numbers of gauge bosons. This forbids the weak bosons to accumulate and postpones the development of the resonance. At this point, the fraction of energy of the Higgs that goes into Standard Model particles is still very small compared with the energy in the oscillations. A relatively large number of oscillations will take place before a significant amount of energy is transferred to the gauge bosons and fermions. Eventually, the decreasing of the Higgs amplitude due to the matter-like expansion of the Universe reduces the decay rate and parametric resonance becomes the dominant effect. The gauge bosons start to build up their occupation numbers very rapidly via parametric amplification. We computed the distribution of the energy budget among all the species present at that time, which roughly coincides with the time at which backreaction from the gauge bosons into the Higgs condensate start to be significant. As a consequence, the Higgs field acquires a large mass and preheating ends. Soon afterwards, the Universe is filled with the remnant condensate of the Higgs and a non-thermal distribution of fermions and bosons, redshifting as radiation and matter respectively. From there on until thermalization [239, 240, 241], the evolution of the system is highly non-linear and non-perturbative, which makes it difficult to make a clear statement about the subsequent stage. Numerical studies in the lattice are needed.

It is interesting to notice that, although the *Combined Preheating* scenario was discussed in the context of Higgs inflation, the formalism is completely general and could be applied to any realistic particle physics theory. Indeed, the described competition between perturbative and non-perturbative physics will take place whenever the inflaton couples to fields able to decay into lighter ones. Whether the energy density of the decay products overcomes that in the inflaton condensate before the development of the resonance or not depends on the specific values of the couplings. Among the many particle physics models that

could be considered, the so-called New Higgs Inflation scenario [242, 243] seems especially interesting. It constitutes an alternative, or rather a complement, to the Higgs inflation models described above, where all the couplings to the Standard Model particles are also known. The *Combined Preheating* mechanism could besides modify the development of the Gravitational Wave Background (GWB) produced as a secondary product of the re-scattering of classical matter waves produced during preheating [244, 245, 246, 247, 248, 249, 250, 251] as well as the production of magnetic fields at preheating [252, 253] or even electroweak baryogenesis [254, 255, 256, 257].

### The Higgs field and Dark Energy

The required dilatation symmetry described above forbids the appearance of a cosmological constant term in the action. Nevertheless, this term can be recovered if one considers a very modest modification of General Relativity. In Unimodular Gravity the metric determinant is fixed to one and the  $\Lambda$  term reappears at the level of the equations of motion. Its physical interpretation is however very different. Rather than a cosmological constant, it becomes the strength of a quintessence potential, being its value related only to initial conditions. The Higgs and dilaton fields are able to provide not only an inflationary stage, with successful preheating, but also a dark energy dominated period. All the parameters of the theory are completely determined from CMB physics, which allows us to make specific predictions in any subsequent period. In particular, we present an extremely appealing connection between the spectral tilt of the CMB anisotropies,  $n_s^*$ , and the present equation of state  $w_{\text{DE}}^0$  of dark energy,  $-3(w_{\text{DE}}^0 + 1) \approx (n_s^* - 1)$ , for  $\Omega_{\text{DE}} = 0.74$ . An extra consistency relation,  $3w_a \approx dn_s^*/d \ln k$ , between the scale-factor dependence of the equation of state for dark energy,  $w(a) = w_0 + w_a(1-a)$  and the logarithmic running of the spectral tilt is also presented. These expressions allowed us to predict within this model the equation of state parameter and its derivative,  $w = -0.987$  and  $w_a < 0.01$ , which constitutes a precise prediction that could potentially allow to accept or reject the model.

### *Something in the distance...*

These are very exciting times for modern physics, where lots of data will be available soon. To know if the particle physics desert assumed throughout this Thesis [60, 57] is the proper answer or a *Beyond the Standard Model* oasis appears in the distance is just a matter of time. Decades of speculations and unsolved questions may turn out into experimental realities, changing our understanding of the Universe or just slightly modifying it. Regarding the cosmological aspects discussed in this work, the results of the LHC, the PLANCK mission and the different surveys aimed to unveil the nature of the dark energy are particularly important. The precise electroweak symmetry breaking mechanism will hopefully be accessible in the LHC, whatever it may be. If the simplest scenario is finally realized and the Higgs boson detected, the measurement of its mass will complete the list of the couplings of the Standard Model. On the other hand, the PLANCK satellite [258] might determine the tensor contribution to the temperature and polarization anisotropies of the CMB, whose amplitude is directly proportional to the energy scale of inflation [259, 260, 261, 262, 263]. Photometric

and Spectroscopic Dark Energy surveys, such as DES, PAU or BOSS [264, 265, 266], will determine the Dark Energy equation of state at the 5 % level, or even better, as well as its evolution with the scale factor at the 10 % level. Unfortunately, the Higgs-Dilaton models consistency relations seem difficult to be tested in the near future.



## CHAPTER 7

# Resumen y Perspectivas

You alwaies end ere you begin.

*The two Gentlemen of Verona*  
W.SHAKESPEARE

## Del Universo primitivo a nuestros días

La Relatividad General y el Modelo Estándar de Física de Partículas constituyen dos de los pilares mejor fundamentados de la física moderna, aunque no por ello libres de problemas. La ausencia de respuestas para cuestiones tan fundamentales como el origen de las masas de los neutrinos, la dinámica del proceso inflacionario o la naturaleza de las componentes oscuras del Universo, motivó la búsqueda de soluciones en las llamadas teorías *Más allá del Modelo Estándar*. Un denominador común de todas estas teorías es la introducción de nuevas escalas físicas y/o partículas para intentar solventar, o al menos aliviar dichas dificultades. En esta tesis se adoptó una visión alternativa y minimalista para afrontar el problema, basada solamente en elementos bien conocidos o susceptibles de ser verificados en un futuro cercano. Se asume que el Modelo Estándar es válido hasta la escala de Planck, restringiendo con ello sustancialmente el número de grados de libertad e imponiendo la búsqueda de respuestas dentro del marco existente. Los modelos obtenidos son por tanto extramadamente frágiles pero al mismo tiempo extraordinariamente predictivos. Si cualquiera de sus predicciones no se viera satisfecha, la idea debería descartarse por completo. De entre todas las posibles consecuencias fenomenológicas, en esta tesis se hizo especial hincapié en los aspectos de índole cosmológico, especialmente en aquellos relacionados con inflación, recalentamiento y energía oscura. En lo que sigue resumimos los principales resultados obtenidos.

## El Higgs e Inflación

Se introdujo un acoplo no-minimo del campo de Higgs a gravedad, adicional al termino de tipo Einstein-Hilbert ya existente. Es fácil demostrar, haciendo uso de una transformación conforme, que el citado modelo es indistinguible del modelo de Starobinsky [97, 98, 99, 100], al menos al nivel de las ecuaciones de movimiento. Al igual que este último, nuestro modelo admite soluciones inflacionarias para acoplos no-mínimos relativamente grandes  $\xi_h \sim 10^4$ , capaces de rescatar al Higgs de las conocidas dificultades para generar inflación. A pesar del enorme valor del acoplo, este no deja ningún tipo de signatura experimental ni en el sistema solar ni en los experimentos de baja energía, ya que al final de inflación el Higgs adquiere un valor de expectación muchos ordenes de magnitud menor que la escala de Planck. La evolución del mismo queda por tanto congelada y las cotas sobre el Principio de Equivalencia Débil [93] satisfechas.

Para intentar unificar los diferentes mecanismos de generación de masa se extendió el anterior modelo con una simetría de escala clásica, potencialmente extendible al regimen cuántico por medio de un proceso de renormalización adecuado [116, 117]. El valor de expectación del Higgs se convierte en este caso un singlete escalar dinámico, el dilatón. Los acoplos entre esta nueva partícula y las ya existentes en el Modelo Estándar están prohibidos por sus números cuánticos, respetandose por tanto todas las cotas experimentales. Sin embargo, el dilaton puede acoplarse no-minimamente a gravedad, igual que el Higgs, en el más puro espíritu de Gravedad Inducida. El lagrangiano resultante no contiene parametro dimensional o escala alguna. Todas las escalas se originan a partir de un único mecanismo: la ruptura espontánea de la invariancia de escala. Si esta se mantiene a nivel cuántico, la masa del Higgs resulta estable frente a correcciones radiativas [116]. Al igual que en el modelo anterior, el sistema admite soluciones inflacionarias. La corriente de Noether asociada a la invariancia de escala actúa como una ligadura que reduce de manera efectiva el número de grados de libertad a uno, no produciendose por tanto perturbaciones isocurvatura durante el proceso inflacionario. En este caso, el espectro de potencias primordial puede relacionarse directamente con las observaciones del Fondo Cósmico de Microondas [1], obteniendo cotas sobre los valores de los acoplos no mínimos del Higgs y del dilaton a gravedad. Estos resultan ser de orden  $\xi_h \sim 10^4$  y  $\xi_\chi \sim 10^{-3}$  respectivamente.

## Sobre las condiciones iniciales del Big Bang

El número de partículas del Modelo Estándar por volumen comóvil al final de proceso inflacionario es completamente despreciable. Cualquier contenido previo a dicho estado se ve completamente diluido por la expansion. Si queremos recuperar el Big Bang o historia térmica del Universo, la energía cinética y potencial almacenada en el condensado de Higgs debe ser transferida a las partículas del Modelo Estándar en un proceso llamado (p)recalentamiento. Dada la estructura sumamente jerarquica de los acoplos no mínimos a gravedad, con uno de ellos mucho mayor que el otro, el estudio del proceso de recalentamiento en Higgs-Dilaton Inflation se reduce de manera efectiva a aquel en Higgs Inflation, salvo pequeñas correcciones o producción de dilatones [219]. Todos los acoplos entre el inflaton y los campos de materia son conocidos a la escala electrodébil, lo que permite su extrapolación hasta la escala de recalentamiento mediante el uso de las ecuaciones del grupo de renormalización. Esta carac-



terística es extremadamente singular, y diferencia los modelos estudiados de otros modelos de recalentamiento. El proceso final resulta ser más complicado de lo esperado, involucrando en él todos los procesos de producción de partículas conocidos [202, 77]. Tras una, casi despreciable, producción taquionica de partículas al final de inflación, el Higgs comienza a oscilar alrededor del mínimo de su potencial, decurvatura aproximada  $10^{13}$  GeV. La alta población inicial del modo cero del Higgs nos permite hacer uso de las técnicas de teoría cuántica de campos para la producción de partículas en *background* no triviales [94, 238]. El Higgs en su oscilación da lugar a un término de masa homogéneo dependiente del tiempo para todos aquellos campos a los que se encuentra acoplado. Nótese que el concepto de partícula solamente está definido si la evolución temporal de dichas masas es suficientemente lenta. Aunque esta condición claramente se satisface durante la mayor parte del periodo de oscilación, se viola en las zonas cercanas al mínimo del potencial, donde la variación temporal del Higgs es máxima. Esto da lugar a inequivalencias entre los diferentes vacíos antes y después de dicho punto, lo que puede interpretarse como producción no perturbativa de partículas [181, 183]. De entre las diferentes especies creadas, destacan por su número los bosones intermedios, mientras que la creación de fermiones está seriamente restringida por la estadística de Fermi-Dirac [206]. Los bosones creados tienden a decaer en fermiones debido al incremento de su masa efectiva por el desplazamiento del Higgs hacia el máximo de su potencial, dando lugar a un proceso muy complicado que llamamos *Recalentamiento Combinado*, para distinguirlo de los mecanismos existentes. El decaimiento de los bosones gauge impide la producción estimulada de los mismos y por tanto el desarrollo de la resonancia paramétrica. La fracción de energía transferida a las partículas del Modelo Estándar es todavía muy pequeña comparada con la almacenada en las oscilaciones. Serán necesarias un gran número de oscilaciones para que la transferencia sea efectiva y el decrecimiento de la amplitud del Higgs permita al efecto resonante dominar sobre el decaimiento en fermiones. A partir de este momento el número de bosones gauge crece exponencialmente vía amplificación paramétrica. Cuando esto ocurre el *backreaction* sobre el condensado de Higgs empieza a ser significativo, lo que da lugar a un incremento de la masa del Higgs y al final del recalentamiento. El estado resultante contiene el remanente del condensado de Higgs, así como una distribución no térmica de fermiones y bosones, escalando como radiación y materia respectivamente. La evolución del sistema hasta termalización [241] es altamente no lineal y no perturbativa, lo que requiere el uso de métodos numéricos en el retículo.

Es destacable que aunque el *Recalentamiento Combinado* previamente descrito fue analizado en el contexto de Higgs Inflation, es un formalismo completamente general que puede ser aplicado a cualquier teoría realista de física de partículas. La competición entre efectos perturbativos y no-perturbativos tendrá lugar en todos aquellos casos en los que el inflatón se acople a campos acoplados a su vez a otros más ligeros. Si la densidad de energía de los productos de decaimiento supera o no a la almacenada en el inflatón antes del desarrollo de la resonancia dependerá de los valores específicos de los acoplos en cada modelo. De entre todas las posibilidades destaca el conocido como *New Higgs Inflation* [242, 243], por constituir una alternativa a *Higgs Inflation* donde también se conocen todos los acoplos. El *Recalentamiento Combinado* podría modificar además el desarrollo del Fondo de Ondas Gravitacionales (GWB) producido como un producto secundario del re-scattering de las ondas de materia producidas durante preheating [244, 245, 246, 247, 248, 249, 250, 251],

así como la producción de campos magnéticos [252, 253] o incluso baryogenesis a la escala electrodébil [254, 255, 256, 257].

### El Higgs y la Energía Oscura

La simetría de dilatación introducida anteriormente prohíbe la aparición de una constante cosmológica al nivel de la acción. Esta puede ser sin embargo recuperada haciendo uso de una modesta modificación de Relatividad General conocida como Gravedad Unimodular. En ella el determinante de la métrica se fija a la unidad y el término  $\Lambda$  reaparece al nivel de las ecuaciones de movimiento, aunque con una interpretación física muy diferente. En lugar de una constante cosmológica debería interpretarse como la amplitud de un potencial, con su valor dictado por las condiciones iniciales. Este potencial se enmarca dentro de los modelos conocidos como de quintaesencia y puede dar lugar a un periodo dominado por energía oscura. Todos los parámetros del modelo se encuentran fijados por el proceso inflacionario inicial, lo que permite hacer predicciones concretas sobre cualquier periodo subsiguiente. Concretamente, presentamos una sorprendente relación entre el tilte espectral de las anisotropías de Fondo Cósmico de Microondas  $n_s^*$  y la ecuación de estado  $w_{\text{DE}}^0$  de la energía oscura,  $-3(w_{\text{DE}}^0 + 1) \approx (n_s^* - 1)$ , para  $\Omega_{\text{DE}} = 0.74$ . Es posible obtener además una relación de consistencia adiacional,  $3w_a \approx dn_s^*/d \ln k$ , entre la evolución de la ecuación de estado para la energía oscura  $w(a) = w_0 + w_a(1 - a)$  y el running del tilte espectral. Estas relaciones permiten derivar una predicción precisa para la ecuación de estado y su derivada,  $w = -0.987$  and  $w_a < 0.01$ , que podría potencialmente descartar o confirmar el modelo.

### *Algo en la distancia...*

Vivimos tiempos de júbilo para la física moderna, donde una gran cantidad de datos experimentales estará pronto a nuestra disposición. Saber si la naturaleza eligió el desierto de partículas y escalas presentado en esta tesis o por el contrario el oasis de otras teorías es solo una cuestión de tiempo. Decadas de especulaciones y preguntas sin resolver podrían convertirse en realidades confirmadas experimentalmente, cambiando ligeramente o por completo nuestra forma de entender el Universo. En lo que respecta a los diversos aspectos cosmológicos discutidos en este trabajo, los resultados del LHC, PLANCK y otras misiones similares son especialmente importantes. Con algo de suerte, el mecanismo (cualquiera que sea) responsable de la ruptura de simetría será pronto desvelado por el LHC. Si el escenario más sencillo es el elegido por la naturaleza, la medida de la masa del bosón de Higgs completará la lista de acoplos del Modelo Estándar. Por otro lado, el satélite PLANCK [258] podría determinar las contribuciones tensoriales a la temperatura y polarización del Fondo Cósmico de Microondas, cuya amplitud está directamente relacionada con la escala de energía de inflación [259, 260, 261, 262, 263]. Rastros fotométricos y espectroscópicos tales como DES, PAU o BOSS [264, 265, 266], determinarán el valor de la ecuación de estado de la energía oscura con una precisión del 5 % , o incluso mejor, así como su evolución con el factor de escala al 10 % . Lamentablemente, las relaciones de consistencia de Higgs-Dilaton inflación serán difíciles de testar en un futuro próximo.

# Appendices



## APPENDIX A

# Parametric resonance as a quantum mechanical problem

This appendix is devoted to the derivation of Eq. (4.66). This expression is indeed generic for any interaction of the form

$$V_{\text{eff}}(\phi, A) = V(\phi) + \frac{1}{2}\mathcal{M}^2(\phi)A^2, \quad (\text{A.1})$$

with  $\mathcal{M}^2(\phi)$  playing the role of an effective mass term

$$\mathcal{M}^2(\phi) \equiv \frac{\partial^2 V_{\text{eff}}(\phi, A)}{\partial A^2}, \quad (\text{A.2})$$

for the  $A$  field. The field  $\phi$  must be understood as an homogeneous highly populated periodic field, satisfying  $\phi(t + \mathcal{T}) = \phi(t)$ . On the other hand,  $A$  is assumed to be in an initial vacuum state<sup>1</sup>. This fact allows us to decompose  $A$  into fluctuations

$$A(t, \mathbf{x}) = \frac{1}{(2\pi)^{3/2}} \int d^3k \left( a_k A_{\mathbf{k}}(t) e^{-i\mathbf{k}\mathbf{x}} + a_k^\dagger A_{\mathbf{k}}^*(t) e^{i\mathbf{k}\mathbf{x}} \right), \quad (\text{A.3})$$

living in an evolving background  $\phi$ . The temporal eigenfunctions  $A_k(t)$  in the previous expression obey the Klein-Gordon equation

$$\ddot{A}_k + 3H\dot{A}_k + \left( \frac{k^2}{a^2} + \mathcal{M}^2(\phi) \right) A_k = 0, \quad (\text{A.4})$$

where the physical momentum  $k_{ph} \equiv k/a(t)$  redshifts with time due to the expansion of the Universe. This equation resembles that of a damped,  $H \neq 0$ , (quantum) harmonic oscillator

---

<sup>1</sup>In the particular Higgs-driven inflationary scenarios  $\phi$  would correspond to the Higgs condensate, while the scalar field  $A$  would play the role of the different gauge fields polarizations.

with a time-dependent mass (frequency). The previous equation can be rewritten in a much more transparent way making use of the field redefinition

$$a^{3/2} A_k(t) \equiv \mathcal{A}_k(t) = \frac{\alpha_k(t)}{\sqrt{2\omega_k}} e^{-i \int^t \omega_k dt} + \frac{\beta_k(t)}{\sqrt{2\omega_k}} e^{+i \int^t \omega_k dt} , \quad (\text{A.5})$$

in terms of which the evolution equation (A.4) becomes<sup>2</sup>

$$\ddot{\mathcal{A}}_k(t) + \omega_k^2(t) \mathcal{A}_k(t) = 0 , \quad (\text{A.6})$$

with

$$\omega_k^2(t) \equiv k^2 + \mathcal{M}^2(t) . \quad (\text{A.7})$$

The functions  $\alpha_k$  and  $\beta_k$  satisfy the so-called Wronskian condition  $|\alpha_k|^2 - |\beta_k|^2 = 1$ . An additional and useful constraint on these functions can be imposed taking the derivative of Eq. (A.5) as if  $\alpha_k$  and  $\beta_k$  were time-independent, to obtain

$$\dot{\alpha}_k = \frac{\dot{\omega}}{2\omega} e^{+2i \int^t \omega dt} \beta_k , \quad \dot{\beta}_k = \frac{\dot{\omega}}{2\omega} e^{+2i \int^t \omega dt} \alpha_k . \quad (\text{A.8})$$

Note that Eq. (A.6) is just the a Schrödinger kind of equation for a wave function  $\mathcal{A}_k(t)$  scattering in a potential  $-\mathcal{M}^2(t)$ . The problem has been therefore translated into a quantum mechanical one, which allows to apply the standard complex time WKB methods (WKB). If the frequency is varying slowly with time

$$\frac{\dot{\omega}_k}{\omega_k^2} \ll 1 , \quad (\text{A.9})$$

then the solution of (A.6) is close to that of the equation in which  $\omega_k^2$  is constant (Born approximation). The region in which this happens is frequently called the *adiabaticity region*, since in this case the particle number,  $n_k = |\beta_k|^2$ , is an adiabatic invariant, evolving slowly with time. Indeed, for  $|\beta_k| \ll 1$  we can obtain an iterative solution

$$\beta_k \simeq \frac{1}{2} \int_{-\infty}^t dt' \frac{\dot{\omega}}{\omega^2} \exp \left( -2i \int_{-\infty}^{t'} dt'' \omega(t'') \right) . \quad (\text{A.10})$$

which clearly shows that for  $\dot{\omega}_k/\omega_k^2 \ll 1$  the particle production is completely negligible<sup>3</sup>. The field  $A$  approximately remains then in its vacuum state, given by initial positive frequency solution

$$\mathcal{A}_k(kt \rightarrow -\infty) = \frac{1}{\sqrt{2\omega_k}} e^{-i\omega_k t} . \quad (\text{A.11})$$

On the other hand, if the effective mass changes rapidly with time  $\dot{\omega}/\omega^2 \gg 1$  the WKB analysis breaks down. The particle number is then no longer an adiabatic invariant and a

<sup>2</sup>We skipped over corrections  $\sim H^2, \dot{H}$ . The smallness of these terms is indeed quite model dependent, but whenever  $a \propto t^n$ , as happens for instance in a radiation or matter dominated Universe, they can be safely neglected soon after inflation.

<sup>3</sup>The integral can be evaluated by the stationary phase method. For three-legs interactions the perturbative result can be interpreted as separate inflatons decaying independently into pairs of  $A$ -particles.

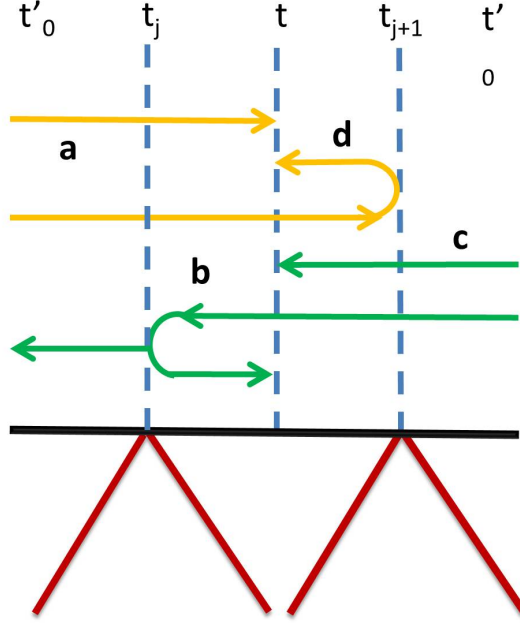


Figure A.1: Complex time WKB trajectories for a periodic potential.

significant particle production should be expected. The violations of the *adiabaticity condition* (A.9) are localized in the vicinity of so the so-called *reflection points*  $t_j$ , which correspond with those time at which the inflaton field  $\phi$  crosses zero. The (complex) points where the time dependent frequency, understood as a complex function, equals zero,  $\omega_k^2 = 0$ , are respectively known as *turning points*. In WKB the resonance particle production occurs due to rotation of currents at the *turning* and *reflection* points. The former kind of production is independent of time and is associated with the *spontaneous particle creation*, while the successive reflections at the points  $t_j$  are associated with *induced particle creation*. Let us define the action for the path that goes from  $t_i$  to  $t_f$

$$\Theta(t_f, t_i) = \int_{t_i}^{t_f} \omega(t) dt, \quad (\text{A.12})$$

and consider the asymptotic in and out boundary conditions

$$\mathcal{A}_k(kt \rightarrow -\infty) = T_k e^{i\Theta(t, t_0)}, \quad \mathcal{A}_k(kt \rightarrow +\infty) = e^{i\Theta(t, t_0)} + R_k e^{-i\Theta(t, t_0)}, \quad (\text{A.13})$$

corresponding to the absence of particles at  $kt \rightarrow -\infty$  and to the potential creation of particles at  $kt \rightarrow +\infty$ . Here  $R_k$  and  $T_k$  are the reflection and transmission amplitudes respectively, related again by the Wronskian condition  $|R_k|^2 + |T_k|^2 = 1$ . Rightmoving waves are chosen as  $\exp[-i\Theta(t, t_0)]$ , while the leftmoving ones evolve  $\exp[+i\Theta(t, t'_0)]$ . As can be seen in (A.13), the transmission and reflection coefficients are defined as  $(T_k, R_k)$  for the rightmoving waves. The left moving one will correspondingly have coefficients  $(T_k^*, R_k^*)$ . Let us focus on the violation of the adiabaticity condition around a given inflaton zero crossing  $t_j$ . The asymptotic adiabatic expressions for the incoming ( $t_{j-1} < t < t_j$ ) and outcoming

waves ( $t_j < t < t_{j+1}$ ) take the form

$$\mathcal{A}_k^j(t) = \frac{\alpha_k^j}{\sqrt{2\omega}} e^{-i\Theta(t,t_0)} + \frac{\beta_k^j}{\sqrt{2\omega}} e^{+i\Theta(t,t_0)}, \quad (\text{A.14})$$

$$\mathcal{A}_k^{j+1}(t) = \frac{\alpha_k^{j+1}}{\sqrt{2\omega}} e^{-i\Theta(t,t'_0)} + \frac{\beta_k^{j+1}}{\sqrt{2\omega}} e^{+i\Theta(t,t'_0)} \quad (\text{A.15})$$

where  $\alpha_k^j$ ,  $\beta_k^j$ ,  $\alpha_k^{j+1}$ ,  $\beta_k^{j+1}$  are constant coefficients in their corresponding intervals. In the region  $t_j < t < t_{j+1}$  the rightmoving component of  $\mathcal{A}_k^{j+1}(t)$

$$\mathcal{A}_{k,RMP}^{j+1} = \left[ \frac{\alpha_k^j}{T_k} + \frac{\beta_k^j R_k^*}{T_k^*} e^{2i\Theta(t_j,t_0)} \right] e^{-i\Theta(t,t_0)}, \quad (\text{A.16})$$

is made of two parts (cf. Fig. A.1). The first one (represented by  $a$  in Fig. A.1) gets the factor  $1/T_k$  after transmission at  $t_j$ . The second contribution to the rightmoving wave comes from  $t > t_j$ . The amplitude  $\beta_k^j \exp[2i\Theta(t_j, t_0)]$  of the leftmoving part (represented by the trajectory  $b$  in Fig. A.1), gets a factor  $1/T_k^*$ , when continued into the region  $t > t_j$ . This factor is again modified by the reflection at  $t_j$ , becoming finally the  $R_k^*/T_k^*$  term in (A.16). Comparing (A.16) with the first term in (A.15) we get

$$\alpha_k^{j+1} = \frac{\alpha_k^j}{T_k} + \frac{\beta_k^j R_k^*}{T_k^*} e^{2i\Theta(t_j,t_0)}. \quad (\text{A.17})$$

The left moving part

$$\mathcal{A}_{k,LMP}^{j+1} = \left[ \frac{\beta_k^j}{T_k^*} + \frac{\alpha_k^j R_k}{T_k} e^{-2i\Theta(t_{j+1},t_0)} \right] e^{+i\Theta(t,t_0)}, \quad (\text{A.18})$$

has also two contributions given by the trajectories  $c$  and  $d$  in Fig. A.1. The trajectory (c) coming from  $t'_0$  gives the left moving part  $\beta_k^{j+2} \exp[i\Theta(t, t'_0)]$  which in the region  $t < t_{j+1}$  gets a factor  $1/T_k^*$ . The continuity condition  $\beta_k^j e^{i\Theta(t_j,t_0)} = \beta_k^{j+2} e^{i\Theta(t_j,t'_0)}$  must be used to convert  $\beta_k^{j+2}$  to  $\beta_k^j$ . On the other hand, the amplitude of the trajectory (d) is modified by the transmission at  $t_j$  and the subsequent reflection at  $t_{j+1}$  acquiring a factor by a factor  $R_k/T_k$ . Comparing (A.18) with the second term in (A.15) provides

$$\beta_k^{j+1} = \frac{\beta_k^j}{T_k^*} + \frac{\alpha_k^j R_k}{T_k} e^{-2i\Theta(t_{j+1},t_0)}. \quad (\text{A.19})$$

Note that the previous expression coincides with that in (4.63). The number of particles just after the  $j$ -th scattering,  $n_k(j^+)$ , in terms of the number of particles  $n_k(j^-)$  just before that scattering, can be computed from (A.19) to obtain

$$n_k(j^+) = \mathcal{C}_k + (2\mathcal{C}_k + 1)n_k(j^-) + 2 \cos \theta_j \sqrt{\mathcal{C}_k(\mathcal{C}_k + 1)} \sqrt{n_k(j^-)(n_k(j^-) + 1)}$$

with  $\mathcal{C}_k \equiv T_k^{-1}(j) - 1$ , recovering therefore (4.66).



## APPENDIX B

# Conformal transformations

An overpresent mathematical tool throughout this thesis has been the use of conformal transformations. A conformal transformation

$$g_{\mu\nu} \rightarrow \tilde{g}_{\mu\nu} = \Omega^2 g_{\mu\nu} , \quad (\text{B.1})$$

is a point-dependent rescaling of a Lorentzian or Riemannian metric tensor in a smooth  $n$ -dimensional manifold  $\mathcal{M}$  by a non-vanishing, and sufficiently regular function  $\Omega = \Omega(x)$ , usually called the conformal factor. In the most interesting and practical applications, it usually depends on the value of one of more scalar fields coupled non-minimally to the curvature in a given frame. We will generically denote these scalar fields as  $\phi$ . The conformal transformation affects the lengths of spacetime intervals as well as the norm of vectors, but it leaves the light cones unchanged, maintaining therefore the causal structure of spacetime. In what follows we summarize some useful rules for conformally transforming the curvature invariants, stress-energy tensors and inflationary observables.

### B.1 Geometrical quantities

We start by considering the changes in the most relevant geometrical quantities. Let us denote by  $g$  the metric determinant  $\det(g_{\mu\nu})$ . Applying the conformal transformation (B.1) one has,

$$\tilde{g} \equiv \det(\tilde{g}_{\mu\nu}) = \Omega^{2n} g . \quad (\text{B.2})$$

On the other hand, the Christoffel symbols acquire an extra contribution due to the conformal factor  $\Omega$

$$\tilde{\Gamma}_{\nu\rho}^{\mu} = \Gamma_{\nu\rho}^{\mu} + \Omega^{-1} (\delta_{\nu}^{\mu} \nabla_{\rho} \Omega + \delta_{\rho}^{\mu} \nabla_{\nu} \Omega - g_{\nu\rho} \nabla^{\mu} \Omega) . \quad (\text{B.3})$$

Something similar happens with the Riemann tensor, and its associated contractions, namely

$$\begin{aligned} \tilde{R}_{\mu\nu\rho}^{\delta} = & R_{\mu\nu\rho}^{\delta} + 2\delta_{[\mu}^{\delta} \nabla_{\nu]} \nabla_{\rho}(\ln \Omega) - 2g^{\delta\sigma} g_{\rho[\mu} \nabla_{\nu]} \nabla_{\sigma}(\ln \Omega) + 2\nabla_{[\mu}(\ln \Omega) \delta_{\nu]}^{\delta} \nabla_{\rho}(\ln \Omega) \\ & - 2\nabla_{[\mu}(\ln \Omega) g_{\nu]\rho} g^{\delta\sigma} \nabla_{\sigma}(\ln \Omega) - 2g_{\rho[\mu} \delta_{\nu]}^{\delta} g^{\sigma\rho} \nabla_{\sigma}(\ln \Omega) \nabla_{\rho}(\ln \Omega) , \end{aligned} \quad (\text{B.4})$$

$$\begin{aligned}\tilde{R}_{\mu\nu} = & R_{\mu\nu} - (n-2)\nabla_\mu\nabla_\nu(\ln\Omega) - g_{\mu\nu}g^{\rho\sigma}\nabla_\rho\nabla_\sigma(\ln\Omega) + (n-2)\nabla_\mu(\ln\Omega)\nabla_\nu(\ln\Omega) \\ & - (n-2)g_{\mu\nu}g^{\rho\sigma}(\nabla_\rho\ln\Omega)(\nabla_\sigma\ln\Omega),\end{aligned}\quad (\text{B.5})$$

$$\tilde{R} = \Omega^{-2} [R - 2(n-1)\square(\ln\Omega) - (n-1)(n-2)g^{\mu\nu}\nabla_\mu(\ln\Omega)\nabla_\nu(\ln\Omega)]. \quad (\text{B.6})$$

At this point, we would like to make explicit the conformal transformation of the scalar curvature in 4 dimensions, since it plays a spacial role in the work developed in this thesis. Particularizing (B.6) to  $n = 4$  we obtain

$$\tilde{R} = \Omega^{-2} \left[ R - \frac{6\square\Omega}{\Omega} \right] = \Omega^{-2} \left[ R - \frac{12\square\sqrt{\Omega}}{\sqrt{\Omega}} - \frac{3g^{\mu\nu}\nabla_\mu\Omega\nabla_\nu\Omega}{\Omega^2} \right]. \quad (\text{B.7})$$

Notice that the inverse transformations of the previous expressions can be easily calculated just by changing  $\Omega \rightarrow \Omega^{-1}$ . As these are written in terms of logarithms, this change translates into a change of sign in some of the terms in the corresponding expression. For instance, the inverse of (B.6) is given by

$$R = \Omega^2 \left[ \tilde{R} + 2(n-1)\tilde{\square}(\ln\Omega) - (n-1)(n-2)\tilde{g}^{\mu\nu}\nabla_\mu(\ln\Omega)\nabla_\nu(\ln\Omega) \right]. \quad (\text{B.8})$$

Finally, we would like to note that there exist a very important quantity for characterizing conformal metric, known as the Weyl or *conformal* tensor, whose form remains, according to its name, invariant under conformal transformations

$$\tilde{C}_{\mu\nu\rho}^\sigma = C_{\mu\nu\rho}^\sigma. \quad (\text{B.9})$$

## B.2 Matter quantities

Recall that in Section 4.3 we presented the transformation rules for the kinetic terms and interactions associated to scalar, vector and fermionic fields. We would like to supplement that study with the transformations rules for the matter content understood in the fluid description commonly used in General Relativity. Under the effect of a conformal transformation the stress energy tensor associated to a given matter lagrangian  $\mathcal{L}_M$

$$T_{\mu\nu} = \frac{-2}{\sqrt{-g}} \frac{\delta(\sqrt{-g}\mathcal{L}_M)}{\delta g_{\mu\nu}} \quad (\text{B.10})$$

becomes

$$\tilde{T}_{\mu\nu} = \Omega^{-n+2} T_{\mu\nu}. \quad (\text{B.11})$$

For the particular case of a perfect barotropic fluid of energy density  $\rho$ , pressure  $p$

$$T_{\mu\nu} = (\rho + p)u_\mu u_\nu + pg_{\mu\nu}, \quad (\text{B.12})$$

the previous equation (B.10) implies

$$\tilde{u}^\mu = \Omega^{-1} u^\mu, \quad \tilde{\rho} = \Omega^{-n} \rho, \quad \tilde{p} = \Omega^{-n} p. \quad (\text{B.13})$$

We conclude therefore that the equation of state of a given barotropic fluid<sup>1</sup> remains unchanged under conformal transformations.

---

<sup>1</sup>Note that the conclusion does not hold for a non-barotropic fluid with a general equation of state  $p(\rho)$ .

### B.3 Cosmological perturbations

In this thesis we chose to work in the Einstein frame, where all the inflationary slow-roll parameters and observables take the usual form used in Chapter 3. However, the analysis could have been also performed, with the same result, in the original Jordan frame, where the fields couple non-minimally to the scalar curvature. To illustrate this point, let us consider the metric perturbations generated during inflation. We start by decomposing the conformal factor (depending on the scalar fields non-minimally coupled to gravity) into a background  $\bar{\Omega}^2(t)$  and a perturbation  $\delta\Omega(\mathbf{x}, t)$  as

$$\Omega^2(\mathbf{x}) = \bar{\Omega}^2(t) + \delta\Omega(\mathbf{x}, t). \quad (\text{B.14})$$

When this transformation is applied to a perturbed Friedmann-Robertson-Walker metric longitudinal gauge

$$ds^2 = -(1 + 2\Psi(\mathbf{x}, t))dt^2 + a^2(t) (1 + 2\Psi(\mathbf{x}, t)) \delta_{ij} dx^i dx^j, \quad (\text{B.15})$$

we obtain the following transformation rules

$$d\tilde{t} = \Omega(t)dt, \quad \tilde{a}(t) = \Omega(t)a(t), \quad \tilde{\Phi} = \Phi + \frac{\delta\Omega}{2\Omega^2}, \quad (\text{B.16})$$

where the bar over the homogeneous part  $\bar{\Omega}(t)$  has been omitted to simplify the notation.

Let us start by analyzing the background evolution. The Hubble rate in the Einstein frame is redefined as

$$\tilde{H} \equiv \frac{1}{\tilde{a}} \frac{d\tilde{a}}{d\tilde{t}} = \frac{H}{\Omega} \left( 1 + \frac{\Omega'}{\Omega} \right), \quad (\text{B.17})$$

where the tilde denotes differentiation *wrt* the number of e-folds  $N$  in the Jordan frame. Taking into account the previous equation, it is easy to obtain an useful relation among the number of e-folds computed in both frames

$$\Delta \equiv \frac{dN}{d\tilde{N}} = 1 - \frac{d \ln \Omega}{d\tilde{N}}. \quad (\text{B.18})$$

Integrating the previous equation from the initial field configuration  $\phi_0$  at the beginning of inflation we get

$$\tilde{N} - N = \ln \frac{\Omega(\phi)}{\Omega(\phi_0)} \leq 0. \quad (\text{B.19})$$

As expected, the number of e-folds is not an invariant under conformal transformations. However, the difference between the two frames turns out to be practically irrelevant during the inflationary stage. As an example, let us consider Higgs-Inflation. To obtain an upper bound, we focus on the value at the end of inflation,  $\ln \Omega_{end}/\Omega_0$ , where the discrepancy between  $\tilde{N}$  and  $N$  is larger. As we saw in Chapter 3, the inflationary are well described by ellipses with constant radius,  $r_0^2 \equiv (1 + 6\xi_h)h_0^2 + (1 + 6\xi_\chi)\chi_0^2$ . Here  $h_0$  and  $\chi_0$  are the initial values for the Higgs and dilaton fields respectively. Let us assume that they are roughly equal. In this case, it is possible to relate the initial and final amplitude of the  $h$  field to obtain

$$\frac{h_{end}}{h_0} \approx \sqrt{\frac{6\xi_\chi}{1 + 12\xi_\chi}}. \quad (\text{B.20})$$

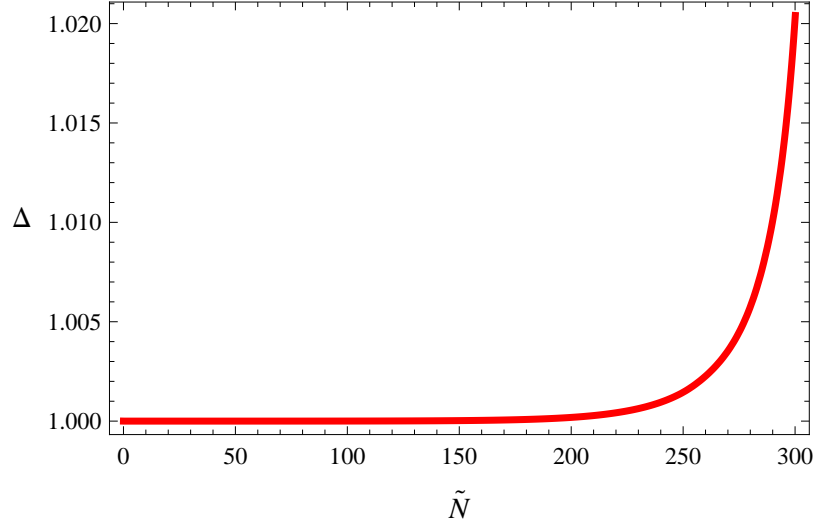


Figure B.1: The quantity  $\Delta \equiv 1 - \frac{d \ln \Omega}{d \tilde{N}}$  for an arbitrary inflationary trajectory. This quantity measures the difference between the number of e-folds computed in Einstein and Jordan frames. For values of  $\Delta$  close to 1 the observables in the Einstein frame can be directly related to those in the Einstein frame.

where we have used  $\xi_h \gg \xi_\chi$  as well as the approximate relation among the field amplitudes at the end of inflation  $\chi \approx \sqrt{\frac{\xi_h}{\xi_\chi}} h$ . Taking into account (B.20), we obtain  $\Omega_{end}/\Omega_0 \approx \sqrt{\frac{12\xi_\chi}{1+12\xi_\chi}}$ , which corresponds, for a typical  $\xi_\chi = 0.005$ , to

$$\left| \frac{N - \tilde{N}}{N} \right| \leq 2\% . \quad (\text{B.21})$$

During most of the inflationary stage the quantity  $\Delta$  in (B.18) is indeed quite smaller than the previous bound, cf. Fig. B.1. Given the small difference between the number of e-folds defined in Jordan and Einstein frame, we will from now on identify  $N = \tilde{N}$ . Regarding the cosmological perturbations produced during inflation, let us notice that the curvature perturbation on comoving slices is not only gauge invariant but also invariant under conformal transformations [267, 268]

$$\tilde{\mathcal{R}} \equiv \Phi - \frac{H}{d\phi/dt} \delta\phi = \tilde{\Phi} - \frac{\tilde{H}}{d\tilde{\phi}/d\tilde{t}} \delta\tilde{\phi} = \tilde{R} , \quad (\text{B.22})$$

as can be easily verified making use of the properties (B.17). This constitutes a fundamental property that can indeed be proved to any order in perturbation theory [269] (see also Ref. [270]). It allows to compute the action for a comoving perturbation in a given frame and then obtain it in another frame by simply performing a conformal transformation [271, 272]. The power spectra computed in the two frames agree

$$\mathcal{P}_\zeta = \tilde{\mathcal{P}}_\zeta . \quad (\text{B.23})$$

The associated spectral indices (for vanishing isocurvature modes) take the form [135]

$$\tilde{n}_s = 1 - 6\tilde{\epsilon} + 2\tilde{p}_{ab}\tilde{N}^{ab}, \quad n_s = 1 - 6\epsilon + 2p_{ab}N^{ab} + 3\frac{d\log\Omega}{dN}, \quad (\text{B.24})$$

in the final (Einstein) and initial (Jordan) frames respectively. The  $\tilde{\epsilon}$  and  $\tilde{N}_{ab}$  slow-roll parameters in the previous expression are defined in the Einstein frame, taking therefore the standard form

$$\tilde{\epsilon} \equiv \frac{M_P^2 \gamma^{ab} \tilde{V}_{,a} \tilde{V}_{,b}}{2\tilde{V}^2}, \quad N_{ab} \equiv \frac{M_P^2 \tilde{V}_{;ab}}{\tilde{V}}. \quad (\text{B.25})$$

with

$$\tilde{p}_{ab} \equiv \frac{\tilde{V}_{,a} \tilde{V}_{,b}}{\gamma^{cd} \tilde{V}_{,c} \tilde{V}_{,d}}, \quad (\text{B.26})$$

The corresponding slow-roll parameters in the Jordan frame are defined as [135]

$$\epsilon \equiv \frac{M_P^2 \gamma^{ab} V_{\text{eff},a} V_{\text{eff},b}}{2V^2}, \quad N_{ab} \equiv \frac{M_P^2 \Omega^2}{V} \left( \frac{V_{\text{eff};b}}{\Omega^2} \right)_{;a}. \quad (\text{B.27})$$

where the effective potential  $V_{\text{eff},a}$  is given by

$$V_{\text{eff},a} \equiv -\Omega^2 \left( \frac{V}{\Omega^2} \right)_{,a} \quad (\text{B.28})$$

and

$$p_{ab} = \frac{\tilde{V}_{\text{eff},a} \tilde{V}_{\text{eff},b}}{\gamma^{cd} \tilde{V}_{\text{eff},c} \tilde{V}_{\text{eff},d}}, \quad (\text{B.29})$$

Tensor perturbations are invariant under conformal transformations [126].



## APPENDIX C

### Higgs-Dilaton trajectories in the Jordan frame

In this Appendix we derive analytic formulae for the temporal evolution of the Higgs and dilaton fields in the Jordan frame and compared them with exact solutions obtained numerically in Jordan and Einstein frames in the way described in [273]. We start by considering the lagrangian density (3.33) for negligible  $\vartheta$ . If we assume the fields to be homogeneous during inflation, together with the standard slow-roll approximation,  $\dot{\phi}_a^2 \ll V$ ,  $\ddot{\phi}_a \ll V_{,a}$  and  $\dot{\phi}_a \ll H\dot{\phi}_a$  the equations of motion for the scalar fields (2.27), expressed in term of the number of e-folds  $N$ , becomes

$$3H^2\phi'_a \approx -V_{,a} + \frac{1}{2}f_{,a}R, \quad (\text{C.1})$$

while the Friedmann equations (2.25) and (2.26) simplify respectively to

$$V \approx 3H^2(f + f'), \quad (\text{C.2})$$

$$fR \approx 4V - 9H^2f'. \quad (\text{C.3})$$

In the last equation, we have assumed extended slow-roll conditions, namely  $1 + 6\xi_a\dot{\phi}_a \ll V(\phi)$  and  $1 + 6\xi_a\dot{\phi}_a \ll H\dot{f}(\phi)$ , which should be checked numerically *a posteriori*. Equations (C.2) and (C.3) imply that the Ricci scalar can be approximated as  $R \approx 12H^2(1 + f'/(4f))$ , which does not correspond to the usual approximation  $\dot{H} \ll H^2$ . Although it can be checked numerically that the contribution of the extra term  $f'/(4f)$  is indeed very small, it must be explicitly maintained to preserve the conservation law (2.23) in the slow-roll regime. Indeed, combining equations (C.1), (C.2) and (C.3) we obtain

$$(1 + 6\xi_\chi)\chi\chi' + (1 + 6\xi_h)hh' \approx 0, \quad (\text{C.4})$$

which can be integrated to obtain the field space constraint

$$r^2 \equiv (1 + 6\xi_h)h^2 + (1 + 6\xi_\chi)\chi^2, \quad (\text{C.5})$$

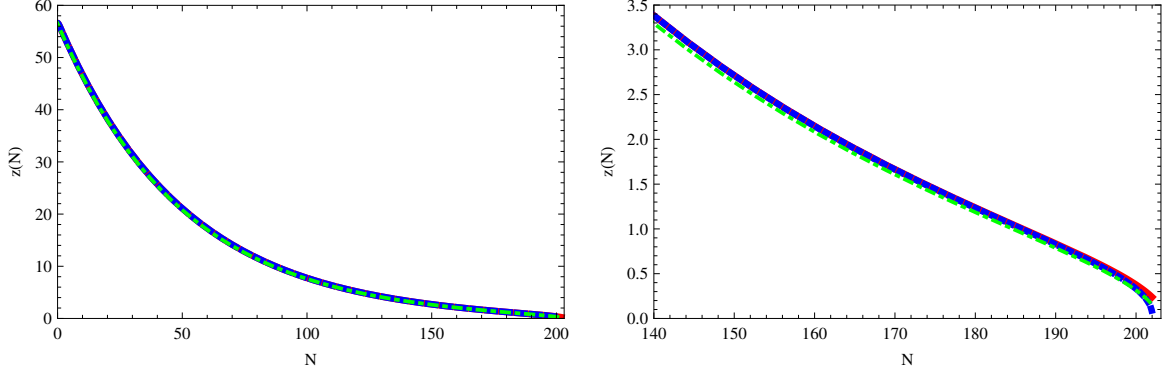


Figure C.1: Evolution of the angular variable  $z$  as a function of the number of e-folds  $N$  and detailed view of the last 60 e-folds. The green (dot-dashed) lines represent the approximate slow-roll solutions given by (C.9), while the red (solid) and blue (dashed) curves correspond to the result of an exact numerical computation performed in the Jordan and Einstein frames respectively.

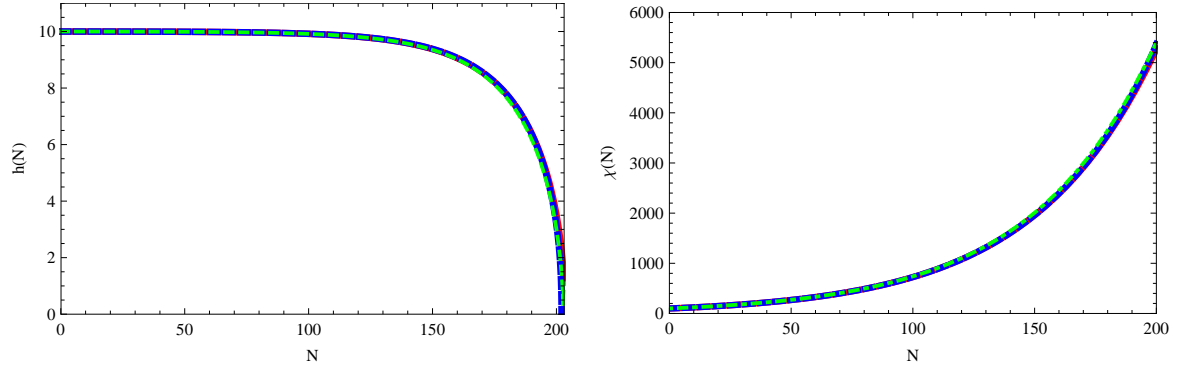


Figure C.2: Evolution of the Higgs  $h$  and dilaton  $\chi$  fields as a function of the number of e-folds  $N$ . The green (dot-dashed) lines represent the approximate slow-roll solutions given by (C.10), while the red (solid) and blue (dashed) curves are exact numerical results in the Jordan and Einstein frames respectively.



where  $r^2 = r_0^2$  is a constant determined by the initial conditions. The inflationary trajectories are therefore ellipses in field space of radius (C.5). This suggests to rewrite the problem in terms of polar coordinates  $(r, z)$ , where  $z$  is defined as

$$z \equiv \sqrt{\frac{(1 + 6\xi_h)}{(1 + 6\xi_\chi)}} \frac{h}{\chi}. \quad (\text{C.6})$$

Notice that this choice is quite natural from the point of view of a scale-invariant theory, where physical quantities can only depend on the ratio of dimensional quantities. The evolution equation for this angular variable can be computed making use of (C.1), (C.2) and (C.3) to obtain

$$\frac{z'}{z} \approx -4\xi_\chi \frac{z^2 + \sigma}{z^2 + \sigma + 2\xi_\chi} \left(1 + \frac{1}{z^2}\right), \quad (\text{C.7})$$

where

$$\sigma \equiv \frac{(1 + 6\xi_h) \xi_\chi}{(1 + 6\xi_\chi) \xi_h}. \quad (\text{C.8})$$

The previous equation can be easily solved to obtain the evolution with the number of e-folds

$$\frac{(1 + z^2)^{1-2\xi_\chi} (z^2 + 6\xi_\chi)^{2\xi_\chi}}{(1 + z_0^2)^{1-2\xi_\chi} (z_0^2 + 6\xi_\chi)^{2\xi_\chi}} = e^{-8\xi_\chi N}, \quad (\text{C.9})$$

where  $r_0$  and  $z_0$  stand for the initial values for the radial and angular coordinates respectively. The comparison between the slow-roll solution (C.9) for the  $z$  variable and the exact solutions obtained numerically in Jordan and Einstein frames is shown in Fig. C.1. Notice that we have identified the number of e-folds computed in Jordan with that computed Einstein frame,  $N$ , given the small difference between the two during the whole inflationary period, cf. Appendix B. The evolution of the non-dimensional quantity  $z$  does not depend on the chosen frame. Finally, making use of Eqs. (C.9) it is also possible to compute the corresponding values of the original Higgs and dilaton fields via

$$h(N) = \frac{r(N)}{\sqrt{1 + 6\xi_h}} (1 + z^{-2}(N))^{-1/2}, \quad \chi(N) = \frac{r(N)}{\sqrt{1 + 6\xi_\chi}} (1 + z^2(N))^{-1/2}, \quad (\text{C.10})$$

whose comparison with the numerical solutions is shown in Fig. C.2. The conservation law (2.23) acts therefore as a constraint equation, reducing the multi-field Higgs-Dilaton scenario to the single field case. This has strong implications, not only for the determination of the model parameters from the CMB observables, but also for the reheating stage after inflation, cf. Chapter 3.



# List of Tables

1	Cosmological Parameters for a $\Lambda$ CDM cosmology with a power-law initial spectrum, spatial flatness and cosmological constant [1]. . . . .	ii
1.1	Particle content of the Standard Model with a minimal Higgs sector (in black) and the $\nu$ MSM extensions (in blue). The number of degrees of freedom in the Standard Model is 98, while there exist 28 bosonic degrees of freedom. The $\nu$ MSM simply restores the symmetry between quarks and leptons in the SM by adding three right handed neutrinos, or equivalently 6 ( $3 \times 2$ ) fermionic degrees of freedom. In the scale-invariant extension of the $\nu$ MSM an extra scalar singlet $\chi$ (in brick red) is added. . . . .	7
3.1	Bounds from the CMB observables on the non-minimal couplings of the Higgs ( $h$ ) and dilaton fields to gravity ( $\chi$ ) for fast ( $\rho_{rh} = \rho_{max}$ ) and slow ( $\rho_{rh} = \rho_{max}$ ) reheating stages. . . . .	41
4.1	Approximate values of the Yukawa couplings in the Standard Model assuming a vacuum expectation value for the Higgs field $v = 249$ GeV. . . . .	60
4.2	Number of semi-oscillations of the Higgs required, as a function of $\lambda$ , for an efficient transfer of energy from the inflaton to the fermions (F) and/or to the gauge fields (B). The numbers are compared with the number of semi-oscillations for the backreaction (BR) of the gauge fields into the Higgs background to become significant. . . . .	80



## List of Figures

- 3.1 Comparative plot of the exact solution (red continuous line) obtained parametrically from (3.12), the analytic formula (3.16) for the potential (blue dashed line), and their parametrization (3.18) (green dotted line). Although the three different expression nicely agrees for positive values of the Higgs field, it can be clearly seen that the analytic formula (3.16) substantially differs from the parametric exact solution. . . . . 25
- 3.2 Shape of the Higgs-Dilaton potential in the Einstein frame (3.38) for the  $\beta = 0$  case (not to scale). The potential displays asymptotic flat regions that can give to inflation. It also possesses two completely degenerate classical ground states that spontaneously break the scale invariance of the corresponding action. . . 29
- 3.3 Numerically computed trajectories of Higgs and Dilaton fields in the Einstein-frame. The lower and upper curves correspond to slow-roll initial conditions. From the very beginning the fields satisfy the constraint  $r^2 = (1 + 6\xi_h)\chi^2 + (1 + 6\xi_\chi)\chi^2 = \text{const.}$ , represented by the dotted line above the lower curve. On the other hand, the initial values for the velocities of the intermediate solid curves have been chosen to be highly non-slow roll. Although the trajectory is initially influenced by the initial conditions, the fields end up describing an ellipse of constant radius in field space. . . . . 32
- 3.4 The approximate expressions (3.78) and (3.80) for the spectral tilt (left) and the tensor-to-scalar ratio (right) respectively as a function of the non-minimal coupling  $\xi_\chi$ . The red dashed curve is evaluated at  $N^* = N_{max}^*$ , corresponding to the fast reheating case,  $\rho_{rh} = \rho_{rh}^{max}$ . On the other hand, the blue solid curve represents the slow reheating case  $\rho_{rh} = \rho_{rh}^{min}$  with  $N^* = N_{min}^*$ . The green diagonal line correspond to the limiting case  $n_s = 1 - 8\xi_\chi$ . The dot-dashed horizontal line and the shaded regions correspond to the absolute maximum (3.84) and the observational  $1\sigma$  and  $2\sigma$  WMAP7 bounds for the scalar tilt respectively, cf. (3.90). . . . . 38

3.5	The allowed WMAP5 $1\sigma$ and $2\sigma$ regions in the $(r, n_s)$ . The prediction of Higgs Inflation (green box) are compared with those of the standard $m^2\phi^2$ and $\lambda\phi^4$ chaotic models and the Harrison-Zeldovich spectrum. . . . .	39
3.6	Parameter regions for which the values of the scalar tilt $n_s(k^*)$ and the amplitude of the scalar spectrum $\Delta_\zeta^2(k^*)$ , lie in the observationally allowed range 3.90, for $0.1 < \lambda < 1$ . The red area is obtained for $\rho_{rh} = \rho_{rh}^{max}$ (fast reheating), while the blue one corresponds to $\rho_{rh} = \rho_{rh}^{min}$ (slow reheating). The fact that the bands are cut on the right hand side is due to the constraint on the scalar tilt $n_s(k^*)$ , cf. (3.78). On the other hand, the band-shape comes from the constraint on the scalar perturbation amplitude $\Delta_\zeta^2(k^*)$ , cf. (3.79). . . . .	41
3.7	Reconstructed Higgs inflationary potential from the WMAP+SN+BA0 dataset as a function of the Higgs mass $m_H$ , the spectral tilt $n_s$ and the tensor to scalar ratio $r$ . The different contours correspond to quark pole masses $m_t = 168$ GeV (green), $m_t = 171.3$ GeV (blue), $m_t = 173$ GeV (magenta) at 68% and 95% C.L. Taken from [174]. . . . .	46
4.1	Numerical evolution of the radial coordinate $\rho$ during the (p)reheating stage. The field displays the shift symmetry $\rho \rightarrow \rho + c$ , associated to the conservation of the dilatational current. This fact reduces the background evolution during preheating to the single field Higgs inflationary case. . . . .	53
4.2	Comparison between the Higgs-Dilaton inflationary potential (blue continuous line) obtained from (4.13) and the corresponding one for the Higgs Inflation model (3.18) (red dotted line). In spite of the slight differences in the upper inflationary region, they nicely agree in the lower part, where the (p)reheating stage takes place. . . . .	54
4.3	Comparison among the exact inflationary potential (4.13) in Higgs-Dilaton inflation (solid black line) and the quadratic approximation in (4.14) with (red dashed line) and without (blue dotted line) taking into account the corrections $\Delta V_{HD}$ . Similar results can be found for Higgs Inflation. . . . .	54
4.4	Numerical evolution during the preheating of the field $\phi$ in (4.11). The amplitude of the oscillations decreases with time due to the expansion of the Universe. The blue solid line corresponds to the evolution on the exact Higgs-Dilaton potential (4.13), while the red dashed line comes from simple quadratic potential (4.14). The curves nicely agree from the very beginning of the preheating stage. . . . .	56
4.5	Spectral distributions (4.68) for the gauge bosons created in a single zero crossing through the first term of (4.66), calculated after $j = 1, 2, 5$ and 10 oscillations (from left to right). The horizontal axis represents $x_j = k/k_*(j)$ , so $x = 1$ is the typical width of the band of momenta of particles created at the first scattering. For later times, the distributions broaden out to greater momenta, since the argument of (4.68), $x_j$ behaves as $\propto j^{-1/3}$ . The typical momenta of the distribution agree with the one calculated in Section 4.6. . . . .	68

- 4.6 Schematic view of gauge boson and fermion production in Higgs Inflation: the slow evolution of the Standard Model effective masses allows to adopt a physically reasonable adiabatic definition of particle during most of the oscillation period. Nevertheless, for values of the Higgs field very close to the minimum of the potential, the adiabaticity condition becomes violated, which can be interpreted as particle production. Most of the created particles are intermediate gauge bosons, since the production of fermions is limited by Pauli blocking. The latter are produced as secondary products of the created gauge bosons, which tend to decay into them via the Standard Model decay widths, amplified by the growing Higgs amplitude. . . . . 69
- 4.7 The Floquet index for a given polarization of the  $W$  and  $Z$  bosons as a function of the variable  $x_j = k/k_*(j)$ . Here we show the maximum (continuous red), the average (short dashed green) and the typical (long dashed blue) indices. . . 74
- 4.8 The initial spectral distribution  $n_k(1^+)$  (lower blue curve) and the Gaussian approximation (4.95) for different  $j$ 's greater than 2 (rest of the curves), describing the resonant behaviour. The approximation is so good that it is hard to distinguish it from the real curve, presenting small deviations just on the tail. The horizontal axis is  $x = k/k_*(1)$  and the curves correspond to different  $j$ 's. It is clearly distinguishable the fact that only the range  $x < 1$  ( $k < k_*(1)$ ) is filtered and therefore excited through parametric resonance, no matter if  $j \gg 2$ . . . . . 76
- 4.9 Successive spectral distributions  $k^2 n_k(1^+) e^{2\pi \sum_{k=2}^j \mu_k(j)}$ , at different  $j$ 's, including the volume factor  $k^2$ . One can see the predicted (4.99) slow displacement of the maxima of the distribution. The x-axis is given in terms of  $x = k/(k_*(1))$ . 76
- 4.10 The ratio  $k^2/\langle m^2 \rangle$  between the typical momenta produced around zero and the averaged mass in every oscillation for the  $W$  (dashed blue line) and  $Z$  bosons (continuous red line) as a function of the number of oscillations. This ratio is significantly smaller than 1 for all crossings, which allows us to consider the produced gauge bosons as non-relativistic. . . . . 77
- 4.11 Schematic representation of the *Combined Preheating* process: The non-perturbatively created gauge bosons in the successive scatterings in the inverted periodic triangular potential (first spontaneously and then via stimulated emission) tend to decay into fermions while their effective masses (4.38) are *boosted* due to the coupling with the Higgs field. These decays initially delay the development of parametric resonance and the consequent exponential particle production. Eventually, the resonant effects overtake the perturbative decays and parametric resonance develops as usual, i.e. as if the produced bosons would not decay perturbatively during each semi-oscillation. . . . . 78
- 4.12 The dependence of the frequency of oscillation in (4.121) as a function of  $A_k$  and  $z$ . The region under the blue dashed line corresponds to  $A_k - 2p|\cos 2z| - p^2 \sin^2 2z < 0$ . Note the periodicity  $T = \pi/2$ . . . . . 82

4.13	The Floquet index $\mu_k$ for dilaton production. It presents a large infrared band at low momenta is reminiscent of a tachyonic mechanism, and a smaller band at higher momenta. The results neglect the expansion of the universe. . . . .	83
5.1	Shape of the Einstein-frame Higgs-Dilaton potential in the original field variables $h$ and $\chi$ for $\Lambda_0 < 0$ (left) and $\Lambda_0 > 0$ (right). The non-equal zero value of $\Lambda_0$ gives rise to the well and chimney shapes in the center of the figures. Its main effect is lifting the valleys, breaking therefore the degeneracy of the classical ground state. For $\Lambda_0 < 0$ the valleys are tilted towards the origin, which induces a trivial classical ground state $(h, \chi) = (0, 0)$ . On the other hand, for $\Lambda_0 > 0$ the potential becomes of runaway type, with an asymptotic ground state at large field values. . . . .	87
5.2	The monotonically increasing function $F(\Omega_\rho)$ (green solid line). Note that it becomes exactly 1/2 for $\Omega_\rho = 0.74$ (red dashed lines). . . . .	90
5.3	Approximate functional relationship (5.24) between the spectral tilt and the dark energy equation of state. The red dashed curve is obtained for fast reheating $\rho_{rh} = \rho_{rh}^{max}$ with $N^* = N_{max}^*$ , while the blue solid curve represents the case of slow reheating $\rho_{rh} = \rho_{rh}^{min}$ with $N^* = N_{min}^*$ . The shaded region shows the WMAP7 $1\sigma$ and $2\sigma$ bounds. The green diagonal line corresponds to the further approximation (5.25). Note that this extra approximation completely fails to describe the behaviour of (5.24) close to the cosmological constant case $w_{DE}^0 = -1$ . However, it might constitute a good approximation, within the expected precision of the forthcoming surveys, for slightly larger values of $w_{DE}^0$ . Gray horizontal dot-dashed line represent the expected accuracy to be achieved by the Planck satellite [237] around an hypothetical central value of the spectral tilt. . . . .	92
5.4	In this schematic plot we summarize the different kind of evolutions that can take place in Higgs-Dilaton inflation according to the different initial conditions. In order to guarantee a sufficient number of e-folds, the initial values of the Higgs and dilaton fields have to lie above the green line, which corresponds to $\theta = \theta^*$ , given by (3.77). For $\Lambda_0 > 0$ the dilaton contributes to the dark energy density in the late universe. For this contribution not to exceed the observational value $\Omega_{DE}^0$ , the initial conditions have to lie above the arc of an ellipse $\rho \simeq \rho_0$ , with $\rho_0$ given by (5.29). The orange region in the figure corresponds therefore to initial field values giving rise to a successful inflationary stage as well as to a dark energy dominated era compatible with the observations. If the dilaton field is completely responsible from the present dark energy, the initial conditions must be fine-tuned to lie on the dotted black segment of the ellipse. The blue region below the hyperbola corresponds to the non-scale-invariant region where the $\Lambda_0$ term becomes dominant. Trajectories starting in that area tend to move away from the origin before entering the scale-invariant region. Such initial conditions can also be acceptable as long as the corresponding trajectories enter the scale-invariant region above the line given by $\rho \simeq \rho_0$ . . . . .	95



A.1	Complex time WKB trajectories for a periodic potential. . . . .	111
B.1	The quantity $\Delta \equiv 1 - \frac{d \ln \Omega}{dN}$ for an arbitrary inflationary trajectory. This quantity measures the difference between the number of e-folds computed in Einstein and Jordan frames. For values of $\Delta$ close to 1 the observables in the Einstein frame can be directly related to those in the Einstein frame. . . . .	116
C.1	Evolution of the angular variable $z$ as a function of the number of e-folds $N$ and detailed view of the last 60 e-folds. The green (dot-dashed) lines represent the approximate slow-roll solutions given by (C.9), while the red (solid) and blue (dashed) curves correspond to the result of an exact numerical computation performed in the Jordan and Einstein frames respectively. . . . .	120
C.2	Evolution of the Higgs $h$ and dilaton $\chi$ fields as a function of the number of e-folds $N$ . The green (dot-dashed) lines represent the approximate slow-roll solutions given by (C.10), while the red (solid) and blue (dashed) curves are exact numerical results in the Jordan and Einstein frames respectively. . . . .	120



## Bibliography

- [1] E. Komatsu *et al.*, “Seven-Year Wilkinson Microwave Anisotropy Probe (WMAP) Observations: Cosmological Interpretation,” [arXiv:1001.4538 \[astro-ph.CO\]](#).  
[arXiv:1001.4538 \[astro-ph.CO\]](#).
- [2] S. L. Glashow, “Partial Symmetries of Weak Interactions,” *Nucl. Phys.* **22** (1961) 579–588.
- [3] S. Weinberg, “A Model of Leptons,” *Phys. Rev. Lett.* **19** (1967) 1264–1266.
- [4] A. Salam, “Weak and Electromagnetic Interactions,”. Originally printed in Svartholm: Elementary Particle Theory, Proceedings Of The Nobel Symposium Held 1968 At Lerum, Sweden, Stockholm 1968, 367-377.
- [5] A. Djouadi, “The Anatomy of electro-weak symmetry breaking. I: The Higgs boson in the standard model,” *Phys.Rept.* **457** (2008) 1–216, [arXiv:hep-ph/0503172 \[hep-ph\]](#).
- [6] A. Einstein, “The Foundation of the General Theory of Relativity,” *Annalen Phys.* **49** (1916) 769–822.
- [7] A. Friedman, “On the Curvature of space,” *Z.Phys.* **10** (1922) 377–386. Original in Germany.
- [8] E. Hubble, “A relation between distance and radial velocity among extra-galactic nebulae,” *Proc.Nat.Acad.Sci.* **15** (1929) 168–173.
- [9] G. Gamow, “Expanding universe and the origin of elements,” *Phys.Rev.* **70** (1946) 572–573.
- [10] R. Alpher, H. Bethe, and G. Gamow, “The origin of chemical elements,” *Phys.Rev.* **73** (1948) 803–804.
- [11] A. A. Penzias and R. W. Wilson, “A Measurement of excess antenna temperature at 4080-Mc/s,” *Astrophys.J.* **142** (1965) 419–421.

- [12] J. Lesgourgues and S. Pastor, “Massive neutrinos and cosmology,” *Phys.Rept.* **429** (2006) 307–379, [arXiv:astro-ph/0603494](#) [[astro-ph](#)].
- [13] J.-P. Uzan, “Varying constants, Gravitation and Cosmology,” *Living Rev.Rel.* **14** (2011) 2, [arXiv:1009.5514](#) [[astro-ph.CO](#)].
- [14] J. Ellis, “Searching for Particle Physics Beyond the Standard Model at the LHC and Elsewhere,” [arXiv:1102.5009](#) [[hep-ph](#)].
- [15] P. Hernandez, “Neutrino physics,” [arXiv:1010.4131](#) [[hep-ph](#)].
- [16] B. Pontecorvo, “Mesonium and antimesonium,” *Sov. Phys. JETP* **6** (1957) 429.
- [17] B. Pontecorvo, “Inverse beta processes and nonconservation of lepton charge,” *Sov. Phys. JETP* **7** (1958) 172–173.
- [18] S. Weinberg, “The Quantum theory of fields. Vol. 1: Foundations,”.
- [19] G. Steigman, “Observational tests of antimatter cosmologies,” *Ann.Rev.Astron.Astrophys.* **14** (1976) 339–372.
- [20] F. Stecker, “On the nature of the Baryon Asymmetry,” *Nucl.Phys.* **B252** (1985) 25–36.
- [21] A. G. Cohen, A. De Rujula, and S. Glashow, “A Matter - antimatter universe?,” *Astrophys.J.* **495** (1998) 539–549, [arXiv:astro-ph/9707087](#) [[astro-ph](#)].
- [22] Particle Data Group , K. Nakamura, “Review of Particle Physics,” *J. Phys.* **G37** (2010) 075021.
- [23] A. D. Sakharov, “Violation of CP Invariance, C Asymmetry, and Baryon Asymmetry of the Universe,” *Pisma Zh. Eksp. Teor. Fiz.* **5** (1967) 32–35.
- [24] K. Kajantie, M. Laine, K. Rummukainen, and M. E. Shaposhnikov, “Is there a hot electroweak phase transition at  $m(H)$  larger or equal to  $m(W)$ ?,” *Phys.Rev.Lett.* **77** (1996) 2887–2890, [arXiv:hep-ph/9605288](#) [[hep-ph](#)].
- [25] C. Jarlskog, “Commutator of the Quark Mass Matrices in the Standard Electroweak Model and a Measure of Maximal CP Violation,” *Phys.Rev.Lett.* **55** (1985) 1039.
- [26] M. Dine and A. Kusenko, “The Origin of the matter - antimatter asymmetry,” *Rev.Mod.Phys.* **76** (2004) 1, [arXiv:hep-ph/0303065](#) [[hep-ph](#)].
- [27] G. Bertone, D. Hooper, and J. Silk, “Particle dark matter: Evidence, candidates and constraints,” *Phys.Rept.* **405** (2005) 279–390, [arXiv:hep-ph/0404175](#) [[hep-ph](#)].
- [28] J. Bond and A. Szalay, “The Collisionless Damping of Density Fluctuations in an Expanding Universe,” *Astrophys.J.* **274** (1983) 443–468.
- [29] Supernova Search Team , A. G. Riess *et al.*, “Observational evidence from supernovae for an accelerating universe and a cosmological constant,” *Astron.J.* **116** (1998) 1009–1038, [arXiv:astro-ph/9805201](#) [[astro-ph](#)].

- [30] Supernova Cosmology Project, S. Perlmutter *et al.*, “Measurements of Omega and Lambda from 42 high redshift supernovae,” *Astrophys.J.* **517** (1999) 565–586, [arXiv:astro-ph/9812133 \[astro-ph\]](#). The Supernova Cosmology Project.
- [31] S. Weinberg, “The Cosmological Constant Problem,” *Rev.Mod.Phys.* **61** (1989) 1–23. Morris Loeb Lectures in Physics, Harvard University, May 2, 3, 5, and 10, 1988.
- [32] S. M. Carroll, “The Cosmological constant,” *Living Rev.Rel.* **4** (2001) 1, [arXiv:astro-ph/0004075 \[astro-ph\]](#).
- [33] T. Padmanabhan, “Cosmological constant: The weight of the vacuum,” *Phys. Rept.* **380** (2003) 235–320, [arXiv:hep-th/0212290](#).
- [34] E. Bianchi and C. Rovelli, “Why all these prejudices against a constant?,” [arXiv:1002.3966 \[astro-ph.CO\]](#).
- [35] S. del Campo, R. Herrera, and D. Pavon, “Toward a solution of the coincidence problem,” *Phys.Rev.* **D78** (2008) 021302, [arXiv:0806.2116 \[astro-ph\]](#).
- [36] N. Dalal, K. Abazajian, E. E. Jenkins, and A. V. Manohar, “Testing the cosmic coincidence problem and the nature of dark energy,” *Phys.Rev.Lett.* **87** (2001) 141302, [arXiv:astro-ph/0105317 \[astro-ph\]](#).
- [37] S. Dodelson, M. Kaplinghat, and E. Stewart, “Solving the coincidence problem : Tracking oscillating energy,” *Phys.Rev.Lett.* **85** (2000) 5276–5279, [arXiv:astro-ph/0002360 \[astro-ph\]](#).
- [38] S. Nojiri and S. D. Odintsov, “Introduction to modified gravity and gravitational alternative for dark energy,” *Int.J.Geom.Meth.Mod.Phys.* **4** (2006) 06, [arXiv:hep-th/0601213 \[hep-th\]](#).
- [39] E. J. Copeland, M. Sami, and S. Tsujikawa, “Dynamics of dark energy,” *Int.J.Mod.Phys.* **D15** (2006) 1753–1936, [arXiv:hep-th/0603057 \[hep-th\]](#).
- [40] J. Garcia-Bellido and T. Haugboelle, “Confronting Lemaitre-Tolman-Bondi models with Observational Cosmology,” *JCAP* **0804** (2008) 003, [arXiv:0802.1523 \[astro-ph\]](#).
- [41] A. H. Guth, “The Inflationary Universe: A Possible Solution to the Horizon and Flatness Problems,” *Phys.Rev.* **D23** (1981) 347–356.
- [42] A. D. Linde, “A New Inflationary Universe Scenario: A Possible Solution of the Horizon, Flatness, Homogeneity, Isotropy and Primordial Monopole Problems,” *Phys. Lett.* **B108** (1982) 389–393.
- [43] A. Albrecht and P. J. Steinhardt, “Cosmology for Grand Unified Theories with Radiatively Induced Symmetry Breaking,” *Phys. Rev. Lett.* **48** (1982) 1220–1223.
- [44] A. D. Linde, “Chaotic Inflation,” *Phys. Lett.* **B129** (1983) 177–181.

- [45] D. H. Lyth and A. Riotto, “Particle physics models of inflation and the cosmological density perturbation,” *Phys. Rept.* **314** (1999) 1–146, [arXiv:hep-ph/9807278](#).
- [46] A. D. Linde, “Inflationary Cosmology,” *Lect. Notes Phys.* **738** (2008) 1–54, [arXiv:0705.0164 \[hep-th\]](#).
- [47] A. Mazumdar and J. Rocher, “Particle physics models of inflation and curvaton scenarios,” *Phys.Rept.* **497** (2011) 85–215, [arXiv:1001.0993 \[hep-ph\]](#).
- [48] S. Raby, “Grand Unified Theories,” [arXiv:hep-ph/0608183 \[hep-ph\]](#).
- [49] H. Georgi, H. R. Quinn, and S. Weinberg, “Hierarchy of Interactions in Unified Gauge Theories,” *Phys.Rev.Lett.* **33** (1974) 451–454.
- [50] M. E. Swanson, W. J. Percival, and O. Lahav, “Neutrino masses from clustering of red and blue galaxies: a test of astrophysical uncertainties,” *Mon.Not.Roy.Astron.Soc.* **409** (2010) 1100–1112, [arXiv:1006.2825 \[astro-ph.CO\]](#). \* Temporary entry \*.
- [51] P. Minkowski, “ $\mu \rightarrow e \gamma$  at a Rate of One Out of 1-Billion Muon Decays?,” *Phys.Lett.* **B67** (1977) 421.
- [52] T. Yanagida, “Horizontal Symmetry and Masses of Neutrinos,” *Prog.Theor.Phys.* **64** (1980) 1103.
- [53] M. Gell-Mann, P. Ramond, and R. Slansky, “Complex spinors and Unified Theories,” Supergravity, P. van Nieuwenhuizen, D.Z. Freedman (eds.), North Holland Publ. Co., 1979.
- [54] S. Weinberg, “Baryon and Lepton Nonconserving Processes,” *Phys.Rev.Lett.* **43** (1979) 1566–1570.
- [55] T. Asaka, S. Blanchet, and M. Shaposhnikov, “The nuMSM, Dark Matter and Neutrino Masses,” *Phys. Lett.* **B631** (2005) 151–156, [arXiv:hep-ph/0503065](#).
- [56] H. Davoudiasl, R. Kitano, T. Li, and H. Murayama, “The New minimal standard model,” *Phys.Lett.* **B609** (2005) 117–123, [arXiv:hep-ph/0405097 \[hep-ph\]](#).
- [57] K. A. Meissner and H. Nicolai, “Conformal Symmetry and the Standard Model,” *Phys.Lett.* **B648** (2007) 312–317, [arXiv:hep-th/0612165 \[hep-th\]](#).
- [58] H. P. Nilles, “Supersymmetry, Supergravity and Particle Physics,” *Phys.Rept.* **110** (1984) 1–162.
- [59] S. P. Martin, “A Supersymmetry primer,” [arXiv:hep-ph/9709356 \[hep-ph\]](#).
- [60] M. Shaposhnikov, “Is there a new physics between electroweak and Planck scales?,” [arXiv:0708.3550 \[hep-th\]](#).
- [61] T. Asaka and M. Shaposhnikov, “The nuMSM, Dark Matter and Baryon Asymmetry of the Universe,” *Phys. Lett.* **B620** (2005) 17–26, [arXiv:hep-ph/0505013](#).

- [62] M. Shaposhnikov, “A possible symmetry of the  $\nu$ MSM,” *Nucl. Phys.* **B763** (2007) 49–59, [arXiv:hep-ph/0605047](#).
- [63] E. K. Akhmedov, V. A. Rubakov, and A. Y. Smirnov, “Baryogenesis via neutrino oscillations,” *Phys. Rev. Lett.* **81** (1998) 1359–1362, [arXiv:hep-ph/9803255](#).
- [64] R. Foot, G. C. Joshi, H. Lew, and R. Volkas, “Charge quantization in the standard model and some of its extensions,” *Mod.Phys.Lett.* **A5** (1990) 2721–2732.
- [65] K. Wilson and J. B. Kogut, “The Renormalization group and the epsilon expansion,” *Phys.Rept.* **12** (1974) 75–200.
- [66] J. Frohlich, “On the Triviality of  $\lambda\phi^4$  in D-Dimensions Theories and the Approach to the Critical Point in Four-Dimensions,” *Nucl.Phys.* **B200** (1982) 281–296.
- [67] A. Marshakov, “String theory or field theory?,” *Phys.Usp.* **45** (2002) 915–954, [arXiv:hep-th/0212114](#) [[hep-th](#)].
- [68] N. Krasnikov, “Restriction of the Fermion Mass in Gauge Theories of Weak and Electromagnetic Interactions,” *Yad.Fiz.* **28** (1978) 549–551.
- [69] P. Q. Hung, “Vacuum Instability and New Constraints on Fermion Masses,” *Phys.Rev.Lett.* **42** (1979) 873.
- [70] H. Politzer and S. Wolfram, “Bounds on Particle Masses in the Weinberg-Salam Model,” *Phys.Lett.* **B82** (1979) 242–246.
- [71] K. Holland and J. Kuti, “How light can the Higgs be?,” *Nucl.Phys.Proc.Suppl.* **129** (2004) 765–767, [arXiv:hep-lat/0308020](#) [[hep-lat](#)].
- [72] L. Maiani, G. Parisi, and R. Petronzio, “Bounds on the Number and Masses of Quarks and Leptons,” *Nucl.Phys.* **B136** (1978) 115.
- [73] N. Cabibbo, L. Maiani, G. Parisi, and R. Petronzio, “Bounds on the Fermions and Higgs Boson Masses in Grand Unified Theories,” *Nucl.Phys.* **B158** (1979) 295–305.
- [74] M. Lindner, “Implications of Triviality for the Standard Model,” *Z.Phys.* **C31** (1986) 295.
- [75] M. Shaposhnikov and D. Zenhausern, “Scale Invariance, Unimodular Gravity and Dark Energy,” *Phys. Lett.* **B671** (2009) 187–192, [arXiv:0809.3395](#) [[hep-th](#)].
- [76] J. Garcia-Bellido, J. Rubio, M. Shaposhnikov, and D. Zenhausern, “Higgs Cosmology: From the Early to the Late Universe. To be published soon,”.
- [77] J. Garcia-Bellido, D. G. Figueroa, and J. Rubio, “Preheating in the Standard Model with the Higgs-Inflaton Coupled to Gravity,” *Phys. Rev.* **D79** (2009) 063531, [arXiv:0812.4624](#) [[hep-ph](#)].
- [78] P. Peebles and A. Vilenkin, “Quintessential inflation,” *Phys.Rev.* **D59** (1999) 063505, [arXiv:astro-ph/9810509](#) [[astro-ph](#)].

- [79] M. Peloso and F. Rosati, “On the construction of quintessential inflation models,” *JHEP* **9912** (1999) 026, [arXiv:hep-ph/9908271 \[hep-ph\]](#).
- [80] K. Dimopoulos and J. Valle, “Modeling quintessential inflation,” *Astropart.Phys.* **18** (2002) 287–306, [arXiv:astro-ph/0111417 \[astro-ph\]](#).
- [81] M. Bastero-Gil, A. Berera, B. M. Jackson, and A. Taylor, “Hybrid Quintessential Inflation,” *Phys.Lett.* **B678** (2009) 157–163, [arXiv:0905.2937 \[hep-ph\]](#).
- [82] H. P. Fister, “Mach’s principle: From Newton’s Bucket to Quantum Gravity,”. Ed. J.Barbour, Birkhauser, Boston (1972).
- [83] K. Godel, “An Example of a new type of cosmological solutions of Einstein’s field equations of graviation,” *Rev.Mod.Phys.* **21** (1949) 447–450.
- [84] E. S. I. Ozsvath, “Recent Developments in General Relativity, p. 339.,”. Pergamon, New York, 1962.
- [85] I. Ciufolini and J. Wheeler, “Gravitation and Inertia,”. USA, Princeton Academic Press (1996).
- [86] C. Brans and R. H. Dicke, “Mach’s principle and a relativistic theory of gravitation,” *Phys. Rev.* **124** (1961) 925–935.
- [87] V. W. Hughes, H. G. Robinson, and V. Beltran-Lopez, “Upper Limit for the Anisotropy of Inertial Mass from Nuclear Resonance Experiments,” *Phys. Rev. Lett.* **4** (1960) 342–344.
- [88] R. W. P. Drever, “A search for anisotropy of inertial mass using a free precession technique,” *Phil. Mag.* **6** (1961) 683–687.
- [89] A. Zee, “A Broken Symmetric Theory of Gravity,” *Phys. Rev. Lett.* **42** (1979) 417.
- [90] L. Smolin, “Towards a Theory of Space-Time Structure at Very Short Distances,” *Nucl. Phys.* **B160** (1979) 253.
- [91] H. Dehnen, H. Frommert, and F. Ghaboussi, “Higgs field gravity,” *Int. J. Theor. Phys.* **29** (1990) 537–546.
- [92] H. Dehnen and H. Frommert, “Higgs field gravity within the standard model,” *Int. J. Theor. Phys.* **30** (1991) 985–998.
- [93] C. M. Will, “The Confrontation between General Relativity and Experiment,” *Living Rev. Rel.* **9** (2005) 3, [arXiv:gr-qc/0510072](#).
- [94] S. M. A.A. Grib and V. Mostepanenko, “Vacuum Quantum Effects in Strong External Fields,”. Friedmann Laboratory Publishing St. Petersburg, Russia.
- [95] A. Dobado, A. Gomez-Nicola, A. L. Maroto, and J. Pelaez, “Effective lagrangians for the standard model,”. See the BOOKS subfile under the following call number: QC174.45:D6:1997.



- [96] A. Dobado and A. L. Maroto, “Inflatonless inflation,” *Phys.Rev.* **D52** (1995) 1895, [arXiv:hep-ph/9406409 \[hep-ph\]](#).
- [97] A. A. Starobinsky, “A new type of isotropic cosmological models without singularity,” *Phys. Lett.* **B91** (1980) 99–102.
- [98] V. F. Mukhanov and G. V. Chibisov, “Quantum Fluctuation and Nonsingular Universe. (In Russian),” *JETP Lett.* **33** (1981) 532–535.
- [99] V. F. Mukhanov and G. V. Chibisov, “The Vacuum energy and large scale structure of the universe,” *Sov. Phys. JETP* **56** (1982) 258–265.
- [100] L. A. Kofman, V. F. Mukhanov, and D. Y. Pogosian, “Evolution of inhomogeneities in inflationary models in a theory of gravitation with higher derivatives,” *Sov. Phys. JETP* **66** (1987) 433–440.
- [101] M. Ferraris, M. Francaviglia, and G. Magnano, “Do non-linear metric theories of gravitation really exist?,” *Class. Quant. Grav.* **5** (1988) L95.
- [102] G. Magnano, M. Ferraris, and M. Francaviglia, “Legendre transformation and dynamical structure of higher derivative gravity,” *Class. Quant. Grav.* **7** (1990) 557–570.
- [103] T. S. Koivisto and D. F. Mota, “Vector Field Models of Inflation and Dark Energy,” *JCAP* **0808** (2008) 021, [arXiv:0805.4229 \[astro-ph\]](#). \* Brief entry \*.
- [104] A. Golovnev, V. Mukhanov, and V. Vanchurin, “Vector Inflation,” *JCAP* **0806** (2008) 009, [arXiv:0802.2068 \[astro-ph\]](#).
- [105] D. Gorbunov and A. Panin, “Scalaron the mighty: producing dark matter and baryon asymmetry at reheating,” *Phys.Lett.* **B700** (2011) 157–162, [arXiv:1009.2448 \[hep-ph\]](#).
- [106] WMAP Collaboration , G. Hinshaw *et al.*, “Five-Year Wilkinson Microwave Anisotropy Probe (WMAP) Observations: Data Processing, Sky Maps, and Basic Results,” *Astrophys.J.Suppl.* **180** (2009) 225–245, [arXiv:0803.0732 \[astro-ph\]](#).
- [107] J. J. van der Bij, “Can Gravity Make the Higgs Particle Decouple?,” *Acta Phys. Polon.* **B25** (1994) 827–832.
- [108] J. L. Cervantes-Cota and H. Dehnen, “Induced Gravity Inflation in the Standard Model of Particle Physics,” *Nucl. Phys.* **B442** (1995) 391–412, [arXiv:astro-ph/9505069](#).
- [109] J. van der Bij, “Can gravity play a role at the electroweak scale?,” *Int.J.Phys.* **1** (1995) 63, [arXiv:hep-ph/9507389 \[hep-ph\]](#).
- [110] D. S. Salopek, J. R. Bond, and J. M. Bardeen, “Designing Density Fluctuation Spectra in Inflation,” *Phys. Rev.* **D40** (1989) 1753.

- [111] F. L. Bezrukov and M. Shaposhnikov, “The Standard Model Higgs Boson as the Inflaton,” *Phys. Lett.* **B659** (2008) 703–706, [arXiv:0710.3755 \[hep-th\]](#).
- [112] P. Jain and S. Mitra, “Cosmological Symmetry Breaking, Pseudo-Scale Invariance, Dark Energy and the Standard Model,” *Mod. Phys. Lett.* **A22** (2007) 1651–1661, [arXiv:0704.2273 \[hep-ph\]](#).
- [113] P. Jain and S. Mitra, “Standard Model with Cosmologically Broken Quantum Scale Invariance,” *Mod. Phys. Lett.* **A25** (2010) 167–177, [arXiv:0903.1683 \[hep-ph\]](#).
- [114] S. Weinberg, “Implications of Dynamical Symmetry Breaking: An Addendum,” *Phys.Rev.* **D19** (1979) 1277–1280. (For original paper see Phys.Rev.D13:974-996,1976).
- [115] E. Gildener and S. Weinberg, “Symmetry Breaking and Scalar Bosons,” *Phys.Rev.* **D13** (1976) 3333.
- [116] M. Shaposhnikov and D. Zenhausern, “Quantum Scale Invariance, Cosmological Constant and Hierarchy Problem,” *Phys. Lett.* **B671** (2009) 162–166, [arXiv:0809.3406 \[hep-th\]](#).
- [117] M. E. Shaposhnikov and I. I. Tkachev, “Quantum Scale Invariance on the Lattice,” [arXiv:0811.1967 \[hep-th\]](#). [arXiv:0811.1967 \[hep-th\]](#).
- [118] R. N. Lerner and J. McDonald, “Gauge singlet scalar as inflaton and thermal relic dark matter,” *Phys.Rev.* **D80** (2009) 123507, [arXiv:0909.0520 \[hep-ph\]](#).
- [119] T. Clark, B. Liu, S. Love, and T. ter Veldhuis, “The Standard Model Higgs Boson-Inflaton and Dark Matter,” *Phys.Rev.* **D80** (2009) 075019, [arXiv:0906.5595 \[hep-ph\]](#).
- [120] I. Antoniadis, J. Iliopoulos, and T. N. Tomaras, “Quantum Instability Of De Sitter Space,” *Phys. Rev. Lett.* **56** (1986) 1319.
- [121] N. C. Tsamis and R. P. Woodard, “Relaxing the Cosmological Constant,” *Phys. Lett.* **B301** (1993) 351–357.
- [122] N. C. Tsamis and R. P. Woodard, “Strong Infrared Effects in Quantum Gravity,” *Ann. Phys.* **238** (1995) 1–82.
- [123] I. Antoniadis, P. O. Mazur, and E. Mottola, “Cosmological Dark Energy: Prospects for a Dynamical Theory,” *New J. Phys.* **9** (2007) 11, [arXiv:gr-qc/0612068](#).
- [124] A. M. Polyakov, “Decay of Vacuum Energy,” *Nucl. Phys.* **B834** (2010) 316–329, [arXiv:0912.5503 \[hep-th\]](#).
- [125] M. E. Peskin and D. V. Schroeder, “An Introduction to Quantum Field Theory,” Reading, USA: Addison-Wesley (1995) 842 p.

- [126] V. F. Mukhanov, H. A. Feldman, and R. H. Brandenberger, “Theory of Cosmological Perturbations. Part 1. Classical Perturbations. Part 2. Quantum Theory of Perturbations. Part 3. Extensions,” *Phys. Rept.* **215** (1992) 203–333.
- [127] D. Polarski and A. A. Starobinsky, “Semiclassicality and decoherence of cosmological perturbations,” *Class. Quant. Grav.* **13** (1996) 377–392, [arXiv:gr-qc/9504030 \[gr-qc\]](#).
- [128] E. E. Flanagan, “The Conformal frame freedom in theories of gravitation,” *Class. Quant. Grav.* **21** (2004) 3817, [arXiv:gr-qc/0403063 \[gr-qc\]](#).
- [129] K. ichi Maeda, “Towards the Einstein-Hilbert Action via Conformal Transformation,” *Phys. Rev.* **D39** (1989) 3159.
- [130] A. R. Liddle, P. Parsons, and J. D. Barrow, “Formalizing the slow roll approximation in inflation,” *Phys. Rev.* **D50** (1994) 7222–7232, [arXiv:astro-ph/9408015 \[astro-ph\]](#).
- [131] D. Salopek and J. Bond, “Nonlinear evolution of long wavelength metric fluctuations in inflationary models,” *Phys. Rev.* **D42** (1990) 3936–3962.
- [132] C. P. Burgess, “Lectures on Cosmic Inflation and its Potential Stringy Realizations,” *PoS P2GC* (2006) 008, [arXiv:0708.2865 \[hep-th\]](#).
- [133] A. D. Linde, “Extended chaotic inflation and spatial variations of the gravitational constant,” *Phys. Lett.* **B238** (1990) 160.
- [134] J. Garcia-Bellido and A. D. Linde, “Stationary solutions in Brans-Dicke stochastic inflationary cosmology,” *Phys. Rev.* **D52** (1995) 6730–6738, [arXiv:gr-qc/9504022](#).
- [135] T. Chiba and M. Yamaguchi, “Extended Slow-Roll Conditions and Primordial Fluctuations: Multiple Scalar Fields and Generalized Gravity,” *JCAP* **0901** (2009) 019, [arXiv:0810.5387 \[astro-ph\]](#).
- [136] R. Durrer, “The Cosmic Microwave Background,”. Cambrige Univ. Pr. (2008).
- [137] J. M. Bardeen, “Gauge Invariant Cosmological Perturbations,” *Phys. Rev.* **D22** (1980) 1882–1905.
- [138] J. Martin and D. J. Schwarz, “The Influence of Cosmological Transitions on the Evolution of Density Perturbations,” *Phys. Rev.* **D57** (1998) 3302–3316, [arXiv:gr-qc/9704049](#).
- [139] H. Kodama and T. Hamazaki, “Evolution of cosmological perturbations in a stage dominated by an oscillatory scalar field,” *Prog. Theor. Phys.* **96** (1996) 949–970, [arXiv:gr-qc/9608022 \[gr-qc\]](#).
- [140] Y. Nambu and A. Taruya, “Evolution of cosmological perturbation in reheating phase of the universe,” *Prog. Theor. Phys.* **97** (1997) 83–89, [arXiv:gr-qc/9609029 \[gr-qc\]](#).

- [141] F. Finelli and R. H. Brandenberger, “Parametric amplification of gravitational fluctuations during reheating,” *Phys.Rev.Lett.* **82** (1999) 1362–1365, [arXiv:hep-ph/9809490 \[hep-ph\]](#).
- [142] B. A. Bassett, D. I. Kaiser, and R. Maartens, “General relativistic preheating after inflation,” *Phys.Lett.* **B455** (1999) 84–89, [arXiv:hep-ph/9808404 \[hep-ph\]](#).
- [143] B. A. Bassett and F. Viniegra, “Massless metric preheating,” *Phys.Rev.* **D62** (2000) 043507, [arXiv:hep-ph/9909353 \[hep-ph\]](#).
- [144] W. Lin, X. Meng, and X.-M. Zhang, “Adiabatic gravitational perturbation during reheating,” *Phys.Rev.* **D61** (2000) 121301, [arXiv:hep-ph/9912510 \[hep-ph\]](#).
- [145] F. Finelli and R. H. Brandenberger, “Parametric amplification of metric fluctuations during reheating in two field models,” *Phys.Rev.* **D62** (2000) 083502, [arXiv:hep-ph/0003172 \[hep-ph\]](#).
- [146] M. Parry and R. Easther, “Preheating and the Einstein field equations,” *Phys.Rev.* **D59** (1999) 061301, [arXiv:hep-ph/9809574 \[hep-ph\]](#).
- [147] R. Easther and M. Parry, “Gravity, parametric resonance and chaotic inflation,” *Phys.Rev.* **D62** (2000) 103503, [arXiv:hep-ph/9910441 \[hep-ph\]](#).
- [148] F. Finelli and S. Khlebnikov, “Large metric perturbations from rescattering,” *Phys.Lett.* **B504** (2001) 309–313, [arXiv:hep-ph/0009093 \[hep-ph\]](#).
- [149] F. Finelli and S. Khlebnikov, “Metric perturbations at reheating: The Use of spherical symmetry,” *Phys.Rev.* **D65** (2002) 043505, [arXiv:hep-ph/0107143 \[hep-ph\]](#).
- [150] Y. Nambu and Y. Araki, “Evolution of non-linear fluctuations in preheating after inflation,” *Class.Quant.Grav.* **23** (2006) 511–526, [arXiv:gr-qc/0512074 \[gr-qc\]](#).
- [151] M. Bastero-Gil, M. Tristram, J. F. Macias-Perez, and D. Santos, “Non-linear Preheating with Scalar Metric Perturbations,” *Phys.Rev.* **D77** (2008) 023520, [arXiv:0709.3510 \[astro-ph\]](#).
- [152] J. Garcia-Bellido and D. Wands, “Constraints from inflation on scalar - tensor gravity theories,” *Phys. Rev.* **D52** (1995) 6739–6749, [arXiv:gr-qc/9506050](#).
- [153] F. Di Marco, F. Finelli, and R. Brandenberger, “Adiabatic and Isocurvature Perturbations for Multifield Generalized Einstein Models,” *Phys. Rev.* **D67** (2003) 063512, [arXiv:astro-ph/0211276](#).
- [154] S. Tsujikawa and B. A. Bassett, “When can preheating affect the CMB?,” *Phys.Lett.* **B536** (2002) 9–17, [arXiv:astro-ph/0204031 \[astro-ph\]](#).
- [155] A. R. Liddle and D. H. Lyth, “The Cold Dark Matter Density Perturbation,” *Phys. Rept.* **231** (1993) 1–105, [arXiv:astro-ph/9303019](#).

- [156] A. Linde, M. Noorbala, and A. Westphal, “Observational consequences of chaotic inflation with nonminimal coupling to gravity,” *JCAP* **1103** (2011) 013, [arXiv:1101.2652 \[hep-th\]](#).
- [157] SDSS Collaboration, B. A. Reid *et al.*, “Baryon Acoustic Oscillations in the Sloan Digital Sky Survey Data Release 7 Galaxy Sample,” *Mon.Not.Roy.Astron.Soc.* **401** (2010) 2148–2168, [arXiv:0907.1660 \[astro-ph.CO\]](#).
- [158] A. G. Riess, L. Macri, S. Casertano, M. Sosey, H. Lampeitl, *et al.*, “A Redetermination of the Hubble Constant with the Hubble Space Telescope from a Differential Distance Ladder,” *Astrophys.J.* **699** (2009) 539–563, [arXiv:0905.0695 \[astro-ph.CO\]](#).
- [159] A. O. Barvinsky, A. Y. Kamenshchik, and A. A. Starobinsky, “Inflation scenario via the Standard Model Higgs boson and LHC,” *JCAP* **0811** (2008) 021, [arXiv:0809.2104 \[hep-ph\]](#).
- [160] A. De Simone, M. P. Hertzberg, and F. Wilczek, “Running Inflation in the Standard Model,” *Phys. Lett.* **B678** (2009) 1–8, [arXiv:0812.4946 \[hep-ph\]](#).
- [161] F. L. Bezrukov, A. Magnin, and M. Shaposhnikov, “Standard Model Higgs boson mass from inflation,” *Phys.Lett.* **B675** (2009) 88–92, [arXiv:0812.4950 \[hep-ph\]](#).
- [162] F. Bezrukov and M. Shaposhnikov, “Standard Model Higgs boson mass from inflation: Two loop analysis,” *JHEP* **0907** (2009) 089, [arXiv:0904.1537 \[hep-ph\]](#).
- [163] A. O. Barvinsky, A. Y. Kamenshchik, C. Kiefer, A. A. Starobinsky, and C. Steinwachs, “Asymptotic freedom in inflationary cosmology with a non- minimally coupled Higgs field,” *JCAP* **0912** (2009) 003, [arXiv:0904.1698 \[hep-ph\]](#).
- [164] J. Barbon and J. Espinosa, “On the Naturalness of Higgs Inflation,” *Phys.Rev.* **D79** (2009) 081302, [arXiv:0903.0355 \[hep-ph\]](#).
- [165] C. Burgess, H. M. Lee, and M. Trott, “Power-counting and the Validity of the Classical Approximation During Inflation,” *JHEP* **0909** (2009) 103, [arXiv:0902.4465 \[hep-ph\]](#).
- [166] C. P. Burgess, H. M. Lee, and M. Trott, “Comment on Higgs Inflation and Naturalness,” *JHEP* **07** (2010) 007, [arXiv:1002.2730 \[hep-ph\]](#).
- [167] F. Bezrukov, A. Magnin, M. Shaposhnikov, and S. Sibiryakov, “Higgs inflation: consistency and generalisations,” *JHEP* **1101** (2011) 016, [arXiv:1008.5157 \[hep-ph\]](#).
- [168] S. R. Huggins and D. J. Toms, “One graviton exchange interaction of nonminimally coupled scalar fields,” *Class.Quant.Grav.* **4** (1987) 1509.
- [169] S. R. Huggins, “Cross-sections from tree level gravitational scattering from a nonminimally coupled scalar field,” *Class.Quant.Grav.* **4** (1987) 1515–1523.

- [170] K. Freese, J. A. Frieman, and A. V. Olinto, “Natural inflation with pseudo - Nambu-Goldstone bosons,” *Phys.Rev.Lett.* **65** (1990) 3233–3236.
- [171] C. Cheung, P. Creminelli, A. Fitzpatrick, J. Kaplan, and L. Senatore, “The Effective Field Theory of Inflation,” *JHEP* **0803** (2008) 014, [arXiv:0709.0293 \[hep-th\]](#).
- [172] C. Wetterich, “Cosmology and the Fate of Dilatation Symmetry,” *Nucl. Phys.* **B302** (1988) 668.
- [173] G. ’t Hooft and M. J. G. Veltman, “Regularization and Renormalization of Gauge Fields,” *Nucl. Phys.* **B44** (1972) 189–213.
- [174] L. Popa and A. Caramete, “Cosmological Constraints on Higgs Boson Mass,” *Astrophys.J.* **723** (2010) 803–811, [arXiv:1009.1293 \[astro-ph.CO\]](#).
- [175] V. Bednyakov, N. Giokaris, and A. Bednyakov, “On Higgs mass generation mechanism in the Standard Model,” *Phys.Part.Nucl.* **39** (2008) 13–36, [arXiv:hep-ph/0703280 \[HEP-PH\]](#).
- [176] A. D. Dolgov and A. D. Linde, “Baryon Asymmetry in Inflationary Universe,” *Phys. Lett.* **B116** (1982) 329.
- [177] L. F. Abbott, E. Farhi, and M. B. Wise, “Particle Production in the New Inflationary Cosmology,” *Phys. Lett.* **B117** (1982) 29.
- [178] A. Albrecht, P. J. Steinhardt, M. S. Turner, and F. Wilczek, “Reheating an Inflationary Universe,” *Phys. Rev. Lett.* **48** (1982) 1437.
- [179] J. H. Traschen and R. H. Brandenberger, “Particle production during out-of-equilibrium phase transitions,” *Phys.Rev.* **D42** (1990) 2491–2504.
- [180] A. Dolgov and D. Kirilova, “On particle creation by a time-dependent scalar field,” *Sov.J.Nucl.Phys.* **51** (1990) 172–177.
- [181] L. Kofman, A. D. Linde, and A. A. Starobinsky, “Reheating after inflation,” *Phys. Rev. Lett.* **73** (1994) 3195–3198, [arXiv:hep-th/9405187](#).
- [182] Y. Shtanov, J. H. Traschen, and R. H. Brandenberger, “Universe reheating after inflation,” *Phys.Rev.* **D51** (1995) 5438–5455, [arXiv:hep-ph/9407247 \[hep-ph\]](#).
- [183] L. Kofman, A. D. Linde, and A. A. Starobinsky, “Towards the theory of reheating after inflation,” *Phys. Rev.* **D56** (1997) 3258–3295, [arXiv:hep-ph/9704452](#).
- [184] B. A. Bassett, S. Tsujikawa, and D. Wands, “Inflation dynamics and reheating,” *Rev.Mod.Phys.* **78** (2006) 537–589, [arXiv:astro-ph/0507632 \[astro-ph\]](#).
- [185] R. Allahverdi, R. Brandenberger, F.-Y. Cyr-Racine, and A. Mazumdar, “Reheating in Inflationary Cosmology: Theory and Applications,” *Ann.Rev.Nucl.Part.Sci.* **60** (2010) 27–51, [arXiv:1001.2600 \[hep-th\]](#).

- [186] S. M. Barr and G. Segre, “Inflation and reheating in induced gravity models,” *Phys.Rev.* **D41** (1990) 2398–2407.
- [187] A. Cerioni, F. Finelli, A. Tronconi, and G. Venturi, “Inflation and Reheating in Induced Gravity,” *Phys.Lett.* **B681** (2009) 383–386, [arXiv:0906.1902 \[astro-ph.CO\]](#). \* Brief entry \*.
- [188] A. Cerioni, F. Finelli, A. Tronconi, and G. Venturi, “Inflation and Reheating in Spontaneously Generated Gravity,” *Phys.Rev.* **D81** (2010) 123505, [arXiv:1005.0935 \[gr-qc\]](#).
- [189] B. A. Bassett and S. Liberati, “Geometric reheating after inflation,” *Phys.Rev.* **D58** (1998) 021302, [arXiv:hep-ph/9709417 \[hep-ph\]](#).
- [190] S. Tsujikawa, K.-i. Maeda, and T. Torii, “Resonant particle production with nonminimally coupled scalar fields in preheating after inflation,” *Phys.Rev.* **D60** (1999) 063515, [arXiv:hep-ph/9901306 \[hep-ph\]](#).
- [191] S. Tsujikawa, K. ichi Maeda, and T. Torii, “Preheating with non-minimally coupled scalar fields in higher-curvature inflation models,” *Phys. Rev.* **D60** (1999) 123505, [arXiv:hep-ph/9906501](#).
- [192] S. Tsujikawa, K.-i. Maeda, and T. Torii, “Preheating of the nonminimally coupled inflaton field,” *Phys.Rev.* **D61** (2000) 103501, [arXiv:hep-ph/9910214 \[hep-ph\]](#).
- [193] L. Abramo, L. Brenig, and E. Gunzig, “On the stability of gravity in the presence of an nmc scalar field,” *Phys.Lett.* **B549** (2002) 13–19, [arXiv:gr-qc/0205022 \[gr-qc\]](#).
- [194] Y. Watanabe and E. Komatsu, “Reheating of the universe after inflation with  $f(\phi)R$  gravity,” *Phys. Rev.* **D75** (2007) 061301, [arXiv:gr-qc/0612120](#).
- [195] O. Bertolami, P. Frazao, and J. Paramos, “Reheating via a generalized non-minimal coupling of curvature to matter,” *Phys.Rev.* **D83** (2011) 044010, [arXiv:1010.2698 \[gr-qc\]](#).
- [196] G. N. Felder *et al.*, “Dynamics of symmetry breaking and tachyonic preheating,” *Phys. Rev. Lett.* **87** (2001) 011601, [arXiv:hep-ph/0012142](#).
- [197] G. N. Felder, L. Kofman, and A. D. Linde, “Tachyonic instability and dynamics of spontaneous symmetry breaking,” *Phys. Rev.* **D64** (2001) 123517, [arXiv:hep-th/0106179](#).
- [198] J. Garcia-Bellido, M. Garcia Perez, and A. Gonzalez-Arroyo, “Symmetry breaking and false vacuum decay after hybrid inflation,” *Phys. Rev.* **D67** (2003) 103501, [arXiv:hep-ph/0208228](#).
- [199] G. N. Felder, L. Kofman, and A. D. Linde, “Instant preheating,” *Phys. Rev.* **D59** (1999) 123523, [arXiv:hep-ph/9812289](#).



- [200] J. Garcia-Bellido and D. Wands, “Metric Perturbations in Two-Field Inflation,” *Phys. Rev. D* **53** (1996) 5437–5445, [arXiv:astro-ph/9511029](#).
- [201] M. Abramowitz and I. Stegun, “Handbook of Mathematical Functions with Formulas, Graphs, and Mathematical Tables,”. New York, Dover (1972).
- [202] F. Bezrukov, D. Gorbunov, and M. Shaposhnikov, “On initial conditions for the Hot Big Bang,” *JCAP* **0906** (2009) 029, [arXiv:0812.3622 \[hep-ph\]](#).
- [203] T. P. Cheng and L. F. Li, “Gauge Theory of Elementary Particle Physics,”. Oxford. U. P., UK, 2006.
- [204] M. Gleiser and R. O. Ramos, “Microphysical approach to nonequilibrium dynamics of quantum fields,” *Phys. Rev. D* **50** (1994) 2441–2455, [arXiv:hep-ph/9311278 \[hep-ph\]](#).
- [205] A. D. Linde, “Hybrid inflation,” *Phys. Rev. D* **49** (1994) 748–754, [arXiv:astro-ph/9307002](#).
- [206] P. B. Greene and L. Kofman, “Preheating of fermions,” *Phys. Lett. B* **448** (1999) 6–12, [arXiv:hep-ph/9807339 \[hep-ph\]](#).
- [207] J. Baacke, K. Heitmann, and C. Patzold, “Nonequilibrium dynamics of fermions in a spatially homogeneous scalar background field,” *Phys. Rev. D* **58** (1998) 125013, [arXiv:hep-ph/9806205 \[hep-ph\]](#).
- [208] J. Garcia-Bellido and E. Ruiz Morales, “Particle production from symmetry breaking after inflation,” *Phys. Lett. B* **536** (2002) 193–202, [arXiv:hep-ph/0109230](#).
- [209] N. Shuhmaher and R. Brandenberger, “Non-perturbative instabilities as a solution of the cosmological moduli problem,” *Phys. Rev. D* **73** (2006) 043519, [arXiv:hep-th/0507103 \[hep-th\]](#).
- [210] J. F. Dufaux, G. N. Felder, L. Kofman, M. Peloso, and D. Podolsky, “Preheating with trilinear interactions: Tachyonic resonance,” *JCAP* **0607** (2006) 006, [arXiv:hep-ph/0602144 \[hep-ph\]](#).
- [211] A. A. Abolhasani, H. Firouzjahi, and M. Sheikh-Jabbari, “Tachyonic Resonance Preheating in Expanding Universe,” *Phys. Rev. D* **81** (2010) 043524, [arXiv:0912.1021 \[hep-th\]](#).
- [212] A. Galindo and P. Pascual, “Mecánica Cuántica,”. Madrid, Ed. Alhambra Universidad, 1978.
- [213] F. Cooper, S. Habib, Y. Kluger, E. Mottola, J. P. Paz, *et al.*, “Nonequilibrium quantum fields in the large N expansion,” *Phys. Rev. D* **50** (1994) 2848–2869, [arXiv:hep-ph/9405352 \[hep-ph\]](#).
- [214] F. Cooper, S. Habib, Y. Kluger, and E. Mottola, “Nonequilibrium dynamics of symmetry breaking in  $\lambda \Phi^4$  field theory,” *Phys. Rev. D* **55** (1997) 6471–6503, [arXiv:hep-ph/9610345 \[hep-ph\]](#).



- [215] G. N. Felder and I. Tkachev, “LATTICEEASY: A Program for lattice simulations of scalar fields in an expanding universe,” *Comput.Phys.Commun.* **178** , [arXiv:hep-ph/0011159](#) [hep-ph].
- [216] A. V. Frolov, “DEFROST: A New Code for Simulating Preheating after Inflation,” *JCAP* **0811** (2008) 009, [arXiv:0809.4904](#) [hep-ph].
- [217] Z. Huang, “The Art of Lattice and Gravity Waves from Preheating,” *Phys.Rev.* **D83** (2011) 123509, [arXiv:1102.0227](#) [astro-ph.CO]. \* Temporary entry \*.
- [218] J. Lachapelle and R. H. Brandenberger, “Preheating with Non-Standard Kinetic Term,” *JCAP* **0904** (2009) 020, [arXiv:0808.0936](#) [hep-th].
- [219] J. Garcia-Bellido, J. Rubio, M. Shaposhnikov, and D. Zenhausern, “Dilaton production in Higgs-Dilaton inflation. In preparation.”.
- [220] K. Urwin and F. Arscott, “Theory of the Whittaker-Hill equation,” *Proceeding of the Royal Society of Edinburgh* **69** (1970) 28–44.
- [221] J. Garcia-Bellido, S. Mollerach, and E. Roulet, “Fermion production during preheating after hybrid inflation,” *JHEP* **0002** (2000) 034, [arXiv:hep-ph/0002076](#) [hep-ph].
- [222] W. Buchmuller and N. Dragon, “Einstein Gravity from Restricted Coordinate Invariance,” *Phys. Lett.* **B207** (1988) 292.
- [223] W. G. Unruh, “A Unimodular Theory of Canonical Quantum Gravity,” *Phys. Rev.* **D40** (1989) 1048.
- [224] E. Alvarez, “Can one tell Einstein’s unimodular theory from Einstein’s general relativity?,” *JHEP* **03** (2005) 002, [arXiv:hep-th/0501146](#).
- [225] W. Buchmuller and N. Dragon, “Gauge Fixing and the Cosmological Constant,” *Phys. Lett.* **B223** (1989) 313.
- [226] N. Dragon and M. Kreuzer, “Quantization Of Restricted Gravity,” *Z. Phys.* **C41** (1988) 485.
- [227] Y. F. Pirogov, “Violating General Covariance,” [arXiv:gr-qc/0609103](#). [arXiv:gr-qc/0609103](#).
- [228] E. Alvarez, D. Blas, J. Garriga, and E. Verdaguer, “Transverse Fierz-Pauli Symmetry,” *Nucl. Phys.* **B756** (2006) 148–170, [arXiv:hep-th/0606019](#).
- [229] D. Blas, “Transverse Symmetry and Spin-3/2 Fields,” *Class. Quant. Grav.* **25** (2008) , [arXiv:0803.4497](#) [hep-th].
- [230] E. Alvarez and R. Vidal, “Weyl Transverse Gravity (WTDiff) and the Cosmological Constant,” *Phys. Rev.* **D81** (2010) 084057, [arXiv:1001.4458](#) [hep-th].

- [231] J. J. van der Bij, H. van Dam, and Y. J. Ng, “The Exchange of Massless Spin Two Particles,” *Physica* **116A** (1982) 307–320.
- [232] R. R. Caldwell and E. V. Linder, “The Limits of Quintessence,” *Phys. Rev. Lett.* **95** (2005) 141301, [arXiv:astro-ph/0505494](#).
- [233] P. G. Ferreira and M. Joyce, “Cosmology with a Primordial Scaling Field,” *Phys. Rev.* **D58** (1998) 023503, [arXiv:astro-ph/9711102](#).
- [234] J. U. Lopes Franca and R. Rosenfeld, “Fine Tuning in Quintessence Models with Exponential Potentials,” *JHEP* **10** (2002) 015, [arXiv:astro-ph/0206194](#).
- [235] R. J. Scherrer and A. A. Sen, “Thawing Quintessence with a Nearly Flat Potential,” *Phys. Rev.* **D77** (2008) 083515, [arXiv:0712.3450 \[astro-ph\]](#).
- [236] S. Sen, A. A. Sen, and M. Sami, “The Thawing Dark Energy Dynamics: Can We Detect It?,” *Phys. Lett.* **B686** (2010) 1–5, [arXiv:0907.2814 \[astro-ph.CO\]](#).
- [237] Planck Collaboration, “The Scientific programme of planck,” [arXiv:astro-ph/0604069 \[astro-ph\]](#).
- [238] N. D. Birrell and P. C. W. Davies, “Quantum fields in curved space,”. Cambridge, Uk: Univ. Pr. (1982) 340p.
- [239] S. Davidson and S. Sarkar, “Thermalization after inflation,” *JHEP* **0011** (2000) 012, [arXiv:hep-ph/0009078 \[hep-ph\]](#).
- [240] R. Micha and I. I. Tkachev, “Relativistic turbulence: A Long way from preheating to equilibrium,” *Phys.Rev.Lett.* **90** (2003) 121301, [arXiv:hep-ph/0210202 \[hep-ph\]](#).
- [241] A. Tranberg, “Quantum field thermalization in expanding backgrounds,” *JHEP* **0811** (2008) 037, [arXiv:0806.3158 \[hep-ph\]](#).
- [242] C. Germani and A. Kehagias, “New Model of Inflation with Non-minimal Derivative Coupling of Standard Model Higgs Boson to Gravity,” *Phys.Rev.Lett.* **105** (2010) 011302, [arXiv:1003.2635 \[hep-ph\]](#).
- [243] C. Germani and A. Kehagias, “Cosmological Perturbations in the New Higgs Inflation,” *JCAP* **1005** (2010) 019, [arXiv:1003.4285 \[astro-ph.CO\]](#).
- [244] S. Khlebnikov and I. Tkachev, “Relic gravitational waves produced after preheating,” *Phys.Rev.* **D56** (1997) 653–660, [arXiv:hep-ph/9701423 \[hep-ph\]](#).
- [245] R. Easther and E. A. Lim, “Stochastic gravitational wave production after inflation,” *JCAP* **0604** (2006) 010, [arXiv:astro-ph/0601617 \[astro-ph\]](#).
- [246] R. Easther, J. Giblin, John T., and E. A. Lim, “Gravitational Wave Production At The End Of Inflation,” *Phys.Rev.Lett.* **99** (2007) 221301, [arXiv:astro-ph/0612294 \[astro-ph\]](#).

- [247] J. Garcia-Bellido and D. G. Figueroa, “A stochastic background of gravitational waves from hybrid preheating,” *Phys.Rev.Lett.* **98** (2007) 061302, [arXiv:astro-ph/0701014](#) [astro-ph].
- [248] J. Garcia-Bellido, D. G. Figueroa, and A. Sastre, “A Gravitational Wave Background from Reheating after Hybrid Inflation,” *Phys.Rev.* **D77** (2008) 043517, [arXiv:0707.0839](#) [hep-ph].
- [249] R. Easther, J. T. Giblin, and E. A. Lim, “Gravitational Waves From the End of Inflation: Computational Strategies,” *Phys.Rev.* **D77** (2008) 103519, [arXiv:0712.2991](#) [astro-ph].
- [250] J. F. Dufaux, G. N. Felder, L. Kofman, and O. Navros, “Gravity Waves from Tachyonic Preheating after Hybrid Inflation,” *JCAP* **0903** (2009) 001, [arXiv:0812.2917](#) [astro-ph]. \* Brief entry \*.
- [251] J.-F. Dufaux, D. G. Figueroa, and J. Garcia-Bellido, “Gravitational Waves from Abelian Gauge Fields and Cosmic Strings at Preheating,” *Phys.Rev.* **D82** (2010) 083518, [arXiv:1006.0217](#) [astro-ph.CO].
- [252] A. Diaz-Gil, J. Garcia-Bellido, M. Garcia Perez, and A. Gonzalez-Arroyo, “Magnetic field production during preheating at the electroweak scale,” *Phys.Rev.Lett.* **100** (2008) 241301, [arXiv:0712.4263](#) [hep-ph].
- [253] A. Diaz-Gil, J. Garcia-Bellido, M. G. Perez, and A. Gonzalez-Arroyo, “Primordial magnetic fields from preheating at the electroweak scale,” *JHEP* **0807** (2008) 043, [arXiv:0805.4159](#) [hep-ph]. \* Temporary entry \*.
- [254] J. Garcia-Bellido, D. Y. Grigoriev, A. Kusenko, and M. E. Shaposhnikov, “Nonequilibrium electroweak baryogenesis from preheating after inflation,” *Phys.Rev.* **D60** (1999) 123504, [arXiv:hep-ph/9902449](#) [hep-ph].
- [255] L. M. Krauss and M. Trodden, “Baryogenesis below the electroweak scale,” *Phys.Rev.Lett.* **83** (1999) 1502–1505, [arXiv:hep-ph/9902420](#) [hep-ph].
- [256] A. Tranberg and J. Smit, “Baryon asymmetry from electroweak tachyonic preheating,” *JHEP* **0311** (2003) 016, [arXiv:hep-ph/0310342](#) [hep-ph].
- [257] J. Garcia-Bellido, M. Garcia-Perez, and A. Gonzalez-Arroyo, “Chern-Simons production during preheating in hybrid inflation models,” *Phys.Rev.* **D69** (2004) 023504, [arXiv:hep-ph/0304285](#) [hep-ph].
- [258] Planck Collaboration . <http://www.rssd.esa.int/index.php?project=Planck>.
- [259] A. R. Liddle and M. S. Turner, “Second order reconstruction of the inflationary potential,” *Phys. Rev.* **D50** (1994) 758, [arXiv:astro-ph/9402021](#).
- [260] M. S. Turner and M. J. White, “Dependence of Inflationary Reconstruction upon Cosmological Parameters,” *Phys. Rev.* **D53** (1996) 6822–6828, [arXiv:astro-ph/9512155](#).

- [261] E. J. Copeland, I. J. Grivell, E. W. Kolb, and A. R. Liddle, “On the reliability of inflaton potential reconstruction,” *Phys. Rev.* **D58** (1998) 043002, [arXiv:astro-ph/9802209](#).
- [262] I. J. Grivell and A. R. Liddle, “Inflaton potential reconstruction without slow-roll,” *Phys. Rev.* **D61** (2000) 081301, [arXiv:astro-ph/9906327](#).
- [263] J. Lesgourgues and W. Valkenburg, “New constraints on the observable inflaton potential from WMAP and SDSS,” *Phys. Rev.* **D75** (2007) 123519, [arXiv:astro-ph/0703625](#).
- [264] Dark Energy Survey Collaboration , T. Abbott *et al.*, “The dark energy survey,” [arXiv:astro-ph/0510346](#) [[astro-ph](#)]. White Paper submitted to Dark Energy Task Force.
- [265] PAU Collaboration . <http://www.pausurvey.org/home-PAU.html>.
- [266] Baryon Oscillation Spectroscopic Survey Collaboration . <http://www.sdss3.org/surveys/boss.php>.
- [267] N. Makino and M. Sasaki, “The Density perturbation in the chaotic inflation with nonminimal coupling,” *Prog. Theor. Phys.* **86** (1991) 103–118.
- [268] R. Fakir, S. Habib, and W. Unruh, “Cosmological density perturbations with modified gravity,” *Astrophys. J.* **394** (1992) 396.
- [269] D. H. Lyth, K. A. Malik, and M. Sasaki, “A general proof of the conservation of the curvature perturbation,” *JCAP* **0505** (2005) 004, [arXiv:astro-ph/0411220](#).
- [270] J. Weenink and T. Prokopec, “Gauge invariant cosmological perturbations for the nonminimally coupled inflaton field,” *Phys.Rev.* **D82** (2010) 123510, [arXiv:1007.2133](#) [[hep-th](#)].
- [271] J.-c. Hwang, “Cosmological perturbations in generalized gravity theories: Conformal transformation,” *Class.Quant.Grav.* **14** (1997) 1981–1991, [arXiv:gr-qc/9605024](#) [[gr-qc](#)].
- [272] J.-c. Hwang and H. Noh, “Cosmological perturbations in generalized gravity theories,” *Phys.Rev.* **D54** (1996) 1460–1473.
- [273] C. Ringeval, “The Exact Numerical Treatment of Inflationary Models,” *Lect. Notes Phys.* **738** (2008) 243–273, [arXiv:astro-ph/0703486](#).



